The Clinical Application of Optical Coherence Tomography for Head and Neck Premalignant/Malignant Lesions

Zaid Hamdoon

BDS, MSc (OMFS), MFDS RCS

A submission presented in partial fulfilment of the requirements of the University College London for Doctor in Philosophy

2013

Abstract

The principle of Optical Coherence Tomography (OCT) is based on the property of light coherence. OCT generates cross-sectional images of two-dimensional objects to obtain *in-vitro* and *in-vivo* images of tissues.

Non–commercially available OCT systems, which have a higher resolution and scanning rate, have been previously reported. However, some clinical research has already been conducted using the first commercially available OCT device (Niris system) to image the larynx; but applications on oral and skin tissue have not been tested yet.

This thesis aims to explore, compare and validate three specific types of commercially available OCT equipment for imaging head and neck tissue.

An animal cancer model has been used to verify the feasibility of one system (Niris) to differentiate normal from malignant oral tissue, using *in-vivo* tissue samples. Since images of oral tissue samples didn't show much structure using the Niris system, a different machine (Michelson Diagnostic bench based) with different specifications and resolution was employed. Great emphasis has been put on validating OCT structurally and histomorphometrically in comparison to the gold standard of pathology. This was tested and validated with *ex-vivo* oral and skin tissues using the lab based version of the machine.

Use of an upgraded system (Michelson vivo sight with probe) has been tested on abnormal oral and skin biopsy tissue but with different timing for the scan (instant *ex-vivo*). One original study evaluated and classified tongue papilla atrophy from patients having their suspicious tongue lesions biopsied.

In conclusion, this thesis concludes that the new version of this commercially approved OCT system can be applied to the diagnosis of superficial premalignant and malignant oral and skin lesions *in-vitro*. Furthermore, OCT holds the promise of complementing surgery to eradicate tumors and monitor the consequences.

Acknowledgments

This task would not have been possible without the guidance and support I received from everyone around me while I was working on the project. My supervisor, Mr. Colin Hopper, through his encouragement and guidance of the subject, played a pivotal role in shaping this project.

Credit goes to other pathology lab members, Amrita Jay and Christina, for all their help. I would also like to thank my second supervisor, Professor Porter, the Director of Eastman Dental Institute, for reviewing this thesis. Thanks also to Mr. Ashraf for revising the English of the manuscript. I also wish to thank the Government of Iraq for their enormous financial support and travel grants, which exceeded 150.000 British pound.

I would also like to thank my study mates,Waseem, Sultan, Dara. I thank all my fellow workers at the Michelson Diagnostic Laboratory, especially Dr. Gorden for the considerable work he did supplying soft ware information on the OCT system, Florian for his assistance with most of the measurements and for great discussions, and Rore for his support and technical advice in the early stage of this work.

My thanks must also go to Max and Sebastion at the University of Gronegen, who kindly offered me their animal lab at no cost for the fruitful work Chapter III is concerned with. Finally, I would like to thank my wife Zainab and my daughter Sara for their great support and patience, and my father for his support and encouragement during this project, and to the soul of my mother who passed away before seeing me graduate.

Declaration

I certify that, except the help listed in the acknowledgments, the contents of this thesis, concerning the *ex-vivo* OCT work except biopsy taking, are based solely upon my independent work and have not been submitted in part or in full for the award of a degree this or any university or examination board. Animal induction by carcinogenic agent was carried out by research group at the University of Gronegen who are the primary license holder with ethical approval. In Animal study, *in-vivo* OCT scan was done by Mr Hamdoon which is the only *in-vivo* work in this thesis. The number of the patients included in this thesis is 245 with overlap in different study all cover by one ethics (REC reference number: 07/Q0504/4). The original ethics application was submitted by Dr Betz

Zaid Hamdoon **Signature……..**

Date…../……/……

List of abbreviations and definitions

AK	Actinic keratosis
BCC	Basal cell carcinoma
BM	Basement membrane
CE	Contact endoscopy
CI	Confidence of interval
CIS	Carcinoma *in- situ*
CM	Conofocal microscopy
CT	Computerized tomography
DEJ	Dermo-epidermal junction
DMBA	7,12-dimethylbenz(a) anthracene
EBV	Epstein–Barr virus
ED	Epithelial dysplasia
EL	Epidermal layer
EP	Epithelium layer
ESS	Elastic scattering spectroscopy
ET	Epithelium thickness
FD-OCT	Fourier-Domain Optical Coherence Tomography
FS	Florescence spectroscopy
H&E	Haematoxylin and Eosin
HGD	High grade dysplasia
HPV	Human papilloma virus
LDR	Lichenoid drug reaction
LGD	Low grade dysplasia
LP	Lamina properia

LM	Lentigo Maligna
LR+	Positive Likelihood Ratio
LR-	Negative Likelihood Ratio
LSS	Light-scattering spectroscopy
MM	Malignant melanoma
MDL	Michelson Diagnostic Limited
MI	Molecular imaging
MPM	Multiphoton microscopy
MRI	Magnetic Resonance Imaging
NHL	Non-homogeneous leukoplakias
NIR	Near-infrared
NMSC	Non-melanoma skin cancer
NPP	Negative predictive value
OCT	Optical Coherence Tomography
OCM	Optical coherence microscopy
ODT	Optical Doppler Tomography
OFK	Oral frictional keratosis
OL	Oral leukoplakia
OLP	Oral lichen planus
OPL	Oral premalignant lesion
OSCC	Oral squamous cell carcinoma
OSF	Oral submucous fibrosis
PD	Papillary dermal layer
PDT	Photodynamic therapy

PL	Premaignant lesion
PMD	Potentially malignant disorders
POC	Premaignant oral condition
PPV	Positive predictive value
PR	Partial response
RS	Raman spectroscopy
RT	Radiotherapy
SC	Stratum corneum
SCC	Squamous cell carcinoma
SD	Stable disease
SD-OCT	Spectral-domain OC
SE	Standard Error
SR-OCT	Speckle reduced OCT
SS-OCT	Swept-source OCT
TD-OCT	Time-domain Optical Coherence Tomography
UADT	Upper aerodigestive tract
UCLH	University College London Hospitals NHS Trust
UV	Ultraviolet
WHO	World Health Organization
4NQ0	4-nitroquinoline l-oxide
µm	Micrometer

List of Figures

List of Tables

Table Page

Table of contents

Chapter 1

Review of Literature

1.0 Introduction

1.1 Normal mucosa

The oral mucosa is not simply a transition zone between the skin and gastrointestinal mucosa but comprises several differing and highly specialized mucosae. The varied histological patterns need to be appreciated to interpret the histological changes in disease.

Three main types of mucosa are distinguished: masticatory mucosa, specialized mucosa and lining mucosa. As a group they differ from the skin in that the papillary and reticular dermis are not distinguishable and the vascularity is greater. Apart from these features the oral mucosa have little connective tissue.

Mitotic figures may be found relatively frequently in normal oral epithelium, whose turnover time is between that of the skin and gut. They are more frequent in non-keratinized lining mucosa than in the more slowly replaced keratinized masticatory epithelium. The epithelial thickness reduces only very slightly with age and the rete ridge morphology becomes flatter.

Although it is widely stated that the oral mucosa becomes atrophic with age in reality there is only a microscopic thinning in healthy individuals and even this varies from site to site. Age-related changes are much less prominent than in skin and significant atrophy should not be dismissed as a normal age change.

Melanocytes, Merkel cells, Langerhans cells and lymphocytes are all found within oral epithelium. Melanocyte density in the mouth is similar to that on the skin although pigmentation is normal only in dark-skinned races. The gingiva is the most common site for racial pigmentation but the lips and buccal mucosa are occasionally also pigmented.

1.1.1 Masticatory mucosa

The masticatory mucosa is adapted to resist masticatory forces and covers the hard palate and attached gingiva. The overlying epithelium is orthokeratinized without a prominent granular layer and posteriorly passes through a transition zone of parakeratinization at the junction between the masticatory mucosa and the lining mucosa of the soft palate. In the midline, as on the gingiva, the mucosa and periosteum are fused into mucoperiosteum.

1.1.1.1 Palate

The palatal rugae are ridges running across the anterior hard palate with no specialized microscopic structure; they are formed by thickening of the fibrous connective tissue.

1.1.1.2 Gingiva

The gingiva, or gum, surrounds the teeth and covers edentulous alveolar ridges. In the upper jaw the palatal gingiva is not demarcated from the hard palate but elsewhere the gingiva is sharply delineated from the alveolar mucosa at the mucogingival junction. Gingiva appears opaque pink in colour. It is firmly bound to the underlying periosteum of the crest of the alveolar bone and to the cementum on the roots of the teeth by a dense collagen network, although the most coronal millimetre at the gingival margin is not bound down; this is termed the free gingival (Figure 1.1).

The gingival connective tissue is densely collagenous, with bundles of fibres passing from tooth to gingival and around the teeth circumferentially. The covering epithelium is para- or lightly orthokeratinized, less so than that in the palate, and has regular elongate rete processes which gradually become smaller and disappear towards the gingival margin.

The masticatory mucosa of the gingival meets the tooth surface at a small crevice which runs right around the tooth. This gingival crevice is absent in complete health but the almost universal presence of a minor degree of inflammation at this site results in it being 1-2 mm deep in most adults. The crevice is lined by a non-keratinized epithelium, the oral sulcular epithelium.

At the base of the crevice, a seal between mucosa and tooth is provided by the specialized junctional epithelium. This non-keratinized epithelium extends from the gingival crevice down the enamel surface of the tooth to the cementoenamel junction, tapering gradually. In adults with a degree of inflammatory periodontal disease the junctional epithelium proliferates and the level of attachment migrates down the root surface towards the root apex.

At the same time the gingiva becomes detached from the enamel and root, deepening the gingival crevice to form a periodontal pocket alongside the root. Although the pocket may extend many millimetres down the root, the epithelial barrier is maintained by the pocket lining epithelium which remains attached to the root at the base of the pocket.

1.1.2 Specialized mucosa

Although it is a masticatory mucosa, that on the dorsal surface of the tongue is distinct in structure. Most of the anterior dorsum is covered by filiform papillae, conical extensions of the mucosa comprising an elongate connective tissue papilla covered by keratinized epithelium which tapers to a point. Each papilla arises from both of the prominent elongate rete processes on each side. Only a narrow fibrous connective tissue lies between the epithelium and the underlying muscle. On the lateral parts of the dorsum the fungiform papillae are scattered among the much more numerous filiform papillae. Each comprises a rounded nodule of 0.25 mm in diameter, which projects little above the mucosal surface but which appears red because of its vascular connective tissue and less keratinized surface (Figure 1.2, 1.3).

The dividing line between the anterior two thirds of the tongue and the pharyngeal portion is marked by the row of 8-10 circumvallate papillae. These much larger structures (up to 3 mm diameter) comprise a nodule surrounded by an epithelium-lined cleft extending deeply to reach the underlying muscle. Serous minor mucous glands discharge in the depths of the sulcus and numerous taste buds lie in the lateral wall of the papilla. Taste buds are composed of a cluster of spindle-shaped epithelial cells, occupying the full thickness of the epithelium and communicating with the mouth through a narrow pore or pores (Figure 1.4).

1.1.3 Lining mucosa

Lining mucosa covers those parts of the mouth which are not subject to masticatory forces (Figure 1.5). It has a less dense connective tissue bound to underlying muscle or alveolar bone and contains minor mucous glands and variable amounts of fat. The covering epithelium is non-keratinized and varies in thickness from 100 µm in the floor of the mouth and the alveolar mucosa to 500 µm on the buccal or labial mucosa. Rete processes are short and wide or completely absent, as in the alveolar, labial and buccal mucosa (Figure 1.6).

Lining mucosa contains minor salivary glands of mucous type. These are particularly frequent in the labial and buccal mucosa and in the soft palate but are also found, in smaller numbers, on the ventral tongue. Sebaceous glands are scattered in the lip and buccal mucosa of almost all adults. When superficial or clustered they are visible to the naked eye (Fordyce spots) and if prominent may form creamy plaques. Heterotopic hair follicles are extremely rarely encountered.

1.2 Head and neck cancer

1.2.1 Incidence

Cancer is one of the major killers of human kind; enormous amount of interest should be taken in its treatment. Cancer is a complex disease to diagnose and treat, and represents a significant burden to patients and their families, the health system, and the community at large.

Head and neck cancer is a general name given for many different forms of cancers and affect different anatomical parts. They include cancers of the mouth, lip or tongue (oral cancers), and the upper parts of the throat (larynx and pharynx), oral cavity and upper part of throat called upper aerodigestive tract (UADT). Cancer of the outer layer of the skin, even if they involve the head and neck region, is not entitled within the head and neck cancer.

Oral and oropharyngeal cancer, grouped together, is the sixth most common cancer in the world. Squamous cell carcinoma (SCC) represents 90% of the UADT carcinoma and the other 10% include other epithelial origin carcinoma. The annual global estimated incidence is around 175,000 for oral and 106,000 for pharyngeal cancers excluding nasopharynx (Parkin *et al*., 2005).

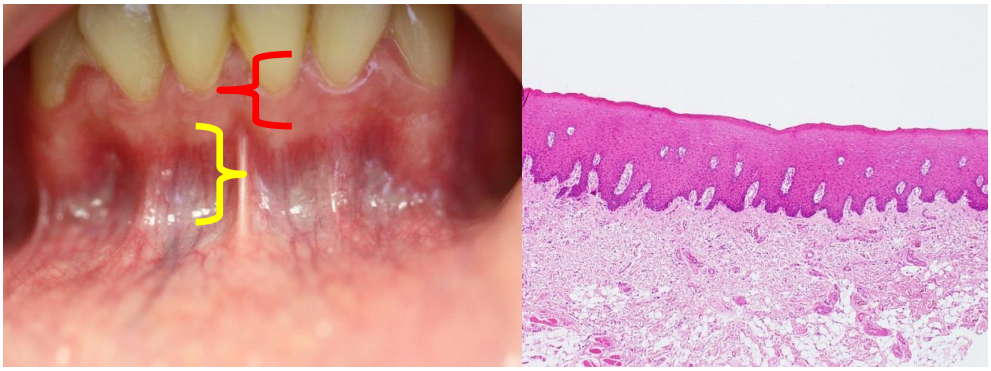

Figure 1.1: A; Attached gingival (masticatory mucosa) with dark pink colour (red bracket) well demarcated from non attached mucosa (alveolar mucosa with yellow bracket). **B;** H&E of attached gingiva, with thick keratin cell layer and thick epithelium.

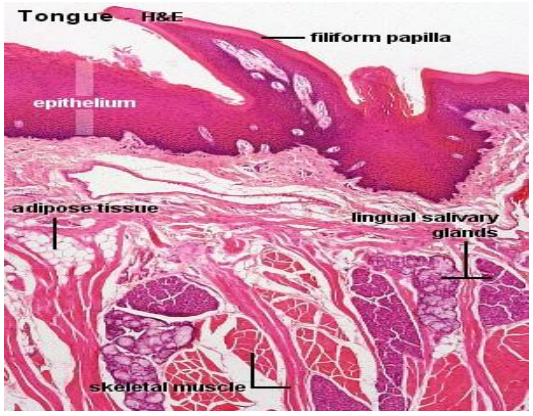

Figure 1.2: Filiform papillae. (Adapter from blue Histology - Oral Cavity and Oesophagus School of Anatomy and Human Biology - The University of Western Australia. http://www.histology-world.com.

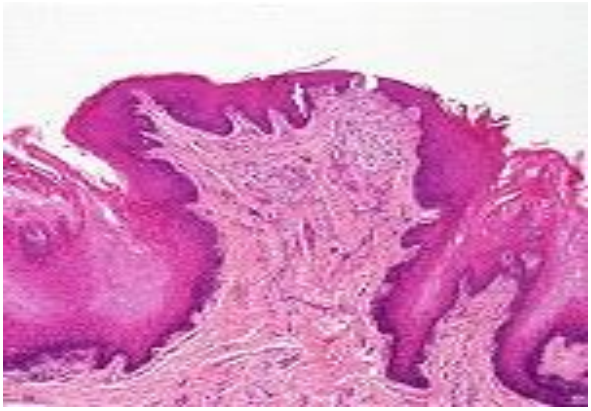

Figure 1.3: Fungiform papillae. (Adapter from blue Histology - Oral Cavity and Oesophagus School of Anatomy and Human Biology - The University of Western Australia. http://www.histology-world.com.

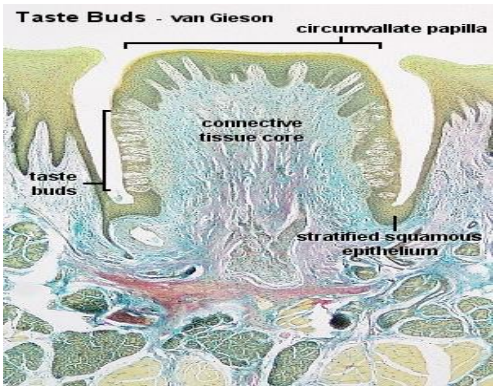

Figure 1.4: Circumvallate papillae. (Adapter from blue Histology - Oral Cavity and Oesophagus School of Anatomy and Human Biology - The University of Western Australia. http://www.histology-world.com.

Figure 1.5: Lingual mucosa at the ventral side of tongue.

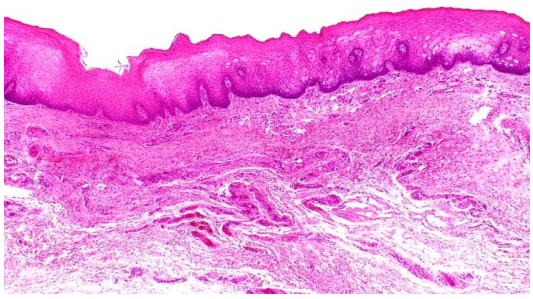

Figure 1.6: Normal non keratinized buccal mucosa with corresponding histology showing short rete pegs and slightly thick epithelium.

In the United Kingdom, oral cancers accounted for 1.6% of all new cancers, outnumbering cervical cancer, ovarian cancer and leukaemia (Warnakulasuriya 2009(b)). The disease is on the increase in young adults and most UK cancer registries record 6% of all oral cancers in young people under the age of 45 years (Warnakulasuriya 2007(b)).

1.2.2 Survival rate

For most countries, five-year survival rates for cancers of the tongue, oral cavity and oropharynx are around 50-58% (Jemal *et al.,* 2009; Bell *et al.,* 2007; de Araújo Jr *et al.,* 2008). The best outcome is for the cancer of the lip, with over 90% of patients surviving for five years. The lowest survival was for hypopharyngeal tumours. In general, prognosis decreases with advanced disease and increasing inaccessibility for the tumour. For cancers of both the tongue and the oral cavity, women had higher survival rates than men. TNM stage at presentation significantly affects five-year survival. For mobile tongue, five-year survival for stage 1 disease is 80%, while for stage 1V survival drops to 15% (Figure 1.7).

1.2.3 Clinical features

Patients who present with UADT malignancies often manifest various signs and symptoms. Generally speaking, early carcinomas often go unnoticed because they are asymptomatic (Scully and Bagan 2009). Mainly non-healing ulcers in the mouth, swelling (Figure 1.8 and 1.9), white lesions (leukoplakia) or red lesions (erythroplakia) (Al-Rawi and Talabani 2008)(Figure 1.10,1.11). They may also note loosened teeth, and a change in their dentition or in how their dentures fit. Occasionally patients may present with cervical lymphadenopathy without any other symptoms. In terminal stages, patients may develop skin fistulas, bleeding, severe anaemia and cachexia (Milian *et al.,* 1993). In addition, dysphagia, odynophagia, hoarseness, respiratory difficulty, referred ear pain, or weight loss may be present. Infrequently, the first sign of an aerodigestive malignancy is the presence of distant metastases. When present, distant metastases may involve the lung, bone, liver or brain.

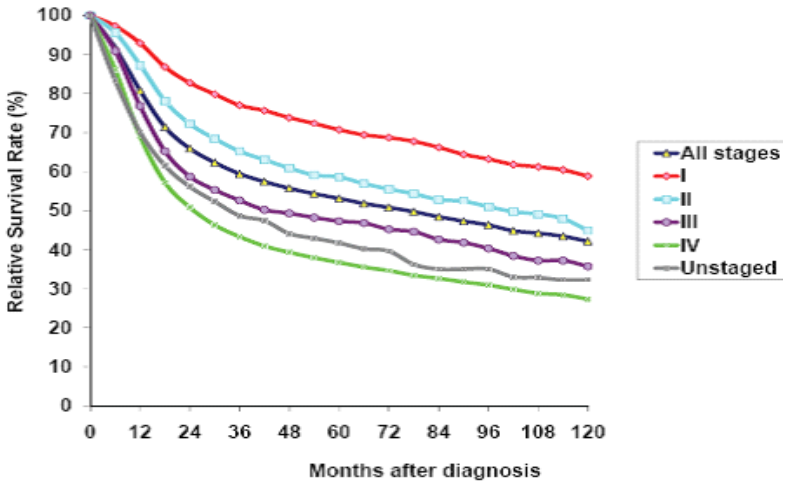

Figure 1.7: 5-year survival rate carve for head and neck cancer patient. (Adapter from Jay *et al* ., 2008).

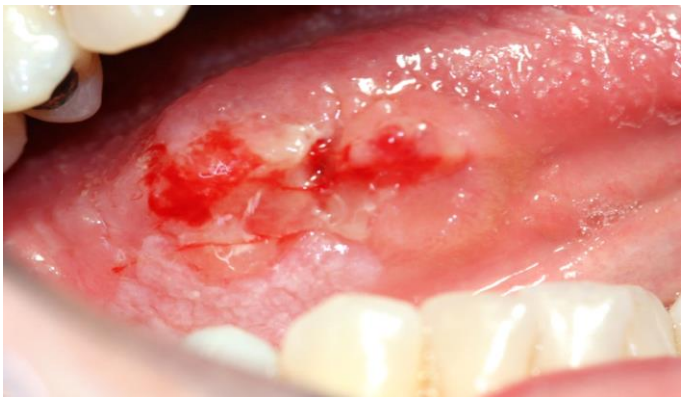

Figure 1.8: Typical SCC ulcer, lateral border of tongue.

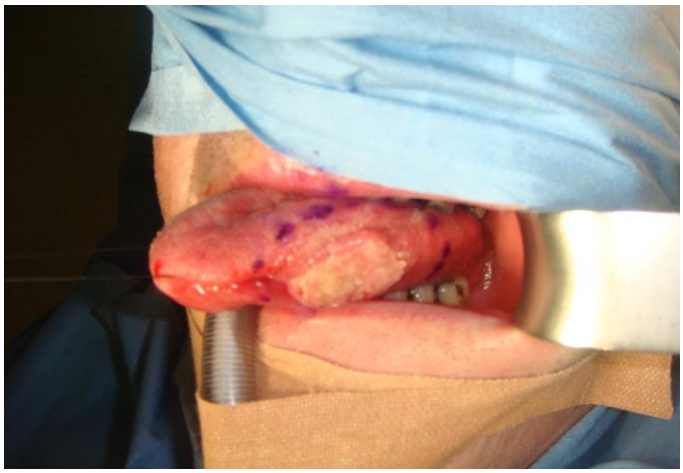

Figure 1.9: Exophytic SCC.

Figure 1.10: Homogenous Leukoplakia (T4 SCC).

Figure 1.11: Homogenous erythroplakia with early invasive carcinoma.

1.2.4 Histopathology of the SCC

In addition to the conventional and instantly recognised oral SCC (OSCC), several subtypes presenting varying diagnostic challenges have been recognised. The OSCC subtypes often occur alone (‘pure’ forms). However, ‘hybrid’ OSCCs, combining varying ratios of more than one subtypes, are now being increasingly recognised and are attributable to proliferation of individual clones expressing different phenotypes. Cervical node metastases of hybrid OSCCs may consist wholly or predominantly of one subtype (Figure 1.12, 1.13).

1.2.5 Location

Oral SCC may appear in any location, although there are certain areas in which it is more commonly found. The most common locations are the tongue and the floor of the mouth (Jovanovic *et al*., 1993; Brandizzi *et al.,* 2008)(Figure 1.14,1.15) . Oliver *et al*. in a review of 92 cases, found that the lateral and ventral surfaces of the tongue were the most frequent locations, followed by the floor of the mouth (Oliver *et al*., 1996). The lateral border of the tongue and the floor of the mouth, with extension to the tonsillar is the area of highest risk of developing cancer (Mashberg *et al.,* 1989).

1.2.6 Pre-malignant lesions

1.2.6.1 Terminology and staging

Terminology and definitions within the field of oral pre-cancer have been widely discussed. The use of the terms 'oral pre-cancer' and 'oral pre-malignancy' in itself poses problems. The use of terms like 'potentially malignant' signifies more precisely what is actually meant. The designations 'pre-cancer', 'pre-cancerous', 'pre-malignant', and 'precursors' will be used synonymously (Warnakulasuriya *et al*., 2007 (a)).

Oral pre-malignant lesions (OPL) are usually occupied by epithelial dysplasia (ED). This characteristically presents itself as a predominantly white, red, speckled or verrocus lesion (Brennan *et al*., 2007) (Figure 1.16, 1.17, 1.18, 1.19). Dysplastic features of a stratified squamous epithelium are characterized by cellular atypia and loss of normal maturation and stratification (Pinholt *et al*., 1997).

Conventionally, dysplasia is divided into grades of mild, moderate and severe: mild cases are those in which changes are seen within the lower third of the epithelium; moderate cases are those in which at least half the epithelium is involved; and severe cases are those in which most of the epithelium is affected (Figure 1.20). The presence of dysplastic areas in the oral epithelium is believed to be associated with an expected progression to malignancies. There is support for the view that in an individual lesion, the more severe the dysplasia, the greater the possibility is of progression to cancer (Reibel 2003).

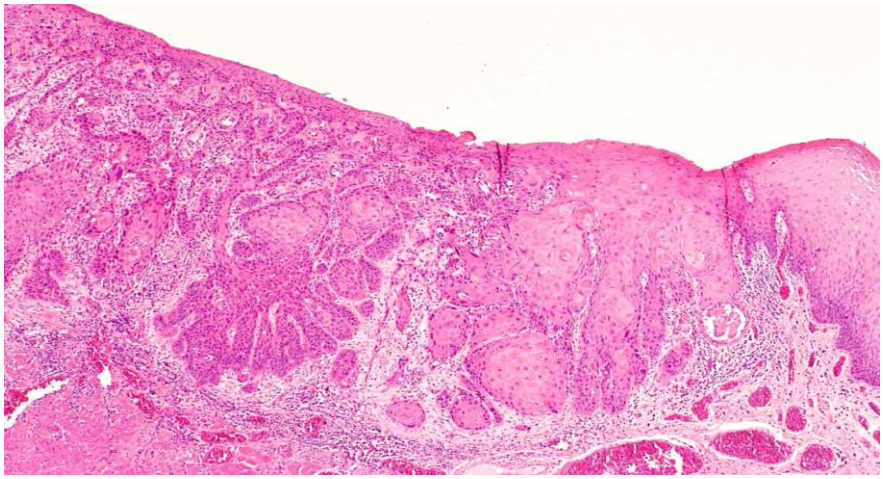

Figure 1.12: Early invasive SCC (2mm invasion).

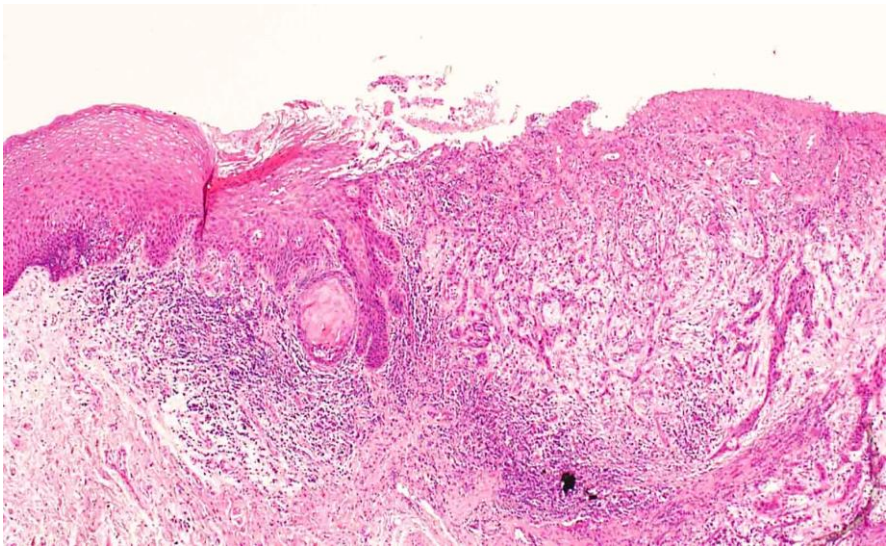

Figure 1.13: Advanced SCC (more than 4 mm invasion).

Figure 1.14: T1 SCC floor of mouth (ulcer).

Figure 1.15: Erythro-leukoplakia surrounding small ulcer (SCC).

Figure 1.16: Homogenous Leukoplakia with mild dysplasia.

Figure 1.17: Homogenous erythroplakia with carcinoma *in-situ*.

Figure 1.18: Erythro-leukoplakia with sever dysplasia on the lateral and ventral side of the tongue.

Figure 1.19: Verrocus leukoplakia.

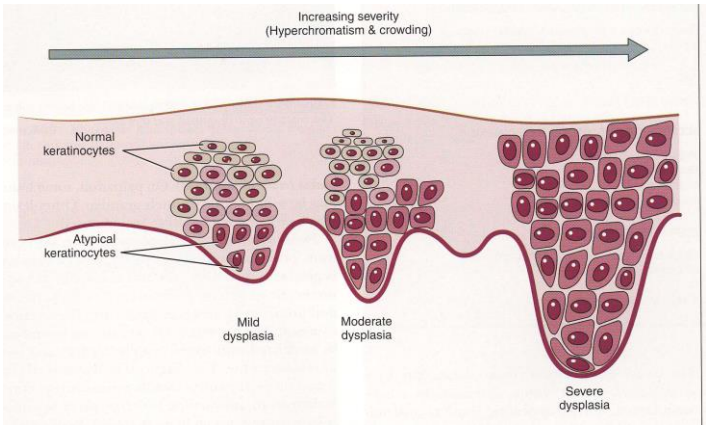

Figure 1.20: Different grades for oral dysplasia**.**

1.2.6.2 Predisposal factors

Alcohol has been found to increase the risk of OPL in the presence of tobacco (Warnakulasuriya 2009(a); Jaber *et al*., 1998). The risk of head and neck cancer in persons who smoke and drink is up to 17 times greater than the risk in persons who neither smoke nor drink. Tobacco is known to have various mutagenic effects through the formation of free radicals and epoxides. While alcohol increases the penetration of carcinogens through the oral mucosa by increasing their solubility and the permeability of oral mucosa (Howie *et al.,* 2001); chronic consumption causes oral mucosal atrophy and hyper-regeneration, thereby making the epithelium more susceptible to chemical carcinogens (Valentine *et al.,* 1985). Other risk factors have be attributed like viruses Epstein–Barr virus (EBV) which cause nasopharyngeal carcinoma, herpes simplex virus (HPV), Betel nut chewing, reversed smoking, iron deficiency (Plummer-Vinson syndrome) and chronic sunlight light exposure (cancer of the lower lip and malignant disease of skin) (Yen *et al*., 2008; Johnson *et al.,* 2009).

1.2.6.3 Spread and prognosis

The clinical type of oral leukoplakia (OL) has a bearing on the prognosis, since the non-homogeneous leukoplakias (NHL) containing an erythematous, nodular, and/or verrucous component have four- to five-times-higher risk of malignant development in the non-homogeneous leukoplakias compared with the homogeneous ones.

OL has an annual malignant transformation rate of 0.1% to 17% (Reibel 2003). In general, it is more or less accepted as an overall statement that approximately 5% of all leukoplakias will transform into cancer in an average period of 5 years. The malignant potential for erythroplakis is different because histological analysis is warrning, 51% of erythroplakic lesions have been shown to demonstrate invasive squamous cell carcinoma (SCC), with 40% demonstrating carcinoma *in-situ* (CIS), and 9% exhibiting mild-moderate dysplasia (Shafer and Waldron 1975)(Table 1.1,1.2).

Table 1.1: Clinical features of Leukoplakia

Feature	Leukoplakia
Definition	white plaque that does not rub off and cannot be clinically identified as another entity
Etiology	Tobacco Chronic hyperplastic candidosis Idiopathic leukoplakia (heterogeneous)
Clinical Feature	• Age : middle aged and elderly • Sex: Male predilection • Common Sites: Alveolar mucosa, buccal mucosa • Dynamic process, shows continuous histological changes
Clinicopathologic correlation	Dysplasia Carcinoma *in-situ* Squamous cell carcinoma
Other designations	Leukoplakia simplex, Leukoplakia verrucosa, Leukoplakia erosive, Verrucous hyperplasia, Leukoplakia speckled, Leukoplakia nodular, Leukoplakia ulcerative, Erythroleukoplakia

Table 1.2: Clinical features of Erythroplakia

Feature	Erythroplakia
Definition	Red velvety plaque that cannot be clinically or pathologically identified as another entity
Etiology	Unknown
Clinical Feature	• Age : elderly • Sex: Male predilection • Common Sites: floor of mouth , ventral and lateral tongue • Often well demarcated from surrounding mucosa • More likely to develop malignancy compared to Leukoplakia
Clinicopathologic correlation	Epithelial dysplasia Carcinoma *insitu* Epithelium is mostly non keratinized and shows atrophy

1.2.7 Prognosis

Early diagnosis of cancer improves the survival rate and increases the chance of cure. Moreover, treatment for a small early lesion is likely to be less mutilating and have a lower morbidity than treatment for a large advanced lesion. The five-year survival rate for persons with localized lesions is four times greater than that for those with distant metastases (Velich *et al*., 2007).

The proportion of patients presenting with advanced disease had not changed in the past 40 years despite public education (McGurk *et al., 2005*). The responsibility of this trend is multifactorial. The major contributing factors for non-improvement in the survival rate might be the late diagnosis of primary tumors and the high incidence of local recurrences due to occurrence of occult cancer cells in tumor margins (Bettendorf *et al*., 2004). Delay in the diagnosis is usually due to patients' delay or physician's delay. Since most head and neck cancers are asymptomatic, this delays patient in seeking advice. In younger people, this delay could be longer as cancer is not suspected by primary care practitioners (Llewellyn *et al.,* 2004).

1.2.8 Mode of treatment

The treatment for head and neck cancers, on the other hand, is most successful if they are diagnosed and treated early. Most head and neck cancers are treated with surgery to remove the tumour, or with radiotherapy (treatment using X-rays), or both. Chemotherapy (treatment using cancer medicines) isn't usually used alone for these cancers but may sometimes be used in combination with radiotherapy (this is called chemo-radiation). The fourth modality (photodynamic therapy) is being currently used in the treatment of advanced head and neck tumours and some early mucosal and skin tumours (Jerjes *et al*., 2009).

1.3 Benign oral lesions mimicking cancer

1.3.1 Oral lichen planus (OLP)

1.3.1.1 Aetiology and feature

Lichen planus is an autoimmune chronic disease mediated by T lymphocytes that involves the stratified squamous epithelial tissue. The designation and description of the pathology were presented by the English physician Erasmus Wilson in 1866. In addition, he suggested that its etiology could result from "nervous tension"(Scully and El-Kom 1985).

Louis-Frederic Wickham added to the description of the lesion *stries et punctuations grisatres* (grayish striae and dots), named Wickham striae in 1895 (Steffen *et al*., 2004). This dermatosis normally affects the oral mucosa, but it may involve the skin, nails, and genital mucosa. It is common in middle-aged women and affects men and women in the ratio of 2:3, respectively. It rarely affects children (Ismail *et al.*, 2007; Scully and Carrozzo 2008)

The etiology of the disease remains unclear, but many causal factors have been associated, among which: anxiety, diabetes, autoimmune diseases, intestinal diseases, drugs, stress, hypertension, infections, dental materials, neoplasms, and genetic predisposition. Even though its etiology has not been fully understood, its pathogenesis is more clearly defined. The main occurrence is the lymphocytic attack to the keratinocytes of the basal layer of the mucosa. T Lymphocytes induce apoptosis and cell degeneration and perpetuate the process by releasing chemokines in the inflammatory site (Scully *et al*., 1998).

1.3.1.2 Diagnosis

The diagnosis of OLP should be done by clinical and histological examination. However, in classical lesions, it is possible to achieve the diagnosis based solely on clinical appearance. The clinical presentations of this pathology vary widely and may, in some cases, have a silent onset and be overlooked in the examination.

Upon inspection, OLP may present with white striae (Wickham striae) in the surface of the mucosa, white papules or plaques, atrophic, erosive or vesicular lesions. The erosive, atrophic or bullous OLP has diverse painful symptoms. The gingival variant

often presents erythemas or ulcers limited to the gingiva. Due to the clinical similarity with gingival inflammation, it is denominated desquamative gingivitis. The most commonly affected areas are the mucosa of the cheek, dorsum of the tongue, gingiva, labial mucosa and lower lip (redness).

1.3.1.3 Clinical presentation

OLP has six classical clinical presentations described in the literature: reticular, erosive, atrophic, plaque-like, papular and bullous (Andreasen 1968).

Reticular: it is the most common clinical form of the disease and it presents with fine, intertwined white striae. Often, these lesions are not static, improving and worsening within weeks or months. Lesions are usually asymptomatic with a bilateral pattern, symmetrical, and involve the posterior mucosa of the cheek in most cases (Ingafou *et al.*, 2006) (Figure 1.21).

Erosive: this is the most significant form of the disease because it shows symptomatic lesions. Clinically, a central irregular ulceration covered or not by a fibrin plaque or pseudomembrane. The lesion is often surrounded by fine radiant keratinized striae with a network appearance (Figure 1.22).

Atrophic: it exhibits diffuse red lesions and it may resemble the combination of two clinical forms, such as the presence of white striae characteristic of the reticular type surrounded by an erythematous area (Silverman 1985) (Figure 1.23).

Plaque-like: this type shows whitish homogeneous irregularities similar to leukoplakia; it mainly involves the dorsum of the tongue and the mucosa of the cheek. Lesions can be multifocal, changing aspect and becoming elevated and/or rugous (especially in smokers) (Figure 1.24).

Papular: this form is rarely observed and is normally followed by some other type of variant described. It presents with small white papules (0.5mm to 1.0 mm of diameter) with fine striae in its periphery (Bricker 1994) (Figure 1.25).

Bullous: it is the most unusual clinical form, exhibiting blisters that increase in size and tend to rupture, leaving the surface ulcerated and painful. The periphery of the lesion is, in general, surrounded by fine keratinized striae (Zegarelli 1993) (Figure 1.26).

1.3.1.4 Histology of OLP

Histologically (Figures 1.27) lesions show a change in keratin pattem ranging from thick orthokeratosis through parakeratin to loss of keratin layer, the last usually being associated with atrophy or erosion.Disturbances of keratinisation vary in frequency with the site involved and it is the change in keratin pattem from the normal, rather than the type of keratinization, which is significant. The subepithelial band of lymphocytes in the mouth is often wider than in the skin but has the same sharply defined deep margin. Varying degrees of basal cell infiltration associated with apoptosis and colloid body formation are seen, depending on disease activity. In typical cases the infiltrate is exclusively lymphocytic, with only a few plasma cells scattered throughout.

The formation within the infiltrate of lymphoid follicles with germinal centres is a regular but infrequent occurrence when lichen planus is ulcerated, very atrophic or infected by candida. In the absence of these features the presence of follicles should suggest a topical lichenoid or hypersensitivity reaction or lupus erythematosus. In all but the least active keratotic lesions squamoid change of the basal cell layers, at least focally, is caused by loss of basal cell morphology and prickle cells at the basement membrane. When basal squamoid change is prominent the epithelial connective tissue attachment is weakened and there may be separation *in vivo*, during biopsy or section preparation.

Rete architecture is disturbed and shows all the variations from hyperplasia to complete loss seen in the skin, except that saw-tooth patterns are rare in the mouth. Elongate rete processes with a more dense lymphocytic infiltration around the tip are sometimes seen, especially on the dorsum of the tongue. A prominent hyalinized and thickened basement membrane may be visible somewhere in the section but is not usually seen in the areas of densest infiltrate or basal cell degeneration (Table 3).

Figure 1.21: Reticular lichen planus – reticular aspect on mucosa of the cheek (Adapter from Scully and Carrozzo 2008).

Figure 1.22: Erosive lichen planus – ulcerated lesion in the lateral area of the tongue with erythematous borders (Adapter from Scully and Carrozzo 2008).

Figure 1.23: Atrophic lichen planus (Adapter from Scully and Carrozzo 2008).

Figure 1.24: Plaque-like lichen planus (Adapter from Scully and Carrozzo 2008).

Figure 1.25: Papular lichen planus (Adapter from Scully and Carrozzo 2008).

Figure 1.26: Bullous lichen planus (Adapter from van Tuyll van Serooskerken *et al*., 2007).

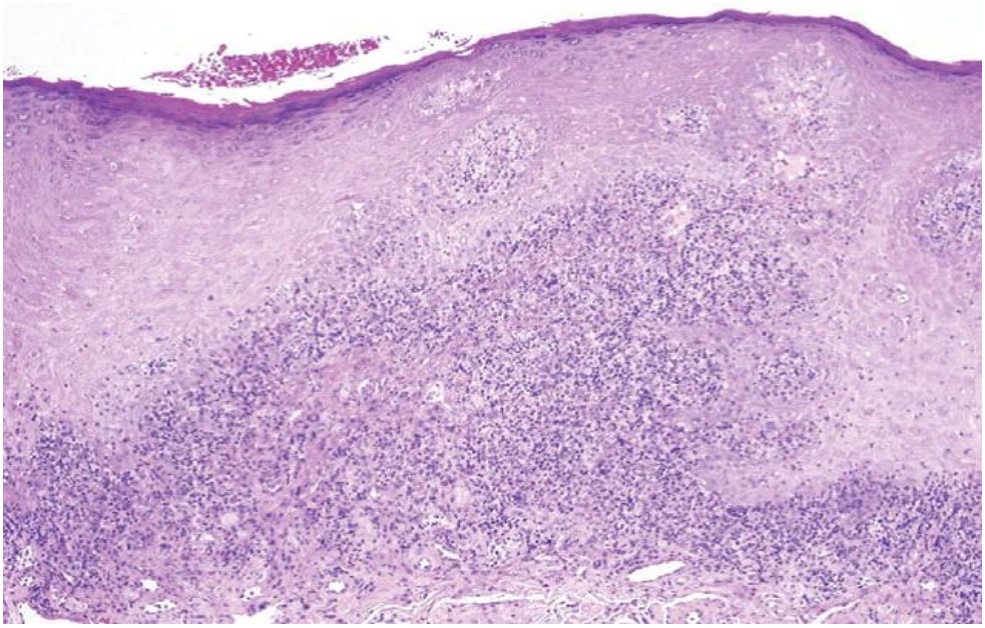

Figure 1.27: Histopathology of oral lichen planus shows a dense, bandlike, lymphocytic infiltrate in the superficial submucosa and wedge-shaped hypergranulosis of the epithelium (100 ×magnification). (Adapter from Schlosser 2010).

Table 1.3: Oral lichen planus: histological criteria and exclusionary features.

Essential features	Signs of "liquefaction degeneration" in the basal cell layer Presence of well-defined bandlike zone of cellular infiltration confined to the superficial part of the connective tissue, consisting mainly of T-lymphocytes Normal epithelial maturation pattern (absence of epithelial dysplasia)
Other non-requisite features	Candle-dripping" or "saw-tooth"-like rete ridge conformation Parakeratosis Civatte bodies Separation of epithelium from lamina propria due to basal cell destruction Exclusionary features Atypical cytomorphology Nuclear enlargement or hyperchromasia Prevalent dyskeratosis Increased number of mitotic figures; aberrant mitosis Blunt rete ridges Disordered stratification Heterogeneous lichenoid infiltrate (deep extension below superficial stroma or perivascular infiltration)

1.3.1.5 Malignization of OLP

The malignancy potential of lichen planus, especially in the erosive form, is not yet fully understood. More concrete evidence of its malignant potential is found in long-term follow-up studies and retrospective incidence of the patients; however, the issue remains controversial. Studies about the development of squamous cell carcinoma in OLP lesions appear to have fairly uniform results. On average, the sample is constituted by 200 patients and the frequency of malignancy varies from 0 to 5.3% in follow-up studies of 6 months to 20 years. Based on the variant of OLP presented, the atrophic, ulcerated and erosive types show greater incidence of malignant transformation. The most common sites are the tongue, gingiva and mucosa of the cheek (Lo Muzio *et al.*, 1998).

The greatest problem of studying the potential of malignancy of OLP is the lack of objective and unanimous criteria for its diagnosis. Some studies base the diagnosis only on clinical characteristics; others, on histopathological findings and others still on both. In addition, many lesions clinically and/or histologically diagnosed as OLP may, in reality, be dysplastic leukoplakias with lichenoid appearance and secondary lichenoid inflammatory infiltrate similar to lichen planus (lichenoid dysplasia). It is important to stress that histological characteristics of epithelial dysplasia are not exclusively premalignant.

The importance of the presence or absence of dysplasia in the early presentation of OLP was described in a study that reported four cases of malignant transformation in 141 patients with OLP. Of the four cases in which malignant transformation occurred, dysplasia was present in the early diagnosis of three of them (Bornstein *et al.*, 2006).

1.3.2 Leukoedema

Leukoedema is a generalized greyish-white keratosis of oral mucosa that characteristically appears on the buccal mucosa, was alleged to occur only in adult populations until Martin and Crump (Martin and Crump 1972) found this lesion in children and youth (Figure 1.28). Leukoedema was first described by Sandstead and Lowe in 1953 (Sandstead and Lowe 1953). leukoedema occurred as "patches" around lesions of leukoplakia or as "filmy" areas merging with leukoplakias and indicted leukoedema as a probable precursor to leukoplakia.

Several investigators have attempted to determine the etiology of this lesion. These independent studies were successful in correlating the clinical and histological aspects of leukoedema. Subsequently all suspicions of malignancy were removed (Martin *et al*., 1970; Archard 1968; Hammer *et al.*, 1971; Durocher *et al*., 1972).

Clinical examination readily differentiates leukoedema from leukoplakia since there is no loss of pliability or flexibility of the involved tissues (Russ 1957). In addition, the tissues affected by leukoedema manifest an edematous state. Leukoedema is distinguished from lichen planus by stretching the buccal mucosa (Crawley and Kerr 1952). Areas exhibiting leukoedema will either disappear or persist upon stretching, whereas lesions of lichen planus will become more pronounced. Leukoedema should also be differentiated from white sponge nevus and habitual cheek-biting (pathomimia morsicatio buccarum).

Histologically the appearances are either normal or may show simple acanthosis with accentuation of the normal basket weave appearance of the prickle cell layer or a thin superficial laver of vacuolated prickle cells' lesions of leukoedema exhibit hyperparakeratosis and are frequently elongated with irregular rete-pegs and intracellular edema of the malpighian layer. Increased mitoses, dyskeratosis, connective tissue atypia, and surface keratinization typical of cancerous lesions are not evident.

1.3.3 Oral frictional keratoses (OFK)

Oral frictional keratosis is a benign, self-limiting oral condition caused by the constant rubbing of two surfaces against each another, whereby the production of keratin filaments produces a haracteristic clinical aspect of white patches (Figure 1.29). OFKs represent a chronic, mechanical process, which tends, in most cases, to reduce or disappear within 1 to 3 weeks if the causative agent is carefully removed. Thus, this condition is more frequent in patients with particular habits and is generally found by chance during routine oral examination. OFK is an especially evident alteration in areas of mechanical trauma and may be due to different conditions:

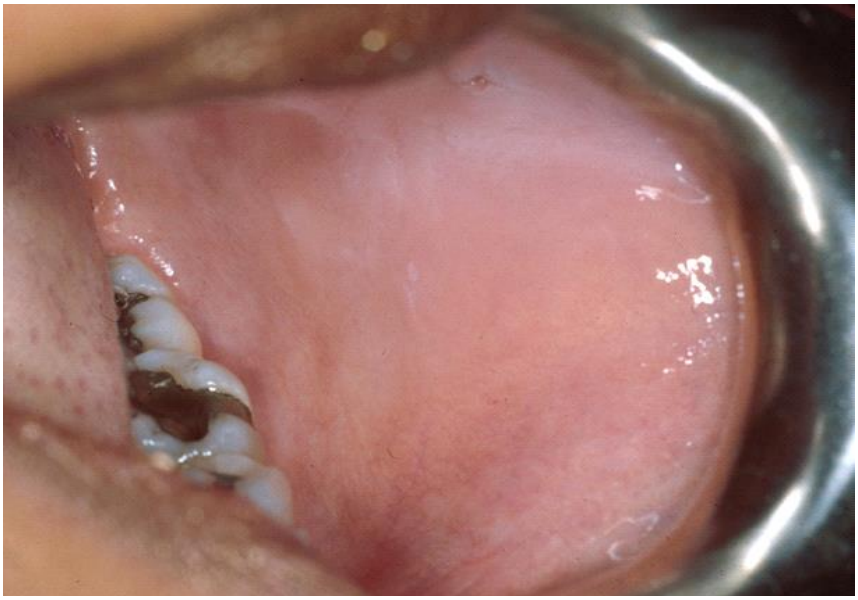

Figure 1.28: Typical case of leukoedema.

Figure 1.29: Frictional keratosis on the buccal mucosa.

1) excessive force while brushing the teeth with an overly stiff brush (toothbrush keratosis)

2) constantly rubbing the tongue against the teeth (tongue thrust keratosis)(Flaitz 2006)

3) constantly pushing the cheeks between the teeth while gently sucking or biting on the buccal tissues along the plane of occlusion (linea alba), often bilaterally (chronic cheek- or lip-bite keratosis)(Woo and Lin 2009)

4) constantly rubbing an external object, such as a tobacco pipe, pen cap, or musical instrument and presence of removable prosthetic appliances and food impaction on the edentulous alveolar ridge and retromolar pad area (Natarajan and Woo 2008).

Although the cause of OFK is clear in most cases, clinicians have to include a wide variety of clinical conditions in the differential diagnosis, such as genetic, physiologic, inflammatory, immunologic, potentially malignant, and malignant disorder, or a local insult, including chemical, thermal, or physical irritants.

1.4 Skin Cancer

Skin cancer is different from mucosal cancer where the former is divided into melanotic and non-melanotic cancers. Both of them account for more than 40% of all cancers. Skin cancer that develops from melanocytes, the pigment-producing cells of the skin, is called melanoma. Melanocytes can also form benign growths called moles (benign lesion). There are many types of non-melanoma skin cancers, but two types are most common basal cell carcinoma and squamous cell carcinoma (Reintgen *et al.*, 2010).

1.4.1 Incidence

Skin cancer, especially non-melanoma type, continues to be a major problem in the developed world. The number of recorded cases of NMSC in the U.K. in 2001 was around 62 700 (Diffey and Langtry 2005). While it is generally accepted that recorded numbers of these cancers underestimate the true figure, Non-melanoma skin cancer (NMSC) involves mainly squamous and basal cell carcinomas, SCC and BCC respectively. BCCs are mostly slow-growing local tumours with minimal invasion,

while SCCs are fast-growing invading tumours and usually metastasise early to loco-regional lymph nodes (Cherpelis *et al.,* 2002).

Non-melanomatous skin tumours are the most frequent tumours in the Caucasians population and mainly caused by cumulative exposure to ultraviolet B radiation. On account of this origination about 80% of all NMSC are located on the head and neck or the arms.

Incidence of basal-cell carcinoma alone is increasing by 10% per year worldwide, suggesting that prevalence of this tumour will soon equal that of all other cancers combined (Hayes *et al.,* 2007). Furthermore, an estimated 40–50% of patients with a primary carcinoma will develop at least one or more further basal-cell carcinomas within 5 years.

1.4.2 Age and gender

About 80% of cases occur in people aged 55 years and over. The incidence of BCC in South Wales in1998 in individuals over 75 years old was approximately five times higher than for individuals aged between 50 and 55 years old (Holme *et al*., 2000). Old age and male sex are associated with higher risk of developing both BCC and squamous cell carcinoma (SCC). More than 99% of individuals with BCC are white and 95% are between the ages of 40 and 79 years. Now it is also being seen in younger people, due to sun bathing (McCormack *et al*., 1997).

1.4.3 Macroscopic and microscopic appearance

Basal cell carcinoma (BCC) begins in the lowest layer of the epidermis called the basal cell layer. About 75% of all skin cancers are basal cell carcinomas (Leiter and Garbe 2008). They usually develop on sun-exposed areas. Up to 90% of these lesions are in the head and neck.

Early BCCs are usually small, translucent, or pearly, with raised telangiectatic edges. Roughly 80% of all BCCs occur on the head and neck, and clinical diagnosis is fairly straightforward. In addition to the classic rodent ulcer with an indurated edge and ulcerated centre, nodular or cystic, superficial, morphoeic, and pigmented basal-cell carcinomas are other common subtypes (Figure 1.30-1.32).

Up to 10–40% of basal-cell carcinomas contain a mixed pattern of two or more of these histological subtypes, drawing attention to the need for a clinicopathological diagnosis (Sexton *et al*., 1990; Rippey 1998). Superficial BCCs can sometimes be difficult to differentiate from psoriasis, discoid eczema, or Bowen's disease and pigmented and nodular subtypes can cause diagnostic confusion with melanoma.

Squamous cell carcinomas develop in higher levels of the epidermis and account for about 20% of all skin cancers. They commonly appear on sun-exposed areas of the body such as the face, ear, neck, lip, and back of the hands (Figure 1.33, 134). They can also develop within scars or skin ulcers elsewhere. Less often, they form in the skin of the genital area. Unlike BCC, SCCs can have precursor lesions, such as actinic keratoses and squamous-cell carcinoma *in-situ* (Bowen's disease), which are considered premalignant. SCCs tend to be more aggressive than basal cell cancers. They are more likely to invade tissues beneath the skin, and slightly more likely to spread to lymph nodes and/or distant parts of the body (Röwert-Huber *et al.*, 2007).

Several prognostic indicators play part in metastasis and recurrence SCC greater than 2.0 mm in thickness, and especially those greater than 6.0 mm, are associated with high risk of metastasis and local recurrence. The histological subtype is associated with poor prognosis such as spindle cell (carcinosarcomas), acantholytic, desmoplastic SCC (Veness 2006; Brantsch *et al*., 2008).

Figure 1.30: Nodular BCC.

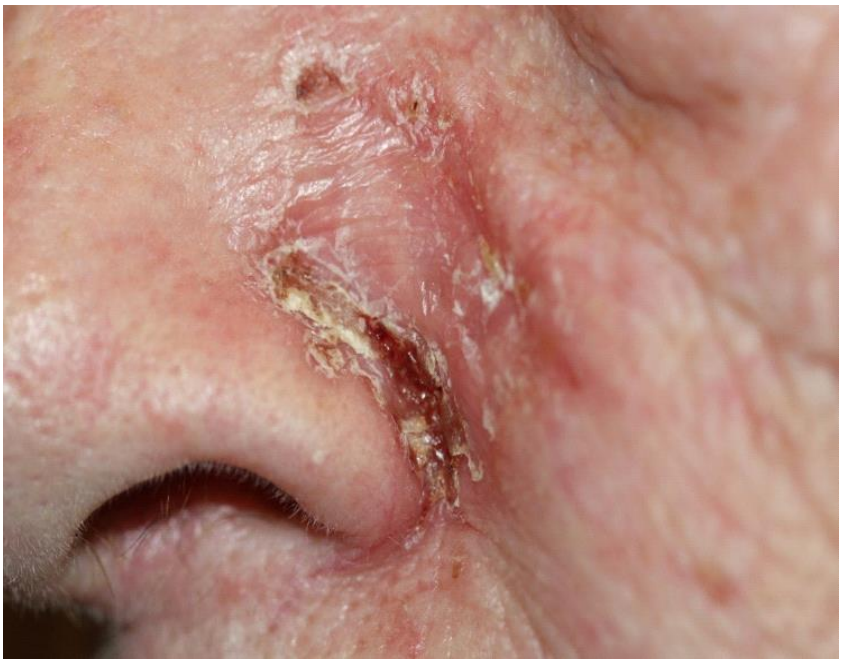

Figure 1.31: Ulcerative BCC at the naso-labial fold.

Figure 1.32: Superficial BCC temple.

Figure 1.33: SCC on the upper lip.

Figure 1.34: SCC on the lower lip.

1.4.4 Prognosis

Basal cell carcinoma is slow-growing. It is highly unusual for a basal cell cancer to spread to lymph nodes or to distant parts of the body. However, if a basal cell cancer is left untreated, it can grow into nearby areas and invade the bone or other tissues beneath the skin. The relative 5-year survival rate for patients with BCC is more than 99%. Less than one-tenth of a percent of basal cell carcinomas spread to lymph nodes or distant organs. However, patients whose basal cell carcinoma has spread to lymph nodes or distant organs have a 5-year survival rate of about 10% (Kyrgidis *et al*., 2010).

The overall 5-year survival rate for patients with SCC of the skin is more than 95%. The likelihood of squamous cell skin cancer spreading to lymph nodes depends on the cancer's size and location, but is estimated to occur in a small percentage of cases. The 5-year survival rate for SCC of the skin that has spread to lymph nodes or distant organs is about 25% (Dormand *et al.*, 2010).

1.4.5 Pre-cancer stage

Precancerous and pervasive skin conditions include mainly actinic keratosis and squamous cell carcinoma *in-situ* (CIS). Actinic keratosis (AK), also known as solar keratosis, is a precancerous skin condition caused by overexposure to the sun. Actinic keratoses are small (usually less than ¼ inch) rough spots that may be pink-red or flesh-colored. Usually they develop on the face, ears, back of the hands, and arms of middle-aged or older people with fair skin, although they can arise on other sun-exposed areas of the skin. People with one actinic keratosis will usually develop many more (Figure 1.35).

Actinic keratoses are slow-growing. They usually do not cause any symptoms or signs other than patches on the skin. It is possible, but not common, for actinic keratoses to turn into squamous cell cancer. They also frequently go away on their own but may come back. Even though most actinic keratoses do not become cancers, they are a warning that the skin has been damaged by the sun and that patients should check their skin regularly. Some actinic keratoses and other skin conditions that could become cancers may have to be removed (Newbold 1972).

The rate of progression of individual actinic keratoses to invasive SCC has been estimated as 1–10% over 10 years; this risk could be much higher in patients with more than five actinic keratoses (Newbold 1972; Marks *et al.,* 1998).

Squamous cell carcinoma *in-situ*, on the other hand, is the earliest form of squamous cell skin cancer. The cells of these cancers are entirely within the epidermis, and have not invaded the dermis. Bowen's disease (another name of squamous cell carcinoma *in-situ*) appears as reddish patches. Compared with actinic keratoses, Bowen's disease patches tend to be larger (often over ½inch), redder, more scaly, and crusted. Like invasive squamous cell skin cancers, the major risk factor is overexposure to the sun. Lesions of Bowen's disease usually present as slowly enlarging erythematous scaly or crusted plaques and have a 3–5% risk of progression to squamous-cell carcinoma (Glogau 2000; Cox *et al.,* 2007).

1.4.6 Risk factors

The Risk Factors for non-melanoma skin cancer is different from epithelium origin carcinoma. Excessive exposure to ultraviolet (UV) radiation is the greater risk of non-melanoma skin cancer. The main source of UV radiation is sunlight. The amount of UV exposure depends on the strength of the light, the length of exposure, and whether the skin is protected. People who live in areas with year-round, bright sunlight have a higher risk. Spending a lot of time outdoors for work or recreation without protective clothing and sunscreen increases the risk. Tanning lamps and tanning booths are other sources of UV radiation that may produce a greater risk of non-melanoma skin cancer.

The type of skin adds another risk factor. People with fair skin are 20 times higher risk of skin cancer than for dark-skinned. This is due to the protective effect of melanin (skin pigment). Other risk factors like chemical exposure**,** radiation treatment and reduced immune system treatment have a higher risk of developing non-melanoma skin (Simić 2010).

A confirmatory diagnosis can be achieved by histopathological examination, which remains the gold standard for diagnosis of non-melanoma skin cancer. As further novel non-invasive therapeutic modalities for non-melanoma skin cancers become available, interest in non-invasive screening and diagnosis of these lesions has also

increased. Dermoscopy (dermatoscopy) with cross-polarised light, high-frequency (20–100 MHz) ultrasound, optical coherence tomography with infrared light, and in-vivo confocal microscopy have been used for early diagnosis of non-melanoma skin cancer (Ulrich *et al*., 2007).

1.4.7 Pre-Melanoma and melanoma skin cancer

Malignant melanoma is the sixth most common cancer among men and women in the United States and accounts for the largest number of skin cancer-related deaths, with tumor thickness being the strongest prognostic indicator (Breslow 1970). Five-year survival rates for patients with nonulcerated tumors 1.0 mm and thinner reach 95%, while for nonulcerated tumors greater than 4.0 mm in depth, survival falls to 67%. Thus, it is imperative to detect and treat melanoma while early in its course (Balch *et al.*, 2001).

The annual incidence rate of malignant melanoma varies between populations, but in general has been in the order of 3–7% per year for fair-skinned Caucasian populations (Diepgen and Mahler 2002). The estimates suggested a doubling of melanoma incidence every 10–20 years (Garbe *et al*., 2000).

The histopathologic recognition of early cutaneous melanoma is to a large extent based on the presence of an atypical lentiginous proliferation of melanocytes along the dermoepidermal junction. This may occur in atrophic sun-damaged skin, such as that seen in lentigo maligna, or in addition to prominent pagetoid spread, as seen in superficial spreading melanoma (Figure 1.36). Mixed patterns of intraepidermal melanocytic proliferation occur in some melanomas, and there are melanomas that cannot be easily classified into the traditional groupings of lentigo maligna, superficial spreading, or acral lentiginous types (Table 4).

The term lentiginous melanoma coined to describe what believed to be a subset of melanomas, usually present in older adults, but also found in middle-aged persons, and in limited biopsies histologically bearing superficial resemblance to lentiginous nevus or atypical (dysplastic) lentiginous nevus of the elderly (King *et al*., 2005; Kossard *et al*., 1991; Kossard 2002).

Figure 1.35: Multiple AK (foot).

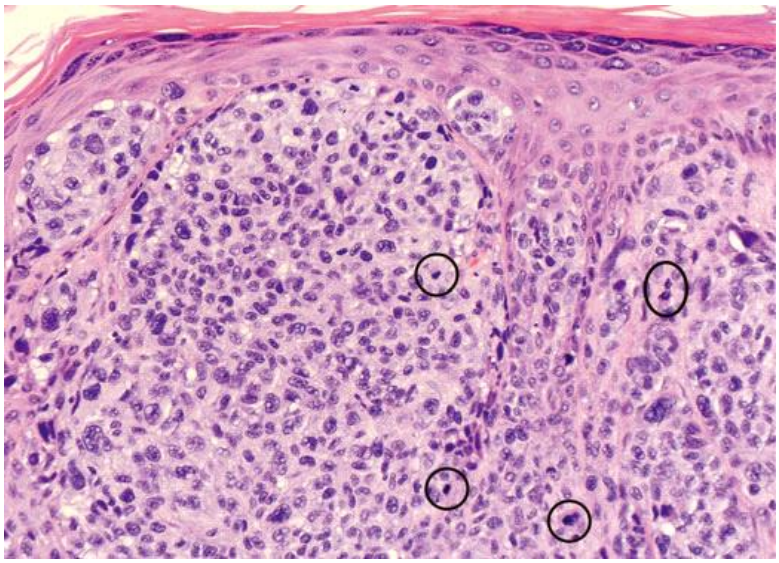

Figure 1.36: Histopathology ogf malignant melanoma. Mitotic figures in a melanoma with large junctional nests of tumor cells invading the corium and forming confluent sheets of cells. Because of invasive tumor growth, mitoses are counted to calculate the mitotic rate. H&E, x20. (Adapter from Garbe *et al*., 2011**).**

Table 1.4: Histologic Criteria for Lentiginous Melanoma

1. Broad proliferation of small nests and single cells at the dermoepidermal junction with areas of confluent growth
2. Preservation of the retiform epidermis
3. Mild to moderate melanocytic atypia with nuclear size equal to keratinocyte nuclei
4. Single-cell pagetoid spread
5. Lack of significant solar elastosis

1.5 Early diagnosis and monitoring of the cancer

1.5.1 Conventional methods of the detection and diagnosis of the oral and skin cancer

1.5.1.1Visual inspection

The most common screening method for the diagnosis of cancer is visual inspection and palpation. Physicians inspect for clinically evident lesions such as leukoplakia or erythroplakia which are associated with increased risk of cancer. Visual examination relies heavily on the experience and skill of the physician to identify and delineate early pre-malignant and cancerous changes. Several benign conditions, such as lichen planus, inflammation, and hyperkeratosis of oral cavity and skin, mimic the clinical presentation of precancerous lesions, and visual inspection with standard white light illumination may not yield sufficient contrast between normal and abnormal tissues. Even experienced specialist might misdiagnose a serious oral lesion and delay the diagnosis of cancer (Wildt *et al.,* 1995).

Once a suspicious lesion is identified, biopsy and histological examination are required for definitive diagnosis. Biopsies are invasive, painful, and costly and require familiarity and skill and are therefore typically limited to highly suspicious lesions. Additionally, many lesions are heterogeneous in morphology and visual appearance, and biopsy diagnosis may not be representative of the entire lesion due to the small sampling area (Margarone *et al*., 1985).

The diagnosis can be delayed by several months or more if the clinician treats the patient's complaints empirically with drugs instead of providing a thorough physical examination and workup. Furthermore, upper digestive tract cancer is known to exhibit "field cancerization" which may result in a second primary tumor which may need long term follow up (Slaughter *et al.,* 1953). Generally speaking, patients with symptoms and signs lasting longer than 2 weeks after removing the aetiological factors should be referred promptly to an appropriate specialist to obtain a definitive diagnosis.

1.5.1.2 Biopsy

1.5.1.2.1 Incisional and excisional biopsy

A biopsy is often the gold standard way to diagnose any abnormally looked lesions or diseases and as with most procedures there is often more than one method of undertaking the biopsy successfully. Whatever the method used, however, the aim is to provide a suitably representative sample for the pathologist to interpret (Oliver *et al* ., 2004).

For diagnosis, the excised material needs to be fixed to stop tissue autolysis prior to the sample reaching the pathology laboratory. The solution of choice to do this is 10% neutral buffered formalin fixative (a 4% solution of formaldehyde). A tight knot close to the specimen, however, is to be avoided as it may result in the tissue being crushed. The use of such a suture can aid the biopsy procedure by providing traction and preventing unwanted movement of tissue when taking a biopsy from mobile structures such as the tongue. It also helps the pathologist to orientate the biopsy sample for sectioning. The 'traditional' technique using toothed tissue forceps to grasp the specimen is acceptable providing care is taken and the area grasped is away from the main site of interest (Golden and Hooley 1994).

If the reason for the biopsy was to exclude malignancy in a long-standing ulcer, a biopsy of the ulcer to include some adjacent clinically normal epithelium would be desirable. The centre of larger tumors should be avoided as this is often necrotic and will not yield diagnostic material. Care should be exercised when handling mucosal biopsy specimens as they can be particularly prone to damage. Sometimes specimens can be rendered of little diagnostic value due to poor handling which produces a crush artifact in histological section (Moule *et al*., 1995).

1.5.1.2.2 Punch biopsy

The punch biopsy technique is an alternative to the traditional incisional biopsy. Essentially the punch comprises a circular blade attached to a plastic handle. This removes a core of tissue the base of which can be simply and atraumatically released using curved scissors. Alternatively, the specimen can be lifted from the mucosal surface and the base undermined with a scalpel (Eisen 1992).

1.5.1.2.3 Exfoliative cytology

Cytopathology is the microscopic study of cell samples collected from mucosal surfaces obtained by exfoliative cytology (via smears, scrapings, or lavage) or from internal sites via fine-needle aspiration (Patton *et al*., 2008).

Exfoliative cytology was first designed for cervical cancer cell early detection and it has been primarily applied in oral medicine practice to detect early changes in oral mucosa related to malignancy (Mehrotra *et al*., 2006). Exfoliative cytology is performed with cytobrushes so as to obtain good-quality smear that includes cells from deeper layers of epithelium, especially of squamous intraepithelial lesions.

According to Mehrotra *et al*. 2009, sensitivity and specificity of conventional exfoliative cytology in carcinoma's suspected lesions, ranged between 76.8%–100%, and 88.9%– 100%, respectively, in a review of 22 articles.

1.5.1.3 Stain

Vital Iodine Stain can be used prior to biopsy and resection and is useful in the determination of the best incision area. Its principle is based on the binding of iodine to glycogen granules in the cytoplasm, resulting in a blackbrown tissue color. In cancer cells, where the glycolysis is elevated (Maeda *et al.,* 2010), this method results in unstained areas whereas the normal mucosa is stained.

Toluidine Blue (also known as tolonium chloride) is a vital metachromatic dye of the thiazine group that has been effectively used in nuclear staining because of its binding to DNA nucleus acid. It has been used for decades as an aid in epithelium dysplasia identification (Epstein and Güneri 2009) and appears to improve precancerous lesion

visualization by showing high-risk areas (areas of high cell proliferation), therefore guiding biopsy (figure 1.37).

Several studies have shown that viral staining with an iodine solution was useful for detecting the extent of epithelial dysplasia. Some studies reported that vital staining with an iodine solution had great potential in determining the precise borders of the dysplastic epithelium. Some investigators described the usefulness of iodine staining.

There are numerous reports on the false positive results obtained from the Toluidine Blue. Reference has earlier been made to the fact that reactive lesions and benign tumors sometimes display features of epithelial dysplasia (Nair *et al*., 2012; Macdonald and Rennie 1975). The reaction patterns are largely unknown; however, a few studies have shown that benign lesions in some cases reveal a reaction pattern similar to that seen in epithelial dysplasias and cancer.

1.5.2 Optical diagnostic techniques

1.5.2.1 Elastic scattering spectroscopy (ESS)

ESS is an emerging technique that generates a wavelength dependant spectrum that reflects structural and morphological change within tissues. Light-scattering spectroscopy provides morphological information about such subcellular constituents as nuclei and mitochondria from elastically scattered visible light (Shim *et al.,* 2000).

Elastic scattering implies that the light returns with the same kinetic energy as the incident photons. The incident light can undergo single, or more commonly, multiple scattering events before being collected again at the same surface by an optical probe and the data analysed. Elastic spectroscopy can provide valuable information about changes that take place in tissue biochemistry during the development of dysplasia. However, the measured tissue spectra can be distorted significantly by unrelated scattering and absorption events. This scattering process has been shown to occur at gradients in the optical index of refraction resulting from differences in densities that occur at a cellular and sub-cellular level. The structures that induce the scattering (scattering centres) are the nucleus, chromatin concentration, and sub-cellular organelles (Sharwani *et al*., 2006) (Figure 1.38).

Clinical evidence of this method for the detection of dysplasia has been shown in a study of 13 patients with high grade dysplasia (HGD) and low grade dysplasia (LGD). Logistic regression and cross-validation were used to compare the spectral classification with that of histopathologic examination. The sensitivity and specificity of ESS for detecting dysplasia (either LGD or HGD) were 90% and 90%, respectively, with all HGD and 87% of LGD sites correctly classified.(Wallace *et al*., 2000). This method has the potential to detect very early changes associated with cancer transformation (Roy *et al.,* 2004).

Elastic-scattering spectroscopy was used to characterize the epithelial cell nuclei, chromatin content, nuclear/cytoplasmic ratio and cellular crowding which are all criteria that the histopathologist looks for when establishing of malignancy within a tissue. The intensity of the ESS spectrum varied in wavelength in an oscillatory manner. The frequency of these oscillations are proportional to the size of the scatterers (cell nuclei), and the depth of the modulations is proportional to the density of the scatterers, which in this case is indicative of nuclear crowding (Perelman *et al*., 1998).

ESS has the advantage of being fast, reliable and cost effective and potentially offers a diagnosis *in-situ*, non-invasively and in real time. The technique has not been used only in the diagnosis of dysplasia and malignancy, but can be used to monitor chemotherapy levels and free-flap oxygenation levels. It also can enable guided rather than random biopsies and to assess surgical margins and regional lymph nodes intraoperatively (Jerjes *et al*., 2004 & 2005).

1.5.2.2 Florescence spectroscopy (FS)

Approximately 30 years ago, it was observed that the autofluorescence of tissues (tissue fluorescence) could potentially be used for cancer detection. As such, there has been considerable interest in the technologies of both fluorescence imaging and spectroscopy in cancer screening for a number of anatomic sites including the oral cavity (Onizawa *et al.,* 1996; Ingrams *et al.,* 1997; Onizawa *et al.,* 1999). Fluorescence spectroscopic diagnosis, either autofluorescence or induced by an extrinsic photosensitizer, has shown encouraging results in differentiating normal from neoplastic tissues in clinical oncology (Wagnières *et al*., 1998) (Figure 1.39, 1.40).

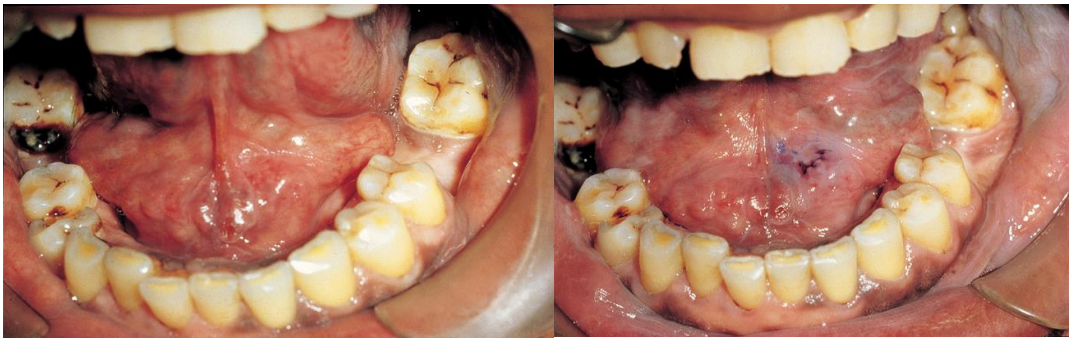

Figure 1.37: Toluidine blue staining of early SCC floor of mouth A; unstained; B: stained.

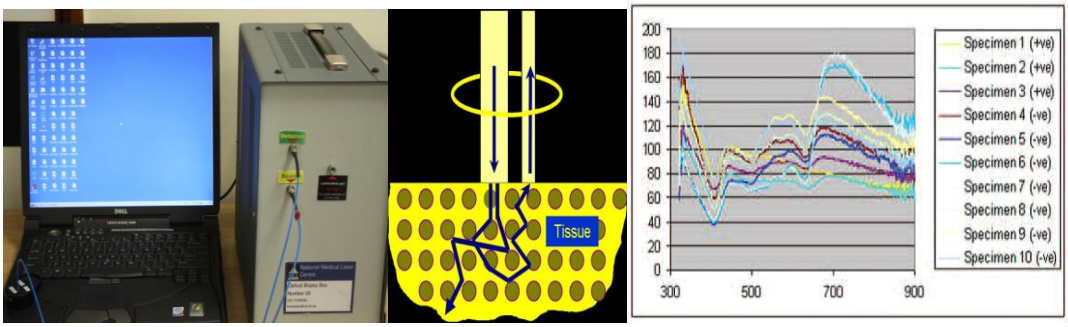

Figure 1.38: Elastic scattering spectroscopy (Adapter from Upile *et al*., 2007b).

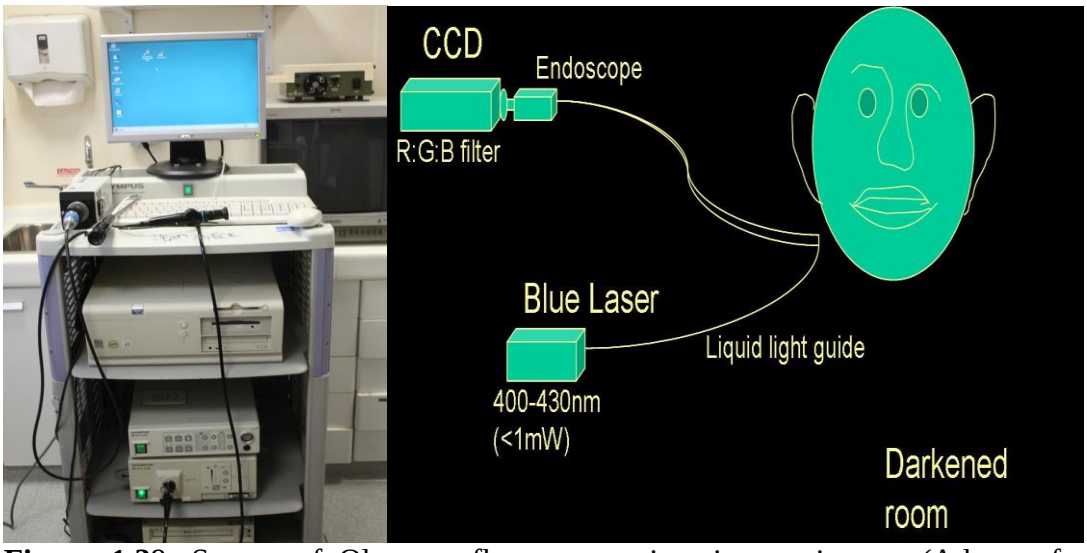

Figure 1.39: Set up of Olympus fluorescence imaging equipment (Adapter from Upile *et al*., 2007b).

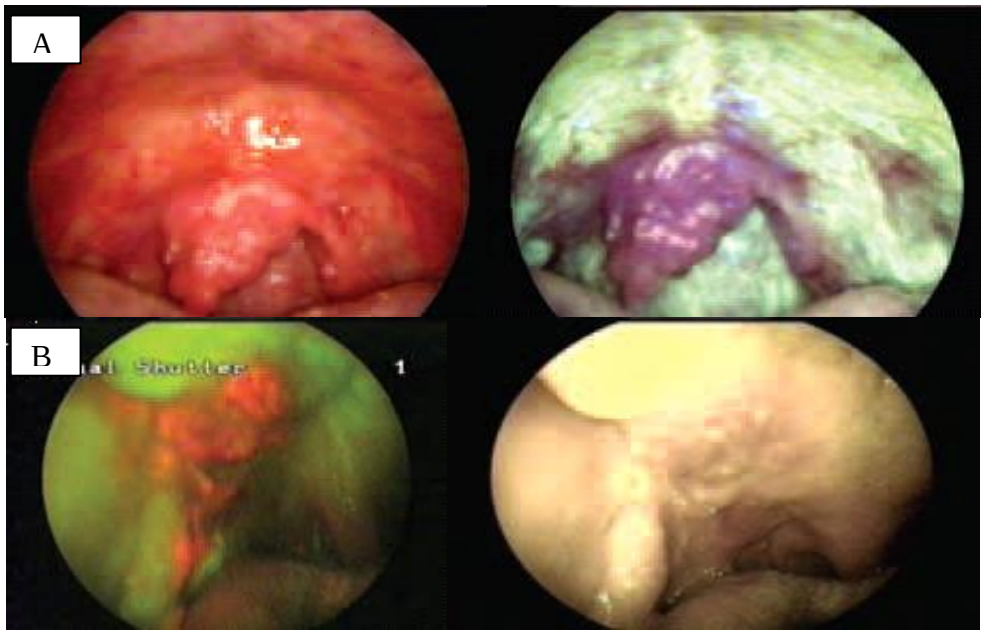

Figure 1.40: Head and neck fluorescence spectroscopy. (A) Autofluorescence image of a T1 SCC of soft palate and uvula. (B) Enhanced fluorescence image of a T1 SCC of the right hard palate (Adapter from Upile *et al*., 2007b).

Autofluorescence spectroscopy, which is highly related to the morphohistological characteristics and intrinsic fluorophores of the tissues, has shown great potential in detecting cancerous tissues. Direct fluorescence visualization is potentially powerful approach that may be used routinely by clinicians in the future to facilitate the visualization and management of nonapparent lesions. Tissue architecture and biochemical composition can be evaluated in near real time using optical spectroscopy using Ultraviolet light for disease detection since the 1950s (Schaffer and Sachs 1953). The device illuminates the oral mucosa, exciting natural fluorophores in the tissue and causing them to emit fluorescence that subtle alterations induced by dysplasia or inflammation can be visualized directly by a human observer non-invasively (Römer *et al*., 1995).

The loss of autofluorescence in clinically occult high-risk oral lesions could reflect histomorphological changes (eg, dysplastic nuclei, thickening of the epithelium, and increased vascularization), and/or biochemical changes such as decreased density of collagen crosslinks (fluorophores), possibly owing to the breakdown of the extracellular matrix in response to the signals from the dysplastic cells and decreased flavin adenine dinucleotide concentration due to increased metabolic. The contrast between normal and neoplastic areas can be increased beyond that which is available

with standard white light by tuning illumination and detection conditions (De Veld 2005).

Studies of fluorescence spectroscopy for the diagnosis of neoplastic changes have been conducted in a variety of sites, including the gastrointestinal tract, cervix, lung, breast tissue and oral mucosa (Ramanujam *et al.,* 1996; Hung *et al.,* 1991; Alfano *et al.,* 1989; Scheer *et al.,* 2011).

Fluorescence diagnosis using extrinsic 5-aminolevulinic acid (ALA) has been developed to improve the detection of neoplastic lesions and applied to oral, oesophageal, bronchial, and urothelial epithelia (Betz *et al.,* 2002). ALA itself is not a photosensitizer and serves as the biological precursor in the heme biosynthetic pathway (Gardner *et al*., 1991). Administration of ALA bypasses the feedback control system in the heme biosynthetic pathway, resulting in cellular accumulation of protoporphyrin IX. (ALA) is preferentially take up by tumour cells and converted to strongly red fluorescing photoporphyrin IX. Malignant tissue also has a limited ability to metabolize iron, so that an exogenous application application of ALA will result in an intracellular increase in photoporphyrin IX which increase red tissue fluorescence (Upile *et al.,* 2007b).

Clinical evidence for the usefulness of endogenous fluorescence endoscopy as a guide for biopsy is beginning to emerge with mixed results. A recent study using targeted biopsy performed first under endogenous fluorescence imaging in 34 patients with short segment Barrett's esophagus found a greater number of sites of high grade dysplasia (HGD) than under subsequent conventional endoscopy (Niepsuj *et al.,* 2003) . In another study, 35 patients with Barrett's esophagus were evaluated first by autofluorescence endoscopy and then by random 4-quadrant biopsy. However, fluorescence imaging was found to have a collective sensitivity of 21% for the detection of neoplastic lesions, including 88, 19, and 12 specimens of low-grade dysplasia (LGD), HGD, and cancer, respectively (Egger *et al*., 2003).

1.5.2.3 Tissue reflectance (Chemiluminescence)

Tissue reflectance has been used for many years as an adjunct in the examination of the cervical mucosa for ‘‘acetowhite’’ premalignant and malignant lesions. Recently, this form of tissue reflectance-based examination has been adapted for use in the oral cavity and is currently marketed under the names ViziLite Plus and MicroLux DL (Figure 1.41). These products are intended to enhance the identification of oral mucosal abnormalities.

This imaging device has been FDA-approved for use in the oral cavity since November 2001. After rinsing with an acetic acid mixed solution, the oral cavity is examined under chemiluminescent illumination at 430, 540 and 580 nm wavelengths. This method allows increased visual distinctions between normal mucosa and oral white lesions (Epstein *et al.,* 2006; Kerr *et al.,* 2006).

The 1% acetic acid wash is used to help remove surface debris and may increase the visibility of epithelial cell nuclei, possibly as a result of mild cellular dehydration. Under blue-white illumination, normal epithelium appears lightly bluish while abnormal epithelium appears distinctly white (acetowhite). ViziLite Plus also provides a tolonium chloride solution (TBlue), which is intended to aid in the marking of an acetowhite lesion for subsequent biopsy once the light source is removed.

ViziLite was used to examine a variety of oral lesions, including linea alba, leukoedema, hairy tongue, leukoplakia, traumatic ulcer, fibroma, amalgam tattoo, tori, and frictional keratosis (Sackett *et al*., 1991). The detected signals may be related to the altered thickness of the epithelium, or to the presence of a higher density of nuclear content and mitochondrial matrix that preferentially reflect light. Hyperkeratinized or dysplastic lesions appear distinctly white when viewed under a diffuse low-energy wavelength light. By contrast, normal epithelium will absorb light and appear dark (Lingen *et al*., 2008).

The majority of studies investigating chemiluminescence reported subjective perceptions of intra-oral lesions in terms of brightness, sharpness and texture vs routine clinical examination, data interpretation may vary significantly between examiners (Huber *et al*., 2004). In January 2005, a combination of both Toluidine

Blue and ViziLite systems (ViziLite Plus with TBlue system; Zila Pharmaceuticals, Inc.) received FDA clearance as an adjunct to visual examination of the oral cavity in populations at increased risk for oral cancer. In a multicenter study of high-risk patients, it was reported that the majority of lesions with a histological diagnosis of dysplasia or carcinoma-in-situ were detected and mapped using (ViziLite) and toluidine blue (Epstein *et al.,* 2008).

1.5.2.4 Contact endoscopy (CE)

Contact endoscopy or microendoscopy is a promising approach for organ imaging *in vivo*. It combines conventional microscopy and miniature endoscopy. Microendoscopy permits direct observation of pathologic change at the microscopic level without the need to remove tissue. Its principal characteristic lies in the "live" evaluation of the cellular patterns of the epithelial layers and the sub-mucosal microvascular network (Figure 1.42**)**.

The main benefit includes earlier detection of precancerous and cancer conditions through improved biopsy selection and examination and more cost-effective solutions to screening. Details of the tissues, cells and cellular ultra-structure as well as the presence of some bacteria, fungi are evident.

The endoscope allow the monitoring of the whole mucosa surface, both normal and abnormal, and allows the detection of patterns specific for pathology, as infection, inflammation, metaplasia, dysplasia and malignancy. The endoscope gives the practitioner immediate result at examination and can be used to guide further surgery, biopsy or simple surveillance of large area of suspected mucosa.

In 1989, L'Estrange *et al*, first applied CE to the oral mucosa (L'Estrange *et al.*, 1989). Then, in 1995, Andrea *et al*. from the University of Lisbon applied this method to the larynx and nasal mucosa. Despite the good results obtained by Andrea *et al*., 1995, CE does not seem to have interested many authors to date, as few reports on this topic are available (Andrea *et al.*, 1995 (a); Andrea *et al.*, 1995 (b); Andrea *et al.*, 1997).

Wardrop *et al*. 2000, employed CE in 8 consecutive patients who underwent bioptic microlaryngoscopy with collection of biopsy specimens, comparing the endoscopic view with the histologic report. In 6 patients (2 of whom with carcinoma *in-situ*), histology confirmed the endoscopic diagnosis. These authors suggest that CE could be used, in the future, for the monitoring of dysplastic and neoplastic laryngeal diseases.

Negoro *et al*. 2004, used CE together with video-microscopy to observe tongue papillae, studying the correlation between the appearance of fungiform papillae and taste function. Patients with taste disorders tended to show flat papillae and a poor vascular network of papillae.

Contact endoscopy with methylene blue, acetic acid, or indigo carmine can produce a resolution of 10 to 71 μm with the capability of observation up to 100 μm below the tissue surface (Nelson *et al*., 2000). Only the most superficial layers of the epithelium can be visualized due to intrinsic optical limitations, and the images are obtained in an en face plane, an orientation that clinicians trained in reading cross-sectional histology are unaccustomed to. Furthermore, many disease processes of the oral mucosa result in immense epithelium thickening, thereby precluding any possibility of BM evaluation using existing technology (Shakhov *et al*., 2001)

One study of microendoscopy technique based on the findings in a 40 patient sample was shown to have sensitivity and specificity of 95% and 90%, respectively, in it is ability to determine abnormal mucosa compared to histopathological examination (Upile *et al*., 2007a)

One limit related to this method concerns the use of a stain. In fact, methylene blue, on account of its poor penetration in the deeper layers, permits the evaluation only of the upper mucosal surface. Therefore, disorders such as cysts or nodules located in the sub-mucosal layers and any deep tumoural infiltration cannot be fully described. For this reason, it is difficult, at times, to decide whether the image obtained is sufficiently diagnostic. Close collaboration with the pathologist is, therefore, clearly necessary.

Further disadvantages related to this technique include the difficulties sometimes experienced, by the operator, in positioning the endoscope on the mucosal surface (particularly when using 150x magnification) and in obtaining homogeneous staining of the mucosal surface, especially in localizations with physiological clearance, such as, for example, the oral cavity and nasal mucosa.

1.5.2.5 Raman spectroscopy (RS)

Raman spectroscopy is performed by illuminating tissue with near-infrared (NIR) photons that are absorbed by the unique vibrational/rotational modes of molecular bonds associated with chemical functional groups specific to mucosal proteins, lipids, and nucleic acids. Raman spectroscopy is one of these optical methods that could permit less invasive and non-destructive analysis of biological samples, allowing one to get precise information on biochemical composition from different types of human tissues (Figure 1.43).

Raman spectra are obtained by exciting the molecules in the sample by a laser beam. The inelastic scattering light results in a frequency shift in the Raman spectra. Once these frequency shifts depends on the type of molecules, the Raman spectra holds important information on the different biochemical compounds. All stages of cancer are marked by fundamental changes in cellular morphology and/or tissue biochemistry, and biochemical tumor markers such as proteins, enzymes, and hormones could be detected by analyzing the differences of Raman spectra obtained from normal and pathologic tissue. Raman spectral differences could be used as a clinical method to provide real-time medical diagnosis less invasively, as well as, important information about the tissue biochemistry (Elizabeth *et al*., 2009; Florence *et al*., 2009).

Within biological tissues there are four principle components that contribute to the spectra; water, lipids (cell membranes), nucleic acids (DNA and RNA) and proteins (hormones, isoenzymes, immunoglobulins and keratins). The resultant spectra from these structures give a characteristic signature for that tissue. The choice of wavelength also enables the operator to probe different depths of tissue due to different wavelength penetrations and the technique therefore represents a true form of optical histochemistry.

Figure 1.41: ViziLite Plus.

Figure 1.42: Cy-scope & monitor.

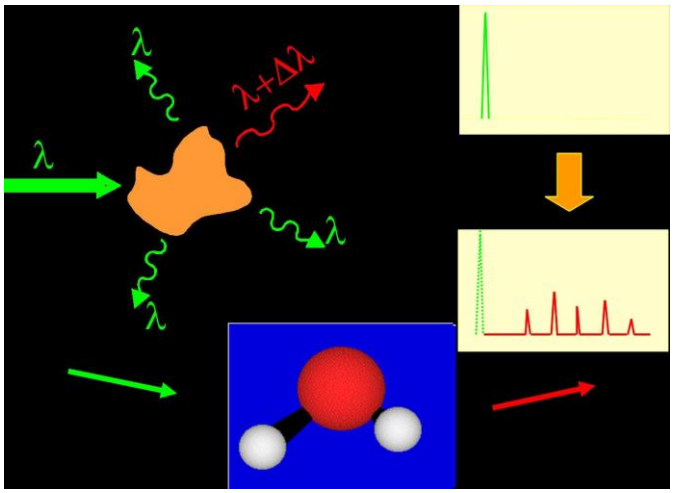

Figure 1.43: Principal of Raman spectroscopy.

The disadvantage, however, is that it is expensive, complex and difficult to adapt for *in vivo* use due to superimposed optical fibre and auto-fluorescence complicating the spectra. Another minor disadvantage of Raman spectroscopy is the autofluorescence emitted from biological tissues that could be almost completely suppressed by using excitation radiation in the near-infrared region. The Raman effect is much weaker than that of fluorescence and can be obscured easily by fluorescence from the tissue or optical fibre itself. Recent advancement in charge-coupled device (CCD) detector sensitivity and special filtered probes have allowed for the collection of Raman spectra *in vivo* (Hanlon *et al.,* 2000).

Raman spectra were first collected *ex-vivo* from non head and neck cancer, 34 adenomatous and 20 hyperplastic polyps in 8 patients to validate the diagnostic algorithm and then collected *in vivo* from 10 adenomatous and 9 hyperplastic polyps in 3 patients to show the ability to distinguish polyp type with 100% sensitivity, 89% specificity, and 95% accuracy (Molckovsky *et al.,* 2003).

1.5.2.6 Molecular Imaging (MI)

Molecular imaging is performed with the use of injected probes consisting of such small molecules as enzyme substrates, receptor ligands, monoclonal antibodies, and peptides tagged to a fluorescence dye to achieve high-affinity binding to specific biochemical and molecular markers of disease (Massoud and Gambhir 2003). This approach is being developed primarily as a research tool with transgenic animals.

The potential of this method has been shown with cathepsin B, a protease that has increased expression in neoplastic cells (Mahmood and Weissleder 2003). This probe is synthesized from a polymer tagged to Cy 5.5, an NIR dye, that is inactive in its native state, but releases fluorescence after being cleaved by cathepsin B.

1.5.2.7 Optical coherence tomography

1.5.2.7.1 History and evolution

Optical coherence tomography (OCT) was first demonstrated for cross sectional retinal imaging in 1991 by a Massachusetts Institute of Technology (MIT) team headed by Fujimoto. (Huang *et al*., 1991). Since then, it has become a clinically useful diagnostic technique in the ophthalmology community. OCT instrumentation, buoyed

by a stream of technological advancements, has undergone substantial improvement in the past decade, and, as a result, is now well positioned for wide adoption in various other clinical and research applications.

A number of promising scientific developments remain on the horizon as well, ensuring that the potential applications for OCT-based techniques will continue to widen for the foreseeable future. OCT is an interferometric imaging technique that maps depth-wise reflections of near-infrared (NIR) light from tissue to form cross sectional images of morphological features at the micrometer scale. In the most basic form, an OCT instrument consists of a Michelson-type interferometer with a focused sample arm beam and a lateral-scanning mechanism.

OCT traces its origins to the field of optical coherence-domain reflectometry, a 1-D distance mapping technique that was originally developed to localize reflections from faults in fibre optic networks and was quickly applied to biological applications. These ties to the telecommunications industry have allowed the OCT community to leverage existing and state of the art low-cost hardware for biomedical applications. Initial OCT technology was licensed by MIT to Humphrey Systems (now Carl Zeiss Meditec Incorporated, Dublin, California), which commercialized the technology for ophthalmic applications, released its first unit in 1996, gained Federal Drug Administration (FDA) clearance in 2002, and has sold more than 6000 of its Stratus OCT™ systems to date.(Tran *et al*., 2004)

The OCT intellectual property landscape has become quite diverse since the development of this first system, with current patent holdings by a variety of corporate and academic entities. Among the approximately 40 U.S. patents with OCT in the title, Carl Zeiss Meditec still dominates corporate patent holders with more than ten, and the University of California leads academic institutions with four.

The corporate landscape itself is also expanding, and clinical OCT systems are now being manufactured for various applications by a group of established and start-up companies that includes Carl Zeiss Meditec Incorporated, LightLab Imaging (Westford, Massachusetts), Imalux Corporation (Cleveland, Ohio), ISIS Optronics GmbH (Mannheim, Germany), OCT Medical Imaging, Incorporated (Irvine,

California), Novacam Technologies, Incorporated (Pointe-Claire, Canada), and Lantis Laser Incorporated (Denville, New Jersey). A new set of companies focusing on high-speed retinal imaging, including OptoVue, Incorporated (Fremont, California), Topcon Corporation (Tokyo, Japan), Optol Technology (Zawiercie, Poland), Heidelberg Engineering (Heidelberg, Germany), and Opthalmic Technologies, Incorporated (Toronto, Canada), has also emerged recently. Today, it is estimated that more than 37,000 OCT scans are performed daily in the U.S.(Xie *et al.*, 2003).

In addition to the widespread development of clinical OCT systems, a significant market has also developed for research targeted systems and components. For example, several companies, including Femtolasers Produktions GmbH (Vienna, Austria), Nippon Telegraph and Telephone Corporation (Tokyo, Japan), and Thorlabs, Incorporated (Newton, New Jersey), through its partner MenloSystems GmbH (Munich, Germany), sell compact broad-bandwidth optical sources that are marketed for OCT application. In addition, full-featured stand-alone OCT systems for research use are sold by Thorlabs, Incorporated and Bioptigen, Incorporated (Research Triangle Park, North Carolina), whose 840- and 1310-nm systems incorporate advanced visualization software and are compatible with a broad selection of application-specific scanners.

This partnership between industry and academia has lowered the cost of entering the OCT research community. When coupled with the accessibility of ophthalmic OCT systems to clinicians, this commercialization has spurred exponential growth in both scientific and medical OCT research.

This surge in OCT investigations has taken place in parallel with the development of next-generation technologies that have opened new frontiers of OCT application. High-speed imaging capabilities are key among these advances, as they have enabled the rapid acquisition rates that are often necessary to reduce artifacts due to patient motion. Additionally, these capabilities have led to the ability to generate 3-D volumetric images within reasonable time constraints. OCT imaging speed increases have been achieved with Fourier domain detection techniques such as spectral-domain OCT (SD-OCT) and swept-source OCT (SS-OCT), where rapid scanning of narrow-band source spectra is performed. These techniques have been made possible by

technological advances in detector and source technologies. Finally, application of OCT deep within the body requires that minimally invasive imaging devices be employed since OCT penetration depths are typically limited to about 1 to 3 mm in highly scattering tissues. In addition to handheld probes, a variety of imaging devices have been integrated into clinical devices to allow for minimally invasive OCT imaging throughout the body with endoscopes, catheters, and biopsy needles.

1.5.2.7.2 Clinical application

Ear, nose, throat and esophageal lesions are another set of promising targets for OCT imaging due to the difficulties presented by traditional visual examination and the accessibility of tissue using specialized endoscopic OCT techniques (Bibas *et al.*, 2004; Armstrong *et al.,* 2006). OCT has been used to evaluate the laryngeal mucosa (Wong *et al*., 2005) the most common site of primary head and neck malignancy development, and has been found to be an effective means of quantifying the thickness of the epithelium, evaluating the integrity of the basement membrane, and visualizing the structure of the lamina propria.(Brand *et al.,* 2000; Jäckle *et al.,* 2000, Upile *et al*., 2009)

In addition, preliminary studies have been conducted to evaluate the application of OCT imaging to the oral cavity, oropharynx, vocal folds, and nasal mucosa. OCT has also been extensively applied in the gastrointestinal tract (Pitris *et al.,* 2000; Tearney *et al.,* 1997, Chak *et al.*, 2005; Faruqi *et al.,* 2004). Patients with Barrett's esophagus, a condition of cellular metaplasia that can progress to esophageal adenocarcinoma, typically undergo regular endoscopic surveillance and biopsy to monitor for dysplastic changes.

Several studies have sought to investigate the diagnostic utility of *in vivo* OCT to detect and diagnose oral pre-malignancy and malignancy (Tsai *et al.*, 2008(a,b); Wilder-Smith *et al*., 2009). In a blinded study involving 50 patients with suspicious lesions including oral leukoplakia or erythroplakia, the effectiveness of OCT was evaluated for detecting oral dysplasia and malignancy (Wilder-Smith *et al*., 2009). OCT images of dysplastic lesions revealed visible epithelial thickening, loss of epithelial stratification, and epithelial down growth.

Areas of OSCC of the buccal mucosa were identified in the OCT images by the absence or disruption of the basement membrane, an epithelial layer that was highly variable in thickness, with areas of erosion and extensive epithelial down-growth and invasion into the sub-epithelial layers.

Other studies have utilized direct analysis of OCT scan profiles, rather than image-based criteria, as a means of delineating the site and margins of oral cancer lesions (Tsai *et al*., 2008a,b). Using numerical parameters from A-scan profiles as diagnostic criteria, the decay constant in the exponential fitting of the OCT signal intensity along the tissue depth decreased as the A-scan point moved laterally across the margin of a lesion.

Additionally, the standard deviation of the OCT signal intensity fluctuation increased significantly across the transition region between the normal and abnormal portions. The authors concluded that such parameters may well be useful for establishing an algorithm for detecting and mapping the margins of oral cancer lesions. Such a capability has huge clinical significance, because of the need to better define excisional margins during surgical removal of oral pre-malignant and malignant lesions.

In the last decade OCT has been widely investigated for imaging of NMSC (Olmedo *et al*., 2006; Olmedo *et al.,* 2007; Welzel *et al.,* 1997; Welzel *et al.,* 1998; Gladkova *et al*., 2000; Bechara *et al.,* 2004; Barton *et al.,* 2003). A break-up of the characteristic layering of normal skin (Gambichler *et al.,* 2006; Mogensen *et al.,* 2008) is found in both OCT images of NMSC (Pierce *et al.,* 2004; Welzel 2001) and melanoma lesions (Gambichler *et al.,* 2007).

However, this disruption of layering is also seen in various benign lesions. Several other NMSC features in OCT images have been described, the most important are: focal changes including thickening of epidermis in AK lesions (Mogensen *et al*., 2009 (a), and dark rounded areas, sometimes surrounded by a white structure in BCC lesions. SCC has mainly been studied on oral mucosal surfaces using OCT but changes similar to BCC have been described.

Accuracy was assessed in three OCT studies (Barton *et al*., 2003; Korde *et al.*, 2007; Mogensen *et al*., 2009 (a)); identification of dark band in epidermis enabled detection of AK with sensitivity 86% and specificity 83% in a study of more than 100 patients. The dark band in OCT images correspond to keratin deposits in thickened SC in AK lesions. The study also reported sensitivity 73% and specificity 65% in diagnosis of AK using ROC-curves displaying quantitative data from OCT images of AK and sun-damaged skin (Korde *et al.*, 2007). In an earlier smaller pilot study Barton *et al*. 2003, had described sensitivity 100% and specificity 70% for diagnosing AK from dark bands in SC in OCT images.

Another study compared OCT and high-frequency ultrasound in diagnosis of eye-lid tumours. Examination of 38 patients (4 BCC, 1 AK and other benign and malignant tumours) showed that OCT was superior in detecting cystic lesions, but due to low penetration of the OCT system in the skin, tumour margins could not be determined (Buchwald *et al*., 2003).

In evaluation of OCT for quantitative assessment of skin cancer thickness (Mogensen *et al* 2009 (b)) found that OCT was more precise and less biased than HFUS for thickness measurement in BCC and AK lesions <2 mm, which is of particular interest as this group of tumours can be treated with non-invasive treatments such as photodynamic therapy. Both methods overestimated thickness but OCT was significantly less biased and OCT had low inter-observer agreement.

No relation between OCT penetration depth and skin colour was found. Using functional OCT imaging as PS-OCT, the presence of a non-birefringent, homogeneous band in the upper part of PS-OCT images corresponding to epidermis and papillar dermis has been described. A gradual transition from normal appearing tissue to tumour tissue could be detected by PSOCT at the BCC borders, indicating an ability of PSOCT to delineate tumour borders (Strasswimmer *et al.*, 2004).

Speckle reduced OCT (SR-OCT) is based on repeated scanning by altering the distance between the probe and the surface of the skin. This corresponds to a change of focus position in the skin between each OCT scan resulting in a number of OCT images with decorrelated speckle noise. A proper registration and averaging of these

images produce an SR-OCT image with reduced speckle noise. In a recent pilot study, SR-OCT results in improved visualisation and accurate thickness measurements in two BCC lesions and OCT was improved to a clinically relevant level in imaging of BCC lesions. Although at present individual diagnostic features do not seem sufficiently discriminatory for accurate OCT diagnosis of skin cancer (Mogensen *et al.*, 2009 (c)).

Machine learning algorithms or neural networks where several OCT features is combined may be useful: in a pilot study 41 BCC and 37 AK lesions were studied and the machine learning analysis established accurate classification in 73% of AK and in 81% of BCC lesions (Jørgensen *et al*., 2008).

In malignant melanoma (MM), only one study (Gambichler *et al.*, 2007) demonstrated large vertical, icicle-shaped structures as the most striking OCT feature of MM. Distinct architectural disarray and vague dermo-epidermal junction was found when comparing MM to benign nevi (BN). OCT of MM infrequently demonstrated a dermoepidermal junction zone with finger-shaped elongated rete ridges as typically seen in BN. Sensitivity and specificity studies also including other skin tumours were not performed. Another study showed that in selected cases OCT allows for *in vivo* correlation between surface dermoscopic parameters and histopathologic correlates, in particular the pigment network and brown globules. The resolution was not high enough to reveal the morphology of the single cells, but it was possible to evaluate the architecture of lesions (de Giorgi *et al*., 2005).

1.5.2.7.3 Clinical Translation

Similarly to the developmental process for pharmaceutical agents, there are five developmental steps that a new medical imaging technique takes as it is developed from the laboratory bench to the bedside is focused on technology development in the laboratory through initial design, calibration, and testing. Step 1 involves pilot studies that are carried out to assess the feasibility and safety of the technique for the clinical application of interest. During this step, the criteria or methods used to differentiate between normal and abnormal tissue are evaluated.

As these studies achieve promising results, research proceeds on to Step 2, which is a limited trial to study the usefulness of the technique in distinguishing between normal and abnormal tissue, grading different disease states or testing sensitivity and specificity. In Step 3, technology standardization is of critical importance as multicenter randomized clinical trials begin. Finally, in Step 4 the new imaging modality is adopted as the standard of care, and is further commercialized for the clinical specialty of interest.

1.5.2.7.3.1 Imaging Validation

In the translation process, there is continuous feedback between tissue phantom studies, cell line studies, animal studies, and human subject studies. In OCT, tissue phantoms, defined as samples designed to mimic human tissue, may copy the optical properties of tissue by incorporating scatterers and absorbers. They may also be constructed to model the physical and spatial properties of tissue through the use of scaffolds or gels.

More sophisticated phantoms may include the use of cell lines such as fibroblasts, and cancer cells. These phantoms are often used to identify biological components that are articulated in a disease of interest and to explore their contribution to observed OCT signals. *Ex-vivo* tissue specimens can be obtained from either animal models or human patients. A number of appropriate animal models exist for human diseases. For example 4-nitroquinoline l-oxide (4NQO), induced rat SCC for oral cavity.

Tissue validation studies are typically compared with light microscopy of histological sections, the medical gold standard. Histological evaluation itself has a degree of

doubt, however, since pathological diagnoses suffer from sampling variability and interobserver variability (Crawford 2006).

Histopathological examination typically requires that the tissue be excised, preserved in formalin, embedded in paraffin wax, thinly sliced, and stained prior to examination. It is clear that significant morphological artefacts may be induced as a result of this processing, and that the histological sections may not truly reflect the structural features *in-vivo*. It is also recognized that a number of optically induced artifacts arise in OCT images.

1.5.2.7.3.2 Clinical System Design

Once the fundamental technology has been proven in a laboratory setting during translation Step 0, imaging instrument hardware and software must be adapted for compatibility with the clinical setting in which it will be used. Many issues must be taken into account, including the size, ease of use of the tool, the speeds of the acquisition of the system, and the sterility of any probes that may be in close contact with tissue.

Fiberbased probes, for instance, are often constructed so that the optical components do not come in direct contact with the tissue but are protected by a transparent sheath, or a metal sheath with a clear window for the imaging beam. Handheld probes with sufficiently long working distances can also be easily protected by covering them with disposable sterile plastic wraps. While these methods are sufficient for *ex-vivo* use, *in-vivo* applications have more rigorous requirements.

System standardization and calibration procedures can reduce system-induced effects. For example, measuring the system's signal-to-noise ratio or imaging a standard tissue phantom prior to an imaging session can be useful for system alignment and the comparison of image quality over time. Other forms of variability, such as specimen or patient health and state of disease, may be overcome by recruiting a sufficient number of study participants to achieve appropriate statistical power. Software standardization is also a significant issue, since many research teams develop unique software to control systems, acquire data, and analyze images. No standard image or visualization formats currently exist in the OCT research community (Pearson 2006).

1.5.2.7.3.3 Clinical Trials and Commercialization

Randomized clinical trials form the basis of evidence-based medicine and are conducted in four phases. In phase 1 trials, the technology is applied to a small group of individuals to evaluate its safety and to identify any potential issues or side effects. Phase 2 trials are expanded to a larger group of patients, further testing the effectiveness and safety of the technology. Phase 3 trials are traditionally multicenter studies and are carried out to confirm the effectiveness of the new technology, compare it to other commonly used diagnostic methods, and collect any information on anomalies or adverse effects that may occur as side effects. Phase 4 trials are almost always carried out by the private sector in an effort to determine the risks, benefits, and optimal uses of the technology.

In the late stages of development and in clinical trials, private sector individuals with specializations in biomedical imaging technologies are often introduced for guidance and funding. Corporate partners frequently prefer to pursue technologies with established manufacturing processes that are easily scalable and transferable, rather than investing in fundamental research and development. Major medical companies also primarily focus investments on technologies with demonstrated clinical success and strong market potential.

Before a technology can be fertile for commercialization, it must be tied to a specific procedure rather than simply a clinical field of application. The tight restrictions surrounding device approval as part of the standard of care require that the approved uses be well developed and validated.

Aims and objectives of the thesis

The purpose of the thesis is to prove the feasibility and explore the benefit of new OCT in the diagnosis of pre- and early malignant lesions of the oral cavity and the facial skin.

The primary objective is to compare three OCT systems to establish a tissue diagnosis (normal, hyper-keratosis, pre-malignant and invasive carcinoma). Two of these systems have a multi-beam feature enabling high-resolution tissue imaging and providing lateral resolution of >7.5 μm over a 1-mm focal range. This is twice the lateral resolution of existing commercial single beam system (Niris system) which is compared in this thesis.

The secondary objectives are to answer the following questions:

- Can the basal membrane (BM) and dermo-epidermal junction (DEJ) and its invasion clearly be distinguished?

- Is it possible to derive important microanatomical information (e.g. extent of cellular crowding, thickness of the epithelial layer, occurrence of structural proteins, thickness of the keratin layer, parameters of the microvasculature and tongue papilla) from the OCT images?

Further objectives are:

- To validate the newly designed OCT system compared to gold standard pathology, if it is better than the other system, and then test the sensitivity, specificity and accuracy in the diagnosis of head and neck cancer.

- Use OCT to monitor premalignant and malignant conditions as an adjunct to biopsy.

Chapter 2

Materials and Methods

2.1 Two major areas of the FD OCT system

2.1.1 Low Coherence Interferometry

The Michelson interferometer is the heart of the Fourier Domain OCT (FD OCT) system. A coupler splits the source light into reference and sample arms and light reflected back is detected by the spectrometer. Individual wavelength components are detected by an array of detectors in the spectrometer camera. In the FD OCT system, the spectrometer measures the interference pattern as a function of frequency. The discrete Fourier transform of the interference pattern provides information about the object's structure.

OCT is based on a low coherence interferometer. Figure 2.1 shows the basic schematic diagram of an OCT system based on the Michelson interferometer. The broadband light source (Ein) illuminates the interferometer. A 50/50 beam splitter splits light into the reference path (Er) and the sample path (Es). The light is reflected back from the mirror in the reference path and from the tissue sample from the sample path. The electrical field of the light in the sample arm is modified when reflected back. Light reflected back from the mirror in the reference arm interferes with the modified light in the sample arm and is detected by the spectrometer.

Due to the broadband nature of the source, when the path length of the sample arm and reference arm matches within the coherence length of the source, an interference signal is observed. Sharp refractive index variations between layers in the sample medium manifest themselves as corresponding intensity peaks in the interference pattern. The amplitude of the interference depends on the refractive index differences at the interfaces.

The axial resolution of the OCT system depends on the coherence length of the source and the transverse resolution depends on the focusing system. The depth (axial) resolution of an OCT system is determined by the temporal coherence of the light source. In OCT imaging any tissue property which changes the amplitude, phase or polarization of the signal gives rise to diagnostically informative signals.

The OCT source wavelength should be good enough to provide better depth resolution. Light at UV frequencies is able to image at only superficial layers; at higher than 2500 nm wavelength vibrational absorption by water limits the depth resolution. Hence these wavelength ranges are not useful. Also the window between 950 and 1000 nm wavelengths should be avoided because the absorption of water in this range is the highest and it would cause tissue surface burns. Thus far, wavelength ranges from 1200nm to 1600nm have been proven the best for tissue imaging.

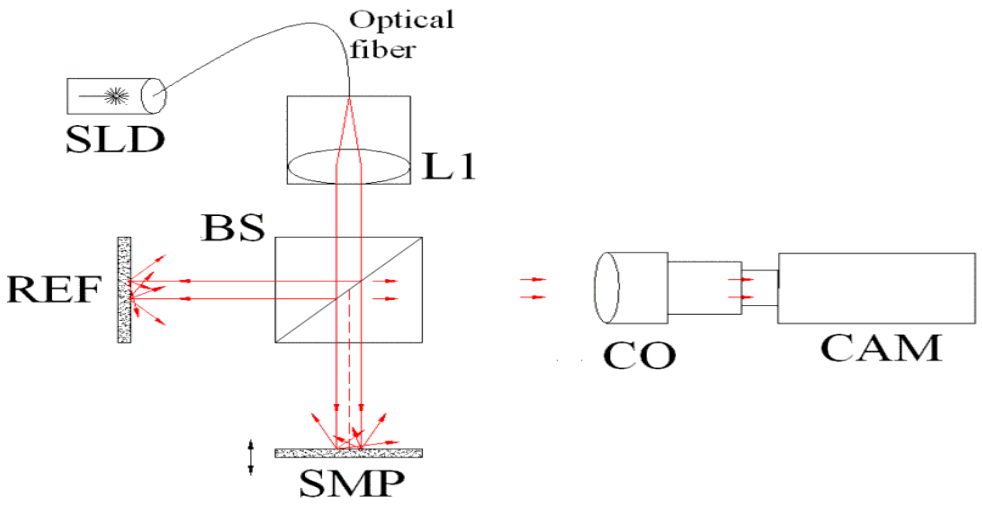

Figure 2.1: Full-field OCT optical setup. Components include: super-luminescent diode (SLD), convex lens (L1), 50/50 beamsplitter (BS), camera objective (CO), CMOS-DSP camera (CAM), reference (REF) and sample (SMP). The camera functions as a two-dimensional detector array, and with the OCT technique facilitating scanning in depth, a non-invasive three dimensional imaging device is achieved.

2.1.2 OCT hardware

The OCT system instrumentation consists of the source, reference arm and sample arm and a detector. All of these play a very important role in deciding the performance of the system and the quality of OCT images. In OCT, the source (laser) is a very important factor that decides the general performance of the system. High irradiance, short temporal coherence and emission in near infrared are basic requirements for the OCT source. Light reflected back from deep tissue is very weak and thus high irradiance is required while imaging tissue samples. Temporal coherence has an inverse relation with bandwidth. Shorter coherence that is higher bandwidth provides better resolution contrast in imaging.

2.2 OCT system setup

For imaging tissue samples three FD OCT systems were used: 1) bulk system (lab-based system with multibeam), 2) *In-vivo* OCT with flexible endoscopic probe (Imalux system with single-beam) *In-vivo* OCT with skin probe (Michelson VivoSight with multibeam). All these systems are based on the principle explained above. The bulk system is used for immediate and delayed *ex-vivo* imaging in the lab, but it cannot be used in clinical applications or for instant *ex-vivo* because of its size and bulky hardware. To overcome this limitation, an *in-vivo* OCT probe was used in a clinical setting to get images in instant *ex-vivo* from human subjects.

2.2.1 Bulk FD OCT system setup

Ex-vivo OCT imaging was done using the FD OCT bulk system (Michelson Diagnostics EX1301 OCT Microscope V1.0). The schematic of the FD OCT bulk system with the components is shown in Figure 2.2. To overcome this fundamental limitation of traditional, single-beam FD-OCT systems, a multichannel optical coherence tomography (multi-beam OCT) system was developed using a swept-source OCT system as a solution to simultaneously scan multiple beams, focused at slightly different depths, and compile an image mosaic from the resulting multiple FD-OCT interferograms.

Using a multichannel interferometer, the beams are sufficiently close together to be effectively simultaneous, so motion artifacts are not a problem. For example, a four-beam system focused over 1.0 mm, with each sub-beam focused over 0.25 mm, produces double the resolution possible from a single beam (Figure 2.3). Each sub-beam has a theoretical full width half maximum (FWHM) diameter of just 10.3 μm. The distal optics were micro-machined to produce a high numerical aperture, multi-focus fibre optic array. This combination resulted in a transverse design resolution of <10 μm FWHM throughout the entire imaging range, while also increasing the signal intensity within the focus of the individual channels.

The light source used is a Santec HSL-2000, with an imaging wavelength of 1310 nm, axial optical resolution of <10 μm, and lateral optical resolution of <10μm. The system provides an image resolution of 5.3 μm/pixel with a maximum image width of 6 mm, a sub-surface imaging depth of 1.5 mm, and a focal depth of 1 mm. Samples can be manipulated to see the full quality results on the screen instantly, with an image capture time of <100 ms and refresh

rate of >1 Hz. Images were acquired in two modes: black and white, and inverted colour mode.

2.2.2 *In-Vivo* OCT probe (Imalux system)

A commercially available clinical imaging system (Niris, Imalux Corporation, Cleveland, OH) was used (Figure 2.4). This portable OCT system uses a low coherence near-infrared light source to acquire real-time images of 200 × 200 pixels at a maximum frame rate of 0.7 Hz. The spatial depth resolution of the system is 10 to 20 μm, with a depth scanning range of 2mm. In practice, owing to the turbidity of living tissues, scanning depth is only about 1.5 mm. The lateral resolution is ≤50 μm, with a lateral scanning range of 1.5 to 2.5 mm while spatial resolution is 10-20 μm. In OCT systems, lateral resolution is diffraction limited, whereas axial resolution depends on the coherence length of the light sources. It uses a 2.7 mm diameter reusable flexible probe to obtain the images. To the user, the probe appears as a single, compact instrument; however, it encases a single-mode optical fibre, which is scanned back and forth within by a solenoid.

The Food and Drug Administration-approved Niris system is a portable OCT imaging system that uses a probe to direct the near-infrared light to the patient's tissues. The light is backscattered from the tissue, collected by the probe's fibre, and combined with a reference signal to produce a high spatial-resolution image of the tissue microstructure. The probe in this system was designed to facilitate OCT imaging within small cavities. The Niris Probe is 2.7 mm in outer diameter and has a length of 4 meters (m) and it is attached on the flexible arm of a lamp. This probe assembly reduces the size of the sample arm and enables fast rate *in-vivo* imaging due to its compact size; it is possible to use this probe for imaging human and animal oral cavities. OCT imaging of the oral cavity in rats was done using this system. The Working distance of the probe is 0-0.5 mm (direct contact with tissue is required) (Figure 2.5).

2.2.3 *In-Vivo* OCT probe (Michelson VivoSight)

A commercially available clinical OCT unit (VivoSight OCT scanner, Michelson Diagnostics, Orpington, Kent) with multibeam technology was used for scanning instant *ex-vivo* tissues. This means that the system uses multiple focus planes to provide a uniform high resolution imaging depth. The VivoSight scanner provides high resolution, at better than 7.5μm lateral and 10μm vertical resolution. This system was designed for skin scanning for the dermatology clinic, with a big probe manufactured for this purpose.

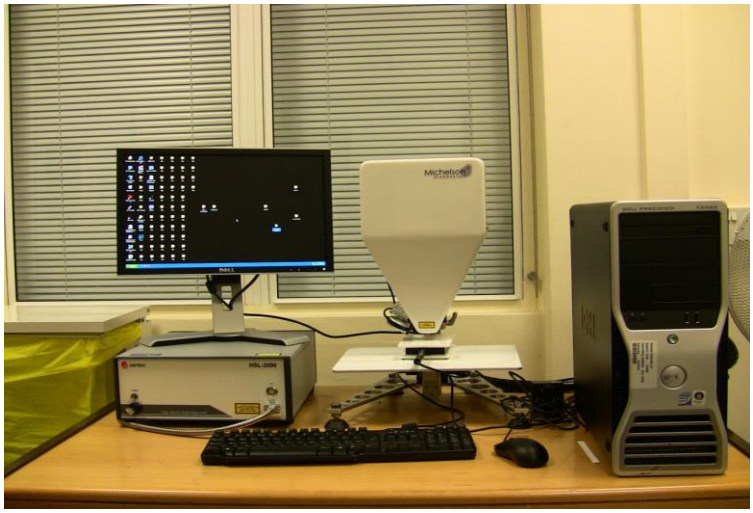

Figure 2.2: Set up of lab-based OCT

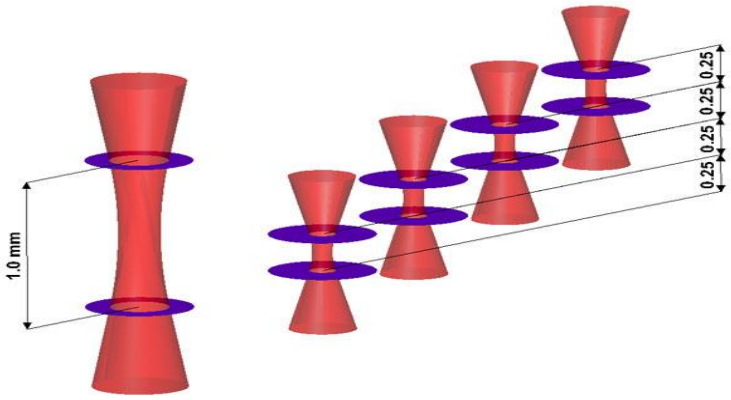

Figure 2.3: The four-beam configuration of the multibeam OCT microscope is focused over 1 mm with each sub-beam focused over 0.25 mm, producing double the resolution possible from a single beam. Each sub-beam has a theoretical FWHM diameter of just 10.3 μm.

Figure 2.4: Imalux system

Figure 2.5: *In-vivo* endoscopic OCT probe (Imalux system)

Figure 2.6: *In-vivo* OCT (Michelson VivoSight) used for instant *ex-vivo* study

2.3 Methodology

2.3.1 *In-vivo* animal study

2.3.1.1 Sensitizing the animals by carcinogen

The 4-nitroquinoline l-oxide (4NQ0) solution (Sigma Chemical, St Louis, MO) was prepared from a refrigerated stock solution (1 gm/SL), which was appropriately diluted with tap water to obtain a concentration of 0.001% for the experiment. Water containing 4NQ0 was administered orally as drinking water ad libitum from a brown, light-shielded, polyvinyl bottle to the 12 rats for 32 weeks. Consumption of 4NQ0 solution was checked once a week and the bottles were refilled with fresh 4NQ0 solution.

Carcinogenic agent was given for the first group (32 weeks group) then the second group was included after 8 weeks (for the 24 week group). The final group was included after 17 weeks (15 weeks group). The control group was kept without any carcinogenic agent at the end of the experiment.

2.3.1.2 Intraoperative imaging

After anaesthetizing of the rat using inhalation anaesthesia (Figure 2.7), the probe was inserted directly using a mouth opener to allow accurate placement of the probe tip on the area of interest. The probe tip was placed in gentle or near-contact with the region of interest (Figure 2.5). OCT images were acquired from the normal tissue, the site of the pathology, and in transition zones in the case of potential cancers. Generally, four areas of interest were focused on in the scans: buccal mucosa, floor of mouth, ventral side of tongue and hard palate. In most of the animals, still images of the lesion were acquired using conventional digital imaging, which also aided in providing a record of the probe position. Images from the rat sub-sites were obtained. Images were then arranged by anatomic site and then sub-divided into the following three categories: (a) normal tissue, (b) benign lesions, (d) premalignant and (c) malignant lesions after histopathological assessment.

2.3.1.3 Images analysis

Three experienced surgeons compared all the images for different stages (normal, keratosis, dysplasia and invasive carcinoma). Clinical images using high resolution camera (Canon EOS 450D) were used to help the examiners to envisage the clinical situation and correlate them with OCT images. The OCT images were also compared with histopathology slides to understand the morphological features.

2.3.2 Immediate *ex-vivo* oral tissue

2.3.2.1 Suspicious oral lesions

The participants in this study underwent surgical excision of the suspicious oral lesions. The specimens were kept in saline before being transferred to be scanned. The OCT instrument captured b-mode scans of the tissue. Our co-registration method was enhanced by using dyes and sutures for better orientation (Figure 2.8). Digital pictures and diagrams were produced to ensure that the histopathologist would be able to identify the scanned planes accurately and provide an exact histopathological image.

A histopathological diagnosis was then achieved after several steps, including embedding in paraffin wax, staining with haematoxylin and eosin (H&E), and examination by light microscopy. Close attention was paid to tissue shrinkage in formalin when comparing microanatomical structures of immediate *ex-vivo* OCT images and paraffin wax slides.

Seven variables were studied on the OCT images to assess for normal oral mucosa microanatomical structures and architectural changes in these areas. This included visibility of the keratin layer, epithelial layer, identification of the basement membrane, identification of blood vessels in the lamina propria, identification of minor salivary gland ducts, and identification of taste papilla (where applicable). Controlled OCT measurements were taken from the edges of the macroscopically normal oral mucosa of the surgical biopsy; these were compared with the OCT images of the suspect area taken from the centre of the lesion. These variables were compared between OCT and pathology by a senior clinician and a senior pathologist who were trained to read OCT images and were not blind to the diagnosis.

2.3.2.2 Histometric validation and sensitivity for oral tissue

2.3.2.2.1 Image acquisition

After removal from formaldehyde, the specimens were dried for 5 minutes on tissue paper. The specimens were then supported by the suspending sutures on a fixed slab for imaging 30 minutes post resection (Figure 2.9). Another two measurements were done 1 hour and 24 hours post resection. The epithelium thickness estimated by OCT was compared with the histology, and the correlation was statistically evaluated with Pearson's correlation coefficient.

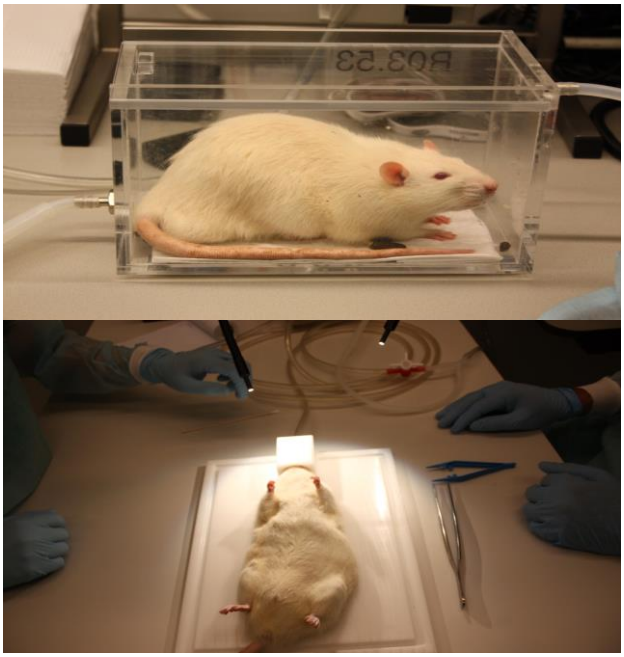

Figure 2.7: Inhalation anesthesia assembly.

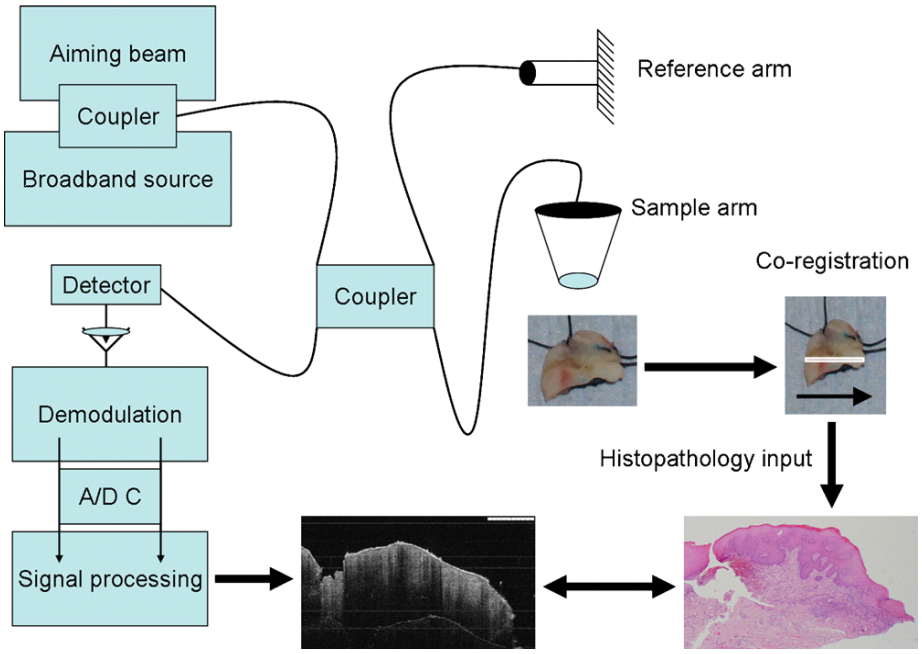

Figure 2.8: Diagram showing the OCT machine and sample tissue, together with our co-registration technique and histopathological and OCT images.

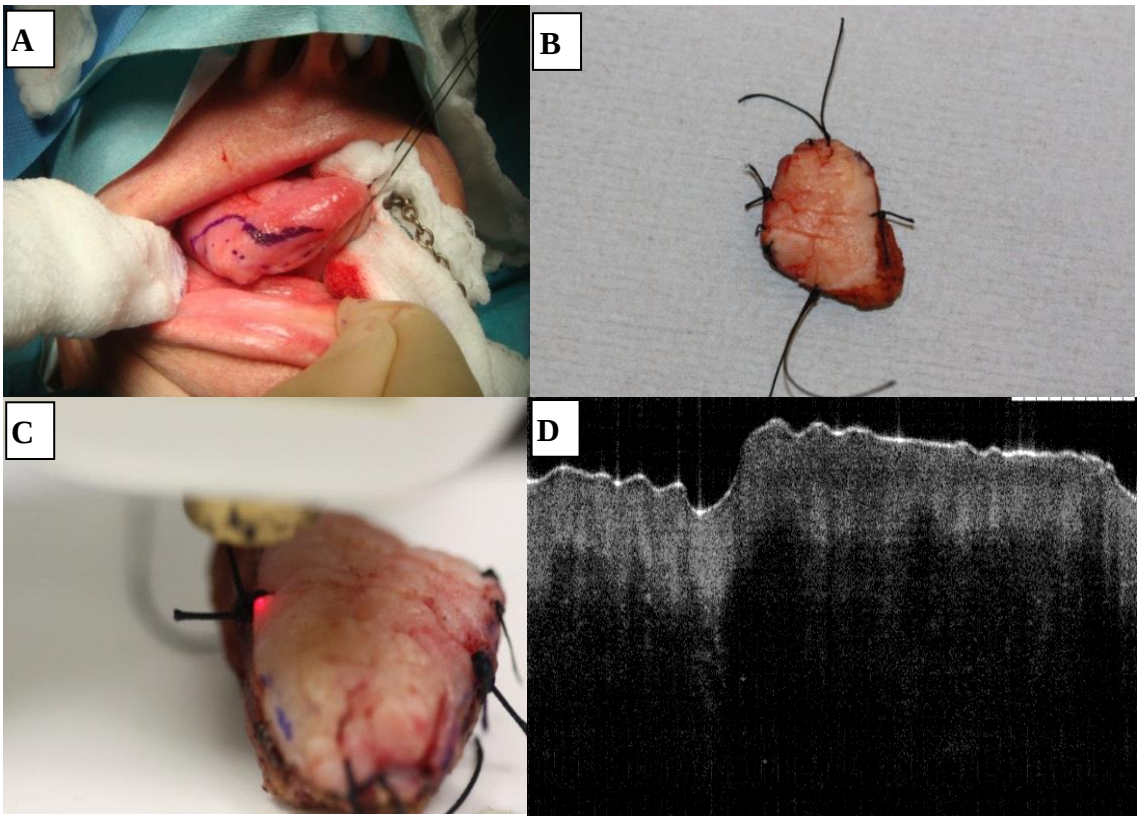

Figure 2.9: Resection margins assessment **A:** Marking tumour prior to resection. **B:** Tumour resected and specimen oriented with sutures and special dyes. **C:** Resected specimen subjected to OCT. **D:** OCT scanning and image acquisition.

2.3.2.2.2 Image analysis

The first two OCT measurements were conducted with 30 minutes gap to avoid shrinkage of specimens, which may ruin the reproducibility of the OCT. The oral epithelium measurement was done in the OCT image at three predetermined points that extended from the surface of the mucosa to the basement membrane, and the average thickness was calculated for the reading of the best correlation for use in further analysis. Then this correlation was used to validate the OCT. The difference between the OCT thickness and histologic thickness was assessed and compared with second OCT reading (1 hour) and the final reading (24 hours).

2.3.2.2.3 Slide preparation and analysis

All the primary lesions were routinely processed by fixation, dehydration, and embedding. Sections 4-µmthick were cut from each tissue block and stained with haematoxylin and eosin. Using a Nikon 80i microscope with a 5 megapixel digital camera connected to a PC, images were captured and stored. Histological specimens were considered suitable for analysis if

1) The tissue slice was complete horizontally, and 2) The oral epithelium surface was intact. Tissue sections were excluded if histological processing had produced a severe artifact.

Epithelium thickness was measured by the standard method using an ocular micrometer. The vertical distance from the uppermost level of the squamous cell layer to the lowest point of the basement membrane was recorded in micrometer units. The examiner who measured the epithelium thickness did not know the thickness of the lesion estimated by OCT (Figure 2.10).

2.3.2.2.4 Validity and reproducibility of OCT measurements

Validity was determined by comparing the average of the histology measurements of each subject with the average of the OCT measurements of the best correlation with the histology. The means were compared using a two-tailed paired t-test and the difference between the means was compared to zero. Similarly, reproducibility of the OCT was assessed by the same statistic but comparing the average of measurements of epithelium thickness at 30 minutes to the average measurements of 1 hour. The degree of reproducibility is expressed by the 95% limits of agreement (mean ± [1.96 × standard deviation]). The difference between the validity and reproducibility is that the former used gold standard measurement as reference, while the later use another measurement which is not standard.

2.3.2.3 Sensitivity, specificity and accuracy of the OCT

The process of co-localisation was described in a previous section (Figure 2.8). The co-registration process involved diagrams, digital images and specimen orientation using sutures and special ink. For each surgical specimen, OCT images were acquired from several areas of interest.

Assessment of OCT images was carried out by a surgeon and a pathologist; both were taught about reading OCT images and provided with a training set to consolidate their knowledge and assessment skills prior to the assessment of the 125 OCT images. However, the same observers had conducted the descriptive correlation study, where they gained enough experience to read the OCT for oral lesions.

Each assessor was provided with a brief clinical history of the suspicious lesion and was asked to comment on every corresponding OCT image using a pre-made proforma. Metric

readings were recorded for both the keratin and the epithelial layers by the principal investigator.

Four main parameters were assessed in every image, including keratin layer, epithelial layer, lamina propria and basement membrane. The assessors were instructed to quantify the thickness (no change, increased or decreased) for each tissue (keratin and epithelium) layers as well as commenting on the status of the basement membrane (intact, breach, difficult to assess), basement membrane quality (excellent, good, adequate or poor) and lamina proprial changes (obvious changes, no clear changes or no changes). Furthermore, each assessor was asked to categorize the diagnosis (normal/benign, dysplasia and invasive cancer) and to report on "the need for surgical biopsy" to confirm the diagnosis, in case of highly suspicious lesion, if this technique was to be applied *in-vivo*.

Statistical analysis

Working upon the data given by both assessors, the sensitivity, specificity, and overall accuracy of OCT were calculated. Agreement was assessed by using Kappa scores (poor=0.00-0.40, good=0.41-0.70, very good=0.71-080, and excellent=0.81-1.00). The average thicknesses of the keratin and epithelial layers were calculated and correlated with the corresponding pathology using Pearson's correlation coefficient.

2.3.2.4 Evaluation of the status for tumour resection margins

Surgical resection was performed under general anaesthesia. The resections were preserved in normal saline and within 24 hours (delayed *ex-vivo*) were subjected to optical coherence tomography scanning. All specimens were then processed for assessment of the surgical margins status. Histopathological assessment was carried out by one maxillofacial pathologist to ensure objectivity. Assessment was conducted according to the World Health Organisation guidelines.

Assessment of OCT images was carried out by two surgeons; both were taught about interpreting OCT images and provided with a training set to consolidate their knowledge and assessment skills prior to the assessment of the 112 OCT images. Each assessor was provided with a brief clinical history of the patient and was asked to comment on every corresponding OCT image using a pre-made proforma. Metric readings were recorded for the epithelial layers at the resection margins area. Four resection margins were assessed per patient; the assessors were asked to comment on the architectural changes and the status of the basement membrane (intact or breached).

Statistical analysis

The overall sensitivity and specificity for interrogating the 112 resection margins were calculated using the SPSS package (Statistical Package for the Social Sciences, Chicago, IL). The inter-observer differences using Kappa and positive and negative predictive values were measured using the same software. A mean value for the epithelium thickness of the resection margins was obtained. Then comparison was made between positive and negative margins.

2.3.3 *Ex-vivo* skin tissue

2.3.3.1 Suspicious skin lesions

The whole skin specimen was placed under the OCT imaging beam and imaged in delayed *ex-vivo* as the transverse virtual line between the two landmarks (Figure 2.11). To provide a linear focal trough, a series of images were taken from edge to edge along the whole length of the specimen. All the pathology slides were examined and the most obvious architectural changes were recorded.

Several variables (5 variable) were studied on the OCT images to assess for normal facial skin microanatomical structures and architectural changes in these areas. This included visibility of stratum corneum, epidermis and the papillary dermis, and other microanatomical structures. Controlled OCT measurements were taken from the edges of the macroscopically normal facial skin of the surgical biopsy; this was compared to the OCT images of the suspect area taken from the centre of the lesion.

These variables were compared between OCT and pathology by a senior clinician and a senior pathologist who were trained to read OCT images and were not blind to the diagnosis. Descriptive diagnostic criteria were then extracted from each OCT image for each pathology according to agreement between the two assessors.

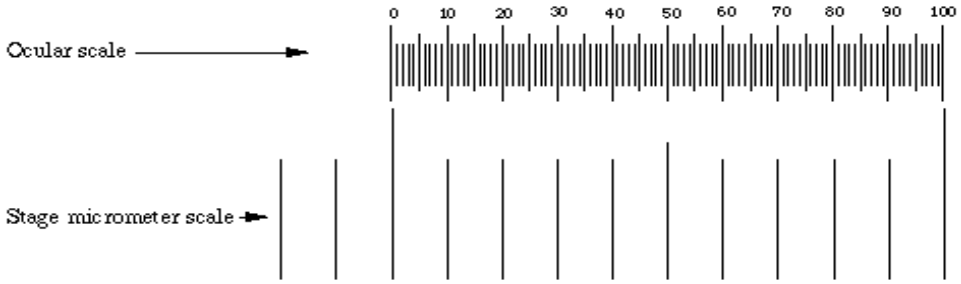

Figure 2.10: Ocular micrometer for epithelium thickness measurement

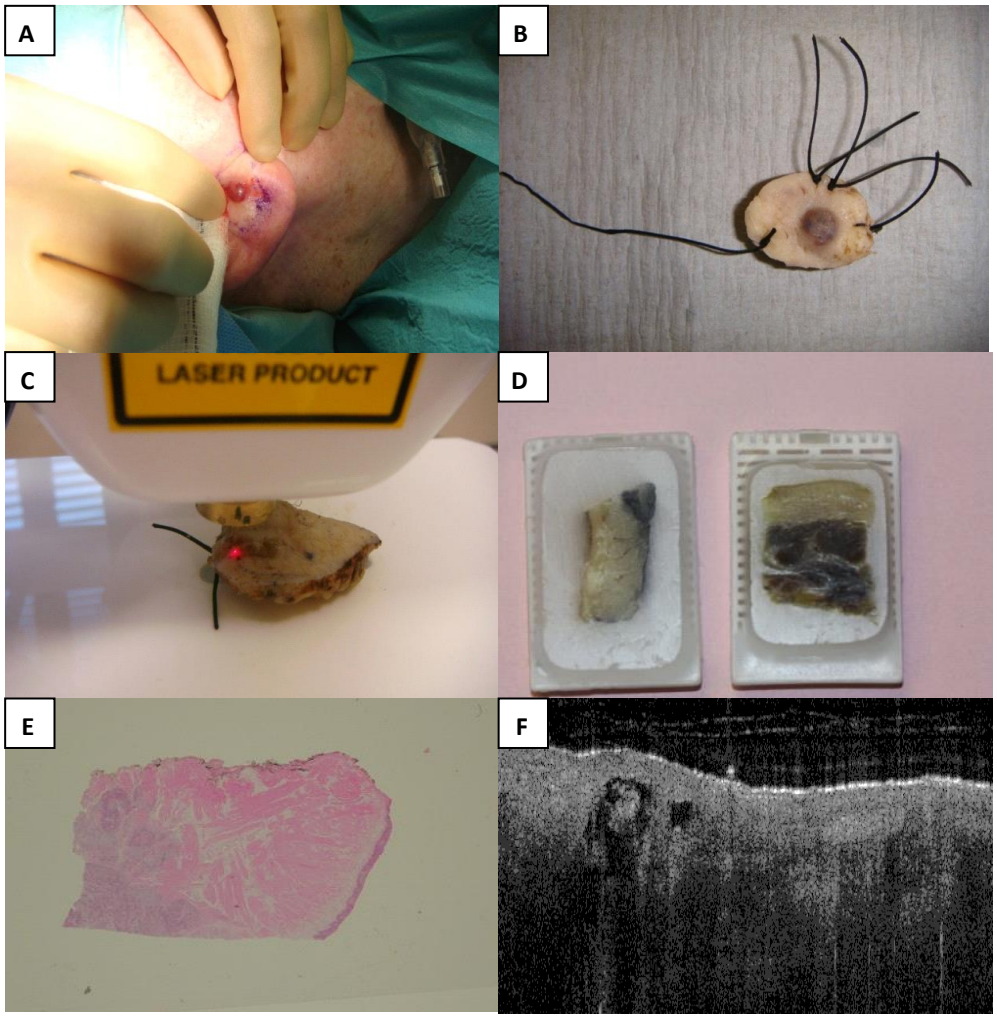

Figure 2.11: Suspicious skin lesion assessment. A: marking tumour prior to resection. B: tumour resection and specimen oriented with sutures. C: Specimen subjected to OCT in *ex-vivo* phase. D: wax embedding. E: H&E slide. F: OCT image acquisition.

2.3.3.2Sensitivity, specificity and accuracy (skin)

The methodology was the same as in **2.3.2.3**.

2.3.3.2.1 Diagnostic parameters

There was consensus in advance that the OCT reading would be performed according to the criteria originally described in our previous study that investigated the major histologic features for diagnosing skin cancer (2.3.3.1). According to this study, a set of OCT imaging criteria was formulated by analyzing biopsy-correlated OCT images. These criteria were:

Single or multiple nodules in the form of a solid or honeycombed compartment (nest) is a typical feature for nodular BCC. Empty space below dermo-epidermal junction (DEJ) is a diagnostic feature for cystic BCC. According to the size of the space, the cystic BCC is sub-classified. We consider 150μm to be the maximum diameter for microcystic BCC.

In malignant melanoma, loss of the typical bright horizontal linear structures with architectural disarray and diffuse or patchy reflectivity, non-edged papillae with cerebriform clusters infiltrating dermal papillae and intact DEJ.

For the SCC, DEJ that have lost their integrity with or without the presence of small bright clusters in the papillary dermis and damage to the superficial epidermal layers (honeycombed, broadened, cobblestone).

Lentigo maligna, characterized by a predominantly uniformly elongated rete ridge. Uniform nests within the epidermis. Hyper parakeratosis/hyperkeratosis and/or stratum corneum disruption are diagnosable features for AK.

2.3.3.2.2 OCT key features for inter and intra observer agreement

Stratum corneum status in terms of hyperkeratosis and any sign of damage (internal clefts) was evaluated. For the epidermal layer, the presence of uniform nests within the epidermis was tested, as was the integrity and thickening of DEJ with or without protruding clusters and the presence of solid nest or honeycomb beyond DEJ. DEJ ridges status (elongated or atrophied rete ridges) was also rated.

2.3.3.2.3 OCT image processing and analysis

All OCT scans were performed by the principal investigator, while the OCT image readings were interpreted independently by two examiners in a blinded way (radiologist and dermatologist). To calibrate the examiners and to avoid inter-observer variation, 6 OCT and correlated pathology images of the main pathological varieties were illustrated with a

description of all normal and pathological changes. These images were used to train the readers in how to read the OCT, as well as how to fill in a special proforma designed for this study.

The principal investigator selected the images showing the best quality (i.e., no artifacts). For example, images displaying some artifact in the form of noise as a result of mismatches in brightness and gain between the different channels of the OCT scanner were excluded.

Each reader was asked to fill in a form consisting of questions and accompanying choices for each image. The form included questions regarding all the descriptive terms for the key features used in the study, stratified by the anatomic skin level. As a result of considerable overlap between the diagnostic parameters for different pathological groups, these parameters were used in the form to give the readers clues about what they might expect to see. However, these criteria were used to rate operators' agreement. Readers were required to first submit their evaluation of each image group, after which they were able to identify the diagnosis. For intraobserver assessment, after the completion of the images evaluations, the same slides were reassigned with random numbers and sent by the principal investigator to be re-examined.

2.3.3.3 Assessment of head and neck tumour resection margins

The methodology was the same as in **2.3.2.4**

2.3.4 Instant *ex-vivo* oral epithelium

2.3.4.1 Normal predictive value for oral epithelium thickness

The hand-held OCT probe is fibre-based and easy to handle. The probe is applied directly to oral mucosa within seconds after excision (instant *ex-vivo*). Each measurement site was scanned twice for further determination of epithelium thickness (ET), and the OCT image showing the best quality (i.e., without artifacts) was selected. For example, we excluded images displaying the appearance of vertical bands that were due to mismatches in brightness and gain between the different LED channels.

Measurements were performed at three different sites perpendicular to the basement membrane and always capturing the maximum depth of the epithelium. An integrated software program for determination of distances in OCT images (B scans) was developed by the manufacturing company on the computer screen using the integrated measuring tool (ruler). The epithelium was delineated manually on the computer screen, and the mean ET

was calculated from 3 predefined ET measurements: the central epithelium (EP) of the OCT image and 2 lateral EP measurements on each side at a fixed distance from the centre.

We measured the OCT image from the surface reflection (entrance signal) to the first well demarcated change of reflectance intensity, as expressed in a more signal-poor zone (basement membrane).The average of the three measurements was calculated corresponding to the mean ET. All OCT measurements were performed by the same investigator. Light microscopic correlation was not sought.

2.3.4.2 Optical coherence tomography of the tongue papilla for patient suffering from taste disorders after head and neck chemoradiotherapy (Instant *ex-vivo* study)

Study design, observer training and images analysis

The results obtained from the 20 subjects for whom tongue biopsy included normal papilla were used to understand normal morphology of the papilla as well as to help our readers learn how to read the normal papilla and compare them with the chemo-radiotherapy group. During the training sessions, examination of the images was performed descriptively and in cooperation with the principal investigator. No processing techniques were necessary to enhance the images.

Training was conducted three times with different time intervals until 95% agreement was reached. The two readers and the principal investigator compared and discussed all the stages of atrophy affecting both filiform and fungiform papilla in an open session using 5-point scaling criteria.

The study co-coordinator (principal investigator) randomly prepared 200 OCT scans showing an equal number of filiform and fungiform papilla of different groups (normal, chemotherapy, radiotherapy). The reviewers were advised to rate the stage of each OCT scan using a special proforma supplied to them. Scores were given by each observer and the agreement was tested using Kappa value. Also readers were instructed to report on the type of the papilla (filliform or fungiform).

2.3.4.3 Risk assessment of oral epithelium thickness (Instant *ex-vivo* study)

Two different investigation methods were applied: a standard examination by white light and an examination by a 400nm wavelength light source and the OCT examination. The clinical white light examination was conducted by one clinician who specialized in oral oncology. The study conducted on oral tissue biopsy which scanned with OCT within seconds after the surgical excision. A standoff device that places the anatomic structures under examination within the focal zone of the transducer is used to obtain the original tissue shape.

According to the specifications of the manufacturer, the area of optimum focusing is approximately 5 mm from the transducer. Close contact of the transducer with the mucosal surface results in blurring and near-field artifacts. Both effects presumably have a negative influence on measurement accuracy. The standoff was constructed specifically for the purpose. The handling of the probe was easy even though the scope was quite rigid and thick. Additionally, the placement of the probe had to be done carefully as a minimal movement could result in moving artifacts. The surface of oral mucosa and the boundary between EP and LP layers were identified for evaluating the EP layer thickness.

Study design

The study was designed to compare epithelium thickness and its changes between different risk groups and compare them with the normal epithelium at the margins after surgical excision. For the PML, only lesions with moderate and severe dysplasia, carcinoma in situ or invasive carcinoma were included. As the study aim was not correlative to histopathology, no comparison was done with OCT images. All of these investigations were performed by the same investigator.

Sites

Biopsies from the vermilion border of the lower lip, buccal mucosa, the ventral side of the tongue and the floor of the mouth were included in this study. Confined lesions such as leukoplakia located out of these territories were excluded due to the limited sample size collected. OCT scans from apparently normal margins were obtained for the purpose of comparison.

2.3.5 Instant *ex-vivo* skin

2.3.5.1 Evaluation of epidermal layer thickness in facial skin

2.3.5.1.1 Sites investigated

Ten sites were included in this study. The sites were selected according to the availability of the biopsy. Measurement areas were defined, namely the frontal skin, tip of nose, nasal dorsum, lateral side of nose, lower eyelid, check, upper lip, lower lip, chin and malar eminence. This study did not intend to correlate the OCT images with accompanying site histology.

2.3.5.1.2 Statistical methods

All the measurements were tabulated using an Excel (Microsoft Corp., Redmond, WA) spreadsheet. Statistical analyses were performed by calculating average values for skin thickness. Mean and standard was calculated for each quantitatively assessed morphologic parameter.

2.3.5.2 Qualitative OCT for pathologic skin lesions

The readings were taken from the central part of the lesion and also at two sites over clinically uninvolved skin at the edge of the lesion at right angles to each other. After assessment by non-invasive techniques, the lesion was taken for histological examination to confirm the clinical diagnosis. No correlation was performed between the pathology and the OCT.

2.4 Ethics

2.4.1 Ethics for all the sub studies in the optical Coherence Tomography (OCT) study involving *ex-vivo* tissue.

Moorfields and Whittington Local Research Ethics committee 07/Q0504/4. A copy of the ethics is supplied in the appendix. All the patients included in this thesis had suspicious oral and/or skin lesions needing biopsy to confirm diagnosis prior to intervention. Different analysis using sub-classifications of this cohort within the thesis using specific grouping parameter.

The total number of the patients included was 245. Many of them presented with more than one lesion at the same time due to field cancerization and no tissue was analysed in excess of clinical need. All the patients consented by the student (Zaid Hamdoon) as sub investigator then by the principal investigator (Mr Colin Hopper) and kept in the research room (at UCLH property) according to the study protocol which is approved by the ethics committee. The whole project was supervised directly by Mr Colin Hopper including consenting patients to scan their biopsies using this minimally-invasive procedure.

All work was *ex-vivo* using the normal resection margins of the specimens to measure the normal epithelium and epidermal layer. It is clinical custom and practice that surgeons take normal tissue from around the biopsy site to ensure complete lesion removal and for comparative analysis by the pathologist.

2.4.2 Ethics for animal studies

license was obtained by Dr Max Witjes, consultant Maxillofacial Surgeon in Groningen university, while ethics obtained by Dr de Visscher (enclosed in the appendix).

Chapter 3

In vivo OCT on animal tumour model

Introduction

OCT-based early cancer detection is limited by the low contrast and resolution obtained in biological tissues, particularly between normal and neoplastic tissues. Various approaches, including Doppler OCT and polarization-sensitive OCT, have been explored to overcome this fundamental limitation of OCT (Yazdanfar *et al.*, 1997; de Boer and Milner, 2002).

With over 15 years of clinical research in OCT imaging in the head and neck in human subjects, these researches to date have used OCT systems designed and constructed in the laboratory. Non-commercially available OCT systems, which have a higher resolution and scanning rate, have previously been described.

Some clinical research has been conducted using the first commercially available OCT device (Niris system). However, this system was designed to image the larynx among other applications which has not been tested like oral and skin tissue (Rubinstein *et al.*, 2010; Wong *et al.*, 2005).

The ultimate goal of this research is to robustly test the noninvasive clinical diagnostic capability of the first commercially approved OCT for the rat oral cavity. This was achieved using an animal cancer model induced by a carcinogenic substance containing all phases of cancer progression (normal epithelium, hyper-/parakeratosis, epithelial dysplasia and invasive carcinoma).

Statement of the problem

Previous work by other researchers using Nitris OCT has shown that the imaging penetration depth of the OCT is sufficient to evaluate the macroscopic characteristics of epithelial and subepithelial structures. However, its use in the head and neck remains pending due to the lack of solid diagnostic criteria.

Objectives

The goal of this study was to evaluate the feasibility of a commercially approved OCT system for the diagnosis of multiple stages of oral cancer progression.

Another aim of this study was to determine whether the basement membrane and its invasion can be distinguished clearly on Niris OCT images. A third aim was to determine whether it is possible to derive important microanatomical information (e.g. extent of cellular crowding, thickness of the epithelial layer, occurrence of structural proteins, thickness of the keratin layer, parameters of the microvasculature) from the OCT images.

Animals

Sixteen male Wistar rates aged 6 weeks old at the start of the experiment and with a mean weight of 125 g were used. All animal studies were approved by the Groningen Health and Science University Institutional Animal Care and Use Committee. Chemical inducement of oral epithelium in rat is a highly controlled model of cancer formation characterized by a three-step process: tumour initiation, promotion and progression.

The rats were randomly divided into four groups, each consisting of four rats. Three groups of rats were treated with 4-nitroquinoline l-oxide (4NQO) to induce premalignant epithelial lesions and squamous cell carcinomas and were examined by OCT and then biopsied at 15, 24 and 32 weeks after 4NQO application (Figure 3.1). One group of rats was not treated with 4NQO and served as the control group.

Results

Observations

All 12 rats given 4NQ0 solution remained alive during the experimental period. The average body weight of rats in the experimental groups increased at almost the same rate as that of rats in the control group. The average amount of carcinogen consumed during the entire experiment was about 0.6 mg per rat.

The 12 rats were examined at 32 weeks. Clinical changes were observed over the tongue, palate, gingiva, buccal mucosa, and floor of the mouth at different times after exposure.

Carcinoma was observed for the first time at 24 weeks. Changes induced during the experimental period included carcinoma in situ and invasive carcinoma. Early epithelial dysplasia began at 15 weeks and progressed from one stage to another with or without progressing to cancer at 32 weeks, as determined by biopsy (Figures 3.2

and 3.3). Initially, dysplastic changes in the epithelium were most pronounced in the gingival area of the palate and floor of the mouth. After longer periods of application of the carcinogen, these changes spread over the entire oral cavity (Figure 3.4).

Most carcinomas developed on the junction between the hard and soft palate, buccal mucosa and floor of the mouth (Figures 3.5–3.7). A papilloma was observed on the floor of the mouth, especially around the torus linguae (Figure 3.8). Frank leukoplakia with different stages of dysplasia foci was detected at the lateral border and on the ventral surface of all tongues (Figure 3.9). No carcinomas were observed at the dorsum or tip of the tongue. Metastases were not found. Carcinoma was also observed in the palate and/or gingiva in many rats. In the group of rats that were treated with 4NQO for 24 weeks, both severe dysplasia and squamous cell carcinoma were observed.

OCT findings

Normal oral epithelium

The Niris system was not able to distinguish between different histological layers in the normal healthy mucosa. Likewise, it was difficult to make a clear distinction between the epithelium and lamina propria. Identification of the basement membrane, as a key diagnostic structure, was difficult. Information regarding the boundary of the oral epithelium, its thickness and structures was unclear (Figure 3.10, 3.11).

There was no difference in the signal reflection intensity of the top keratic cell layer, although it was supposed to be brighter than the rest of the epithelium. Furthermore, there were no graded intensity differences between different histological sub layers of the same epithelium. Subepithelial areas in normal tissues contained a variety of dark areas, which could probably be attributed to poor light penetration with no evidence of any microscopic structures, including papillae, glands, ducts, or blood vessels, which had unclear optical characteristics (Figure 3.12).

Figure 3.1: Three rats in each cage where the carcinogenic agent given.

Figure 3.2: Epithelial dysplasia at the hard palate clinically manifested as homogenous leukoplakia at week 15.

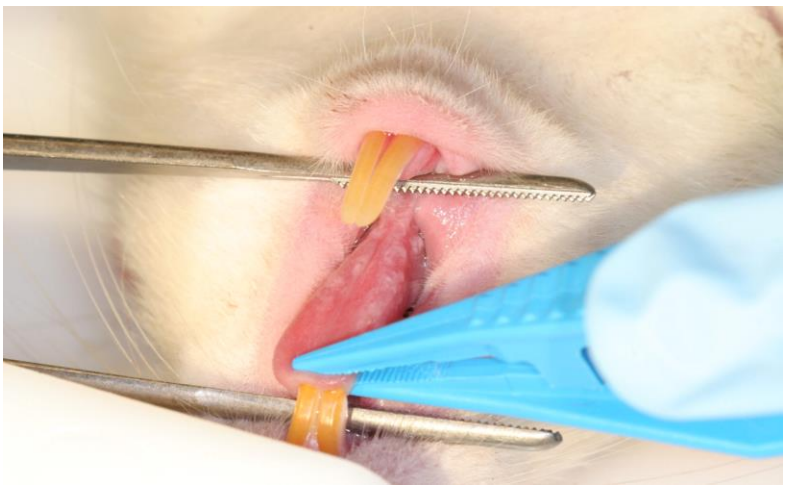

Figure 3.3: Leukoplakia with epithelial dysplasia at the ventral side of the tongue at week 15.

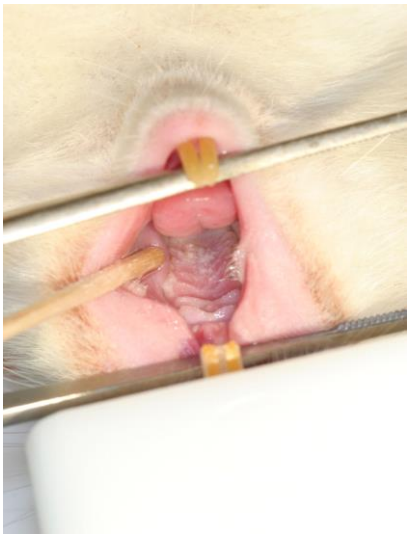

Figure 3.4: Epithelial dysplasia at the junction between the hard and soft palate.

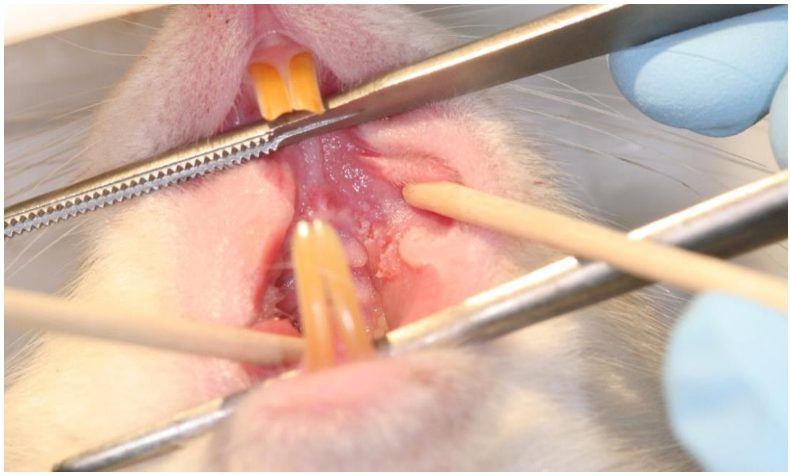

Figure 3.5: Well developed carcinoma at the buccal mucosa (exophytic masses) at week 32.

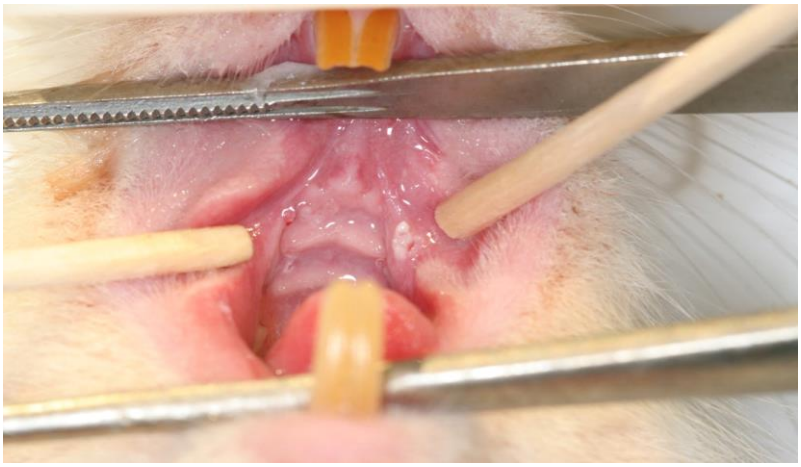

Figure 3.6: Early Invasive carcinoma at the buccal mucosa (ulcer) at week 32.

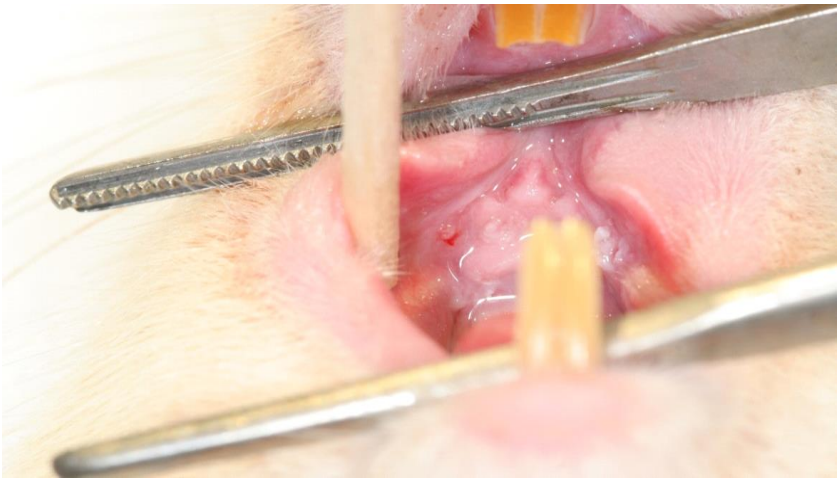

Figure 3.7: Invasive carcinoma floor of mouth at week 32.

Figure 3.8: Squamous cell papilloma (cornflower appearance).

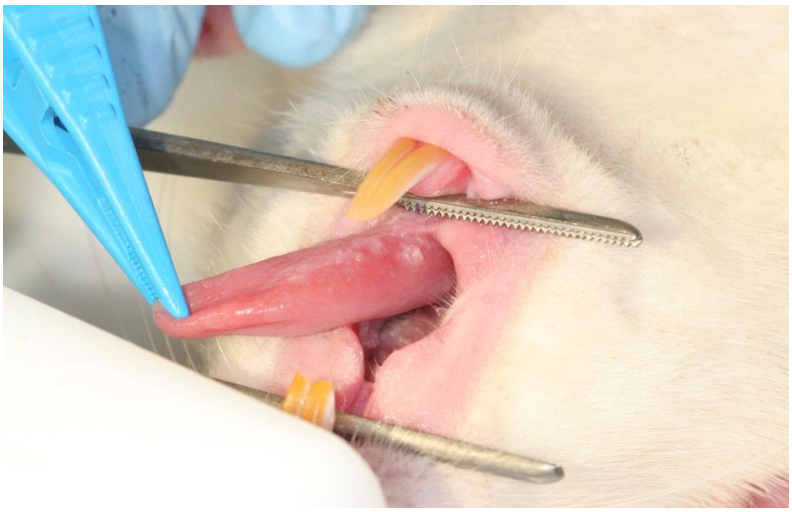

Figure 3.9: Sublingual keratosis as homogenous leukoplakia.

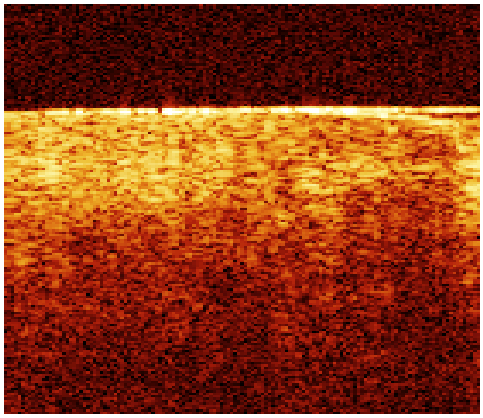

Figure 3.10: OCT scan from the normal epithelium of the buccal mucosa. No clear structure can be distinguished.

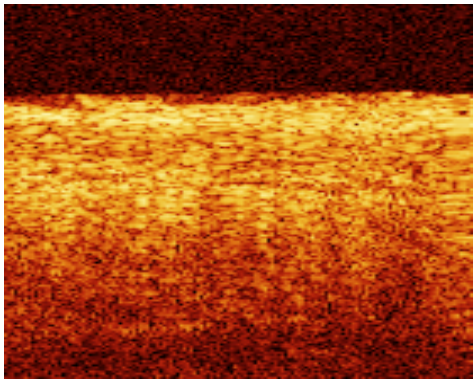

Figure 3.11: OCT scan from normal epithelium of the floor of mouth. Homogenous signal reflection from the different histological structures.

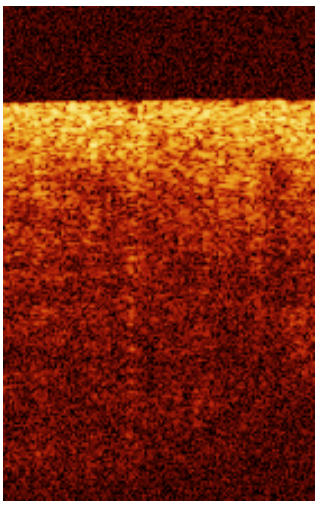

Figure 3.12: OCT scan from normal epithelium of tongue showing no clear structure for the keratin cell layer or the papilla. Oppositely, the keratin cell layer appears as hyporeflective area on the scan. No evidence to see the basement membrane, epithelium rete pegs, and blood vessels.

Oral dysplasia group

No correlation was observed between histopathology and OCT. We were unable to identify similar morphological structures on both the OCT scans and histopathology slides. Microanatomical information (e.g. extent of cellular crowding, thickness of the epithelial layer, thickness of the keratin layer, parameters of elongated rete pegs from the OCT images) was difficult to determine. The non-homogenous image was murky, especially when the lesions had a thicker keratin cell layer, which may indicate poor light penetration and scattering (Figure 3.13, 3.14).

Invasive carcinoma

Malignant tumours in the third group of rats had more non-homogenous structures compared to normal group in which it was hard to distinguish any detail. The attempt to measure epithelial thickness was in vain due to the difficulty finding the basement membrane. Attempts to detect epithelial invasion within the lamina propria were also unsuccessful, even after trying to move the probe along the normal boundary of the lesion to extract information.

OCT images from neoplastic lesions displayed irregular, ragged, dark lines between two light areas that had the appearance of a fracture in the subepithelium (Figures 3.15–3.17). No distinction was possible between invasive carcinoma and squamous cell papilloma except for the top epithelial layer, which sometimes appeared damaged in invasive carcinomas and wavy in papillomas (Figure 3.18).

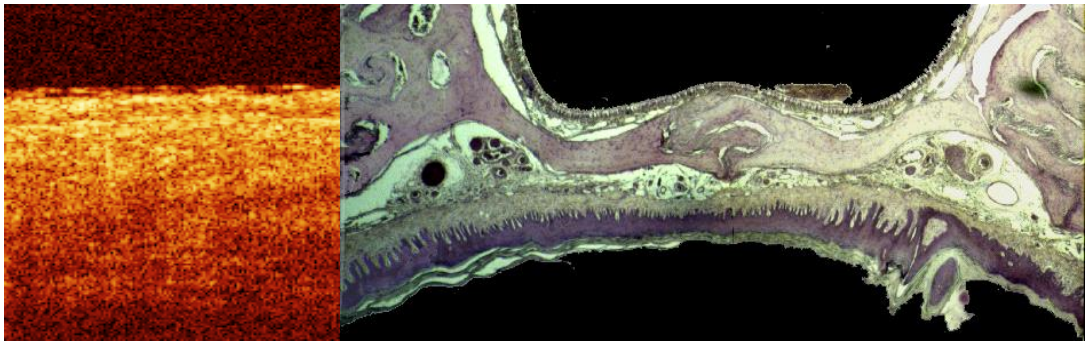

Figure 3.13: OCT scan with the corresponding histopathology with moderate epithelial dysplasia on the floor of the mouth. No clear features can be extracted from the OCT scan.

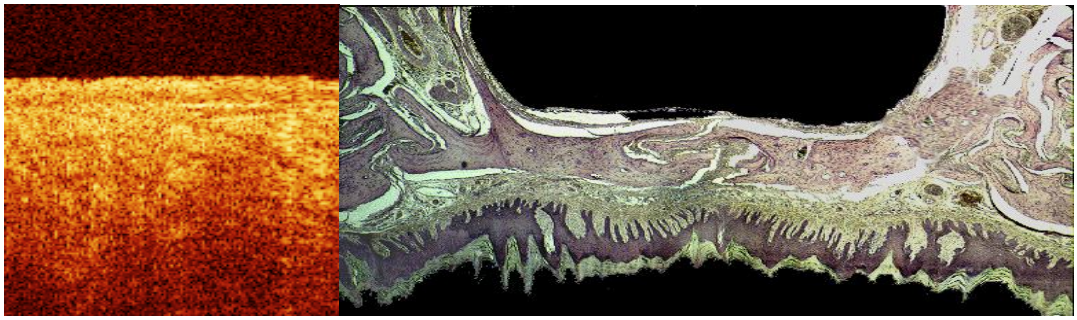

Figure 3.14: OCT scan with the corresponding histopathology with severe dysplasia in the hard palate.

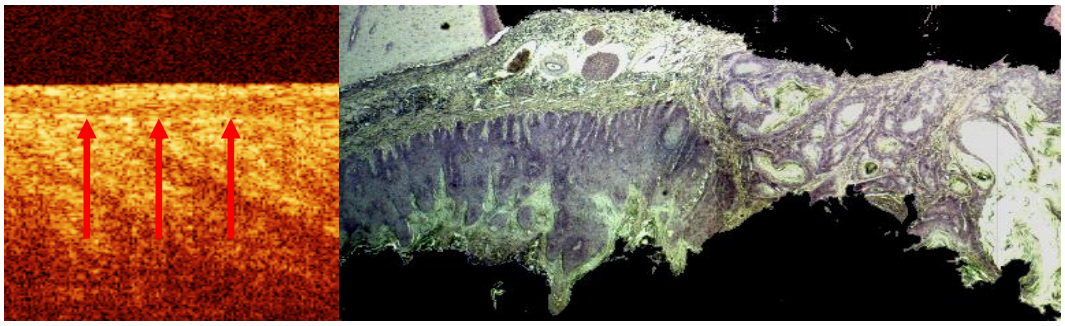

Figure 3.15: OCT scan with the corresponding histopathology with early invasive carcinoma in the buccal mucosa. The misleading distinction between different areas of signal refection (red arrows) gives the impression to the reader of an intact basement membrane.

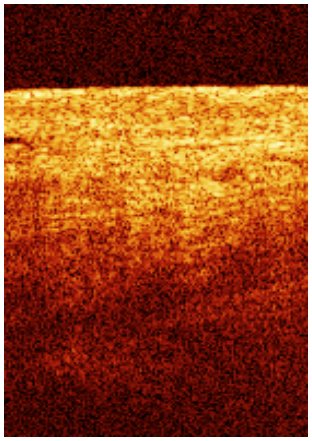

Figure 3.16: OCT scan of invasive carcinoma in the hard palate.

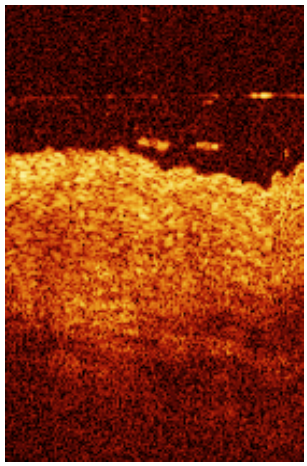

Figure 3.17: OCT scan of advanced invasive carcinoma on the ventral side of the tongue showing a small depression on the top surface which represents the ulcer.

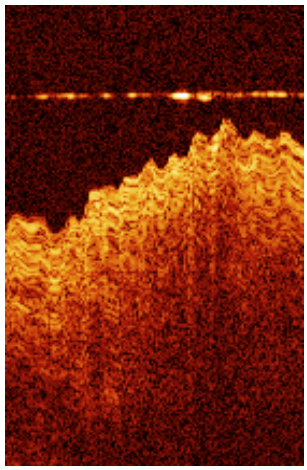

Figure 3.18: OCT scan of squamous cell papilloma with wavy top representing the keratin cell layer. No clear demarcation can be seen between the different layers.

Discussion

All investigations to date have used OCT systems designed and constructed in the laboratory. However, some clinical research has been conducted using the first commercially available OCT device (Niris system) (Rubinstein *et al*., 2010).

However, this system was designed to image the larynx as well as having other applications for oral and skin diagnosis. Other non-commercially available OCT systems have previously been described, but none of these systems have been used in the head and neck (Jeon *et al.,* 2008; Potsaid *et al.,* 2008).

Currently, other commercially available OCT devices are available for use in other medical fields, such as ophthalmology (Savini *et al.,* 2006), gastroenterology (Testoni *et al.,* 2007) and cardiology (Kume *et al.,* 2006). However, these systems do not work in otolaryngology due to the complexity of the endoscopic probe, which play negatively in the resolution.

Researchers at the University of California Irvine at the Beckman Laser Institute and Medical Clinic compared this system with those previously used in their research (Rubinstein *et al.,* 2010; Wong *et al.,* 2005; Armstrong *et al.,* 2006; Sepehr *et al.,* 2008). They found that Niris has limited lateral resolution, a slower frame rate, and a limited depth of imaging. The scanning mechanism for Niris is at the tip, and the optical elements move right to left across the target region in the tissue.

Previous devices constructed by the same group and others obtained cross-sectional images with the probe tip moving in and out of the probe long axis. Left to right imaging allows easier targeting of regions of interest.

Another finding of these studies was that OCT has limited capabilities in imaging large and bulky laryngeal lesions because the basement membrane (BM) cannot be consistently identified, making it difficult to evaluate BM infiltration and to distinguish between benign and malignant lesions. Thus, OCT has its greatest potential value in examining superficial and subtle lesions and disease processes in thin tissue such as the laryngeal mucosa. This device has limited utility for imaging bulky lesions or normal tissue that has a thicker epithelium, such as the oral mucosa.

In this investigation imaging of normal, benign, and pathologic oral conditions in rats using the first commercial OCT device designed for use in head and neck endoscopic applications was conducted. In this study, OCT primarily aimed to aid in the identification of the normal tissue, and compared this with pathological tissue with the aim of assessing its feasibility in differentiating normal from benign and malignant tissue.

Several animal models for oral carcinoma development are available, including hamster, rat and mouse models. Experimental oral carcinoma can be induced by local injection or application of various carcinogens on the oral tissue of rodents (Levy, 1958; Fujino, 1965; Dachi, 1967; Kameyama, 1969). The most commonly used model is the 7,12-dimethylbenz(a)anthracene (DMBA)-induced hamster cheek pouch carcinogenesis model (Gimenez-Conti and Slaga, 1992).

In 1981 Qhne and colleagues reported that oral administration of 0.001% 4-nitroquinoline l-oxide (4NQQ) in the drinking water of rats resulted in a 100% incidence of squamous cell carcinoma in the oral mucosa (tongue, palate and gingiva), while tumour induction in other organs was rare.

This method can induce tumours in the oral cavity in rats (Tanaka *et al*., 1991) and mice (Tang *et al*., 2004). Oral SCCs induced by 4-NQO in rats, which show morphological and histopathological similarities to those of human tumours, have been extensively used to investigate and test a wide range of possibilities for the early diagnosis or therapy of oral cancer.

In this study, the researchers found that the current system has a limited depth of penetration that prevents even superficial tissue architecture from being imaged. Imaging moderately thick epithelium could therefore be challenging. Images from normal areas displayed no defined layers of epithelium, basement membrane or lamina. Small blood vessels were not apparent, even to an experienced operator.

The only structure that was apparent on the OCT was the keratin cell layer. However, this structure demonstrated a slightly different signal at the top of images obtained from areas with clinically severe leukoplakia, sometimes appearing as a wavy or

corrugated pattern. This finding has no significant clinical importance as no distinction could be made between cancerous and non-cancerous lesions.

This study assume that the negative results obtained were due to the weak resolution of the machine being used. To reliably characterize pathologic processes in the mucosa an imaging modality must have a functional resolution approaching 10 μm. This is a fundamental requirement in the OCT in order to obtain clear and informative information from thick tissue such as the skin or oral mucosa.

A second important factor in OCT imaging is the stability of the tissue during examination, which should remain motionless to prevent any motion artefact. The use of general anaesthesia in our experiments to enable endoscopy to visualize the region of interest without any motion excluded this possibility as an explanation for the negative results. Because of the combined requirement for the patients to remain motionless and the need for general anaesthesia in most head and neck endoscopies, this study focused on animal tissues.

Conclusion

Unfortunately, considerable challenges exist in distinguishing different histological layers. Discrimination between premalignant lesions and early tumour development using this current noninvasive modality was impossible. Characterization of both normal and pathological lesions was limited by its inability to penetrate the tissues. OCT imaging provides information about the surface of the lesion, but only limited information about the BM and subsurface structures.

Chapter 4
Ex-vivo histopathologic versus OCT for oral mucosa

Introduction

Oral cancer is the sixth most common cancer worldwide. It represents about 2% of cancer cases in the UK. Unfortunately, despite advances in surgery, radiotherapy and chemotherapy, the 5-year survival rate continues to be only slightly above 50%. The single greatest determinant of long-term patient survival remains early detection and intervention.

Taking tissue samples for microscopic interpretation of cellular and morphological features is the gold standard for the diagnosis of any suspicious lesion (Oliver *et al*., 2004). One of the major problems in histopathology is subjectivity. This subjectivity is most evident when grading dysplasia affecting the upper digestive tract.

Optical diagnostics have developed from the need for clinicians to provide patients with non-intrusive mechanisms to aid treatment. Our aim was to develop real-time non-invasive diagnostic methods for investigating suspect tissue. This will help reduce tissue trauma, the workload in pathology departments and the time the anxious patient has to wait for a diagnosis.

Precise and accurate quantification of disease is a prerequisite for the practice of evidence-based medicine. For OCT to become clinically interpretable and relevant, the structures visualized must correlate with the corresponding tissue microstructures. To date, the interpretation of OCT images has been largely intuitive and empirical.

Knowledge of the normal thickness of the oral epithelium will assist in understanding premalignant/malignant conditions. It has been hypothesized that dysplasia causes thickening of the epithelium due to the increase in rate of turnover of the epithelium (Cör *et al*., 1997). Moreover, the status of surgical margins based on epithelial thickness might help discriminate or map cancer-free resection margins for oral cancer.

Another unresolved clinical issue is the absence of any objectively reliable and accurate assessment modality for resection margin status. In most cases, intraoperative visual inspection and palpation is the standard approach. Unfortunately,

this technique resulted in positive or close surgical margins in almost 40% of patients in one study (McMahon *et al*., 2003).

The UK guidelines judge both mucosal and deep margins of ≥5 mm free of tumour to be clear, 1–5 mm as close and ≤1 mm as involved. These distances usually ignore the effect of formalin shrinkage, which can reach 30%. So in order to achieve a 5 mm pathological clearance, an 8–10 mm *in-situ* surgical margin needs to be taken (Woolgar and Triantafyllou, 2005).

Positive (tumour-involved) or close margins are associated with an increase in local recurrence and have a negative effect on survival. Furthermore, several studies have shown that local recurrence and overall survival benefit from achieving negative resection margins.

Intraoperative frozen sections, although widely used, have their own inherent problems. This technique is costly and time consuming. Additionally, the frozen samples do not represent the entire margin but just a random sample, which may misrepresent the real situation (Shafir *et al.,* 1983; Jüttner *et al.,* 1990). To help overcome these clinical challenges, a highly sensitive, non-invasive, cost-effective and *in-vivo* diagnostic tool is required.

In this *ex-vivo* study we aimed (1) to identify the cellular structures of normal oral mucosa using OCT and to compare these with the gold standard histology, (2) to differentiate between the structural changes of normal and pathological oral mucosa, (3) to develop diagnostic criteria for the use of OCT in the detection of suspicious oral lesions, (4) to verify the validity and reproducibility of OCT, (5) to correlate data from OCT and histopathology, (6) to evaluate the use of OCT in the assessment of suspicious lesions of the oral cavity, and (7) to assess the role of OCT in identifying tumour-involved resection margins in patients undergoing surgical resection for oral squamous cell carcinoma. The thickness of the epithelial layer and architectural changes were the main parameters assessed at each of the resection margins.

Section I: Structural validation of oral mucosa

Background

A new OCT has been released for commercial use. To validate its usefulness, normative data are required.

Objectives

In this *ex-vivo* study we aimed (1) to identify the structures of normal oral mucosa using OCT and compare the system to the "gold standard" of paraffin section histology, (2) to differentiate between the structural changes of normal and pathological oral mucosa, and (3) to develop diagnostic criteria for the use of OCT in the detection of suspicious oral lesions.

Materials

Seventy-eight oral lesions from 73 patients (age range 32–68 years, mean age 50 years; 44 women and 29 men) who presented with suspicious lesions to the UCLH Head & Neck Centre, London, were recruited for this study.

The study protocol was approved by Moorfields & Whittington Local Research Ethics Committee for Human Research. The protocol was devised in collaboration with the Departments of Pathology at University College London..

Informed consent was obtained from each patient after explaining the nature of the study. Exclusion criteria were patients under 18 years of age and patients with a previous history of oropharyngeal carcinoma who had received chemoradiotherapy.

Seven variables were studied on the OCT images to assess normal oral mucosa microanatomical structures and architectural changes in these areas. These included the visibility of the keratin layer, epithelial layer, identification of the basement membrane, identification of blood vessels in the lamina propria, identification of minor salivary gland ducts, and identification of taste bud papillae (where applicable). Control OCT measurements were taken from the edges of the macroscopically normal oral mucosa of the surgical biopsy; these were compared with the OCT images of the suspect area taken from the centre of the lesion.

The data revealed by OCT and pathology were compared by a senior clinician and a senior pathologist who were trained to read OCT images and were not blind to the diagnosis.

Analysis and results

All data were entered and stored in a computerized database designed using Microsoft Excel 2010. The statistical analysis was performed using the statistical software package SPSS 13.0 (SPSS, Chicago, Ill).

Clinical examination of the suspicious oral lesions revealed 8 with apparently normal oral mucosa, 26 leukoplakias, 9 erythroplakias and 24 erythroleukoplakias (speckled leukoplakia). Thirty of the lesions came from the oral tongue, 21 from the buccal mucosa, 13 from the floor of the mouth, 8 from the hard palate and 6 from the soft palate. The clinical presentation of these lesions was variable; the majority were papules (n=26), plaque (n=22) and ulcers (n=18). Histopathological diagnosis showed 25 squamous cell carcinomas (SCC), 4 carcinoma in situ and 30 dysplasias; the remainder involved benign conditions (Table 4.1).

Correlation between OCT and histopathology

OCT imaging showed distinct zones of normal and altered architectural changes. Basic histological layers (keratin cell layer, epithelium and lamina propria) and microanatomical histological structures (including blood vessels, tongue papillae and glandular ducts) were identified on most of the images (Figures 4.1, 4.2). The basement membrane was clearly identified in many specimens.

Structural identification and validation with histopathology were variable. Correlation between OCT and histopathology was achieved in 98.5% of specimens when identifying the basement membrane, in 97% when identifying the epithelial layer and its changes, and in 94% when identifying the keratin cell layer and its changes. Correlation was lower for blood vessels (77%) and salivary gland ducts (60%). Rete ridges were correlated and validated histopathologically in 89% of the OCT specimens (Table 4.2). For normal resection margins, OCT and histology showed a high degree of correlation, as summarized in Table 4.3.

Qualitative OCT analysis for different pathologies

Description of keratin layer

In normal keratinised mucosa, the keratin layer appears as a thin bright line on the uppermost part of the epithelium. This layer is absent in non-keratinised epithelium (Figure 4.3). In frictional keratosis, this layer shows hyper-reflection with slight to moderate thickening (Figure 4.4). Other benign cases show high backscattering signals from reactive keratosis.

Early stages (mild, moderate) of dysplasia mainly demonstrate hyper-signal; however, severe dysplasia and carcinoma *in-situ* have a hypo-reflective layer due to disorganised tissue differentiation. Invasive carcinoma is mostly hypo-reflective or has no reflective layer due to structural damage following ulceration.

Description of epithelial layer

The epithelial layer in normal mucosa has lower signal intensity than the keratin cell layer and lamina propria. This layer has a homogenous structure with little distinction between the spinous and granular cell layer (Figure 4.5). In benign lesions this layer may show a slight increase in thickness, mainly in cases of tissue hyperplasia.

A slight to moderate increase in this layer is usually associated with different stages of dysplasia, with the most significant changes seen in severe dysplasia and carcinoma *in-situ*. In invasive carcinoma this layer shows a significant increase in thickness in the areas of focal invasion where some of the basement membrane is still visible. Following frank invasion, accurate identification of the real boundary is difficult and is usually associated with non-homogenous mixed areas.

Description of lamina propria

In normal tissue, this layer is noticeably demarcated from the upper epithelium, with less reflection of the signal. Small blood vessels may be seen as a signal-poor area surrounded by two signal-rich lines (Figure 4.5).

Description of basement membrane

The demarcation between the different signal intensities of the epithelium and lamina propria represents the basement membrane. This junction may appear as a linear or undulating structure due to tissue shrinkage after biopsy. Small projections toward the lamina propria may be seen which represent rete pegs. Intact basement membrane was observed in both benign and dysplasia cases. Complete or partial loss (breach) of the basement membrane may occur in cases of invasive carcinoma (Figure 4.3).

Description of other microanatomical structures

In the normal part of the dorsum of tongue biopsies, mushroom or featherlike humps represent the fungeform and filliform papillae. Small salivary gland ducts might be seen in some biopsies as minute tortuous signal-free cavities that are sometimes very difficult to differentiate from blood vessels. Rete pegs appear as shadowy extensions from the epithelium, at the same signal intensity.

Agreement in the descriptive interpretation of OCT images by two readers

With regard to hyperkeratosis, agreement was achieved in 100% of the specimens when identifying the basement membrane and 80% of epithelial layer and its changes. The keratin cell layer demonstrated hyper-reflective features in 100% of cases. With regard to other benign oral lesions, agreement was achieved in 78% of the specimens when identifying the basement membrane, in 78% when describing the epithelial layer as being of normal thickness and in 64% when describing the keratin cell layer as normal reflective.

In the oral dysplasia group, agreement was achieved in 90% of specimens when identifying the basement membrane, in 83% when describing the thickness of the epithelial layer as increased, and in 13% when describing the keratin cell layer as hypo-reflective. For oral cancer, agreement was achieved in 100% of the specimens when describing the status of the basement membrane (demarcated or non-demarcated), and in 100% when describing a significant increase in the thickness of the epithelial layer (Table 4.4).

Diagnostic criteria

During examination of an invasive carcinoma, OCT images showed break down of the basement membrane that correlated well with the histological findings in the same specimen. Neoplastic lesions also showed an irregular and unclear architecture in the lower lamina propria, with a non-homogenous structure. The majority of the invasive lesions had hypo-reflective signals from the keratic cell layer, while epithelial thickness increased in all OCT images. Advanced malignant lesions extending into deeper tissue layers are beyond the scope of this technology as OCT cannot penetrate more than 2 mm into the tissue.

OCT was able to differentiate normal from pathological tissue and pathological tissue of different entities. OCT failed to provide enough cellular and subcellular information for staging of oral dysplasia. Differentiation between normal and pathological tissue was mainly based on the identification of a thickened oral epithelium and a disorganised keratin layer and subepithelial structures.

Differentiation between invasive carcinoma and other benign entities was accurate based on basement membrane status (intact or breached). During early invasive carcinoma the epithelium is highly variable in thickness, with areas of invasion into the subepithelial layers with invisible basement membrane. However, the OCT image of a dysplastic lesion showed epithelial thickening without frank breach of the basement membrane; this was sometimes difficult to differentiate from some benign lesions. The thickness of the epithelium for two lesions with carcinoma in situ was higher that that of benign lesions removed from the same anatomic area.

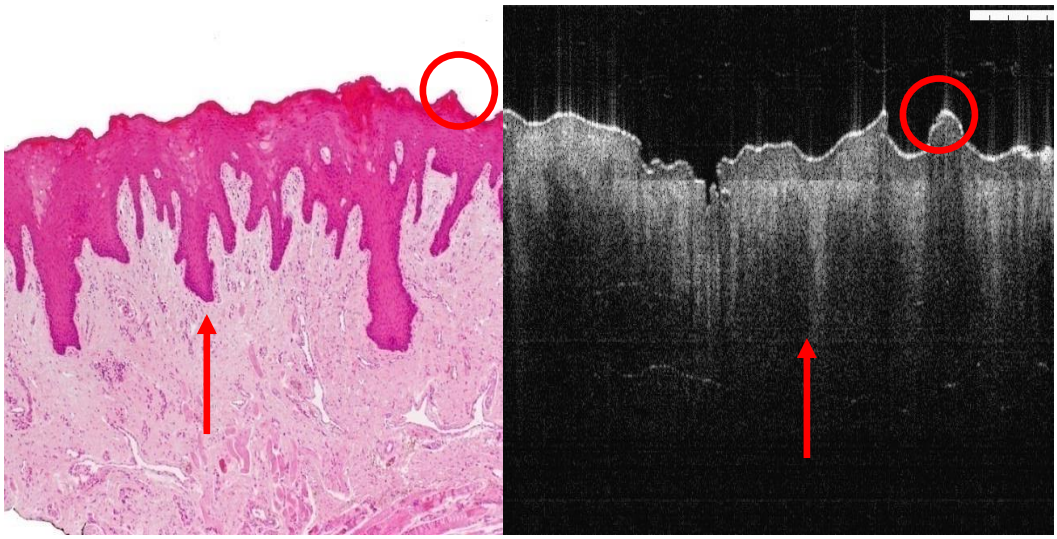

Figure 4.1: Corresponding H&E and OCT images of tongue biopsy showing prominent epithelium ridges (red arrows) and tongue papilla (red circle).

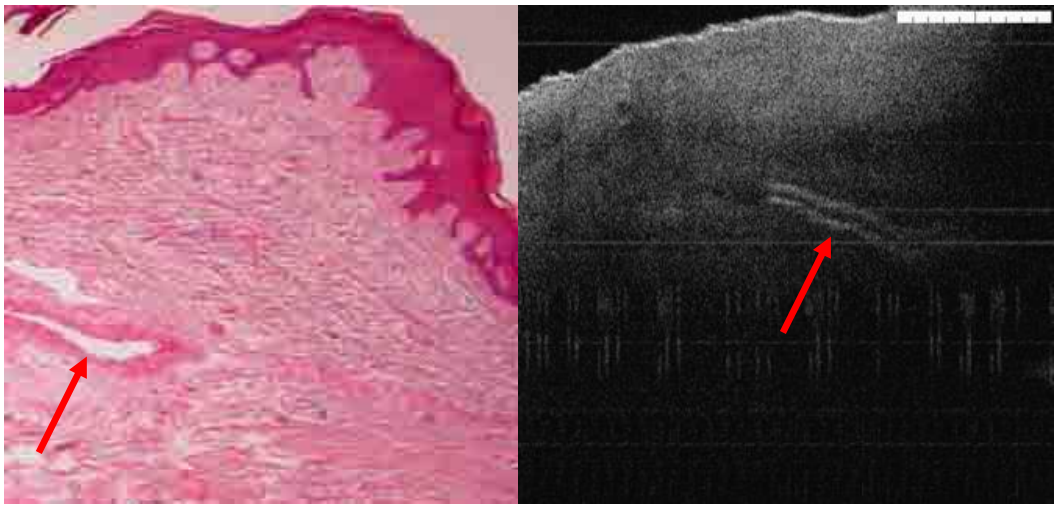

Figure 4.2: Prominent blood vessel appears as two lines with hyper-echoic signal and central hypo-echoic shadow (red arrows).

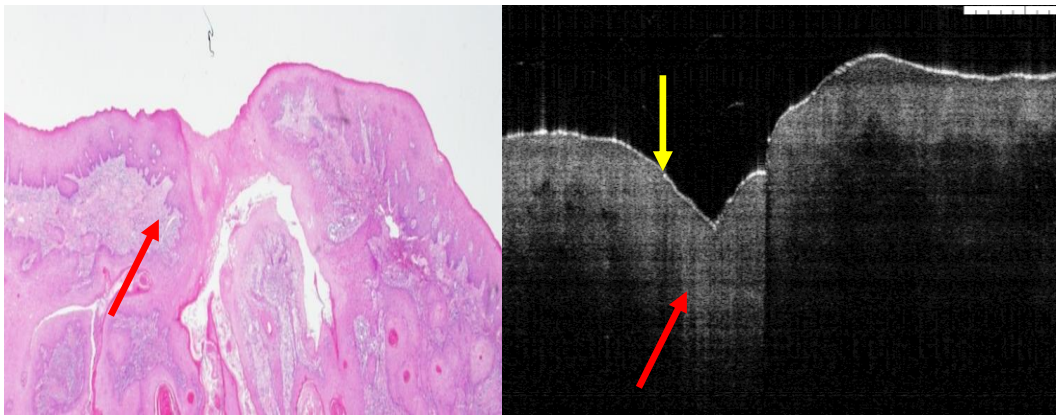

Figure 4.3: Focal invasive carcinoma of buccal mucosa with localized breach of basement membrane (red arrows) with thin or no keratin cell layer (yellow arrow).

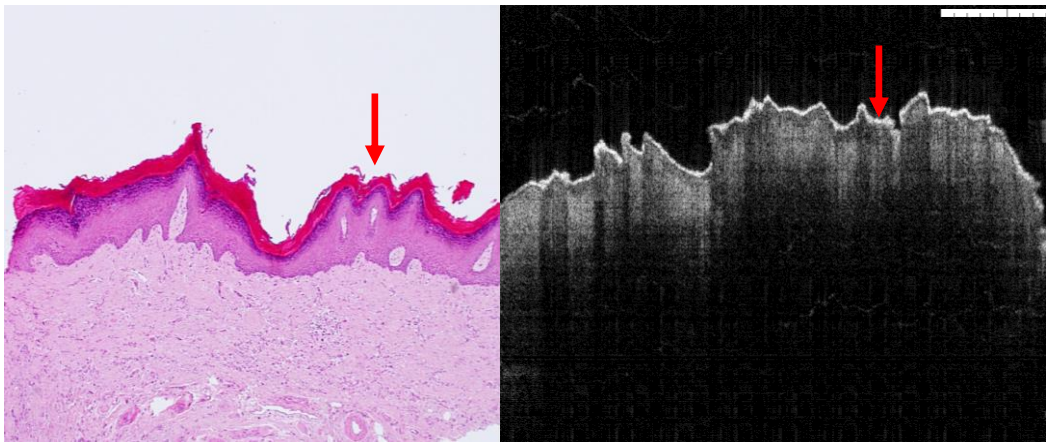

Figure 4.4: Frictional keratosis showing hyper-reflective OCT signal from the top layer (red arrows).

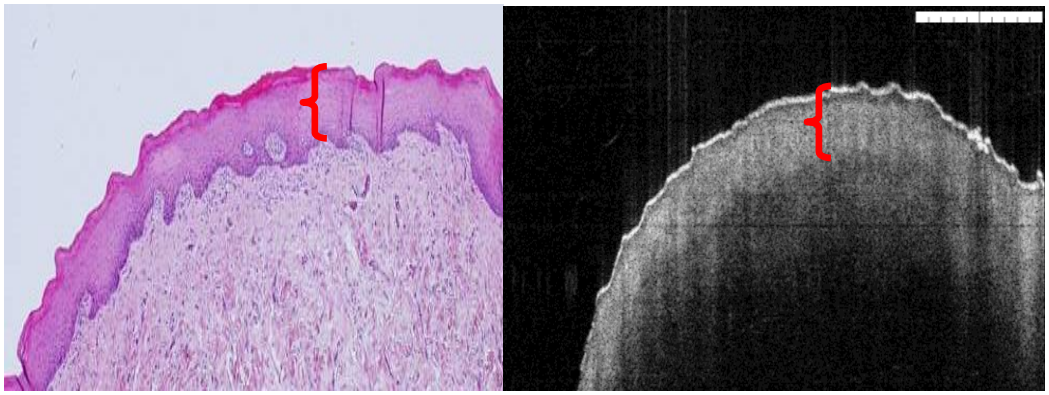

Figure 4.5: Normal epithelium showing normal reflective keratin cell layer, basement membrane and homogenous lamina propria. The area between the basement membrane and uppermost layer is the oral epithelium (red bracket).

Table 4.1: Characteristics of imaged lesions and their demographic location.

	No. (%)
Gender	
Female	44 (60.2)
Male	29 (39.8)
Location	
Tongue	30 (38.4)
Buccal mucosa	21 (26.9)
Floor of mouth	13 (16.6)
Hard palate	8 (10.2)
Soft palate	6 (7.6)
Colour	
Leukoplakia	26 (33.3)
Speckled leukoplakia	24 (30)
Erythroplakia	9 (11.5)
Bluish	9 (11.5)
Normal	8 (10.2)

	No. (%)
Clinical features	
Papule	26 (33.3)
Plaque	22 (28.2)
Ulcer	18 (23)
Others	12 (15.3)
Symptoms	
Oral discomfort and soreness	29 (39.7)
Symptomless	20 (27.3)
Pain	13 (17.8)
Bleeding	11 (15)
Histologic diagnosis	
Dysplasia	30 (38.4)
Carcinoma in situ	4 (5.1)
Invasive carcinoma	25 (32)
Other benign lesion	14 (18)
Frictional keratosis	5 (6.5)

Table 4.2: Common descriptive features in OCT and pathology from oral tissue agreed by two observers.

Keratin cell layer	**OCT**	**Pathology**	**Total**
Clearly seen	62	66	128
Not seen	16	12	28
Total	78	78	156
Basement membrane	**OCT**	**Pathology**	**Total**
Clearly identified	67	68	135
Not identified	11	10	21
Total	78	78	156
Blood vessel in the lamina propria	**OCT**	**Pathology**	**Total**
Clearly seen	17	22	39
Not seen	61	56	117
Total	78	78	156
Tongue papilla	**OCT**	**Pathology**	**Total**
Clearly seen	14	16	30
Not seen	16	14	30
Total	30	30	60
Epithelial boundary	**OCT**	**Pathology**	**Total**
Clearly seen	68	70	138
Not seen	10	8	18
Total	78	78	156
Salivary gland duct	**OCT**	**Pathology**	**Total**
Clearly seen	6	10	16
Not seen	72	68	140
Total	78	78	156
Rete ridges	**OCT**	**Pathology**	**Total**
Clearly seen	55	62	117
Not seen	23	16	39
Total	78	78	156

Table 4.3: Common descriptive features in OCT and histology from normal resection oral tissue agreed by two observers.

Keratin cell layer	**OCT**	**Histology**	**Total**
Clearly seen	30	30	60
Not seen	0	0	0
Total	30	30	60
Basement membrane	**OCT**	**Histology**	**Total**
Clearly identified	30	30	60
Not identified	0	0	0
Total	30	30	60
Blood vessel in the lamina propria	**OCT**	**Histology**	**Total**
Clearly seen	12	15	27
Not seen	18	15	33
Total	30	30	60
Tongue papilla	**OCT**	**Histology**	**Total**
Clearly seen	10	10	20
Not seen	20	20	40
Total	30	30	60
Epithelium boundary	**OCT**	**Histology**	**Total**
Clearly seen	30	30	60
Not seen	0	0	0
Total	30	30	60
Salivary gland duct	**OCT**	**Histology**	**Total**
Clearly seen	6	7	13
Not seen	24	23	47
Total	30	30	60
Rete ridges	**OCT**	**Histology**	**Total**
Clearly seen	22	25	47
Not seen	8	5	13
Total	30	30	60

Table 4.4: Descriptive interpretation of changes in OCT image. KL: keratin cell layer. EP: epithelium. BM; basement membrane. LP; lamina propria. ↑ increase: ↓ decrease; ↔ no change.

Pathological entity	**KL hyper-reflective**	**K hypo-reflective**	**KL normo-reflective**	**not applicable**	**EP ↑**	**EP ↓**	**EP ↔**	**not identified**	**BM demarcated**	**BM non-demarcated**	**not applicable**	**LP homogenous**	**LP non-homogenous**
Keratosis (n=5)	5	0	0	0	1	0	4	0	5	0	0	5	0
Benign oral lesions (n=14)	2	0	9	3	1	1	11	1	11	2	0	12	2
Oral dysplasia (n=30)	17	4	7	2	25	0	3	2	27	1	2	26	4
Carcinoma in situ (n=4)	1	1	2	0	4	0	0	0	4	0	0	4	0
Invasive carcinoma (n=25)	10	10	5	0	25	0	0	0	1	24	0	0	25
Normal margin (n=30)	0	0	30	0	0	0	30	0	30	0	0	30	0

Section II: Histometric validation of the OCT using tumour resection margins

Background

An accurate evaluation of oral epithelium thickness is essential for early diagnosis of premalignant/malignant oral lesions and their progression.

Objectives

The purpose of this research was 1) to evaluate the validity and reproducibility of the OCT for measuring epithelial thickness across different oral sites and to compare these measurements with the gold standard histology, and 2) to correlate epithelial thickness obtained from three different OCT readings with histology and quantify epithelial thickness according to the best correlation.

Participants

The study was approved by the Moorfields & Whittington Local Research Ethics Committee according to the principles of the Declaration of Helsinki. Patients presenting with oral squamous cell carcinoma for the first time were recruited. Patients with T1&T2 N0 lesions were treated with resection of the primary tumour without elective neck dissection. Those patients with T3/T4 lesions who were treated with resection of the primary tumour along with ipsilateral selective neck dissection were excluded from the study due to the difficulty of conducting margin analysis. Any patient who had received radiotherapy or chemotherapy was excluded from the study due to their effects on epithelial thickness. Forty-two patients satisfied the inclusion criteria and signed the consent form.

Results

Demographic information

A total of 42 primary oral cancers were examined using the OCT equipment, showing a total of 142 tumour-free margins. Twenty six resection margins out of 168 showed involvement with tumour (pathology-involved margins). Six tumour-free margins were excluded from the study due to a distorted histopathology image, which may have affected the accuracy of epithelial measurements. In 136 resection margins, OCT showed good to excellent structural demarcation. The anatomical distribution of the

oral lesions differed between the various oral sites. The tongue (*n*=9), floor of mouth (*n*=7) and ventral side of tongue (*n*=7) were the most commonly affected oral sites, followed by the buccal mucosa (*n*=4). The hard palate (*n*=4), soft palate (*n*=4), lower lip (*n*=4) and alveolar mucosa (*n*=3) were the least commonly affected sites. The mean age of the subjects was 57 years (range 41 to 87 years; 29 male, 13 female).

Pearson correlation coefficient and validity of OCT measurements

OCT and histological measurements of epithelial thickness showed good correlation between different readings at all oral sites (Table 4.5). The higher correlation at 24 hours post specimens' resection (r=0.964) compared to the first and the last reading (r=0.948, r=0.932 respectively) (Figure 4.6,4.7,4.8) . In alveolar mucosa the correlation was (r=0.951; P >0.01) (Table 4.6). In the 16 buccal mucosa resection margins, the OCT and histological measurements showed much better correlation (r =0.971) compared to other anatomic sites (Table 4.7). The 25 well-visualized floor of mouth mucosa samples were tomographically and histologically well correlated (r=0.903) (Table 4.8). The correlation between the OCT and histological measurements of the soft palate, tongue and ventral side of the tongue was excellent (r =0.982, r =0.966 and r =0.987, respectively) (Table 4.9, 4.10, 4.11). The correlation for the hard palate was r =0.895 (P =0.01) (Table 4.12). The lowest correlation was for the lip (vermilion border and mucosal surface) (r =0.881, r =0.578) (Table 4.13, 4.14).

Benchmark epithelial thickness

The best correlations, obtained at 24 hours post-resection, were used to calculate the average thickness for different types of oral epithelium. The difference between the OCT thickness and histometric thickness (underestimation) was more than 40 µm in 16 margins (5 floor of mouth, 4, ventral side of tongue, 4 buccal mucosa , 3 from lower lip) (Figure 4.9). The tomographic thicknesses of 106 margins were correctly quantified by OCT with a maximum of 30 µm difference. However, the thickness of OCT was severely underestimated in six normal resection margins affecting the floor of the mouth and ventral side of tongue, for which the OCT thickness was less than 150 µm, but the histological thickness was more than 250 µm. Overestimation by OCT of 30 µm to 40 µm occurred in 10 margins (4 tongue, 4 hard palate, and 2 alveolar mucosa).

The mean epithelial thickness of the 16 buccal mucosa margins on OCT vs. histology was (430 vs. 470 µm), and was thicker than the mucosal surface of the hard palate (260 vs. 270 µm). The oral epithelium was thickest on the buccal mucosa and thinnest on the floor of the mouth (100 vs. 130 µm) and ventral part of the tongue (130 vs. 170 µm). There was a perfect match between the OCT and histology reading of the soft palate (230 vs. 230 µm). In the vermilion border group, the average thickness of the epithelium on OCT was similar to that of the tongue and almost similar on histology (420 vs. 420 µm), but thicker than the mucosal region of the lip (390 vs. 410 µm). In the alveolar group, the mean thickness on OCT and histology was 430 vs. 440 µm.

Reproducibility of OCT measurements

The mean epithelial thickness for the all measurements at first and second measurements with no significantly different ($t = 2.297$, $p > 0.01$, with a confidence of interval (CI) of -0.784 to 1.048) (Table 4.15). The means of the differences in epithelial thickness between the two measurements plus 95% confidence limits for the alveolar mucosa, buccal mucosa, floor of the mouth, hard palate, mucosal and vermilion surface of the lip, soft palate, dorsum and ventral part of the tongue are summarized in Tables 4.16 to 4.24.

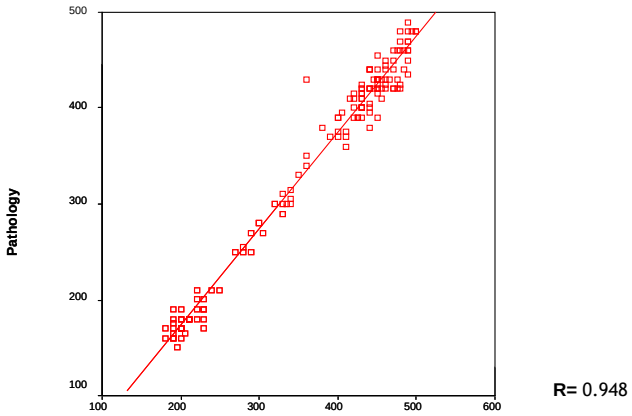

Figure 4.6: Correlation between OCT and histological epithelium thickness 30 minutes post-lesion resection.

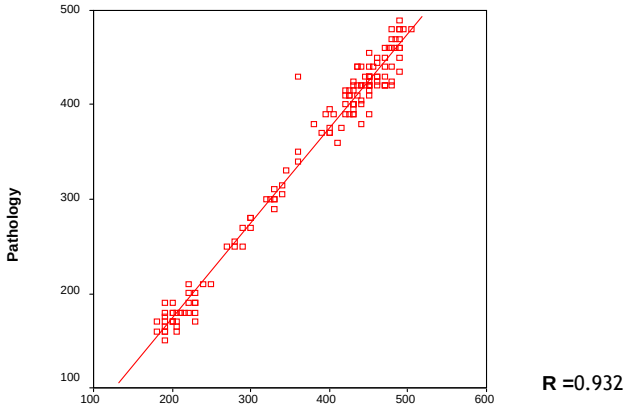

Figure 4.7: Correlation between OCT and histological epithelium thickness 60 minutes post-lesion resection.

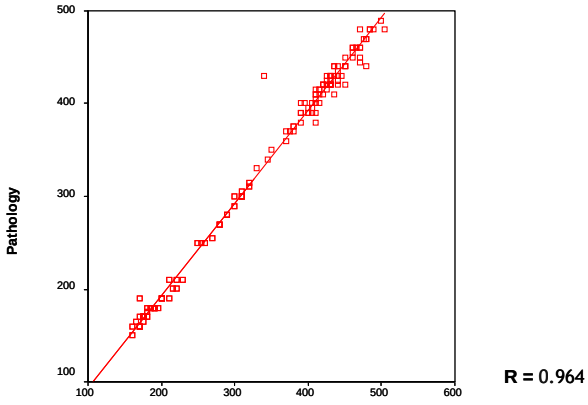

Figure 4.8: Correlation between OCT and histological epithelium thickness 24 hours post-lesion resection.

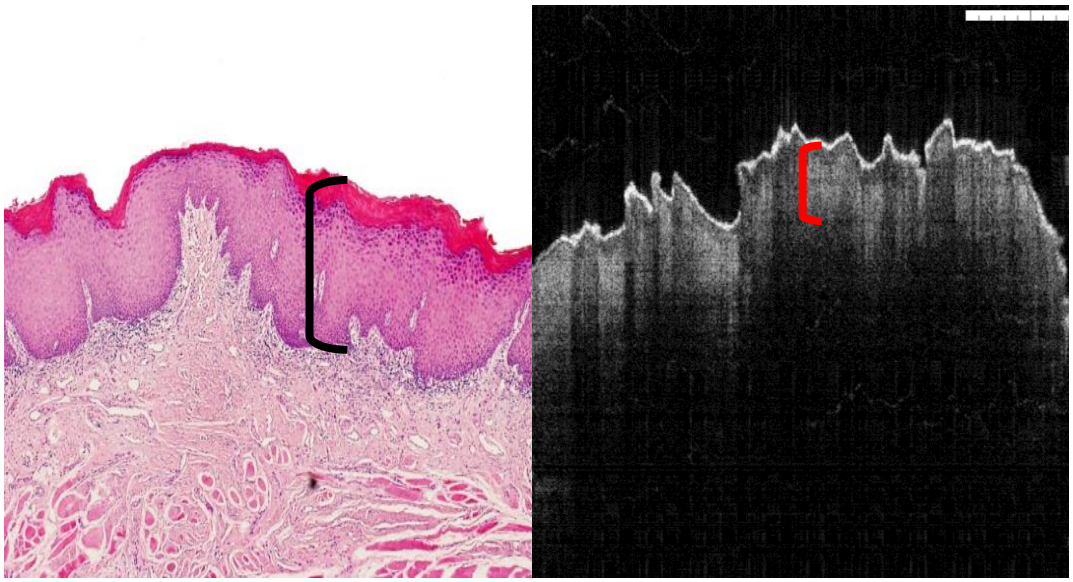

Figure 4.9: Microphotograph of H&E-stained normal palatal epithelium used for histometric measurement and corresponding OCT scan with 60 µm underestimation.

Table 4.5: Correlations between different OCT readings and pathology for the overall measurements.

		CONTROL
ONE	Pearson Correlation	.948**
	Sig. (2-tailed)	.000
	N	142
TWO	Pearson Correlation	.932**
	Sig. (2-tailed)	.000
	N	142
THREE	Pearson Correlation	.964**
	Sig. (2-tailed)	.000
	N	142
CONTROL	Pearson Correlation	1
	Sig. (2-tailed)	.
	N	142

**. Correlation is significant at the 0.01 level

Table 4.6: Correlations between different OCT readings and pathology for alveolar oral mucosa.

		CONTROL
ONE	Pearson Correlation	.780**
	Sig. (2-tailed)	.005
	N	11
TWO	Pearson Correlation	.734*
	Sig. (2-tailed)	.010
	N	11
THREE	Pearson Correlation	.951**
	Sig. (2-tailed)	.000
	N	11
CONTROL	Pearson Correlation	1
	Sig. (2-tailed)	.
	N	11

**. Correlation is significant at the 0.01 level

*. Correlation is significant at the 0.05 level (2-tailed).

Table 4.7: Correlations between different OCT readings and pathology for buccal mucosa.

		CONTROL
ONE	Pearson Correlation	.827**
	Sig. (2-tailed)	.000
	N	27
TWO	Pearson Correlation	.840**
	Sig. (2-tailed)	.000
	N	27
THREE	Pearson Correlation	.971**
	Sig. (2-tailed)	.000
	N	27
CONTROL	Pearson Correlation	1
	Sig. (2-tailed)	.
	N	27

**. Correlation is significant at the 0.01 level

Table 4.8: Correlations between different OCT readings and pathology for floor of mouth.

		CONTROL
ONE	Pearson Correlation	.764**
	Sig. (2-tailed)	.000
	N	25
TWO	Pearson Correlation	.735**
	Sig. (2-tailed)	.000
	N	25
THREE	Pearson Correlation	.903**
	Sig. (2-tailed)	.000
	N	25
CONTROL	Pearson Correlation	1
	Sig. (2-tailed)	.
	N	25

**. Correlation is significant at the 0.01 level

Table 4.9: Correlations between different OCT readings and pathology for soft palate.

		CONTROL
ONE	Pearson Correlation	.944**
	Sig. (2-tailed)	.000
	N	14
TWO	Pearson Correlation	.952**
	Sig. (2-tailed)	.000
	N	14
THREE	Pearson Correlation	.982**
	Sig. (2-tailed)	.000
	N	14
CONTROL	Pearson Correlation	1
	Sig. (2-tailed)	.
	N	14

**. Correlation is significant at the 0.01 level

Table 4.10: Correlations between different OCT readings and pathology for tongue.

		CONTROL
ONE	Pearson Correlation	.718**
	Sig. (2-tailed)	.000
	N	25
TWO	Pearson Correlation	.710**
	Sig. (2-tailed)	.000
	N	25
THREE	Pearson Correlation	.966**
	Sig. (2-tailed)	.000
	N	25
CONTROL	Pearson Correlation	1
	Sig. (2-tailed)	.
	N	25

**. Correlation is significant at the 0.01 level

Table 4.11: Correlations between different OCT readings and pathology for ventral side of tongue.

		CONTROL
ONE	Pearson Correlation	.841**
	Sig. (2-tailed)	.005
	N	9
TWO	Pearson Correlation	.838**
	Sig. (2-tailed)	.005
	N	9
THREE	Pearson Correlation	.987**
	Sig. (2-tailed)	.000
	N	9
CONTROL	Pearson Correlation	1
	Sig. (2-tailed)	.
	N	9

**. Correlation is significant at the 0.01 level

Table 4.12: Correlations between different OCT readings and pathology for hard palate.

		CONTROL
ONE	Pearson Correlation	.862**
	Sig. (2-tailed)	.000
	N	15
TWO	Pearson Correlation	.838**
	Sig. (2-tailed)	.000
	N	15
THREE	Pearson Correlation	.895**
	Sig. (2-tailed)	.000
	N	15
CONTROL	Pearson Correlation	1
	Sig. (2-tailed)	.
	N	15

**. Correlation is significant at the 0.01 level

Table 4.13: Correlations between different OCT readings and pathology for vermilion border of lower lip.

		CONTROL
ONE	Pearson Correlation	.310
	Sig. (2-tailed)	.454
	N	8
TWO	Pearson Correlation	.506
	Sig. (2-tailed)	.201
	N	8
THREE	Pearson Correlation	.881**
	Sig. (2-tailed)	.004
	N	8
CONTROL	Pearson Correlation	1
	Sig. (2-tailed)	.
	N	8

**. Correlation is significant at the 0.01 level

Table 4.14: Correlations between different OCT readings and pathology for mucosal surface of lower lip.

		CONTROL
ONE	Pearson Correlation	.648
	Sig. (2-tailed)	.082
	N	8
TWO	Pearson Correlation	.670
	Sig. (2-tailed)	.069
	N	8
THREE	Pearson Correlation	.578
	Sig. (2-tailed)	.134
	N	8
CONTROL	Pearson Correlation	1
	Sig. (2-tailed)	.
	N	8

Table 4.15: Confidence interval (CI) from T-test between OCT measurements at 30 and 60 minutes post-specimen-excision for overall measurements, $P < 0.01$.

		Mean	N	Std. Deviation	Std. Error Mean
Pair 1	ONE	372.9577	142	106.17321	8.90986
	TWO	372.3944	142	105.88820	8.88594

	Paired Differences					
		95% Confidence Interval of the Difference				
	Mean	Lower	Upper	t	df	Sig. (2-tailed)
Pair 1 ONE - TWO	1.5634	-.0784	1.0484	2.297	141	.023

Table 4.16: Confidence interval (CI) from T-test between OCT measurements at 30 and 60 minutes post–specimen-excision for alveolar mucosa, P < 0.01.

		Mean	N	Std. Deviation	Std. Error Mean
Pair 1	ONE	441.8182	11	21.36267	6.44109
	TWO	440.9091	11	21.42641	6.46030

		Paired Differences			t	df	Sig. (2-tailed)
			95% Confidence Interval of the Difference				
		Mean	Lower	Upper			
Pair 1	ONE - TWO	.9091	-1.1165	2.9347	1.000	10	.341

Table 4.17: Confidence interval (CI) from T-test between OCT measurements at 30 and 60 minutes post-specimen-excision for buccal mucosa, P < 0.01.

		Mean	N	Std. Deviation	Std. Error Mean
Pair 1	ONE	427.7778	27	16.77529	3.22841
	TWO	427.4074	27	16.83462	3.23982

		Paired Differences			t	df	Sig. (2-tailed)
			95% Confidence Interval of the Difference				
		Mean	Lower	Upper			
Pair 1	ONE - TWO	.3704	-1.0733	1.8141	.527	26	.602

Table 4.18: Confidence interval (CI) from T-test between OCT measurements at 30 and 60 minutes post–specimen-excision for floor of mouth, P < 0.01.

		Mean	N	Std. Deviation	Std. Error Mean
Pair 1	ONE	205.2000	25	16.86219	3.37244
	TWO	205.8000	25	16.87454	3.37491

		Paired Differences			t	df	Sig. (2-tailed)
			95% Confidence Interval of the Difference				
		Mean	Lower	Upper			
Pair 1	ONE - TWO	-.6000	-1.2845	.0845	-1.809	24	.083

Table 4.19: Confidence interval (CI) from T-test between OCT measurements at 30 and 60 minutes post-specimen-excision for hard palate, $P < 0.01$.

		Mean	N	Std. Deviation	Std. Error Mean
Pair 1	ONE	443.6667	15	15.86401	4.09607
	TWO	444.3333	15	15.56859	4.01979

	Paired Differences					
		95% Confidence Interval of the Difference				
	Mean	Lower	Upper	t	df	Sig. (2-tailed)
Pair 1 ONE - TWO	-.6667	-2.0965	.7632	-1.000	14	.334

Table 4.20: Confidence interval (CI) from T-test between OCT measurements at 30 and 60 minutes post-specimen-excision for mucosal surface of lower lip, $P < 0.01$.

		Mean	N	Std. Deviation	Std. Error Mean
Pair 1	ONE	358.1250	8	20.34304	7.19235
	TWO	356.8750	8	21.53693	7.61445

	Paired Differences					
		95% Confidence Interval of the Difference				
	Mean	Lower	Upper	t	df	Sig. (2-tailed)
Pair 1 ONE - TWO	1.2500	-.6850	3.1850	1.528	7	.170

Table 4.21: Confidence interval (CI) from T-test between OCT measurements at 30 and 60 minutes post-specimen-excision for vermilion border of lower lip, $P < 0.01$.

		Mean	N	Std. Deviation	Std. Error Mean
Pair 1	ONE	449.3750	8	8.63444	3.05274
	TWO	448.1250	8	9.97765	3.52763

	Paired Differences					
		95% Confidence Interval of the Difference				
	Mean	Lower	Upper	t	df	Sig. (2-tailed)
Pair 1 ONE - TWO	1.2500	-2.4553	4.9553	.798	7	.451

Table 4.22: Confidence interval (CI) from T-test between OCT measurements at 30 and 60 minutes post-specimen-excision for soft palate, $P < 0.01$.

		Mean	N	Std. Deviation	Std. Error Mean
Pair 1	ONE	308.2143	14	24.77647	6.62179
	TWO	306.7857	14	23.66490	6.32471

	Paired Differences					
		95% Confidence Interval of the Difference				
	Mean	Lower	Upper	t	df	Sig. (2-tailed)
Pair 1 ONE - TWO	1.4286	-.3361	3.1932	1.749	13	.104

Table 4.23: Confidence interval (CI) from T-test between OCT measurements at 30 and 60 minutes post-specimen-excision for tongue, $P < 0.01$.

		Mean	N	Std. Deviation	Std. Error Mean
Pair 1	ONE	482.8000	25	10.80895	2.16179
	TWO	481.4000	25	11.86030	2.37206

	Paired Differences					
		95% Confidence Interval of the Difference				
	Mean	Lower	Upper	t	df	Sig. (2-tailed)
Pair 1 ONE - TWO	1.4000	.2822	2.5178	2.585	24	.016

Table 4.24: Confidence interval (CI) from T-test between OCT measurements at 30 and 60 minutes post-specimen-excision for ventral side of tongue, $P < 0.01$.

		Mean	N	Std. Deviation	Std. Error Mean
Pair 1	ONE	213.3333	9	19.52562	6.50854
	TWO	212.2222	9	20.32718	6.77573

	Paired Differences					
		95% Confidence Interval of the Difference				
	Mean	Lower	Upper	t	df	Sig. (2-tailed)
Pair 1 ONE - TWO	1.1111	-.5836	2.8059	1.512	8	.169

Section III: Assessment of suspicious oral lesions

Background

In the previous section, OCT was structurally and morphometrically validated. However, its diagnostic accuracy has not yet been tested using specific image criteria.

Objectives

The purpose of this prospective clinical study was: (1) to assess the sensitivity and specificity of OCT in identifying potentially malignant and malignant oral lesions, (2) to determine the inter-observer agreement in the analysis of specific image parameters, and (3) to measure the oral epithelial thickness in different pathologies.

Materials

Identical protocols were used to recruit 125 consecutive patients who presented with suspicious oral lesions to the UCLH Head and Neck Centre. The study protocol was approved by the Moorfields & Whittington Local Research Ethics Committee for Human Research..

All patients presented with clinical features suggestive of suspicious oral mucosal disease. Written informed consent was obtained from each subject. Demographic information was collected from each patient on pre-made proformas. A detailed clinical examination was performed on each patient to assess the site, size and clinical characteristics of the lesion (Table 2.25). The presenting complaints, smoking and drinking habits were also recorded.

Following examination, surgical (excisional or incisional, when appropriate) biopsies were acquired from each patient. The total number of surgical biopsies was 125. The resections were preserved in formalin and were subjected to optical coherence tomography scanning within 24 hours (delayed *ex-vivo*). All specimens were then processed for histopathological diagnosis. Histopathological assessment was carried out by one oral and maxillofacial pathologist to ensure objectivity. Assessment was conducted according to the World Health Organization guidelines. The pathological categories included: normal/benign, dysplasia (mild, moderate, severe, and carcinoma *in situ*), and invasive cancer.

The process of co-localisation was described in the equipment and methods. The co-registration was aided by digital images and specimen orientation using sutures and special ink. For each surgical specimen, OCT images were acquired from several areas of interest.

Assessment of OCT images was carried out by a surgeon and a pathologist; both were taught how to read OCT images and were provided with a training set to consolidate their knowledge and assessment skills prior to the assessment of the 125 OCT images (Figures 4.10, 4.11, 4.12). Each assessor was provided with a brief clinical history of the suspicious lesion and was asked to comment on every corresponding OCT image using a pre-made proforma. OCT scans with normal and abnormal structure labelled with metric measurement of the epithelium and keratin cell layer provided. This helped reader to assess epithelium thickness changes according to normal reference. Metric readings were recorded for both the keratin and the epithelial layers by the principal investigator.

Four main parameters were assessed in each image, including the keratin layer, epithelial layer, lamina propria and basement membrane. The assessors were instructed to quantify the thickness (no change, increased or decreased) of each tissue (keratin and epithelium) layer as well as commenting on the status of the basement membrane (intact, breached, difficult to assess), basement membrane quality (excellent, good, adequate or poor) and changes in the lamina propria (obvious changes, no clear changes or no changes). Furthermore, each assessor was required to provide a diagnosis and was asked to report on "the need for surgical biopsy" to confirm the diagnosis, in case of highly suspicious lesion, if this technique was to be applied *in- vivo*.

Results

Seventy-two males (57.6%) and 53 females (42.4%) participated in this clinical study; their age range was 20–88 years and 32–89 years, respectively. The median age was 58 years. Most of the biopsied lesions were located on the posterior dorsal tongue (*n*=28), followed by buccal mucosa (*n*=20), anterior dorsal tongue (*n*=12), floor of the mouth (*n*=11), soft palate (*n*=11) and vermilion border of the lower lip (*n*=10) (Table 4.25).

All patients presented with clinical features suggestive of potentially malignant oral mucosal disease. The majority of the lesions (*n*=65) appeared clinically as plaques, 40 lesions were papular and 20 presented as ulcers. Lesion colour was variable: 85 (68.0%) were leucoplakic, 26 (20.8%) were erythroplakic, 13 (10.4%) were leukoerythroplakic and 1 (0.8) was bluish. The pathological diagnosis revealed 43 microinvasive carcinomas and 41 dysplasias. Benign oral lesions were less common and included 22 keratoses, 11 non-specific inflammatory reactions, 6 mucoceles and 2 papillomas (Table 4.25).

The results of the assessment of the epithelial structures made by the pathologist and clinician are recorded in Table 4.26. The pathologist's sensitivity and specificity was 78% and 81%, respectively. The positive predictive value (PPV) was 87% and the negative predictive value (NPP) was 70%. The accuracy of OCT was 79% (Table 4.27). The sensitivity and specificity of the surgeon were 92% and 75%, respectively. The PPV was 86% and the NPP was 85%. The accuracy of OCT was 85% (Table 4.28). The collective sensitivity and specificity for both assessors was 85% and 78%, respectively. The PPV and NPV were 86.5% and 77.5%, respectively.

The average thickness of the keratin and epithelial layers was variable depending on the pathological process. Their mean thickness in benign lesions was 20 µm and 330 µm, respectively. In the dysplasia group, the mean thickness of the keratin and epithelial layers was 20 µm and 450 µm respectively. Their mean thickness in carcinoma *in situ* on the OCT images was 10 µm and 570 µm, respectively. In the presence of microinvasive carcinoma, the average thickness of the epithelium was 650 µm, a much higher value than any other pathological process; however, the thickness of the keratin layer was the same as in severe dysplasia (20 µm) (Table 4.29).

The Kappa agreement for the subjective OCT image analysis was variable. There was poor agreement regarding thickness of the keratin layer, good agreement regarding thickness of the epithelial layer, poor agreement regarding changes in the lamina propria and good agreement when assessing the status of the basement membrane. Agreement on "the need for biopsy" was very good (Table 4.30).

Table 4.25: Demographics of the cohort included in this study.

	No. (%)			No. (%)
Gender			**Medical history**	
Male	72 (57.6)		ASA I	123 (98.4)
Female	53 (42.4)		ASA II	2 (1.6)
Location			**Symptoms**	
Post. dorsal tongue	28 (22.4)		Soreness	17 (13.6)
Buccal mucosa	20 (16.0)		Pain	16 (12.8)
Ant. dorsal tongue	12 (9.6)		Itchiness	2 (1.6)
Floor of mouth	11 (8.8)		Bleeding	1 (0.8)
Soft palate	11 (8.8)		Asymptomatic	89 (71.2)
Vermilion border	10 (8.0)			
Gingival mucosa	9 (7.2)		**Smoking status**	
Ventral tongue	7 (5.6)		Current smoking	44 (35.2)
Lower lip	5 (4.0)		Ex-smoker	48 (38.4)
Hard palate	4 (3.2)		Non-smoker	33 (26.4)
Retromolar trigone	3 (2.4)			
Upper lip	3 (2.4)		**Drinking status**	
Tonsil	2 (1.6)		Current drinker	89 (71.2)
			Ex-drinker	16 (12.8)
Colour			Non-drinker	20 (16.0)
Leukoplakia	85 (68.0)			
Erythroplakia	26 (20.8)		Pan chewing	3 (2.4)
Speckled leukoplakia	13 (10.4)			
Bluish	1 (0.8)		**Diagnosis**	
			Microinvasive carcinoma	43 (34.4)
Clinical features			Dysplasia	41 (32.8)
Macule	65 (52.0)		Keratosis	22 (17.6)
Papule	40 (32.0)		Non-specific inflammatory	11 (8.8)
Ulcer	20 (16.0)		Mucoceles	6 (4.8)
			Papillomas	2 (1.6)
Biopsy type				
Excisional	86 (68.8)			
Incisional	39 (31.2)			

Table 4.26: Assessment of the epithelial structures by the pathologist and clinician.

Pathologist	**No. (%)**		**Clinician**	**No. (%)**
Keratin layer			**Keratin layer**	
Increased	59 (47.2)		Increased	61 (48.8)
Decreased	19 (15.2)		Decreased	31 (24.8)
No change	47 (37.6)		No change	33 (26.4)
Epithelial layer			**Epithelial layer**	
Increased	72 (57.6)		Increased	84 (67.2)
Decreased	3 (2.4)		Decreased	5 (4.0)
No change	50 (40.0)		No change	36 (28.8)
LP layer			**LP layer**	
Obvious changes	34 (27.2)		Obvious changes	26 (20.8)
No clear changes	20 (16.0)		No clear changes	20 (16.0)
No changes	71 (56.8)		No changes	79 (63.2)
BM quality			**BM quality**	
Excellent	23 (18.4)		Excellent	1 (0.8)
Good	50 (40.0)		Good	35 (28.0)
Adequate	32 (25.6)		Adequate	73 (58.4)
Poor	20 (16.0)		Poor	16 (12.8)
BM status			**BM status**	
Intact	78 (62.4)		Intact	77 (61.6)
Breached	35 (28.0)		Breached	47 (37.6)
Difficult to assess	12 (9.6)		Difficult to assess	1 (0.8)

Table 4.27: Pathological assessment. Sensitivity 78%; Specificity 81%; Positive predictive value (PPV) 87%; Negative predictive value (NPV) 70%; Accuracy of OCT 79%. TP: true positive, FP: false positive, TN: true negative, FN: false negative.

	Histology			
OCT		**Positive**	**Negative**	**Total**
	Positive	61 (TP)	9 (FP)	70
	Negative	17 (FN)	38 (TN)	55
	Total	78	47	125

Table 4.28: Clinical assessment. Sensitivity 92%; Specificity 75%; Positive predictive value (PPV) 86%; Negative predictive value (NPV) 85%; Accuracy 85%. TP: true positive, FP: false positive, TN: true negative, FN: false negative.

	Histology			
OCT		**Positive**	**Negative**	**Total**
	Positive	72 (TP)	12 (FP)	84
	Negative	6 (FN)	35 (TN)	41
	Total	77	48	125

Table 4.29: The average thickness of the keratin layer (KL) and epithelial layer (EL) per pathological process.

Pathology	**Range**	**Minimum**	**Maximum**	**Mean**
Benign				
KL thickness	30 µm	10 µm	40 µm	20 µm
EL thickness	420 µm	170 µm	590 µm	330 µm
Mucocele				
KL thickness	10 µm	0 µm	10 µm	10 µm
EL thickness	60 µm	170 µm	230 µm	190 µm
Keratosis & papilloma				
KL thickness	20 µm	20 µm	40 µm	30 µm
EL thickness	370 µm	190 µm	560 µm	360 µm
Non-specific				
KL thickness	20 µm	10 µm	30 µm	20 µm
EL thickness	346 µm	234 µm	580 µm	387 µm
Dysplasia (all)				
KL thickness	20 µm	20 µm	40 µm	20 µm
EL thickness	600 µm	170 µm	770 µm	450 µm
Mild dysplasia				
KL thickness	10 µm	10 µm	20 µm	20 µm
EL thickness	260 µm	170 µm	430 µm	410 µm
Moderate dysplasia				
KL thickness	30 µm	0 µm	30 µm	20 µm
EL thickness	360 µm	230 µm	590 µm	453 µm
Severe dysplasia				
KL thickness	20 µm	10 µm	30 µm	20 µm
EL thickness	540 µm	230 µm	770 µm	480 µm
Carcinoma *in situ*				
KL thickness	20 µm	0 µm	20 µm	10 µm
EL thickness	40 µm	550 µm	590 µm	570 µm
SCC				
KL thickness	40 µm	0 µm	40 µm	20 µm
EL thickness	590 µm	380 µm	970 µm	650 µm

Table 4.30: Kappa agreement between the pathologist and clinician when assessing the OCT images from the 125 patients.

Assessment of pathologist vs. clinician	**Kappa**
Biopsy	0.720
Keratin layer	0.279
Epithelial layer	0.452
Lamina propria	0.306
Basement membrane quality	0.590
Basement membrane status	0.656

.

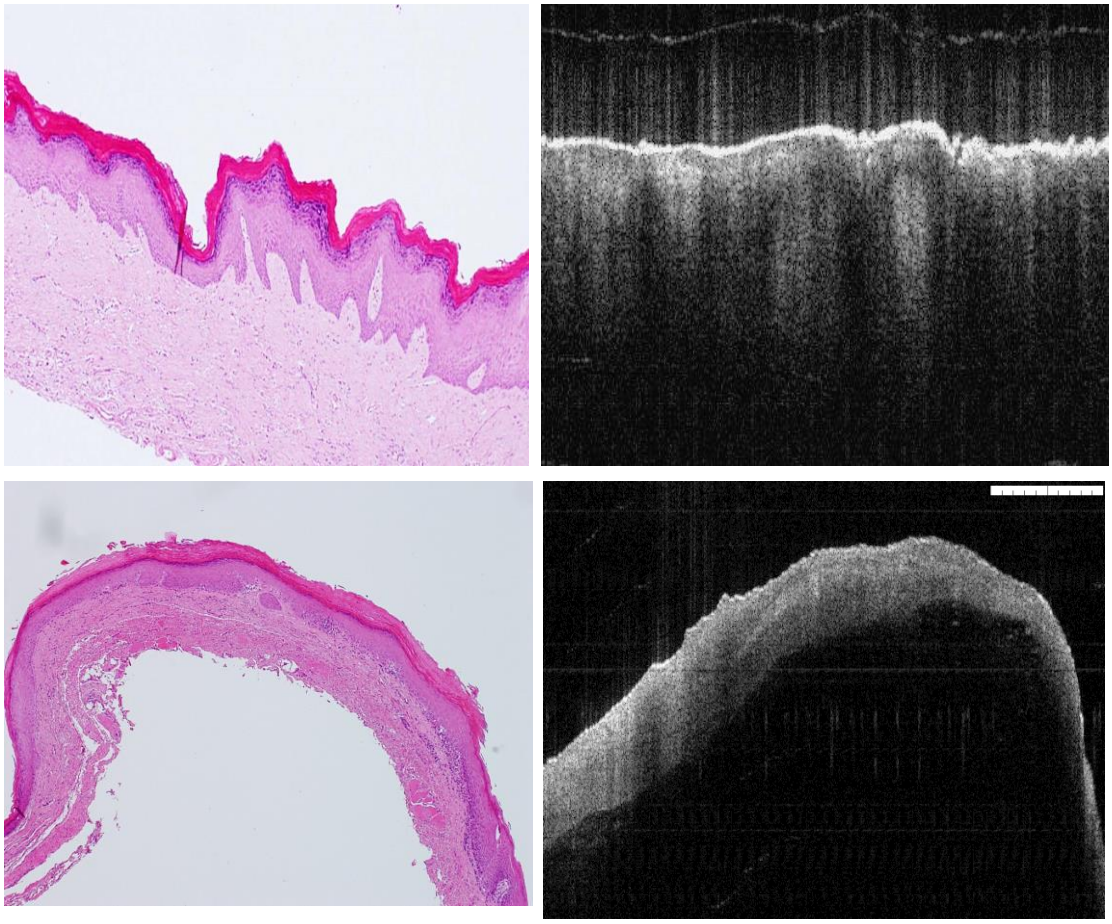

Figure 4.10: Data (OCT images) used for training the clinician and pathologist to identify pathological processes. The images were compared to the gold standard histopathology. Top image: hyperkeratosis with epithelial hyperplasia (30, 320µm KL/EL thickness on histopathology vs. 30, 330 µm on OCT); bottom image: cystic lesion (0/120µm KL/EL thickness on histopathology vs. 0/100µm on OCT).

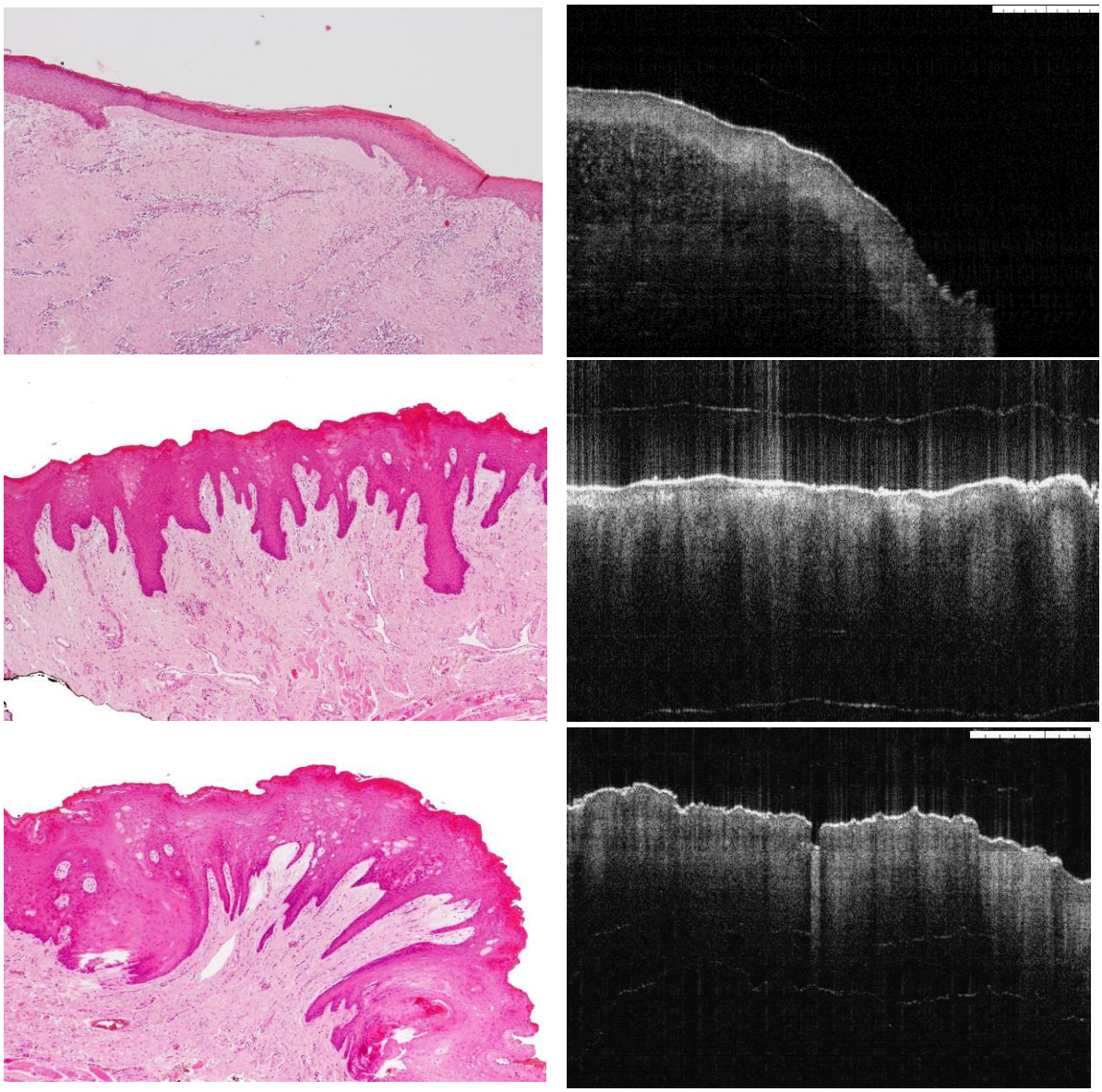

Figure 4.11: Data (OCT images) used to train the clinician and pathologist to identify pathological processes. The images were compared to the gold standard histopathology. Top image: normal epithelium of the floor of the mouth (20, 200µm KL/EL thickness on histology vs. 10, 180 µm on OCT) ; Middle image: normal epithelium of the tongue (10, 350µm KL/EL thickness on histology vs. 10, 340 µm on OCT) ; bottom image: epithelium dysplasia from buccal mucosa (10, 450µm KL/EL thickness on histopathology vs. 10, 430 µm on OCT).

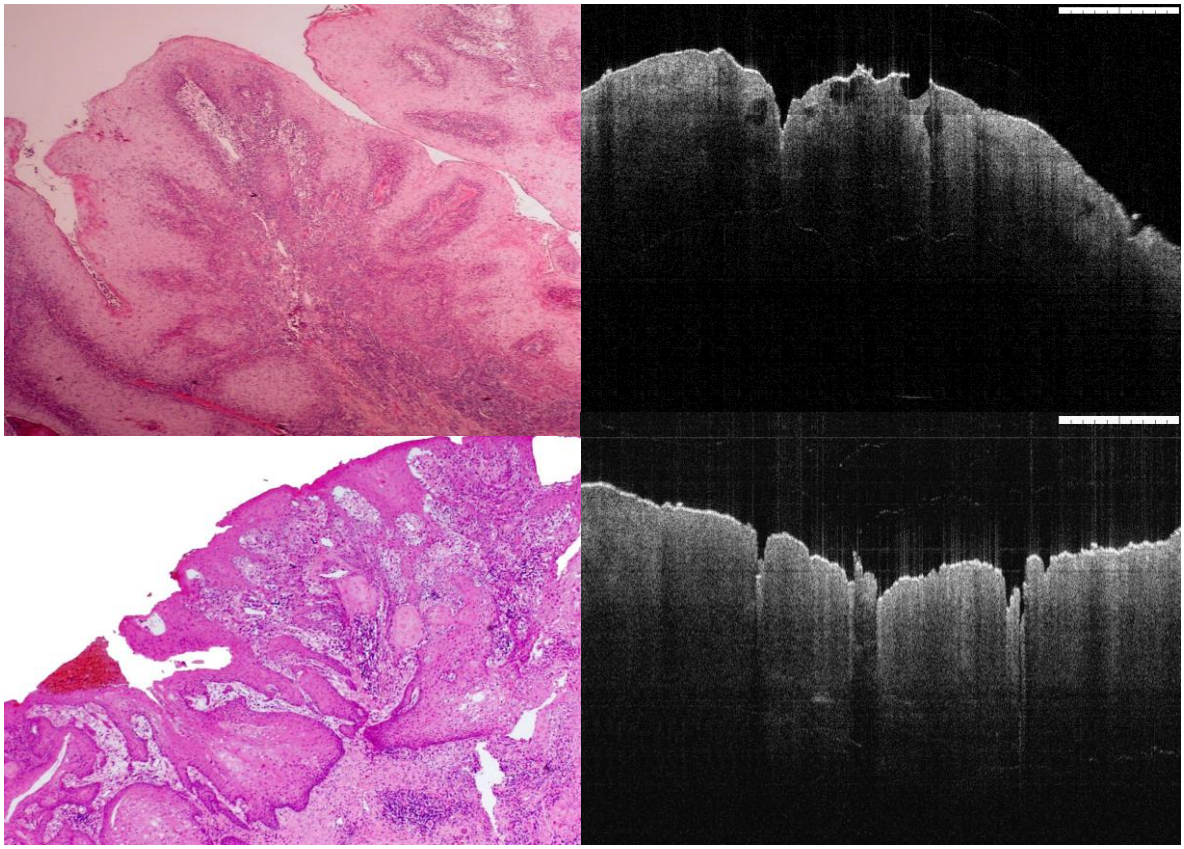

Figure 4.12: Data (OCT images) used to train the clinician and pathologist to identify pathological processes. The images were compared to the gold standard histopathology. Top image: focal SCC (0, 600µm KL/EL thickness on histopathology vs. 0, 500 µm on OCT); bottom image: multi-focal SCC (10, 650µm KL/EL thickness on histopathology vs. 10, 620 µm on OCT).

Section IV: Assessment of oral squamous cell carcinoma resection margins

Background

Incomplete surgical removal of cancer is believed to be the main cause of local recurrence and high mortality. In previous section of this chapter, OCT proved successful to identify tissue structure in healthy and pathology specimens with good sensitivity, specificity and accuracy.

Objectives

This study assessed the use of the OCT in examining oral squamous cell carcinoma resection margins to see if this modality could guide the surgeon during surgical resections.

Materials

Identical protocols were used to recruit 28 consecutive patients who presented with oral squamous cell carcinoma (OSCC) to the UCLH Head and Neck Centre. The study protocol was approved by the Moorfields & Whittington Local Research Ethics Committee for Human Research.

All the patients presented with clinical features suggestive of malignant oral mucosal disease. Detailed clinical examination was performed on each patient to assess the site, size, and the clinical characteristics of the lesion. Incisional surgical biopsy was acquired from each patient and confirmed the diagnoses of OSCC. Clinical staging at time of presentation showed that 20 patients had T1N0 disease and 8 patients had T2N0 disease.

Discussion at the multidisciplinary meeting advised that all patients to undergo surgical removal of the tumour with no prophylactic dissection of the cervical chain. Written informed consent was obtained from every subject. Demographic information of each patient was collected in pre-made proformas. The inclusion criteria included only T1-T2 OSCC with no nodal disease was aimed to facilitate the scanning of the thin resection margins via OCT rather than including patients with bulky tumours.

Assessment of OCT images was carried out by two surgeons; both were taught about interpreting OCT images and provided with training set to consolidate their knowledge and assessment skills prior to the assessment of the 112 OCT images (Figure 4.13). Each assessor was provided with brief clinical history of the patient and was asked to comment on every corresponding OCT image using a pre-made proforma. Metric readings were recorded for the epithelial layers at the resection margins area by the principal investigator.

Results

Nineteen patients were males (67.9%) and nine were females (32.1%); with a mean age of 61 years (range 36-103 years). Approximately one-third of the patients were current smokers. Over 40% of the patients consumed alcohol on a regular basis and less than 10% chewed betel nut (Table 4.31).

Half of the lesions presented as ulcers; and the rest manifested as plagues or papules. Fifty percent (n=14) of the lesions manifested as erythroplakia, 35.7% presented as leukoerythroplakia and 14.3% as homogeneous leukoplakia. The anatomical distribution of the lesions showed 7 in the ventro-lateral tongue, 6 in the floor of mouth, 4 in retromolar trigone (n=4) and 3 in the buccal mucosa (Table 4.31).

The pathological results of the margins status revealed 90 (80.35%) were defined as tumor-free and 22 (19.65%) as having some degree of tumor (Table 4.32). The resection margin of tumour may be involved partially or completely with certain stage of tumour which manifested in the OCT as sudden change in epithelium thickness or partial loss of basement membrane which indicates presence of tumour (Figures 4.14, 4.15, 4.16). The mean thickness of the epithelial layer of the tumour-free margin was 360µm, and for the tumour involved margin 560µm (Table 4.33). Their relationship was significant ($P<0.001$).

The sensitivity and specificity for the first reader was 86% and 88%, respectively. Whilst the positive predictive value (PPV) was 66% and the negative predictive value (NPP) was 96%. The accuracy of OCT was 88% (Table 4.34). There were 10 false positives and 3 false negatives, with a Positive Likelihood Ratio (LR+) of 7.16 and

Negative Likelihood Ratio (LR-) of 1.13. The sensitivity and specificity for the second reader was 77% and 86%, respectively. The PPV was 57% and the NPP was 94%. The accuracy of OCT was 84% (Table 4.35). There were 13 false positives and 5 false negatives, with a LR+ of 5.5 and LR- of 1.16.

The average sensitivity and specificity was 81.5% and 87%, respectively. The PPV and NPP was 61.5% and 95%, respectively. The accuracy was 86%. The inter-observer agreement was very good when assessing all margins except the lateral margin (0.644), (Table 4.36).

Table 4.31: Demographics of the cohort included in this study.

	No. (%)			No. (%)
Gender			**Symptoms**	
Male	19 (67.9)		Asymptomatic	19 (67.9)
Female	9 (32.1)		Pain	4 (14.3)
			Bleeding	5 (17.9)
Location				
Ventro-lateral tongue	7 (25.0)		**Smoking status**	
Floor of mouth	6 (21.4)		Current smoking	10 (35.7)
Retromolar trigone	4 (14.2)		Ex-smoker	12 (42.9)
Buccal mucosa	3 (10.7)		Non-smoker	6 (21.4)
Lower lip	2 (7.1)			
Hard palate	2 (7.1)		**Drinking status**	
Upper lip	2 (7.1)		Current drinker	12 (42.9)
Soft palate	2 (7.1)		Ex-drinker	6 (21.4)
			Non-drinker	10 (35.7)
Colour				
Leukoplakia	4 (14.3)		**Pan chewing**	3 (10.7)
Erythroplakia	14 (50.0)			
Speckled leukoplakia	10 (35.7)		**Diagnosis**	
			T1 disease	20 (71.4)
Clinical features			T2 disease	8 (28.6)
Plague	6 (21.4)			
Papule	6 (21.4)		**Resection**	
Ulcer	16 (57.1)		CO2 Laser	7 (25.0)
			Surgical resection	17 (60.7)
Medical history			Electrosurgical	4 (14.3)
ASA I	20 (71.4)			
ASA II	8 (28.6)			

Table 4.32: Histopathogical status of the four resection margins of the cohort.

Superior margin	No. (%)
Free	24 (85.7)
Involved	4 (14.3)
Inferior margin	
Free	22 (78.6)
Involved	6 (21.4)
Medial margin	
Free	21 (75.0)
Involved	7 (25.0)
Lateral margin	
Free	23 (82.1)
Involved	5 (17.9)

Table 4.33: Measurement of resection margins using OCT. KL: keratin cell layer, EL: epithelial layer.

	Range	Minimum	Maximum	Mean
Tumour free margins				
KL thickness	20µm	0µm	20µm	20µm
EL thickness	290µm	190µm	480µm	360µm
Tumour involved margins				
KL thickness	20µm	10µm	30µm	20µm
EL thickness	230µm	530µm	760µm	560µm

Table 4.34: Clinical assessment by the first reader. Sensitivity 86%; Specificity 88; (PPV) 66%; (NPV) 96%; Accuracy of OCT 88%. TP: true positive, FP: false positive, TN: true negative, FN: false negative.

	Histology			
OCT		Positive	Negative	Total
	Positive	19	10	29
	Negative	3	80	83
	Total	22	90	112

Table 4.35: Clinical assessment by the second reader. Sensitivity 77%; Specificity 86; (PPV) 57%; (NPV) 94%; Accuracy of OCT 84%. TP: true positive, FP: false positive, TN: true negative, FN: false negative.

	Histology			
OCT		Positive	Negative	Total
	Positive	17	13	30
	Negative	5	77	82
	Total	22	90	112

Table 4.36: Raw kappa scores showing levels of un-weighted agreement between the two readers.

	Kappa
Superior margin	0.806
Inferior margin	0.713
Lateral margin	0.644
Medial margin	0.718

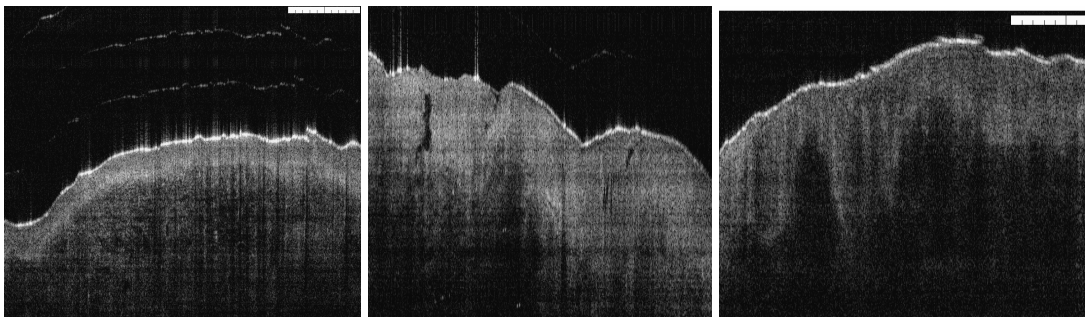

Figure 4.13: Data (OCT images) used in training both clinicians in identifying pathological processes. The images were compared to the gold standard histopathology. Left image: tumour free margin; Middle image: completely involved margin; Right image: partially involved margin.

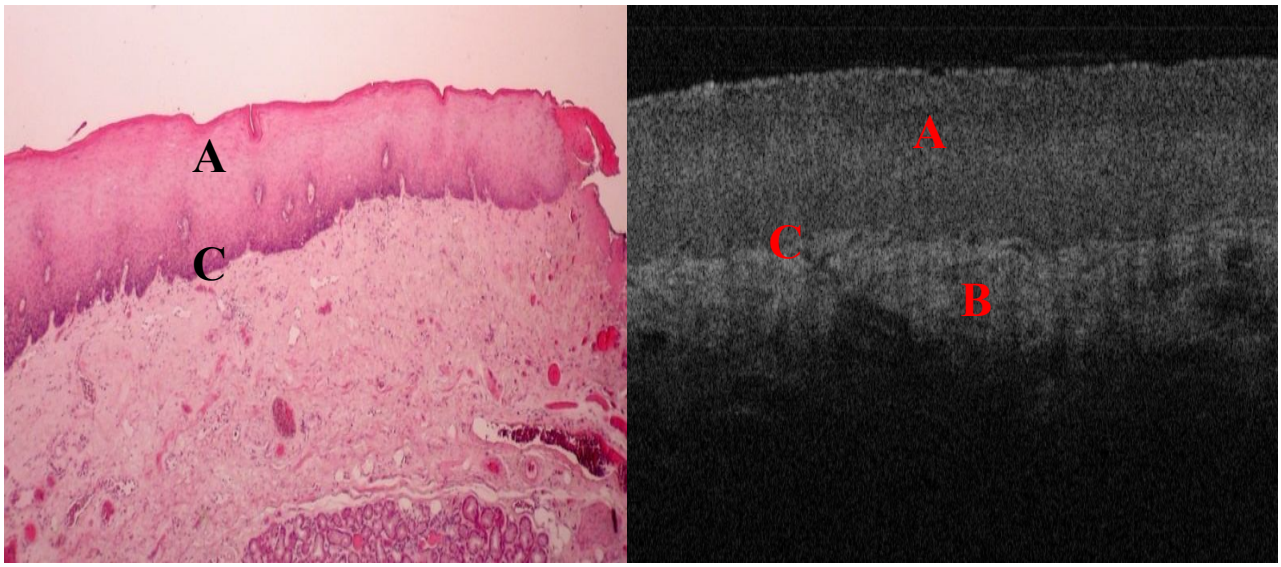

Figure 4.14: Microphotograph for H&E of buccal mucosa resection margin with OCT scan. **(A):** Well defined epithelium; **(B):** No tumour elements in the lamina properia can be found which appear on OCT as homogenous structure; **(C):** intact basement membrane.

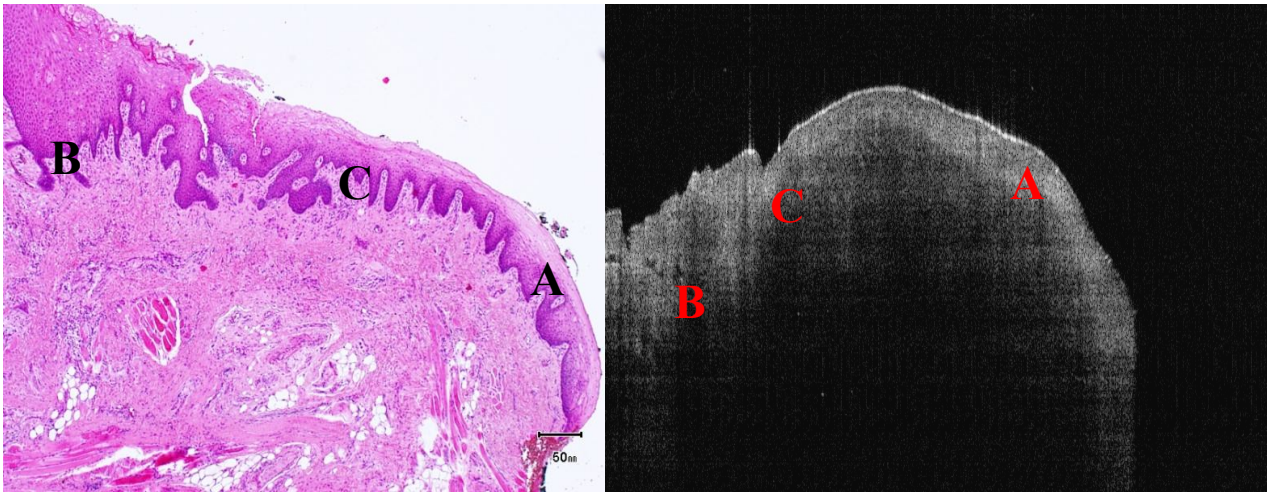

Figure 4.15: Microphotograph for H&E of floor of mouth mucosa resection margin with OCT scan showing partial tumour involvement (within the 3mm edge). **(A):** area with intact basement membrane; **(B):** breached basement membrane. **(C):** Area of transition between intact and damaged basement membrane.

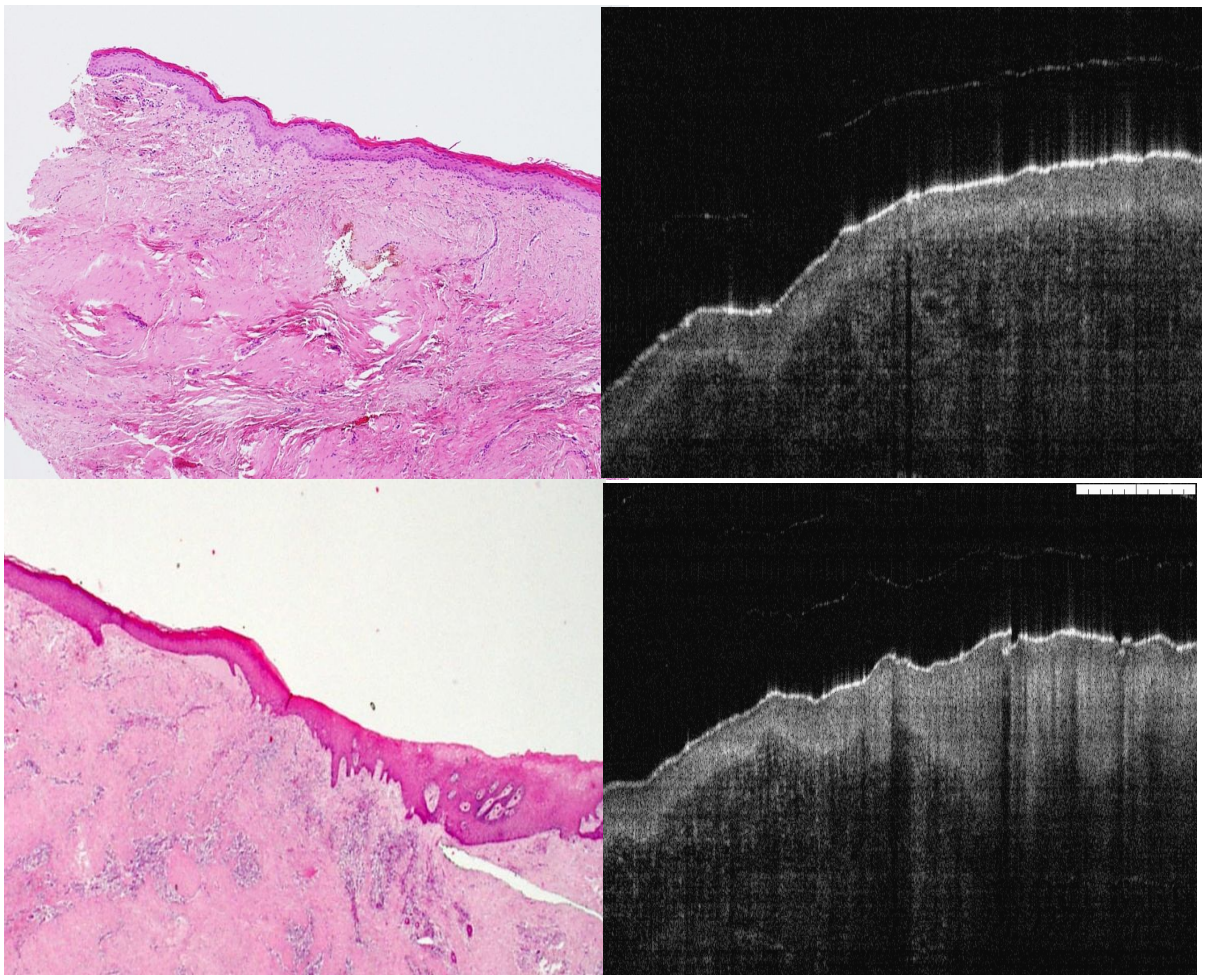

Figure 4.16: Top: tumour free margin with intact basement membrane from oral cancer lesion; bottom: cancer involved margin with breached basement membrane.

Discussion

The term "optical biopsy" refers to methods that use the properties of light to enable the operator to make an instant diagnosis in "real time". However, the term optical biopsy is a misnomer as biopsy mean surgical removal of tissue. "Optical diagnostics" seems a more appropriate term for such techniques.

Although OCT may able to evaluate frank cancer, oral dysplasia can be difficult to stage. Dysplasia is identified by cytological and architectural changes. The former includes nuclear size and shape, nuclear/cytoplasmic ratio and nuclear stratification, and is beyond the resolution of OCT. Visualization of subcellular features, such as nuclei (size, number and chromatin content) and organelles was impossible using the current set-up.

Several studies have sought to investigate the diagnostic utility of *in-vivo* OCT to detect and diagnose oral pre-malignancy and malignancy (Thomson, 2002; Tsai *et al*., 2008 (a&b)). No study adhered to solid diagnostic criteria to reach a diagnosis, mainly of oral dysplasia.

One clinical study of 97 patients used OCT imaging to detect neoplasia in the oral cavity (Lee *et al.,* 2009), revealing that the main diagnostic criterion for high-grade dysplasia/carcinoma in situ was the lack of a layered structural pattern. Diagnosis based on this criterion for dysplastic/malignant vs. benign/reactive conditions was more difficult.

The result of this study found that OCT images of the oral cavity and oropharynx provided microanatomical information about the epithelium, basement membrane and supporting lamina propria of the mucosa, and showed distinct zones of normal, altered and ablated tissue microstructures for each pathological process studied.

OCT images of dysplastic lesions revealed visible epithelial thickening, loss of epithelial stratification and epithelial down growth. However, these criteria are not sufficient to draw firm conclusions and to grade oral dysplasia.

SCC of the oral mucosa were identified in the OCT images by the absence or disruption of the basement membrane, an epithelial layer that was highly variable in thickness, plus areas of erosion and extensive epithelial down-growth and invasion into the sub-epithelial layers.

Therefore, adequate normal tissue from different part of the oral cavity is necessary for thickness measurement. Measurement of normal resection margins of oral SCC lesions is one of the best approaches for validating the OCT in comparison with the gold standard of histology. Moreover, comparison with pathology is very important when validating the OCT as a reliable tool.

Ideally, this experiment measure the epithelial thickness of the oral cavity of young healthy individuals by OCT and light microscopy, but, of course, this would be unethical because it would require healthy individuals without oral disease to undergo further histological examination.

OCT histometric measurement has received renewed interest in recent years following its adaptation for the measurement of corneal thickness (Prakash *et al*. 2009). Its ability to measure epithelial thickness *in-vivo* is a major advantage over traditional instruments designed to measure biochemical and morphological changes. However although its application in oral tissue has been explored in previous studies, its use in the assessment of oral epithelial thickness has been ignored. Our study is the only study to date to establish a quantitative comparison between epithelial thickness with OCT and light microscopy *ex- vivo*.

This study examined the volumetric dimensions of normal tissue to enable a better understanding of the prospective features of tumour-bearing and or dysplasia-bearing sections of oral mucosa. Accurate measurements of the normal epithelial dimensions of the oral cavity are important in order to understand the development of oral dysplasia or cancer as well as to monitor progressive dysplasia or benign-looking lesions.

Similar studies have been conducted elsewhere in the body, particularly in the eye. Chauhan and Marshall (1999) found that the total thickness of both fixed and fresh

bovine retinas as determined by OCT showed a strong linear correlation with measurements obtained by light microscopy, although this work has been criticized as describing artifacts. Wirbelauer *et al.* (2002) found that the thickness of diseased human corneas measured by *in-vivo* OCT was directly proportional to that measured by light microscopy of the same specimens when fixed *ex- vivo*.

Kraft *et al*. (2008) used OCT to measure the thickness of the laryngeal epithelium but only those that were diseased. Their study attempted to quantify the epithelial thickness of the vocal cord *in vivo* but the authors did not report the thickness of normal epithelium. Another limitation of the above mentioned study is that the volumetric analysis was restricted to the larynx itself, rather than the entire upper digestive system wall.

Using OCT to compare epithelium thickness at the floor of the mouth, tongue, buccal mucosa, palate and lip was a bright aspect of the current study. This rise important point that there is a difference even in physiologically similar group like buccal and floor of mouth.

In this research, the difference in oral epithelium thickness measured via OCT was marginal in the first two readings was found. The smaller difference in the final readings in the current study is likely attributable to shrinkage, which made the OCT readings more similar to those obtained via histology. However, the optical density and image resolution appeared similar in all readings. The significant difference in the correlation between the second and third reading may be attributed to the delay in examination of these specimens, allowing tissue decomposition to influence the morphology of the different tissue layers.

The 30-minute gap between the first and second reading was intended to test reproducibility. The reproducibility of the coherence interferometry measurement techniques used in this study has a significant impact to use OCT to monitor oral lesions. This study demonstrated excellent reproducibility in the novel use of the OCT to measure the thickness of the oral epithelium. Furthermore, the study demonstrated the validity of the OCT, which is currently widely used in head and neck research without any previous indication of reliability.

To optimize topographic repeatability, sutures were used as a landmark to provide guidance for specimen orientation. These sutures were also used to help correlate OCT scans with histopathology.

In comparison to histological images, the OCT produced thinner measurements of the epithelium thickness although the difference of more than 40 μm was noticed in the tissue of the buccal mucosa and floor of mouth. This may be because the contraction index of non-keratinized tissue such as the buccal mucosa, lip and floor of mouth was slightly greater than that of the palate, tongue and gingiva. Another possible reason could be that the OCT measurements were not made on the exact section used for histopathology, resulting in a slight error in the measurements. In some biopsies we found a discrepancy between OCT and histology measurements due to prominent rete pegs, which were not usually visible by OCT due to insufficient image resolution.

In contrast, Wirbelauer *et al*. (2002) found the thickness of corneas measured *in vivo* by OCT was, in fact, greater than the thickness of the same corneas measured *ex vivo* by light microscopy, by about 9%. This is in keeping with histological shrinkage. However, Chauhan and Marshall, working with *ex-vivo* bovine retinas, found the opposite: that light microscopy measurements were often larger than those of OCT by a comparable factor. Given that histological preparation generally results in tissue shrinkage, our findings are somewhat surprising in that the OCT measurements were similar to or even smaller than light microscopy measurements for several subsites.

The confidence interval (CI) of the OCT measurements of thickness in this study ranged from -0.78 to +1.04, demonstrating that the measurements were relatively precise. The difference between measurements made by OCT and histology reported for the buccal epithelium may not be clinically meaningless as the difference was less than that recorded on the *in-vivo* scan.

The use of histological slides and light microscopy to measure normal epithelial thickness is not without its disadvantages. For microscopic examination, tissue must first be removed and then subjected to fixation, sectioning and staining, which may result in artifacts. Our study design (*ex-vivo*) meant that we avoided the typical 33%

shrinkage of the tissue after resection. However, further manipulation for histological preparation such as embedding and sectioning may result in up to 20% further reduction in size (Kimura *et al*., 2003).

In the future it may be valuable to image oral tumours during and immediately after surgery, and then after each step in the histological processing cascade to determine the effect of perfusion, formalin fixation, ethanol dehydration and paraffin embedding on the epithelial thickness. Nevertheless, morphometry of histological specimens will always be subject to highly variable shrinkage artifacts, and these can vary considerably depending on the nature of the tissue (e.g., lamina propria versus epithelium).

Our study was more controlled than that of Kaiser *et al*. (2009), who encountered problems with direct probe contact with the tissue under investigation. Even slight pressure created by the probe may be sufficient to alter the measurements, and it is impossible to gauge the amplitude of the pressure exerted by a hand-held probe.

Few studies have evaluated the thickness of the healthy epithelium within the oral cavity and oropharynx using light microscopy alone. Klein-Szanto and Schroeder, 1977 reported that the oral epithelium varies from 75 to 550 μm in thickness. The epithelium of the floor of the mouth was thin (86 ± 13 μm). The epithelium of the alveolar mucosa was thicker (260 ± 40 μm) than that of the floor of the mouth. The buccal epithelium, on average, was 480+90 μm thick. The hard palate was 248±37 μm thick and the attached gingiva was 255 ± 57 μm thick, whereas the underlying LP may extend up to 2000 μm (Paulsen and Thale, 1998). Our values were consistent with these results, particularly in the buccal mucosa and floor of the mouth. However, the values for the alveolar mucosa were rather different.

The angle of measurement played a pivotal role in our results. A tilted measurement produced smaller values, and an oblique measurement produced smaller or larger values than the perpendicular measurement. Such errors can be minimized in OCT by capturing and measuring the axial dimension of the thickest part of the mucosa. In contrast, some of the oblique measurement is difficult to be avoided with OCT because there is no way to ensure that the thickest portion of the mucosa is

consistently measured. This is of particular interest when studying *ex-vivo* samples as the peripheral end of the specimen may kink as a result of contraction of the collage bundle.

In order to obtain an image of the entire 5 mm normal edge, the OCT light was focused perpendicularly to the mucosa while the end of the suture was pulled to counteract the contraction of the collagen.

OCT instrumentation is typically more readily available and precise than other systems that can provide information on the oral epithelium, such as confocal microscopy. However, the limited penetration depth of up 350 μm of confocal microscopy may not be sufficient to allow characterization of pre-malignant and malignant lesions of different histological origins (White *et al*., 1999; Farahati *et al*., 2010). Unlike in OCT, the basement membrane cannot be identified in confocal microscopy, which makes discriminating malignant lesions difficult as visualization of neoplastic cells is restricted to the superficial layer of the epithelium. However, confocal microscopy gives the opportunity for rapid acquisition of high-quality images similarly to OCT even in *ex-vivo* specimens (Just *et al*., 2007; Just *et al*., 2006).

The study on sensitivity and specificity of the OCT to diagnosis suspicious oral lesions demonstrated that the thickness of the keratin cell layer alone is not diagnostic in term of discriminating malignant from non malignant lesion. There was a marginal difference between all groups such that it was hard to ascertain whether the increase in thickness of the layer was part of the cancerous process or a reaction to local irritation.

Within the benign lesions, hyperkeratosis only involved an increase in the thickness of the parakeratin or orthokeratin layer of the epithelium, while the other layers of the epithelium remained unchanged, with or without some degree of hyperplasia. In contrast, epithelial dysplasias may or may not show parakeratinization, which might reflect the stage of dysplasia and cellular immaturity. This means that assessment of these layers individually by OCT is fruitless.

On the other hand, mucoceles had the thinnest keratin cell layer, while keratosis had the thickest layer. Amazingly, a thin keratin cell layer was linked with invasive carcinoma as we expected to see thick layer as part of poor differentiation of the epithelium. One cause of this could be the atrophy of the top layer, especially when the lesion manifests clinically as erythroplakia and/or ulceration.

The highest epithelial thickness was found in cancerous lesions. Dysplastic lesions show fluctuations in thickness, so it is difficult to draw any conclusions regarding the benign and early pre-cancer stage. Our results demonstrate that it is possible to distinguish healthy/benign lesions from advanced dysplastic lesions. We achieved excellent results in discriminating cancerous tumours from healthy tissue. Interestingly, this was based on good agreement between observers regarding basement membrane status.

Our results confirm and expand the findings of previous investigations. Wilder-Smith *et al*. (2009) analysed 50 patients with different oral lesions *in-vivo*. The sensitivity and specificity of the diagnostic algorithm was assessed according to the criteria established by Macdonald *et al*. (1981), which score epithelial dysplasia in the hamster cheek pouch according to criteria based on human oral mucosa. On the contrary, our results revealed the difficulties of differentiating between different grades of oral dysplasia using the classification system of the cellular component.

The sensitivity and specificity of this investigation were generally lower than expected. This may be attributed to two factors. First we used *ex-vivo* samples that lacked fluid perfusion, which ultimately affected optical scattering properties and image resolution. The effects of ischaemia, such as cell lysis, alter tissue microstructure and therefore can affect optical scattering and imaging contrast. Secondly, the differences in sensitivity and specificity compared with other studies were almost certainly related to the difference in the methodologies used to score sensitivity and specificity.

A study conducted by Isenberg *et al*. (2005) reported the accuracy of their OCT system in detecting dysplasia in Barrett's oesophagus, with a sensitivity of 68% and a specificity of 82%. The positive predictive value of OCT for dysplasia was 53%, and

the negative predictive value was 89%. Although dysplasia in the oesophagus differs from that in the oral cavity, the diagnostic accuracy of the OCT in the latter study was 78%, which was lower than that in the current study. This is equivalent to the level of accuracy of microscopic assessment of dysplasia tissue sections by pathologists. Furthermore, the high negative predictive value for one of the examiners (the clinician) may be potentially advantageous for future clinical applications.

Fomina *et al*. (2004) investigated the capability of *in-vivo* OCT for the diagnosis of oral lesions. In comparison to our results, the specificity of their study was much higher, with very good inter-observer agreement. We assume that the *in-vivo* application of OCT would help clinicians to be more sensitive and specific. This speculation comes from the fact that the contralateral anatomical side helps to control the benchmark reference point. In terms of specificity, the former study reported 83%, which is within the range of our value.

An unanticipated result of the present study was the poor agreement regarding changes in the keratin cell layer. The reasons for this are unclear. However, the training exercise was robust and placed great emphasis on reducing discrepancy. The degree of variation in interpretation of this parameter did not influence the accuracy.

Another important outcome of the statistical analysis was the ability of OCT to separate benign lesions from all other lesion types despite having the same or similar outward appearance. Many optical techniques are capable of discerning normal from malignant oral mucosa with a high degree of sensitivity and specificity, but the discrimination of benign lesions from precancer and cancer is more elusive (Wilder-Smith *et al*., 2010).

The result of this study was consistent with that of Kraft *et al*. (2008) in terms of the increase in epithelial thickness from benign lesions towards well-established SCC. However, the laryngeal mucosa is a distinctive tissue, unlike the oral mucosa, which is versatile and divided into three categories: masticatory, lining mucosa and specialized mucosa.

The basement membrane has previously been used as a key landmark in order to discriminate between benign or premalignant oral lesions and frank malignant tumours. The basement membrane helps examiners to decide whether the lesions are cancerous or not. Other parameters also help to differentiate pre-cancer from benign lesions. However, changes in these variables can also help to differentiate benign from pre-cancerous lesions.

Despite the excellent sensitivity, specificity and good agreement on basement membrane status, we found only moderate agreement on basement membrane quality. This means that the basement membrane, as a parameter, is highly subjective. However, although there may be an issue regarding its quality, overall the basement membrane was identifiable. One may conjecture that the most likely cause of the good agreement, as opposed to very good or excellent agreement, may be the shadows produced as a result of partial tissue thickness, which would not occur in the real clinical situation.

The current study suggests that good agreement can be achieved in the assessment of epithelial thickness. Our overall kappa value (0.452) was slightly lower than that for the basement membrane. The intra-observer agreement was similar for the lamina propria and keratin cell layer. It was reassuring to observe good agreement for biopsy taking between the observers, despite the discrepancy in sensitivity and specificity.

The poor agreement seen in the status of the lamina propria is a concern. A number of reasons for this have been suggested, including the lack of tissue perfusion, which may alter light scattering or decrease light penetration. It is also possible that about one third of the suspicious lesions were originally SCCs, which may bewilder the examiner regarding the status of the lamina propria.

The kappa agreement between the pathologist and the clinician regarding the basement membrane status was 0.6, which means that OCT is able to discriminate SCC. The precise assessment of a tumour in its horizontal extent was investigated in the last section of this chapter. This factor is paramount to ensure complete surgical removal and to predict local or regional failures (Yuen *et al*., 2000).

The potential of OCT in objective disease assessment of tumour margins was explored, based on the hypothesis that OCT-assessed epithelium may be a measure of marginal status. The results indicated that epithelium as measured by OCT reflects disease severity at both normal and abnormal margins. Although the number of tumour-laden margins was small, a range of relevant morphologies was represented, and the results indicated that some of the *ex-vivo* OCT images matched some of the histopathological features demonstrated in oral cancer.

The limited depth of penetration of OCT was not thought to play a role in our results since the poorest results were obtained in the lateral rather than the deep margins. A significant difference in oral epithelial thickness was found and attributed to the abnormal cell function and breach of the natural barrier of the basement membrane.

It is critical to accurately evaluate the extent of the tumour using conventional visual examination and palpation. Computed tomography (CT) and magnetic resonance imaging (MRI) are currently used to evaluate tumour extent. These radiological techniques do not have enough resolution and density to accurately measure tumour dimensions with certainty. The delineation between the normal tissue and tumour is confusing, making it difficult to identify most of the tumour within 5 mm margin, which is not suitable for most T1 and T2 oral cancers (Heissler *et al*., 1994).

In comparison to ultrasound, OCT showed good resolution with the ability to acquire detailed data concerning the tongue and floor of the mouth. Songra *et al*. (2006) reported on 14 patients with oral carcinoma undergoing ultrasound imaging. They found ultrasound detection of close surgical margins to have a sensitivity of 83% and a specificity of 63%.

The mean sensitivity and specificity obtained by Songra *et al.* (2006) were 81% and 87%, respectively, being slightly lower in terms of sensitivity compared with our results. However, specificity was much higher despite the difference in study design. Tumour thickness and margin status were measurable when tumour thickness was more than 1 mm according to the sonograph, which is invaluable in shallow tumours.

Shintani *et al*. (1997) used ultrasound to assess the thickness of tongue carcinomas preoperatively. Scans and measurements were compared with those from histological sections after resection of the primary tumour. Their study showed a significant correlation between the two measures.

Determination of marginal status by frozen section has been reported not only in oral cancer but also in breast and prostate carcinoma (Riedl *et al.,* 2009; Eichelberg *et al*., 2006). However, this technique is currently limited by low accuracy to define the involvement of the margins of resection by neoplasia at the time of resection.

Shrinkage of the specimen may lead to under- or overestimation of tumour thickness. Shrinkage is usually subdivided into two types: shrinkage that occurs immediately after tissue resection due to collagen and muscle fibre contraction and shrinkage that affects tissue during embedding and preparation of the specimens during lab processing. Regardless of the type of shrinkage, tissue changes occur volumetrically in three dimensions. Contraction of the vertical collagen and muscle fibres in the connective tissue may increase the actual epithelial thickness. However, contraction of the vertical bundles may not alter epithelial thickness substantially because it is difficult for cells to slide in a vertical manner.

Johnson *et al*. (1997) reported the mean of loss of depth in tongue specimens following resection to be 30.7%. Our study design led to minimum tissue shrinkage for two reasons. Firstly, a tumour consists of non-contractile tissue while the surrounding tissue is filled with contractile musculature, which makes the tumour un-shrinkable. Secondly, the *ex-vivo* specimen absorbs most of the shrinkage, which makes comparison of OCT images with pathology more accurate and precise.

The potential interpretation bias inherent in this prospective clinicopathological study was limited by the single blind style of the study and the two observers' records. This study design is an ideal stepping stone in providing a real-world example of the use of OCT to assess tumour margins.

The cause of some false negatives may be due to the fact that the tumour's vertical depth of invasion, like an iceberg, is much more difficult to assess with OCT due to limited light penetration. Furthermore, if the tumour has a non-cohesive invasive front, even conventional assessments of depth measurements may be inaccurate. This fact was confirmed on two margins in the specimen as the tumour extended from the central part toward the edges without breaking the basement membrane. In addition, tumours frequently develop fingerlike extensions. This type of sub-mucosal tumour extension is very difficult to identify by OCT. However, scanning of the central part of the tumour may give an overall indication of the shape and extent of the tumour. It may even be possible by surveying the exposed margin to predict a non-cohesive front and to estimate the other margins.

Positive margins for specimens are not only present in the thickness of the mucosal membrane, but, as reported by Yuen and colleagues, sub-mucosal and intramuscular spreads are both important zones of positive margins (Yuen *et al.,* 1998).

One limitation of the *ex-vivo* study design was the co-localisation of images with histology. The method used in this study provided as accurate as possible matching between the region of pathology and histology. However, exact control of the histological plane is difficult. Processing artifacts may also be a problem in histology. Another limitation was the lack of a blood supply, which may affect image quality.

Conclusion

This study validates the use of OCT in identifying structural changes in healthy and pathological oral mucosa. Measurements made with the OCT were also valid and reproducible with minor underestimation. Furthermore, OCT demonstrates the ability to discriminate cancerous oral lesions with a variable degree of sensitivity, specificity and accuracy. This may lessen the delay in cancer diagnosis and significantly improve the examiner's ability to correctly diagnose invasive carcinoma. Epithelial thickness and the status of the basement membrane play key roles in OCT image interpretation. Keratin cell layers provide little diagnostic information alone. However, combining the clinical information regarding the thickness of the epithelium and keratin cell layer may provide valuable diagnostic information.

For the assessment of resection margins, our study demonstrates that OCT interrogation of the margins of oral cancer specimens is moderately accurate. A tumour-free margin can be predicted with a moderate degree of certainty. The most important point for clinical practice is the high level of agreement found between observers. The OCT prediction of the tumour-involved margin is therefore as reliable as the prediction of tumour thickness. The predictive information obtained from this study regarding tumour thickness and resection margin status could be of significant use in treatment decision-making in future *in-vivo* research.

Chapter 5
Ex-vivo histopathologic versus OCT work for skin

Introduction

Skin cancer is the most common cancer in the western world. It encompasses basal cell carcinoma (BCC), squamous cell carcinoma (SCC) and malignant melanoma (MM) (Diepgen and Mahler 2002). The incidence of skin cancer is still increasing globally, which introduces a huge health and financial burden on health systems (Holme *et al*., 2000; Levi *et al*., 1988). This trend can be counteracted by means of primary prevention (avoidance of risk factors) and secondary prevention (early diagnosis and intervention).

Early diagnosis is usually achieved by regular visual inspection and a surgical biopsy when required. It is clearly impractical to conduct a biopsy on everyone, and there are no consistent guidelines for taking biopsies. In recent years, advances have been made in human skin imaging by OCT. Numerous studies comparing and identifying structures imaged by conventional histological sectioning and OCT have been conducted. However, step by step validations of the system are still scarce. For example, normal skin histometric measurements are important, not only for cancer application but also for physiological and cosmetic applications such as wrinkles that deepen and align in a parallel pattern.

Light microscopy may still be considered the "gold standard" of diagnosis and for the measurement of epidermal thickness, and the standard by which other methods are compared. However, conventional comparison between *in-vivo* OCT with formalin-paraffin processing used in earlier studies (Gambichler *et al.,* 2006(a); Freeman *et al.,* 1962; Southwood, 1955) is unsuitable for the determination of stratum corneum and epidermal layer thicknesses due to tissue shrinkage (Therkildsen *et al*., 1998).

With the interventional approach (surgery), tumour involvement in resection margins is found in 11–16% of all surgical excisions for patients who undergo skin-conserving surgery (Talbot and Hitchcock, 2004), namely those patients requiring additional surgery or intensified radiotherapy. As a result, high local recurrence rates are reported, even in patients with tumour-free specimen margins treated with surgery.

In this study we aim to:

(1) identify cellular structures of normal facial skin using OCT and compare it to the gold standard histology
(2) correlate the OCT resolution ability to count epidermal ridges
(3) differentiate between the structural changes of normal and pathological facial skin
(4) build on a diagnostic criterion for the use of OCT in the detection of suspicious facial skin lesions
(5) determine the sensitivity and specificity of pre-agreed OCT imaging criteria for the *ex-vivo* diagnosis of skin lesions
(6) test the degree of agreement of certain criteria with the anticipation that these criteria could provide a useful adjunct *in-vivo* modality for the diagnosis of skin cancer
(7) assess the role of OCT in identifying tumour-involved resection margins in patients undergoing surgical resection

Section I: Structural validation of facial skin

Background

OCT is an optical imaging technology that allows real-time imaging with micrometre resolution offering the potential to map skin abnormalities.

Objectives

In this study we aim to (1) identify the cellular structures of normal facial skin using OCT and compare it to the gold standard of parafin section histology, (2) differentiate between the structural changes in normal and pathological facial skin, and (3) build on a diagnostic criterion for the use of OCT in the detection of suspicious facial skin lesions.

Materials

Fifty-seven facial lesions from 53 patients who were presented with suspicious lesions to the UCLH Head & Neck Centre, London, were recruited for this study. The study protocol was approved by the Moorfields & Whittington Local Research Ethics Committee of Human Research. The protocol was devised in cooperation with the Departments of Pathology at University College London. Informed consent was obtained from each patient, explaining the nature of the study. Inclusion criteria included that the patients were 18 years of age or older and had no prior skin cancer in the same area or any skin procedures (i.e. electrosurgical excision, PDT, cryotherapy, etc.).

Result

All data were entered and stored in a computerised database designed in Microsoft Excel 2000. The statistical analysis was performed using the statistical software package SPSS 13.0 (SPSS, Chicago, Ill).

Fifty-seven clinical and pathologically different skin lesions from 53 patients were obtained. The lesions were obtained from 34 women (64.1%) and 19 men (35.9%), ranging in age from 38 to 84 years (median age: 48.4 years). Twenty-nine (53%) were located on the cheek, 16 (28%) were on the nose, 6 (10.5%) on the ear, 3 (5.0%) were on the forehead and 3 (5.0%) on the lower lip.

Histopathological evaluation revealed that 26 (45.5%) patients had basal cell carcinoma (BCC), 12 (21%) had squamous cell carcinoma (SCC), 9 (15.9%) had actinic keratosis (AK), 7 (12.3%) had invasive malignant melanoma (MM) and 3 (5.3%) were diagnosed with lentigo maligna (LM).

The most common histological subtype for the BCC was nodular (53.5%), major cystic (21.5%), microcystic (17.8%) and the least common type was superficial (7.2%) BCC. The majority of SCC was located on the ear, followed by cheek and forehead (Table 5.1).

OCT and histology correlation (normal margins)

OCT was able to visualise and differentiate skin layers and structures such as stratum corneum, epidermis, and papillary dermis. Only a few large and prominent epidermal papilla can be correlated 50%. Description of features in normal facial skin was straightforward for the assessors (Figure 5.1). This resulted in 93% of the specimens identified in the dermal-epidermal junction, 100% in identified in the epidermal layer, and 100% in the stratum corneum layer (Table 5.2).

OCT and histopathology correlation

With respect to actinic keratosis, correlation was achieved in 60% of the specimens by identifying thickening in the DEJ, 100% by identifying the destruction in the corneum layer and 89% by identifying thickening in this layer.

With regards to basal cell carcinoma, correlation was achieved in 100% of the specimens by identifying the dermal-epidermal junction, 100% in identifying epidermal, keratin cell layer. With nodular BCC, the areas beyond the dermal–epidermal junction exhibited a solid nest or honeycomb form in 93% of cases. While major or microcystic BCC showed small multiple empty spaces in 100% of cases. Superficial spreading BCC were mainly represented by cords or small buds protruding from the epidermis into the superficial dermis in 100% of cases.

With regards to squamous cell carcinoma, correlation was achieved in 91% of the specimens by identifying the dermal-epidermal junction as damaged, 83% in by identifying epidermal layer as increased, and 100% in the description of the stratun cornium layer and its changes. Other features included small bright clusters (nonhomogenousness) within the papillary dermis (80%).

With regards to lentigio maligna, correlation was achieved in 30% of the specimens by identifying the rete ridges as elongated, and 30% by identifying nests or lobules within the epidermal layer near the DEJ.

With regards to malignant melanoma, correlation was achieved in 85% of the specimens by identifying abnormal signals within the papillary dermis layer, which was exhibited as diffuse or patchy reflectivity and loss of the typical bright horizontal linear structures, and 57% the dermal-epidermal junction was described as intact with prominent junctional densities (Table 5.3).

Qualitative OCT analysis for different pathology

In normal skin, the majority of the top layer (stratum corneum (SC)) shows more signal reflection than the lower layer that represents the epidermis. The SC was fissured and wrinkled in the areas on the face. The epidermis, the second layer below the SC layer, appears significantly darker (low signal reflection) until the transition with the dermis. The signal intensity between the lower boundary of the epidermis represents the dermo-epidermal junction. There is no boundary for the dermo-epidermal junction except the smooth or undulated demarcation between the less reflective/backscattering layers of the epidermis to the highly reflective/backscattering papillary dermal layer.

Discretion of stratum corneum layer (SC)

In AK, the SC layer demonstrates hyper-reflective features (bright) due to a water/SC refractive index difference, mostly with focal areas of damage. The damaged area appears as a punched out depression, with or without lifting of the stub from the epidermal layer (Figure 5.2). In the nodular and infiltrating BCCs, this layer has normal-reflective features because the tumour infiltrates the deeper tissue dissimilar to

the ulcerative type. In LM and MM this layer either disappears or presents very thin hypo-reflective features.

Description of epidermal layer (EL)

Epidermal thickness is of considerable significance in AK, with homogeneity similar to the surrounding normal margins. The situation is similar in BCCs with dark spaces (solid or empty) within the epidermal layer with different sizes (Figures 5.3 and 5.4). Unlike the AK, BCCs have EP layer thicknesses which vary significantly for different histologic sub-types.

In LM, the EP layer usually becomes atrophied in the active areas, with some hypoecoic areas which represent junctional activity in the rete ridges (Figure 5.5). With MM, elongated rete ridges are mainly seen (Figure 5.6).

Description of dermal layer

In AK, the dermal layer is completely normal with signal-poor snail-track like cavities corresponding to blood vessels, hair follicle and some sweat glands. Some tumours aggregate as signal-poor round spots surrounded by hyporeflective bands in some case of BCCs.

For SCCs and MMs these non-homogenous areas are signal-free globules, and are concentrations of melanin or keratin pearl in spherical or elliptical arrangements below breached dermo-epidermal junction usually extending from EL so there is no band surrounding the spaces.

Description of dermal-epidermal junction (DEJ)

The dermo-epidermal junction is rather flat with intact border between the epidermis and dermis as in the case of AK and BCC. Breaches in case of SCC (Figures 5.7, 5.8) may disappear in infiltrative growing melanoma or display the typical saw teeth appearance from damage to the junction which pushes the rete ridges in the case of the early stages. This appears as echo-poor, low scattering projections sharply demarcated from the echo-rich homogeneous dermis.

Diagnostic criteria

For the SC, OCT images are assessed with regards to reflectivity, hyper-reflective for thick SC (thick), normal-reflective for normal SC or hypo-reflective for atrophied or absent SC. Surface damage confined within the SC is one of the most important diagnostic criteria. Epidermal layer was evaluated as increased, decreased or showing no change according to normal margins. The epidermal layer may show a non-homogenous lobule with an active single or multiple tumour nest collection lobule inside. DEJ are demarcated without protrusion toward the dermis, demarcated with protrusion or are non demarcated (breach).

Signs within the papillary dermis include: homogenous or non-homogenous signals indicating connective tissue invasion, and he presence of solid or empty spaces surrounded by a hyper-reflective band within the dermal layer. The main architectural features for AC were a hyper-reflective and/or disruption of the SC, and demarcated DEJ. For squamous cell skin cancer, the DEJ lost its integrity; other features included superficial epidermal layer disintegration (honeycombing and cobblestoning) with small bright clusters within the papillary dermis.

With melanoma, non-edged papillae, cerebriform clusters infiltrating dermal papillae, diffuse or patchy reflectivity, and loss of the typical bright horizontal linear structures were diagnostic. Lentigo maligna was characterised by predominantly uniformly elongated rete ridges as well as uniform nests within the epidermis (Table 5.4).

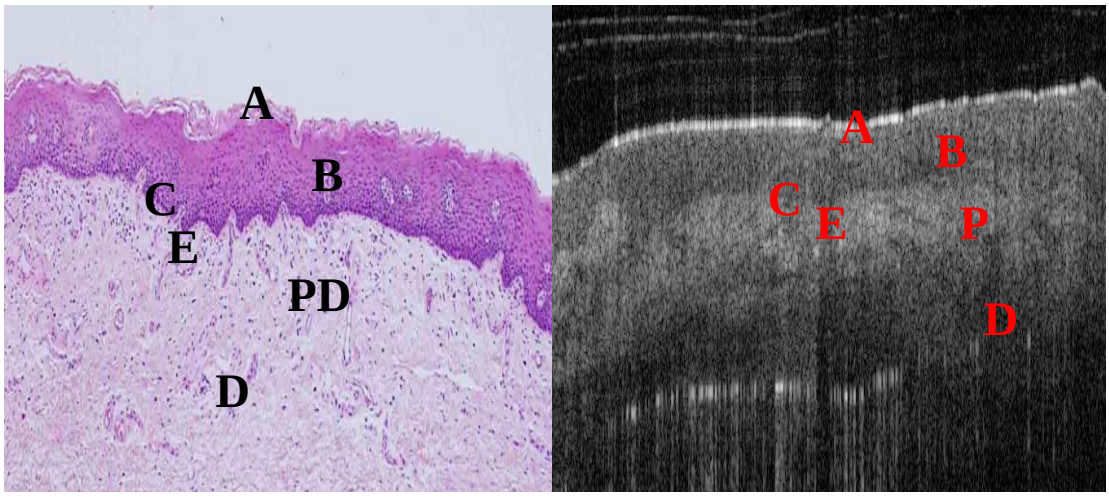

Figure 5.1: Histology versus OCT scan for normal skin margin of the cheek showing three distinct layers. A: representing the SC, B: epidermis, C: DEJ, D: Dermis, E: papilla, PD: papillary dermis. Correlation was good for the SC and epidermis while a few large and prominent papilla have been correlated.

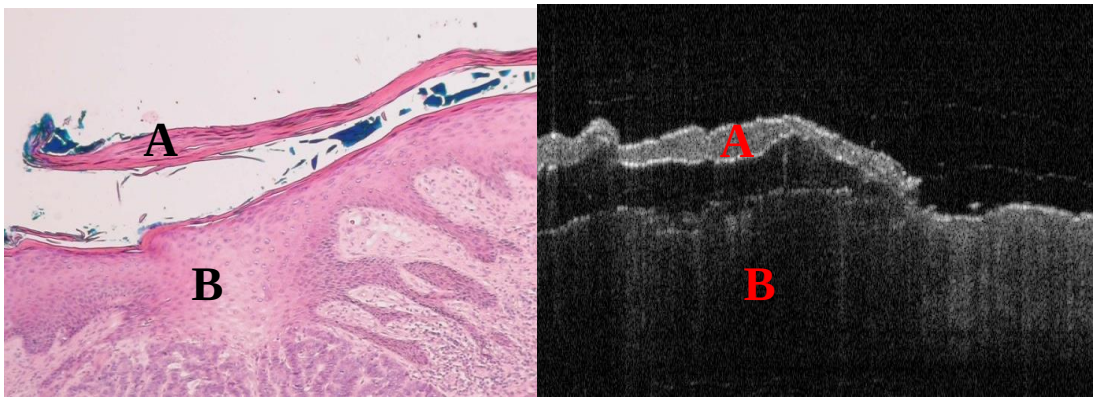

Figure 5.2: AK showing damage to stratum corneum layer (A) with thick epidermis but intact dermo-epidermal junction (B).

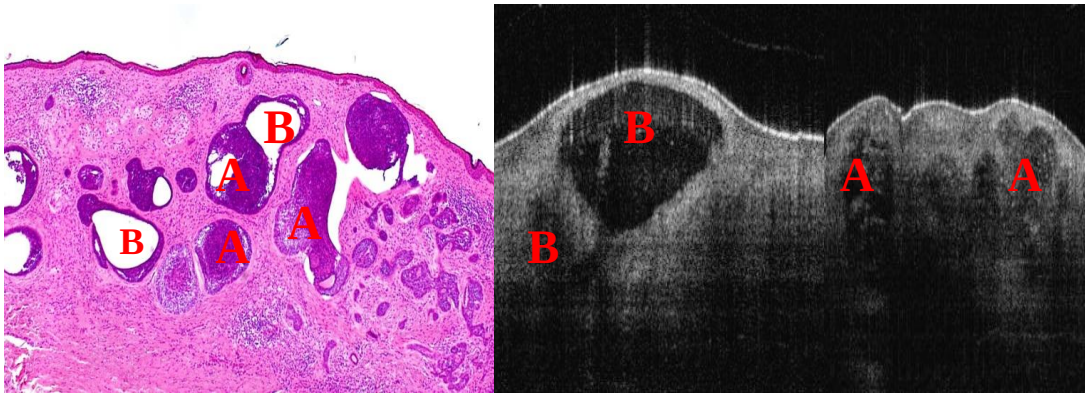

Figure 5.3: Mixed solid (A) and cystic (B) BCC.

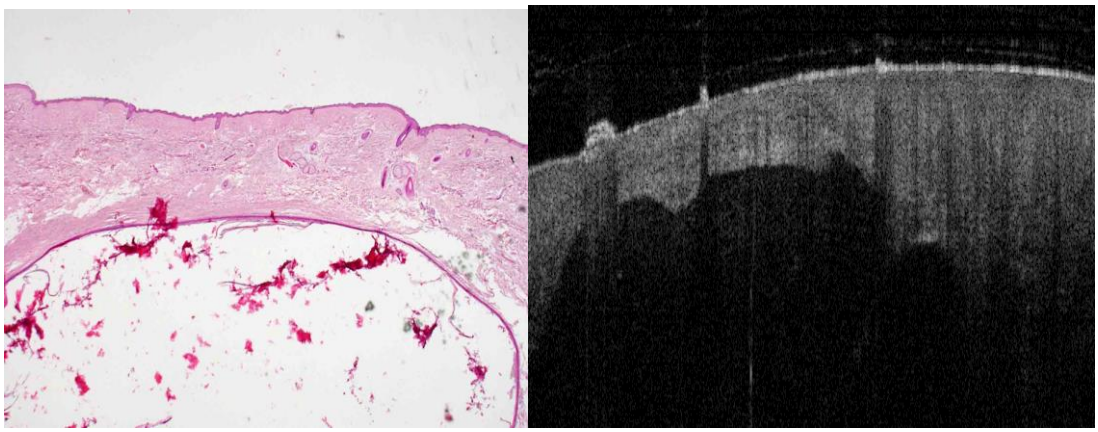

Figure 5: Giant cystic BCC showing a lobular hypo-ecoic OCT feature occupying a large portion of the dermis layer.

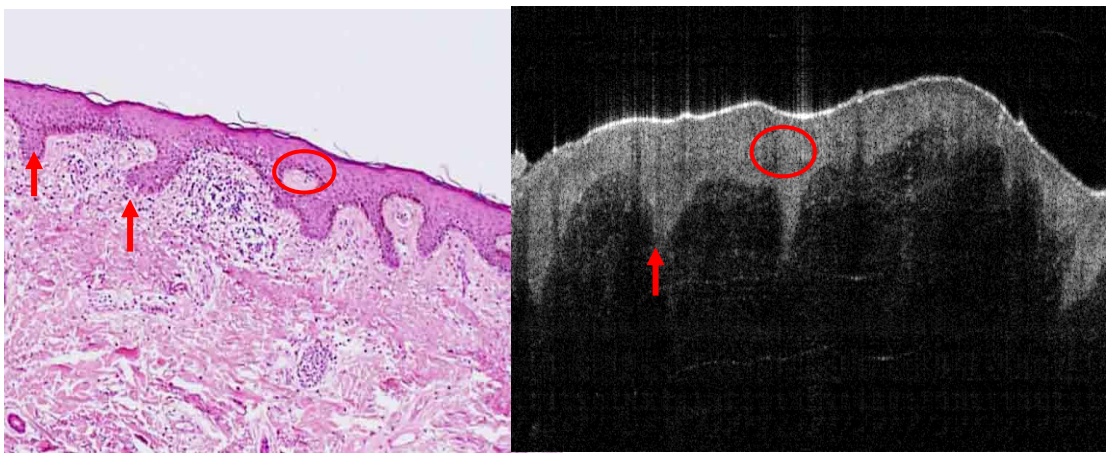

Figure 5.5: Lentigo maligna, characterised by predominantly uniformly elongated rete ridges (arrows). Uniform nests within the epidermis (circles).

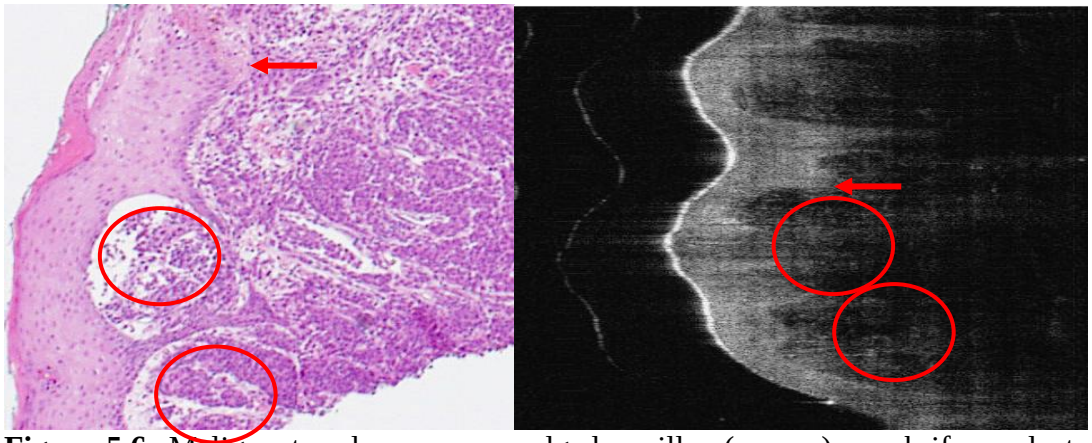

Figure 5.6: Malignant melanoma, non-edged papillae (arrows), cerebriform clusters infiltrating dermal papillae (circles), diffuse or patchy reflectivity, and partial loss of the typical bright horizontal linear structures.

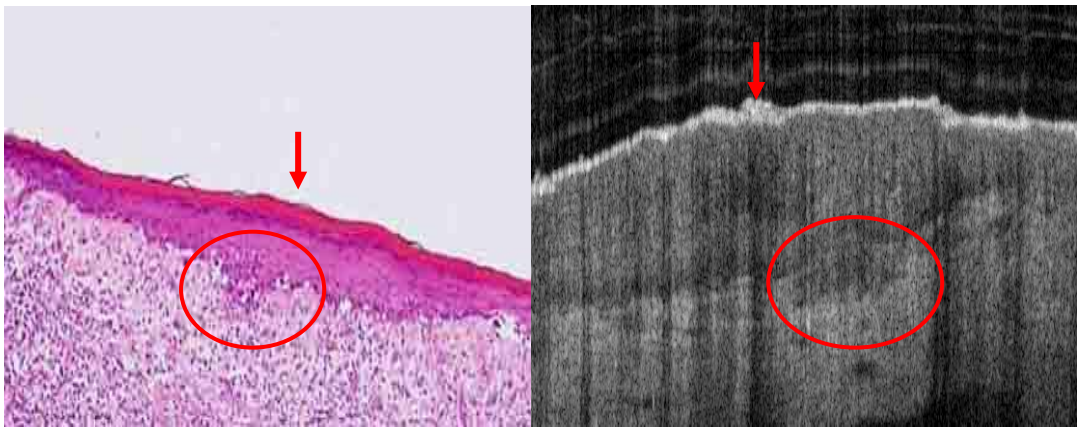

Figure 5.7: SCC in situ (Bowen's disease) from temple, showing thick stratum corenum ,hyperkeratosis (arrow), thickening of the epidermal layer with broadening of DEJ as an early sign of pallipary dermal layer invasion (circle).

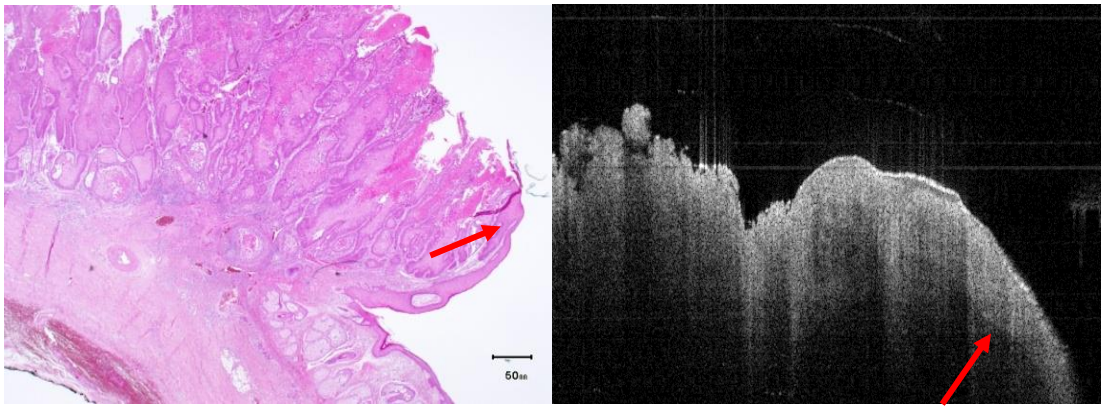

Figure 5.8: SCC showing the transitional area between intact and damaged DEJ (red arrow).

T**able 5.1:** Patient demographic information

	No. (%)			No. (%)
Gender			**Symptoms**	
male	19 (35,9)		itchness	15 (28.3)
female	34 (64.1)		symptomless	13 (24.5)
			scaly	10 (18.8)
Location			lumpy	10 (18.8)
cheek	29 (53)		bleeding	5 (9.4)
nose	16 (28)			
ear	6 (10.5)		**Clinical features**	
forehead	3 (5)		papule	17 (29.8)
lower lip	3 (5)		erosion	15 (26.3)
			ulcer	12 (21)
Colour			nodule	10 (17.5)
mixed	30 (52.6)		others	3 (5.2)
red	11 (19.2)			
brown	7 (12.2)		**Histologic diagnosis**	
black	4 (7)		BCC	26 (45.5)
white	3 (5.2)		SCC	12 (21)
non specific	6 (10.5)		AK	9 (15.9)
			LM	3 (5.3)
Skin type			MM	7 (12.3)
type II	21 (39.6)			
type III	18 (33.9)			
type VI	14 (26.4)			

Table 5.2: Correlation between OCT and normal histology

Normal resection margins			
1- identification of the stratum corneum	**OCT**	**Histology**	**Total**
Yes	30	30	60
No	0	0	0
2- identification of the epidermis	**OCT**	**Histology**	**Total**
Yes	30	30	60
No	0	0	0
3- identification of epidermal papilla	15	30	
4- identification of (DEJ)	**OCT**	**Histology**	**Total**
Yes	28	30	58
No	2	0	2
5- homogenous papillary dermal layer	**OCT**	**Histology**	**Total**
Yes	30	30	60
No	0	0	0

Table 5.3: Common descriptive features between OCT and pathology from skin lesions agreed by two observers.

SCC			
1- dermal–epidermal junction (DEJ) lost integrity	**OCT**	**Pathology**	**Total**
Yes	11	12	23
No	1	0	1
2- superficial epidermal layers (honeycombed)	**OCT**	**Pathology**	**Total**
Yes	5	6	11
No	7	6	13
3- small bright cluster at the papillary dermis	**OCT**	**Pathology**	**Total**
Yes	4	5	9
No	8	7	15
BCC			
4- stratum corneum disruption or thickening	**OCT**	**Pathology**	**Total**
	12	12	24
	0	0	0
1- solid nest or honeycomb beyond (DEJ) within the epidermis	**OCT**	**Pathology**	**Total**
Yes	14	15	29
No	12	11	23
2- small multiple empty spaces	**OCT**	**Pathology**	**Total**
Yes	8	8	16
No	18	18	36
3- cystic BCC, large one or two empty space	**OCT**	**Pathology**	**Total**
Yes	6	6	12
No	20	20	40
4- cords or small buds protruding from epidermis	**OCT**	**Pathology**	**Total**
Yes	2	2	4
No	24	24	48
AK			
1- parakeratosis/hyperkeratosis	**OCT**	**Pathology**	**Total**
Yes	8	9	17
No	1	0	1
2- stratum corneum disruption	**OCT**	**Pathology**	**Total**
Yes	9	9	18
No	0	0	0
3- dermal–epidermal junction thickening	**OCT**	**Pathology**	**Total**
Yes	3	5	8
No	6	4	10
MM			
1- non-edged rete ridges with clusters infiltrating papillary dermal layer	**OCT**	**Pathology**	**Total**
Yes	4	7	11
No	3	0	3

2- loss of typical bright horizontal linear structures	**OCT**	**Pathology**	**Total**
Yes	6	7	13
No	1	0	1
3- intact dermo–epidermal junction	**OCT**	**Pathology**	**Total**
Yes	7	7	14
No	0	0	0
LM			
1- elongated rete ridges	**OCT**	**Pathology**	**Total**
Yes	1	3	4
No	2	0	2
2- uniform nest within the epidermis	**OCT**	**Pathology**	**Total**
Yes	1	3	4
No	2	0	2

Table 5.4: Descriptive interpretation of OCT image changes

	SC hyperreflective	**SC hyporeflective**	**SC normoreflective**	**damaged**	**EL ↑**	**EL ↓**	**EL ↔**	**nest or lobule in EL**	**homogenous EL**	**DEJ demarcated without protrusion toward D**	**DEJ demarcated with protrusion toward D**	**DEJ not demarcated**	**empty space in D**	**solid space in D**	**non-homogenous D**
Pathology entity															
BCC (n= 26)	10	5	8	3	7	3	16	17	9	18	2	0	16	9	1
SCC (n=12)	8	0	2	2	10	0	2	0	12	0	1	11	6	0	6
AK (n=9)	8	0	0	1	3	0	6	1	8	9	0	0	0	0	0
LM (n=3)	0	0	3	0	1	1	1	3	0	1	2	0	0	0	0
MM (n=7)	2	0	5	0	2	3	2	1	6	1	4	2	4	1	2
Normal resection margins (n=30)	0	0	30	0	0	0	30	0	30	30	0	0	0	0	0

SC=stratum corneum layer, ↑=increase, ↓=decrease, ↔=no change, **D**= dermis**, EL=** epidermal layer.

Section II: Sensitivity and specificity of OCT in the diagnosis of head and neck pre-cancerous and cancerous skin lesions

Background

Optical coherence tomography has been shown in the previous section to reliably identify skin changes with the advantage of combining resolution and penetration depth. However, specific studies of diagnostic sensitivity, specificity and the degree of agreement on certain morphological diagnostic criteria are generally lacking.

Objectives

The objective of this study was: 1) to assess the diagnostic value of defined histologic parameters in differentiating skin cancer in terms of sensitivity and specificity, and 2) to test the interobserver and intraobserver agreement of the these standard terminologies for the description and diagnosis of skin lesions.

Patients

In this study, 103 patients with 110 lesions were included who were suspected of having skin cancer. All patients were presented to the Head & Neck Centre, University College London Hospital, with non-healing lesions, pigmented lesions and other lesions of which there was a high degree of suspicion that they were pre-malignant or malignant condition.

The lesions were presented in 8 predetermined anatomical sites: forehead, ear, tip of the nose, bridge of the nose, cheek, chin, neck, lip and mastoid. Only excisonal biopsies have been included. Some of the large and serious lesions have been diagnosed by incisional biopsy and then surgical resection has been performed.

The study protocol was approved by the Moorfields & Whittington Local Research Ethics Committee of Human Research, in light of the Declaration of Helsinki. Informed consent was obtained from each patient. Inclusion criteria included patients being over 18 years of age. All inflammatory skin diseases have been excluded from the study.

All the removed lesions have been scanned with OCT, but only malignant and premalignant lesions of up to 1 cm in diameter were included, as confirmed on the histology. Lesions with vesicle or bullae or both were excluded from the study. Benign non-malignant skin lesions were excluded from the OCT database.

Results

A total of 110 surgical specimens were excised from 103 subjects. Patients comprised 64 (62.2%) women and 39 (37.8%) men. 75% of the participant were Caucasian, 23% Asian, and 2% Africo-Caribbean. Fifty-five of them had Fitzpatric type III skin, 37 type II and 8 type I, and there was a mean age of 67 years (range 39–95). Lesion characteristics are presented in Table 5.6.

Of the 110 lesions that were scanned, 54 were identified by histologic examination as basal cell carcinomas, 23 were diagnosed as actinic keratosis (AK), 15 as squamous cell carcinomas, 10 lentigo maligna, and 8 as melanomas.

Sensitivity and specificity of OCT for overall lesions

Tables 5.7–5.16 summarise the sensitivity and specificity results for each OCT diagnosis. The sensitivity and specificity results were also broken down by BCC subtype. Thus, the specificity was the same for both superficial and nodular BCCs (100%).

The collective sensitivity and specificity for both assessors to differentiate AK was 97.5% and 100%, respectively. The overall diagnostic accuracy has been assessed to differentiate SCC was 93.3. An accuracy of 100% has been found in the AK diagnosis, compared to 96.5% for the dissemination of BCC. For the diagnosis of LM a sensitivity of 55% and specificity of 89.5% were found, this is higher than that for malignant melanomas (43.5% and 82% respectively).

Inter- and intraobserver agreement

Intraobserver agreement was calculated from the assessment of both observers. The findings for different features are shown in Tables 5.17 and 5.18.

Interobserver reproducibility was generally lower than intraobserver reproducibility. The interobserver agreement for integrity (DEJ) was good, with a weighted kappa value of 0.89. For the presence of solid nest compartments within the epidermis, the percentage agreement was high (0.92). However, agreement on the thickening of DEJ with or without protruding clusters was small and the kappa values were 0.60. Higher agreement was obtained for DEJ ridge status (elongated or atrophied), which helps differentiate MM from LM with a k value of 0.55.

The k scores ranged from 0.72 for SC disruption to 0.8 for hyperkeratosis. The mean weighted kappa for the interobserver agreement of parameters is shown in Table 5.19.

Table 5. 6: Characteristics of imaged lesion demographic location.

	No. (%)			No. (%)
Gender			**Skin type**	
Male	39 (37.8)		Type I	8(7.7)
Female	64 (62.2)		Type II	37(35.9)
			Type III	55(53.3)
Location			Type VI	10(9.7)
Cheek	30 (27.2)			
Nose	25 (22.7)		**Clinical features**	
Ear	16 (14.5)			
Forehead	13 (11.8)		Papule	20 (18.1)
Lip	13(11.8)		Erosion	32 (29)
Neck Mastoid	8 (7.2) 5 (4.5)		Ulcer	18 (16.3)
Colour			Nodule	33 (30)
Mixed	40 (36.3)		Others	7 (6.3)
Red	22 (20)			
Brown	8 (7.2)		**Histologic diagnosis**	
Black	5 (4.5)			
White	5 (4.5)		BCC	54 (49)
Non specific	30 (27.2)		SCC	15 (13.6)
			AK	23 (20.9)
Main symptoms			LM	10 (9)
Itchiness	23 (20.9)		MM	8 (7.2)
Symptomless	20 (18.1)			
Scaly	25 (22.7)			
Lumpy	30 (27.2)			
Bleeding	12 (10.9)			

Table 5.7: Assessment of the BCCs by radiologist. Sensitivity 98%; Specificity 96%; Positive predictive value (PPV) 96%; Negative predictive value (NPV) 98%; Accuracy of OCT 97%. TP: true positive, FP: false positive, TN: true negative, FN: false negative.

	Histology			
OCT		**Positive**	**Negative**	**Total**
	Positive	53 (TP)	2 (FP)	55
	Negative	1 (FN)	54 (TN)	55
	Total	54	56	110

Table 5.8: Assessment of the SCCs by radiologist. Sensitivity 80%; Specificity 95%; (PPV) 75%; (NPV) 96%; Accuracy of OCT 93%. TP: true positive, FP: false positive, TN: true negative, FN: false negative.

	Histology			
OCT		**Positive**	**Negative**	**Total**
	Positive	12 (TP)	4 (FP)	16
	Negative	3 (FN)	91 (TN)	94
	Total	15	95	110

Table 5.9: Assessment of the AK by radiologist. Sensitivity 95%; Specificity 100%; (PPV) 100%; (NPV) 99%; Accuracy of OCT 99%. TP: true positive, FP: false positive, TN: true negative, FN: false negative.

	Histology			
OCT		**Positive**	**Negative**	**Total**
	Positive	22 (TP)	0 (FP)	22
	Negative	1 (FN)	87 (TN)	88
	Total	23	87	110

Table 5.10: Assessment of the MM by radiologist. Sensitivity 50%; Specificity 75%; (PPV) 13%; (NPV) 95%; Accuracy of OCT 73.5%. TP: true positive, FP: false positive, TN: true negative, FN: false negative.

	Histology			
OCT		**Positive**	**Negative**	**Total**
	Positive	4 (TP)	25 (FP)	22
	Negative	4 (FN)	77 (TN)	96
	Total	8	102	110

Table 5.11: Assessment of the LM by radiologist. Sensitivity 60%; Specificity 90%; (PPV) 73%; (NPV) 95%; Accuracy of OCT 85%. TP: true positive, FP: false positive, TN: true negative, FN: false negative.

	Histology			
OCT		**Positive**	**Negative**	**Total**
	Positive	6 (TP)	10(FP)	12
	Negative	4 (FN)	90 (TN)	98
	Total	10	100	110

Table 5.12: Assessment of the BCCs by dermatologist. Sensitivity 98%; Specificity 94.5%; Positive predictive value (PPV) 94.5%; Negative predictive value (NPV) 98%; Accuracy of OCT 96%. TP: true positive, FP: false positive, TN: true negative.

	Histology			
OCT		**Positive**	**Negative**	**Total**
	Positive	53 (TP)	3 (FP)	56
	Negative	1 (FN)	53 (TN)	54
	Total	54	56	110

Table 5.13: Assessment of the SCCs by dermatologist. Sensitivity 86.6%; Specificity 94.7%; (PPV) 72%; (NPV) 97.8 %; Accuracy of OCT 93.6%. TP: true positive, FP: false positive, TN: true negative, FN: false negative.

	Histology			
OCT		**Positive**	**Negative**	**Total**
	Positive	13 (TP)	5 (FP)	18
	Negative	2 (FN)	90 (TN)	92
	Total	15	95	110

Table 5.14: Assessment of the AK by dermatologist. Sensitivity 100%; Specificity 100%; (PPV) 100%; (NPV) 100%; Accuracy of OCT 100%. TP: true positive, FP: false positive, TN: true negative, FN: false negative.

	Histology			
OCT		**Positive**	**Negative**	**Total**
	Positive	23 (TP)	0 (FP)	23
	Negative	0 (FN)	87 (TN)	87
	Total	23	87	110

Table 5.15: Assessment of the MM by dermatologist. Sensitivity 37.5%; Specificity 77.4%; (PPV) 11.5%; (NPV) 94%; Accuracy of OCT 74.5%. TP: true positive, FP: false positive, TN: true negative, FN: false negative.

	Histology			
OCT		**Positive**	**Negative**	**Total**
	Positive	3 (TP)	23 (FP)	26
	Negative	5 (FN)	79 (TN)	94
	Total	8	102	110

Table 5.16: Assessment of the LM by dermatologist. Sensitivity 50%; Specificity 89%; (PPV) 31%; (NPV) 94.6%; Accuracy of OCT 85.4%. TP: true positive, FP: false positive, TN: true negative, FN: false negative.

	Histology			
OCT		**Positive**	**Negative**	**Total**
	Positive	5(TP)	11(FP)	16
	Negative	5(FN)	89 (TN)	94
	Total	10	100	110

Table 5.17: Agreement with the radiologist (intraobserver agreement)

Assessment of radiologist	**Kappa**
Integrity DEJ	0.95
Solid nest within the epidermis	0.98
Thickening of DEJ with or out protruding clusters	0.88
DEJ status	0.80
Stratum corneum disruption	0.75
Stratum corneum thickening	0.90

Table 5.18: Agreement with the dermatologist (intraobserver agreement)

Assessment of dermatologist	**Kappa**
Integrity DEJ	0.90
Solid nest within the epidermis	0.95
Thickening of DEJ with or out protruding clusters	0.70
DEJ status	0.80
Stratum corneum disruption	0.90
Stratum corneum thickening	0.95

Table 5.19: Kappa agreement between the dermatologist and the radiologist when assessing the OCT images for the 110 biopsies (interobserver agreement).

Assessment of dermatologist vs. radiologist	**Kappa**
Integrity DEJ	0.89
Solid nest within the epidermis	0.92
Thickening of DEJ with or out protruding clusters	0.60
DEJ status	0.55
Stratum corneum disruption	0.75
Stratum corneum thickening	0.80

Section III: Assessment of head and neck tumour resection margins

Background

Achieving tumour free surgical margins is one of the most essential factors to reduce recurrence of skin cancer.

Objectives

The purpose of this study is: 1) to confirm the accuracy of OCT in discerning normal facial skin cancer margins by comparison with histopathologic diagnosis, 2) to calculate the sensitivity, specificity, and positive and negative predictive values, and 3) to correlate tumour thickness with histopathology.

Materials

The specimens assessed in this study were surgically removed from patients who had a history of facial skin cancer. Seventy surgically removed facial skin lesions were examined by OCT to verify margin status. Four margins per specimen were studied (total number 280). The majority of specimens was basal cell carcinoma (n=40), followed by squamous cell carcinoma (n=30). The margins were processed with hematoxylin and eosin (H&E) staining. The criteria used for rating a margin as negative (tumor free), regardless of whether the lesion is BCC or SCC, is the presence of a normal epidermal layer with intact DEJ and homogenous dermis layer (Figures 5.9, 5.10). Whilst the criteria for differentiating a tumour laden margin as BCC is based on the presence of a tumor nest within the epidermis layer, with or without damaged DEJ (Figure 5.11). The criteria for differentiating a tumour bearing margin for SCC is based on the lobular tumour nests extension beyond the DEJ which is damaged (Figure 5.12). Tumour thickness at the centre was also documented. The study protocol was approved by Moorfields & Whittington Local Research Ethics Committee for Human Research with patient consenting .

Images were assessed by one dermatologist. For every image, the observers assessed the presence of the following structures: surrounding epidermis; surrounding dermis and tumour aggregates. The diagnoses, tumour thicknesses and status of the margins were obtained from the pathologist involved in this study. The principal investigator (study co-ordinator) liaised between the and pathologist scan reader.

Results

Characterization of the population

The mean age of the patients was 60 years (range 40–88 years). Twenty-five of the subjects were men and forty-five were women. All the patients were treated with surgery alone without any pre-operative chemo or radiotherapy. The most common lesion location was the cheek (20) and scalp (20), followed by nose (12), forehead/temple (8), ears (6), and eyelid (4). The pathology result of 280 margins revealed 240 tumour free margins and 40 tumour involved margins. 15 margins were excluded due to distortion during histologic processing. For the 160 margins of BCCs, 17 were tumour involved, whiles 23 margins were tumour involved from 120 margins for SCCs (Table 5.20**)**.

Reliability of differentiating tumour involved from tumour non-involved margins

The sensitivity and specificity for all margins, regardless of whether the tumor was SCC or BCC, was 77.5% and 95.8%, respectively. Whilst the positive predictive value (PPV) was 75.6% and the negative predictive value (NPP) was 96%. The accuracy of OCT was 93% (Table 5.21). There were 10 false positives and 9 false negatives (Figures 5.13, 5.14).

Reliability of differentiating tumour involved as BCC or SCC

The sensitivity and specificity for discriminating the margins for BCCs was 82.5% and 98.5%, respectively. Whilst the positive predictive value (PPV) was 87.5% and the negative predictive value (NPP) was 98%. The accuracy of OCT was 96.5% (Table 5.22). There were 2 false positives and 3 false negatives.

The sensitivity and specificity for the SCCs was 82.5% and 95.5%, respectively. The PPV was 82.5% and the NPP was 95.5%. The accuracy of OCT was 93% (Table 5.23). There were 4 false positives and 4 false negatives.

OCT and histopathology correlation with tumour thickness

There was a statistically poor correlation for tumour thickness in the active centre for BCCs and SCCs in general (r=0.43) (Figure 5.15). However, A better correlation were found for thin BCC (r=0.69) (Figure 5.16).

Table 5.20: Characteristics of imaged lesions: patient demographic and lesion location and features.

	No. (%)			No. (%)
Gender			**Skin type**	
Male	25 (35.7)		Type I	2 (2.8)
Female	45 (64.3)		Type II	10(14)
			Type III	30(42.8)
Location			Type VI	10(14.2)
Cheek	20 (28.5)			
Scalp	20 (28.5)		**Clinical features**	
Nose	12 (17)			
Forehead	8 (11.4)		Erosion	20 (28.5)
Ear	6 (8.5)		Nodule	20 (28.5)
Eyelid	4 (5.7)		Papule	15 (21.5)
			Ulcer	10 (14)
Main symptoms			Others	5 (7)
Itchiness	22 (31.4)			
Symptomless	18 (25.7)		**Histologic diagnosis**	
Scaly	15 (21.4)			
Lumpy	10 (14)		BCC	40 (57)
Bleeding	5 (7)		SCC	30 (43)

Table 5.21: OCT assessment for all margins (265 margins). Sensitivity 77.5%; Specificity 95.5%; (PPV) 75.6%; (NPV) 96%; Accuracy of OCT 93%. TP: true positive, FP: false positive, TN: true negative, FN: false negative.

	Histology			
OCT		Positive	Negative	Total
	Positive	31 (TP)	10 (FP)	41
	Negative	9 (FN)	215 (TN)	224
	Total	40	225	265

Table 5.22: OCT assessment for BCCs margins (150 margins, 10 margins were excluded). Sensitivity 82.5%; Specificity 98.5%; (PPV) 87.5%; (NPV) 98%.; Accuracy of OCT 96.5%. TP: true positive, FP: false positive, TN: true negative, FN: false negative.

	Histology			
OCT		Positive	Negative	Total
	Positive	14 (TP)	2 (FP)	16
	Negative	3 (FN)	131 (TN)	144
	Total	17	123	150

Table 5.23: OCT assessment for SCCs margins (115 margins, 5 margins were excluded). Sensitivity 82.5%; Specificity 95.5%; (PPV) 82.5%; (NPV) 95.5%; Accuracy of OCT 93%. TP: true positive, FP: false positive, TN: true negative, FN: false negative.

	Histology			
OCT		Positive	Negative	Total
	Positive	19 (TP)	4 (FP)	23
	Negative	4 (FN)	88 (TN)	92
	Total	23	92	115

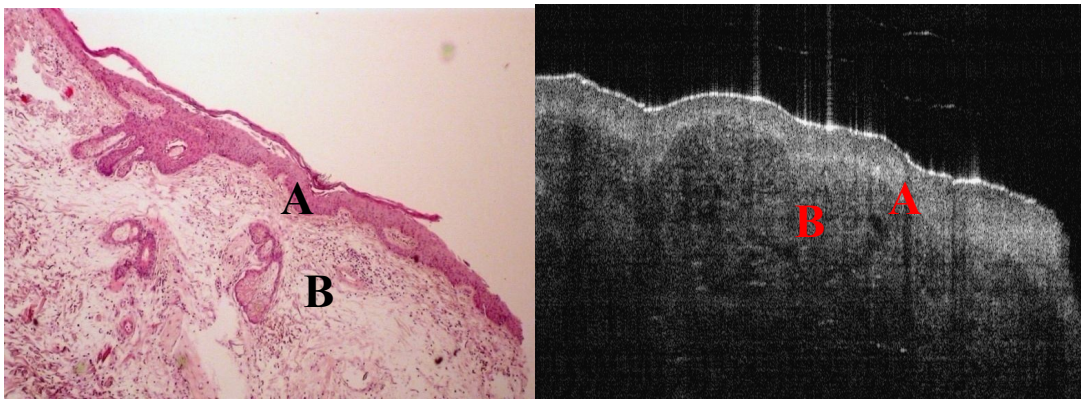

Figure 5.9: True negative margin from BCC lesion. OCT scan showing no tumour, intact DEJ (A) and homogenous demise within the 5 mm scan length (B).

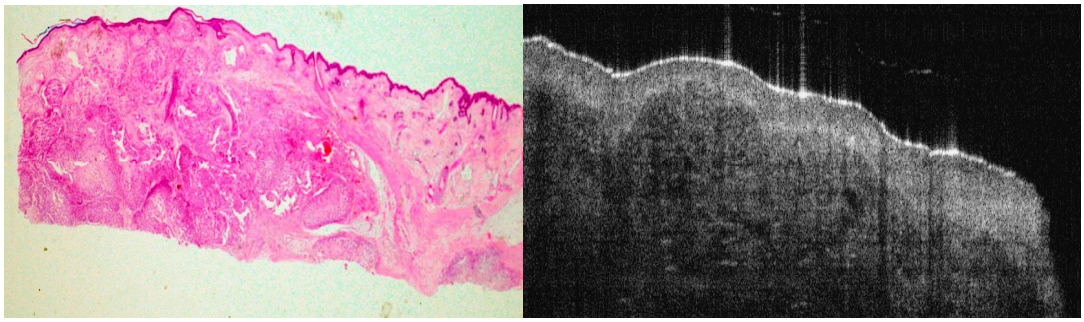

Figure 5.10: True negative margin from SCC lesion. OCT scan showing no tumour nests, intact DEJ and homogenous demise within the 5 mm scan length.

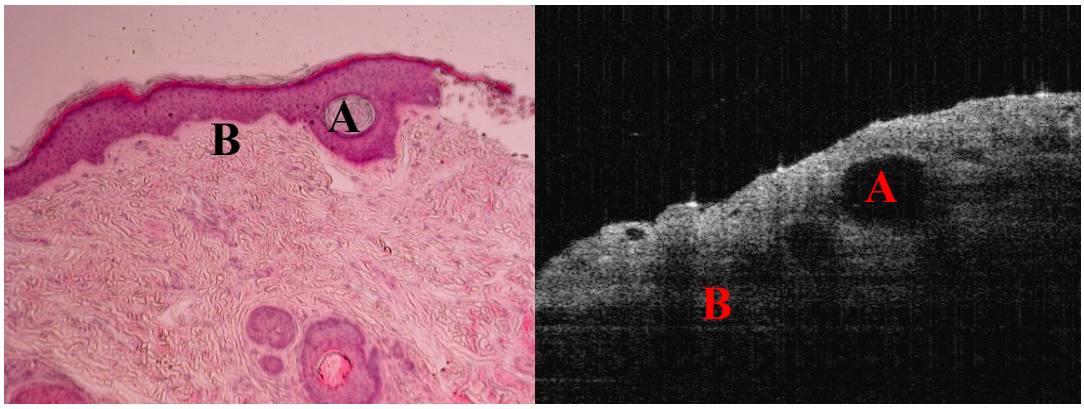

Figure 5.11: True positive margin OCT scan from BCC tumour-bearing resection margin, showing tumour nest within the epidermis layer (A) without damaged DEJ (B).

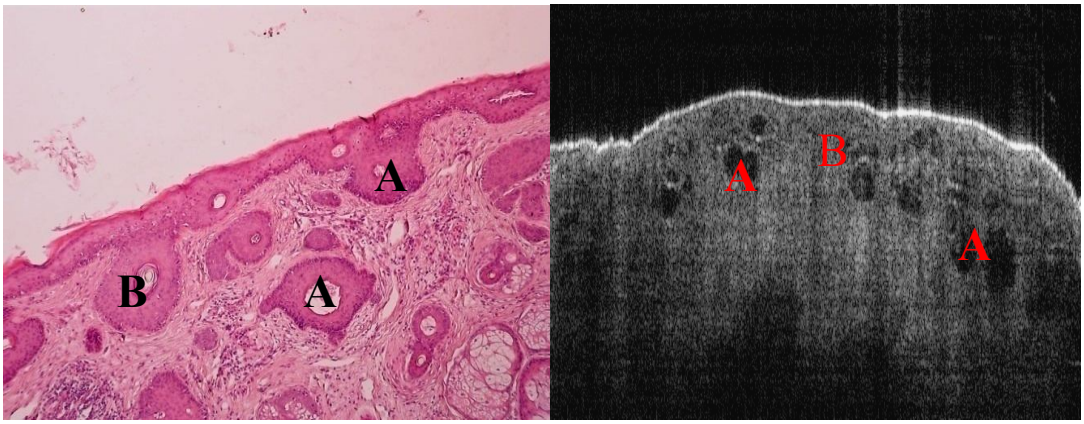

Figure 5.12: True positive OCT scan from SCC tumour-bearing resection margin, showing superficial and deep lobular tumour nests (A) extending beyond the DEJ which is damaged in some areas (B).

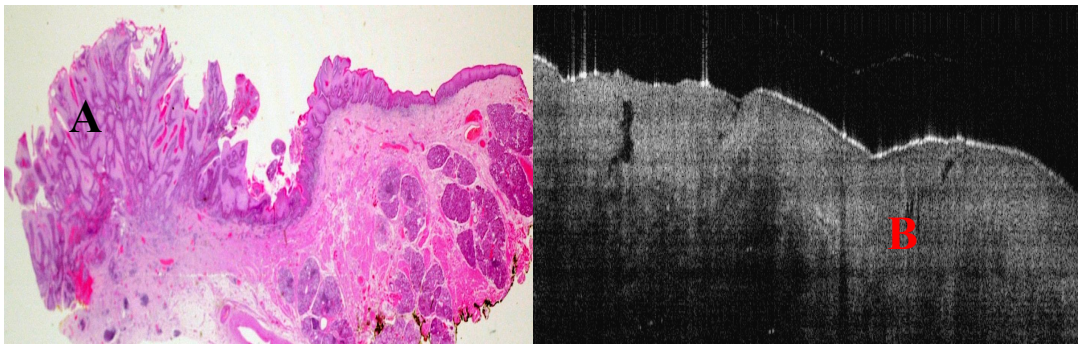

Figure 5.13: False positive margin for SCC lesion with epidermal hyperplasia and reactive keratosis of stratum corneum layer (A). OCT scan revealing non-homogenous non-organized structure (B).

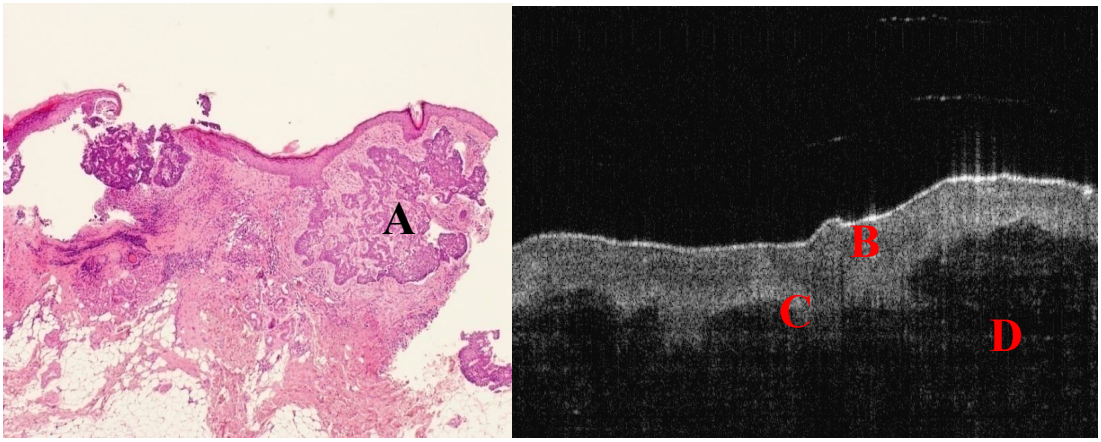

Figure 5.14: False negative OCT tumour resection margin, H&E slide showing deep sub-epidermal tumour extension which could not be detected by OCT (A). OCT scan showing distinct epidermis (B), intact DEJ (C) and homogenous dermis (D).

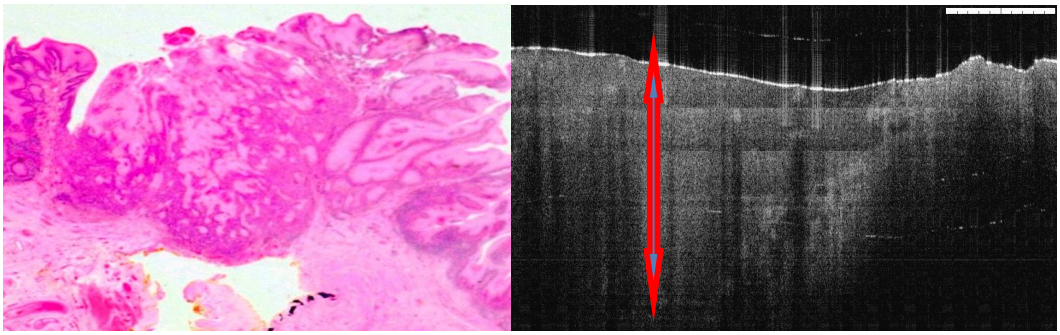

Figure 5.15: OCT and pathology images showing SCC tumour thickness exceeding 2 mm.

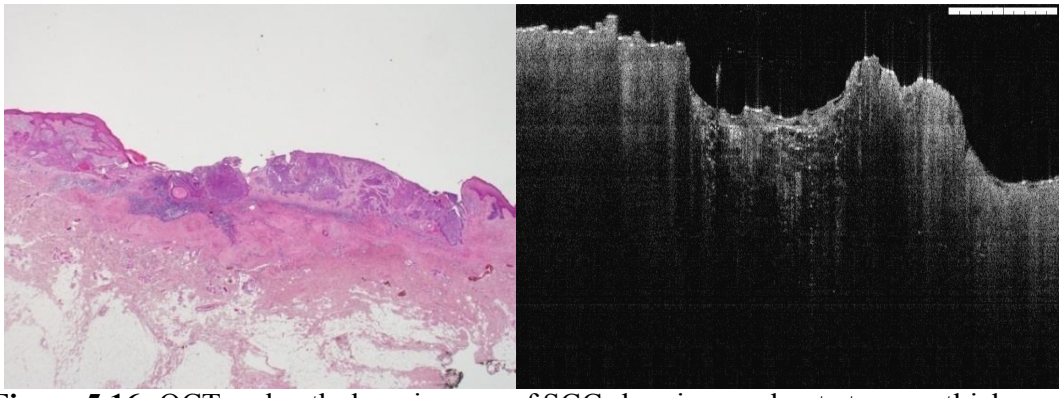

Figure 5.16: OCT and pathology images of SCC showing moderate tumour thickness correlation when tumor thickness is within the 2 mm range.

Discussion

The first part of this chapter reports on the morphologic features observed in OCT imaging performed on fresh facial skin specimens *ex-vivo*. Although the material is small, it represents the range of relevant morphologies needed for future *in- vivo* diagnosis, and the results indicate that morphological changes in OCT images match the histopathology.

To interpret the OCT images of abnormal skin, it is necessary to be familiar with normal skin architecture. In normal skin histology, the epidermis is primarily comprised by keratinocytes and a smaller population of dendritic cells, which are the melanocytes and langerhans cells. The dermis is comprised by blood vessels, nerves, inflammatory cells and fibroblasts surrounded by collagen and elastin fibres.

Papillary dermis forms projections onto the epidermis, named dermal papillae. The meeting point between the epidermis and the dermis is named the dermal-epidermal junction (DEJ). In the epidermis, the keratinocytes are differentiated to form four different layers. Stratum corneum is the most superficial layer of the epidermis, which is comprised of flat anucleated keratinocytes.

Histopathologically there are many histological variants of a BCC, including nodular, superficial, morpheaform (or sclerosing), infiltrative, and micronodular (Hutcheson *et al*., 2005). A typical BCC lesion has a pearly or waxy appearance. The shape of the lesion is flat or slightly raised, white or light pink, flesh-coloured or brown, with visible blood vessels in the lesion or adjacent skin. It usually has a central ulceration and a well-defined border. It also may appear as a scar-like lesion without a history of injury to the skin in that area. The less common infiltrative type can be seen as poorly defined, lightly pigmented, indurated, flat skin lesions, occasionally with overlying telangiectasia.

Squamous cell carcinoma is the second most common skin cancer and it represents 20% of all cutaneous malignancies (Miller *et al*., 1994). The histologic spectrum of squamous cell carcinoma begins with actinic keratosis (AK). Actinic keratoses (AK) are the most common pre-malignant skin pathology (Heaphy *et al*., 2000). Histologically the difference between AK, SCC *in situ* and frank SCC is described as follows: AK involves

only part of the epidermis, SCC *in situ* occupies the full thickness of the epidermis, and invasive SCC penetrates the basement membrane of the epidermis.

In the current study, the results showed that traditional normal histological landmarks such as stratum corneum, DEJ and papillary dermal layer can be clearly identified using OCT. This study indicates that the characteristic layering of normal skin is lost both in BCCs and SCCs, and this is identifiable on OCT.

The depth of the OCT in this study is limited to a maximum of only 2mm, which is satisfactory to visualise the epidermis and dermis layers where most of the pathological changes occur. The axial resolution of 10μm would not allow the detection of a single cell. However, the investigation of single cells or sub-cellular structural changes is part of ongoing research. Unlike other imaging techniques, reflectance confocal microscopy enables the identification of these layers based on architecture and cytological characteristics.

One of the great advantages of OCT, which is not seen in confocal microscopy, is the possibility of only analysing microanatomical structures up to a depth of 1500μm. This means that any abnormalities extending from the papillary dermis to the reticular dermis are diagnosable. For this reason, tumours that invade the depth can be properly assessed. This includes areas where the epidermis has shallow thickness, in which part of the reticular epidermis is also be assessed.

The technical development of OCT, such as polarization-sensitive OCT (PS-OCT) or speckle-reduced OCT, may increase the diagnostic accuracy. Finally the introduction of image analysis, machine-learning algorithms, or neural networks may provide a more precise classification of AK and BCC lesions than simply relying on the human eye.

In this study, nodular BCC showing a single significant feature (i.e. the formation of tumour aggregates in the epidermis) was found to be a characteristic feature in the lesions investigated. This study revealed that the diagnostic ability of OCT is ideal for the detection of sub-types and the early stages of BCC However, partial loss of normal OCT architecture may not be seen in various pre-BCC lesions.

In AK lesions focal changes and thickening of epidermis were the main diagnostic features. OCT investigation for the AK showed another diagnostic feature in the form of buds and irregular proliferation of tumour tissue attached to the undersurface of the epidermis, or in the form of thickening of the DEJ (SCC *in-situ*). The DEJ appeared less well demarcated compared to healthy skin, which is probably due to the cell aggregates of this lesion. The OCT ability to detect cell aggregate at DEJ, as a pre-invasion stage, is a very profound finding in the early detection of the invasion phase of skin cancer.

Korde *et al.* (2007) studied OCT images of sundamaged skin and AK and described the accuracy of dark elongated bands in the epidermis for the diagnosis of AK. These bands correspond to keratin deposits in a thickened SC. The main problem in AK diagnosis is the thickening of the SC layer which reduces the penetration depth of OCT, and this is attributed to the optical properties of hyperkeratosis in AK.

The OCT features in SCC are distinct. Both BCCs and SCCs in the current study demonstrated very reliable diagnostic features. This is in contrast to the finding of Mogensen *et al.* (2009a) who concluded that the naked eye is superior to OCT for the diagnosis of non melanoma skin cancer.

Other research has been performed OCT studies on basal cell carcinoma. It was found that the epidermis and associated basal cell carcinoma had identifiable structural features that were apparent in both the OCT images and histologic pictures. The lobules, islands, and infiltrating strands of basal cell carcinoma appeared similar in OCT images and histologic sections, regardless of the type of tumour (Gambichler *et al*., 2007a).

Interestingly, this study demonstrates that OCT is capable of distinguishing malignant melanoma with the ability to differentiate the early stages of lentigo maligna. Futhermore, OCT is still helpful in distinguishing the late stages of lentigo maligna. In malignant melanoma, the OCT image shows irregular structures in the lower epidermis with the DEJ.

De Giorgi *et al*, (2005). recently performed a pilot study on 9 dysplastic nevi and 1 superficial spreading melanoma OCT *in-vivo*. The authors reported that in selected cases OCT allows for *in-vivo* correlation to be established between the surface dermoscopic parameters and histopathologic correlates, in particular the pigment network and brown globules.

Other research conducted on melanoma skin lesions failed to detect any definitive features in OCT images that enabled us to differentiate tumour subtypes (e.g. junctional nevi, compound nevi), but demonstrated useful discriminating parameters between benign nevi and malignant melanoma (Gambichler *et al.*, 2007b).

There are three basic differences from OCT in relation to the conventional histology routine. OCT images are obtained horizontally from the lesion, whereas in conventional histology the sections are made vertically. The images are obtained in greyscale, similarly to what occurs in radiographs. Moreover, OCT imaging is instantaneous, thus dynamic images of the skin may show events such as blood flow in the case of *in-vivo* OCT which poorly agree with routine histology using formalin-fixed and paraffin-embedded cut sections.

Our observations in this descriptive study indicate that despite the *ex-vivo* nature of the specimen, the level of resolution of seems adequate for clinical practice. However, the first section of this chapter does not evaluate the sensitivity and specificity of the OCT. This is evaluated in the second part of the chapter.

OCT accuracy for the diagnosis of BCC (96.5%) exceeds that of the published rates for physical examination at 92% (Berg and Atkins 2002). Additionally, OCT has the ability to confirm the diagnoses noninvasively and remotely, whereas physical examination has to be followed by a biopsy. We found that OCT is sensitive and specific for the diagnosis of BCC, with no great difference between different BCCs subtypes using specified simple criteria.

Korde and colleagues studied OCT images of sun-damaged skin and AK with a sensitivity of 86% and a specificity of 83% in their study (Korde *et al.*, 2007). Other studies found similar diagnostic criteria in differentiating AK. The presence of a dark band in the SC was 79% sensitive and 100% specific for AK in one such study (Barton *et al*., 2003).

In this study, dark bands specifically was not evaluated, but some of them were identified, suggesting that they may not be a general feature. Some OCT images from solar damage skin in our study displayed characteristics of AK, not surprisingly, given OCT features. The decreased penetration depth of OCT in AK that we identified is attributed to the optical properties of hyperkeratosis in AK.

The current investigation demonstrated that OCT diagnosis was generally more accurate than other *in-vivo* clinical studies. Using experienced observers might be one of the causes of obtaining high accuracy in distinguishing AK from other skin lesions: specificity 100% and sensitivity of 97.5%.

The greatest practical importance of the present study is defining the characteristics of benign lentigines that distinguish these lesions from melanomas. Nevertheless, it is difficult to distinguish between the different types of melanoma. Junctional activity and the cluster cells beyond it were also distinguishable in cross-sectional OCT images. In the diagnosis of cutaneous melanoma, we can reach sensitivity of 43.5% and specificity of 82%.

In the tumour resection margins study, we demonstrated the feasibility of OCT in the identification of skin tumour resection margins. The improved accuracy of excisions by any optical diagnostic technique may benefit the patients by preserving normal tissue and reducing the number of repeat surgeries.

Skin cancer of the face tends to be widespread below the surface and poorly delineated is some cases, requiring multiple biopsies to determine the cancer's margins. Preparation of frozen or permanent pathology can take hours to days or, in some tissues, is not possible. This would significantly affect the prognosis of early stage disease.

Mohs micrographic surgery (MMS) is used, on other hand, as a tissue- preserving technique. During MMS, the tumour is excised with narrow margins and the surgeon assesses the margins on frozen histopathological sections; any residual tumour is mapped and corresponding tissue is further excised. Processing frozen sections takes 20–45 min per MMS stage.

Pre-operative mapping of the margins of skin cancer is important for two reasons: first, despite the high cure rates of excision, there is a high rate of local recurrence. Secondly, the sub-clinical margins – i.e. margins below the skin surface that are not seen by the clinician in the form of thin root-like extensions.

The prognostic significance of the status of the surgical margin in local recurrence is well established; incomplete excision of a tumour increases the risk of primary site recurrence and the status of the surgical margin is an important factor to consider when planning additional treatment (Looser *et al.,* 1978).

Incomplete excision of the tumour may result in operator reluctance to widely excise in areas of high functional or cosmetic concern, which may promote tumour recurrence with incomplete removal. This is due to recognition of the fact that skin cancers in difficult anatomic areas such as the head and neck unit have predictably higher rates of recurrence.

In this study, the correlation between OCT skin thickness and tumour thickness is not very well correlated. This relationship implies that OCT is not a reliable tool for measuring skin tumour thickness despite its ability to measure fine lesions. This negativity in the result not related to light penetration rate rather than the study design (immediate *ex vivo*) and tissue property.

Since the maximum penetration depth for OCT imaging is currently around 2mm, it is unlikely that intraoperative imaging will detect occult lesions at a distance of several millimetres from the primary tumour. This usually makes resection margin analysis difficult in the case of iceberg shaped cancers. This fact attributes to the majority of false negative readings in this study.

Despite that, the real time morphological information gained by OCT regarding the epidermal and dermal layer together with the ability to demonstrate the junction between them makes OCT a promising mapping tool. These are the best performing parameters in terms of diagnostic ability to discriminate tumour involved margins. Our imaging-based scoring system to discriminate between BCC and SCC performed well. However, some cases of SCC may demonstrate tumour nodules similar to BCC extending from the centre toward the periphery without actual damage of DEJ.

In this study, the acquisition time of the OCT is very fast (10 seconds). Moreover, the field-of-view of the system is 6 mm diameter. Therefore, the time needed to evaluate tumour margins and excisions is at most several seconds. Consequently, this real-time intraoperative technique is unlikely to significantly prolong surgical time.

Higher accuracy has been achieved from dermatologist assessing the margins for the BCCs and SCCs and comparing to whole margins regardless of tumour type, although both assessments are subject to the same diagnostic criteria. Many factors may influence the variance in the degree of the sensitivity and accuracy between different margins in the evaluation of individual OCT components, including the experience of the assessor, and varying interpretations in the definition of the categories in each OCT parameter. Tumour heterogeneity is also a factor as variability in tumour appearance that may lead to different decisions.

Examination of the border of basal cell carcinomas revealed a gradual transition from more normal appearing images to frank tumours. OCT can detect features that distinguish normal skin from tumour tissue. Accordingly, Gossage *et al*. (2003) proposed that statistical and spectral texture analysis, combined with OCT imaging, may have the potential to provide an automated means of the diagnostic differentiation of tissue.

Conclusion

This study proved the success of OCT in identifying structural changes in healthy and pathological facial skin. OCT showed a good correlation with the histopathology. Furthermore, this study indicates that OCT shows promise as a useful technique for identifying and characterising different skin pathologies. OCT may not only be able to discriminate between various skin pathologies, but also between sub-pathologies. OCT features in melanoma skin lesion were identified, and MM and LM can be differentiated with a degree of certainty. OCT diagnosis for SCC is less accurate than BCC, but is shows a high accuracy in distinguishing AK lesions from pathology skin.

OCT provides moderate accuracy in identifying tumour borders, although tumour identification may be more difficult to measure accurately in thick tumours that stretch beyond the penetration of the OCT signal. OCT however remains imprecise in the measurement and correlation of tumour thickness in thick tumours. Imaging of the resection margins by OCT shows its feasibility in detecting the residual foci of basal cell carcinoma and squamous cell carcinoma. In the long-term, such imaging may guide the excision of these cancers during intraoperative Mohs surgery, directly on the patient.

Chapter 6
Instant *ex-vivo* OCT for pathologic oral mucosa

Introduction

To date, little normative data on the thickness of oral epithelium exists. Quantitative information on the thickness of oral epithelium has been determined in chapter 4 using a delayed *ex-vivo* technique. However, this previously described method is subject to tissue changes.

Taste disorders are common in cancer patients, particularly in those who have received radiotherapy, as they may experience taste loss (ageusia), taste alterations (dysgeusia), or heightened sensitivity (hypergeusia). The impact of altered sensations can lead to a reduction in caloric intake, a change to a more sugary diet, and also a reduced quality of life (Scott *et al*., 1985).

The management of patients with established taste disturbance following RT or other therapies still remains unsatisfactory, however, and there are few reports utilising good outcome measures due to the lack of proper assessment of atrophy. Subjective methods using operator eyes were widely used to assess the status of the papilla and to monitor responses to treatment (Porter *et al*., 2010).

Only a few studies have been conducted on the effects and the damage of irradiation on the morphology and size of the papilla. As a result, these characteristics are understudied and likely to be underestimated, making recommendations concerning diagnosis, therapy and prognosis difficult.

In this chapter, the applicability of the OCT is examined for a number of reasons, including the collection of baseline data on normal oral mucosa from different parts of the oral cavity using an instant *ex-vivo* study. This technique was used as it may retain the tissue in the same state as it is when it is *in-vivo*. Furthermore, the use of OCT may help to gain more information about its influence in improving oral cancer prediction by screening high risk patients, which can be achieved by obtaining quantitative measurements of the thickness of the oral epithelium. Further aims include describing typical aspects of the healthy human tongue, including morphological features of the peripheral taste organs using OCT, and setting the criteria for assessment and staging of the atrophy and calculating the degree of agreement between readers. Finally, the study aimed to compare the OCT morphologic changes of the tongue after radiation and chemotherapy with normal control groups.

Section I: Normal predictive value for oral epithelium thickness using instant *ex-vivo* tissues.

Background

Human tissue changes within minutes of surgical excision. As a result, measuring epithelium thickness immediately following resection may provide accurate information about the normal thickness.

Objectives

The purpose of this study is to assess OCT in terms of epithelium thickness using instant *ex-vivo* scanning.

Patients

The present prospective study includes 56 patients who had benign oral lesions, mainly mucocele and firoepithelium polyps, which were used for the histometric measurement of normal epithelial thickness. Patients included in this study were of the same race, had no history of cigarette smoking and were of a similar age group. The exclusion criteria included patients with any risk factor for oral cancer, potential malignant oral lesions and/or other conditions.

The study was conducted in accordance with the ethical standards stated in the 1964 Declaration of Helsinki and was approved by the Moorfields & Whittington Local Research Ethics Committee. Informed consent was obtained from all patients prior to scan acquisition.

Results

From the 56 oral biopsies performed by OCT, 12 were taken from the ventral part of tongue tongue, 9 from the buccal mucosa, 8 from the mucosal surface of lower lip, 6 from the vermilion of the lower lip, 5 from the mucosa of the upper lip, 5 from the floor of the mouth, 4 from the gingiva, 4 from the vermilion of the upper lip and 3 from the dorsum of the tongue.

The mean thicknesses measured for each region of the overall epithelium, regardless of gender, are presented in table 6.1. Epithelium thickness for the dorsum of the tongue was greater than in other parts of the oral cavity (mean 450µm, range 60µm) followed by the buccal mucosa and the gingiva, where the mean thickness was 410µm. The mean values for the lower and upper vermilion surfaces of the lip were 390µm (range 60µm) and 400µm (range 50µm), respectively. In addition, the mean mucosal thicknesses of the upper and lower lips were 400µm (range 100µm) and 380µm (range 90µm), respectively. Oral epithelium on the ventral part of the tongue and the floor of the mouth were easily measurable and the mean thicknesses were 230µm (range 70µm) and 200µm (range 80µm), respectively (Figure 6.1-6.5).

Figure 6.1: Epithelial thickness for the floor of mouth (200µm).

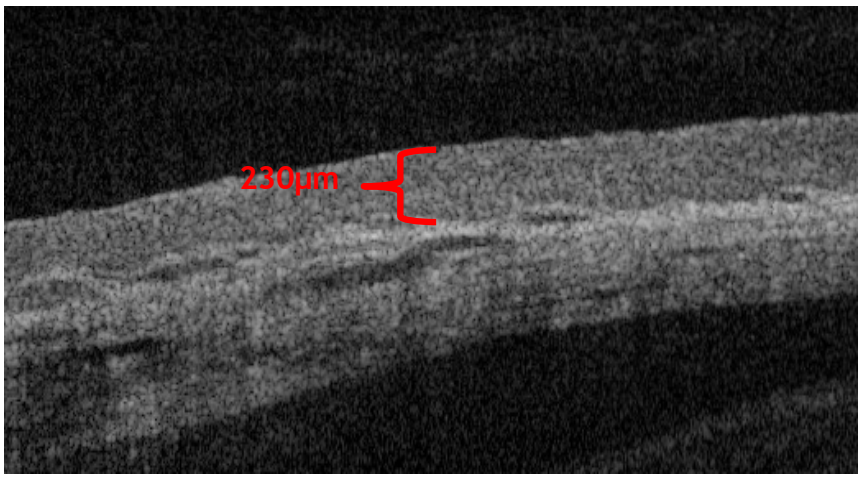

Figure 6.2: Epithelial thickness of the ventral part of tongue (230µm).

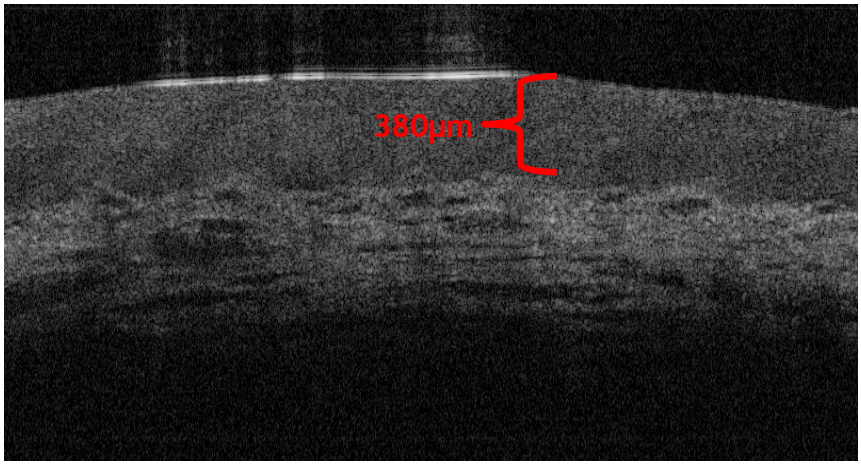

Figure 6.3: Epithelial thickness of the mucosal part of the lip (380µm).

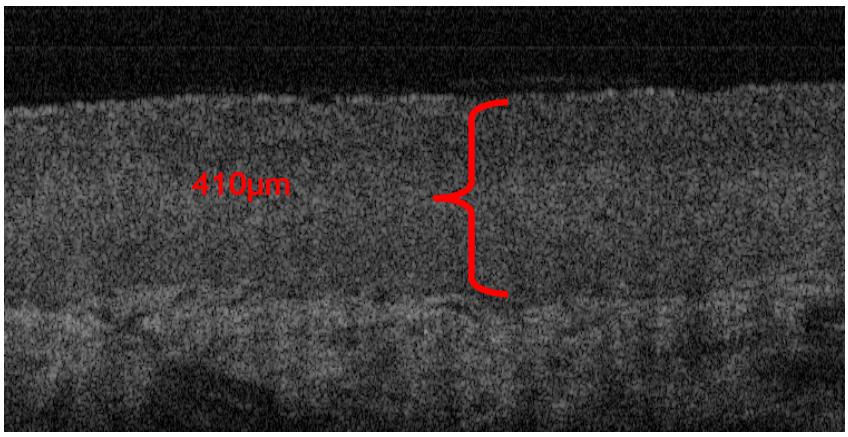

Figure 6.4: Epithelial thickness of the buccal mucosa (410µm).

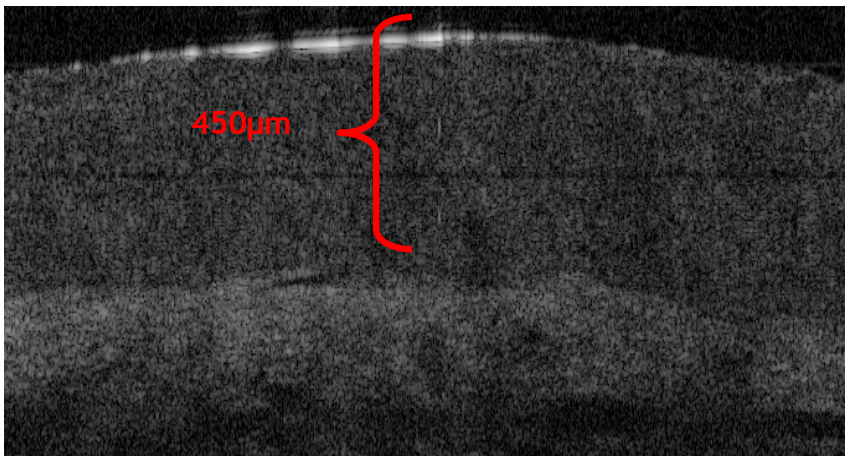

Figure 6.5: Epithelial thickness of the tongue (450µm).

Table 6.1: Mean values for epithelial thicknesses of nine oral sites

Epithelium	**Mean (µm)**	**Maximum (µm)**	**Minimum (µm)**	**Range (µm)**
Mucosa of the lower lip	380	410	320	90
Mucosa of the upper lip	400	420	320	100
Vermilion of the upper lip	400	440	380	50
Vermilion of the lower lip	390	420	370	60
Buccal mucosa	410	490	360	130
Gingiva	410	440	400	40
Dorsal of the tongue	450	480	420	60
Ventral of the tongue	230	250	180	70
Floor of the mouth	200	230	150	80

Section II: Evaluation of the tongue papilla for patients suffering from taste disorders after head and neck chemoradiotherapy

Background

Instant *ex-vivo* OCT has shown a successful application in the assessment of the oral cavity epithelium thickness in the previous section of this chapter. The penetration depth of approximately 2mm allows for visualization of tongue papillae structures and assessment of their geometry.

Objective

To use OCT to identify structural changes in the tongue papillae in patients with taste disorders following chemoradiotherapy.

Chemo-radiotherapy patients

The subjects included 10 patients who underwent RT and 12 who were treated with chemotherapy (CT) for their head and neck cancers at the University College of London Hospital. All of the patients included in this study had reported suspicious oral lesions which indicated that they were suitable for surgical biopsy. Incisional biopsies were taken from the suspicious area towards the apparently normal looking area, which was either atrophied or non–atrophied, depending on the patient. None of the patients were treated with surgery to the tongue prior to RT or CT. The malignancies were distributed among the 22 patients as follows: six had buccal mucosa cancer, five had retromolar cancer, four had floor of the mouth cancer, four had malignancy of the tonsil and three had a soft palate malignancy. The mean age was 64 years (range: 39–70 years), and there were sixteen men and six women.

According to UCLH guidelines, the RT was administered as a dose of 2Gy once a day, five times a week. The total RT period ranged from 38 to 62 days, with an average of 47 days. Conventional radiation techniques were used in this study. The anterior oral tongue was deflected from the radiation volume after off-cord reduction. Concurrent chemotherapy was included in this study, provided that the biopsies taken at the end of the cycle before commencing radiotherapy.

For the patients to be eligible for this study they should have reported moderate to severe taste disturbances after chemotherapy, or after a minimum of 20Gy of radiation had been received within the first three months during and following the therapy. This is because normal taste sensations generally return within 6–24 months.

The cancers were limited to the head and neck area. Patients who had only a part of their tongue within the radiation field were excluded from the study. No tumour ablative procedures or alterations of salivary beds were performed during this study, and none of the enrolled subjects had total or partial glossectomies. All of the subjects gave written informed consent before entry into the study.

Normal individuals

A panel of 20 subjects with benign tongue lesions were biopsied (excisional with normal margins). The ages of participants ranged from 20–36 years, with a mean age of 29 years, and there were 12 women and 8 men. All subjects were informed of the nature of the examination and agreed to participate. The study was conducted in strict accordance with the Helsinki Declaration and was approved by the Moorfields & Whittington Local Research Ethics Committee.

Results

Normal papilla

The agreement between observers for differentiating between filliform and fungiform papillae was very high using the Kappa value (K=0.72). The dorsal surface of the anterior and posterior parts contained fungiform papillae, with the apical parts of these papillae containing hypo-reflective OCT signals, indicating minimal keratin. The interpapillar space was covered by keratin-free squamous stratified epithelium. Taste pores were not easily seen by OCT, making the differentiation of taste buds extremely difficult. Three major morphological forms were clearly identified: dome, conical and mushroom-like papilla (Figures 6.6 and 6.7).

No structural difference was seen between these different forms, except with regards to blood supply. Both dome shape and mushroom papilla demonstrated worm track cavities, which represented the blood vessels supply (Figure 6.8). Filiform papillae

showed four forms, with the most common being thorn-shaped projections, which were uniform in size and stemming from a thick stalk. The second types as similar as the first type with prominent fine thread like structure. The main stalk represents the primary papilla while all other fine thread-like structures represent the secondary papillae (Figure 6.9,6.10). The third pattern was finger like projection, while the fourth pattern was thorn like shape single projection (Figures 6.11-6.12).

Chemo-radiotherapy patients

Five patterns of structural characteristics or changes were recognised in fungiform papilla: (I) a normal pattern with a clear morphology, where the papilla is clear in shape with an average height between 400µm and 750µm; (II) a slight decrease of the papillae height to 300-400µm, where the papillae are less clear in shape with slight depressions on their apical epithelia, and fungiform papillae often show no change in width (the diameter of the papillae at this stage ranges from 50µm to 80µm; (III) moderate decreases of height as the papillae are flattened, with average heights between 100µm and 300µm; (IV) severe decreases in height to 10-100µm; and (V) extreme, completely flattened patterns, as papillae are diminished). Atrophy of the papillae, as well as the diminished blood supply of the connective core in the papillae, were the predominant changes (Figure 6.13-6.16).

Filiform papillae still maintain an irregular shape, with some appearing oval and others appearing ellipsoid. The finger-like, bending filiform papillae consist of keratinised epithelium. In group (I), the papillae are pointed and normally keratinised, and range from 250-500µm. Group (II) papillae are rounded and less keratinised, with sizes from 150-250µm. Group (III) papillae are flattened and not keratinised, and range from 50-150µm. Papillae in group (IV) have stubs ranging from 10-50µm, and group (V) papilla are diminished (Figures 6.17-6.20 and Table 6.2).

The difference was significant between RT patients and healthy subjects (P <0.005), but no significant differences were seen between chemotherapy patients and healthy subjects (P <0.005). Agreements in the scoring of atrophic changes of tongue papillae between 2 examiners using the Kappa test were very high for the filiform papilla (K=0.71) and very good for fungiform papilla (K=0.76).

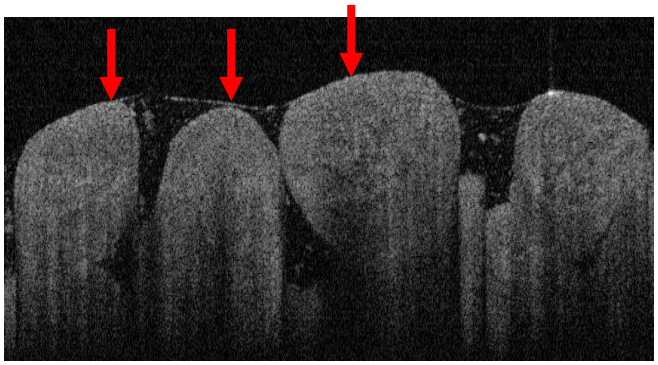

Figure 6.6: Normal fungiform papilla showing a common dome shape papillary pattern (red arrow); Score 1.

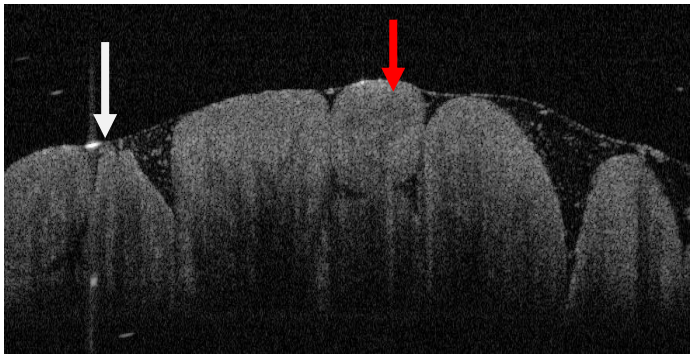

Figure 6.7: Normal fungiform papilla geometry; typical mushroom-like papilla (red arrow); conical papilla (white arrow); Score 1.

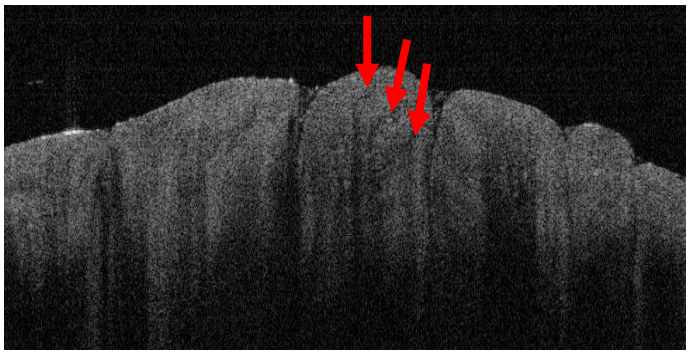

Figure 6.8: Normal fungiform papilla with 3 clear taste bud pores and descending assembly (red arrows).

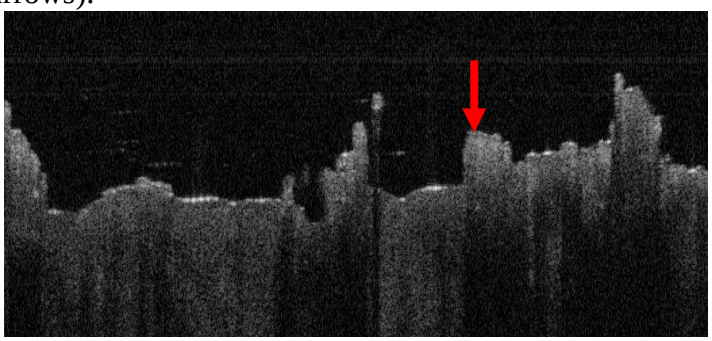

Figure 6.9: 1st pattern of normal filliform papilla from the anterior-lateral part of the tongue: a single uniform papilla (red arrow).

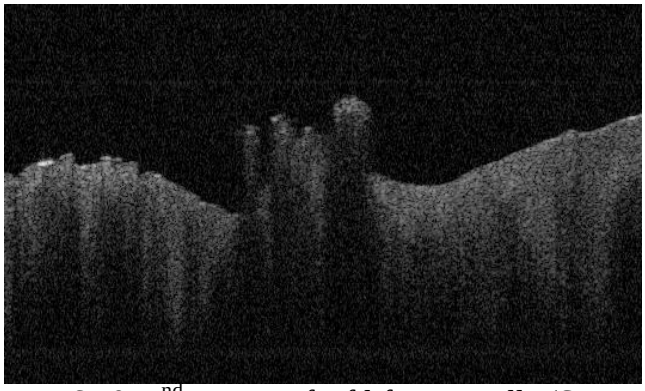

Figure 6.10: 2nd pattern of a filiform papilla (Score 1).

Figure 6.11: 3rd pattern of a filiform papilla (Score 1).

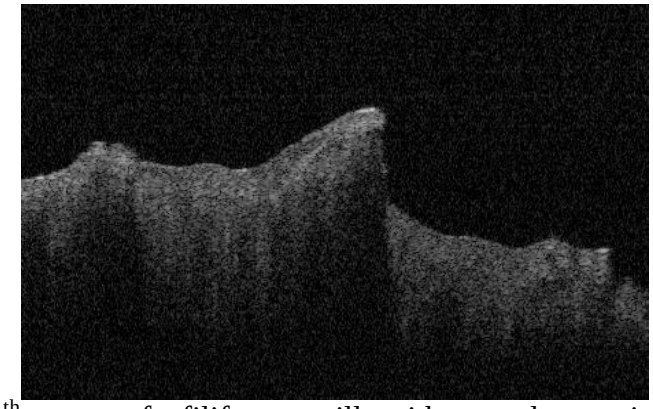

Figure 6.12: 4th pattern of a filiform papilla with secondary projections (Score 1).

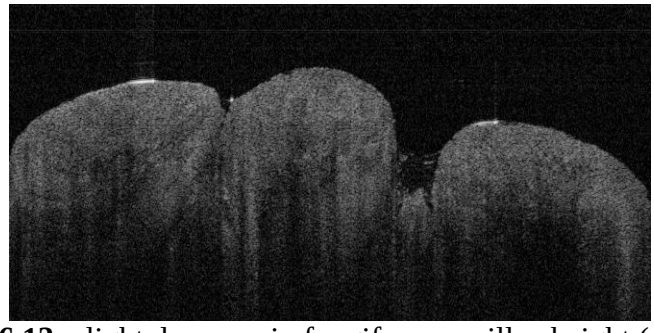

Figure 6.13: slight decrease in fungiform papillae height (score 2).

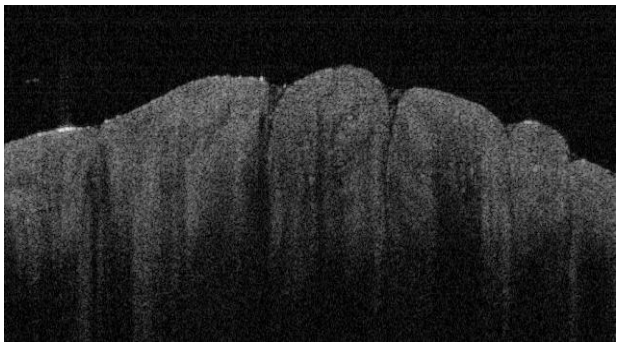

Figure 6.14: Moderate decrease in the height and width of the base in fungiform papillae with pointed tips (score 3).

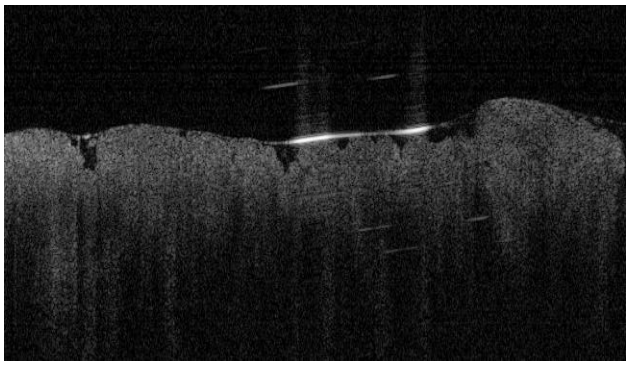

Figure 6.15: Fungiform papillae (Score 4).

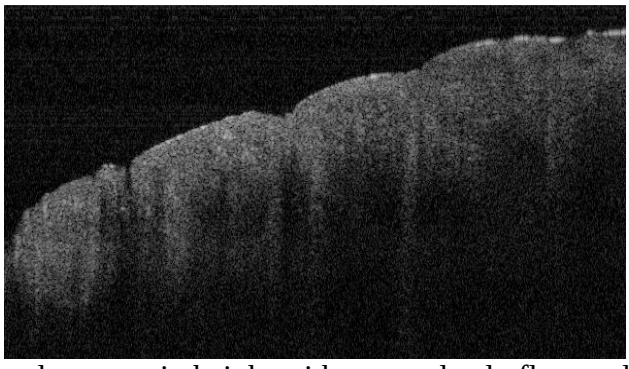

Figure 6.16: Severe decreases in height with a completely flattened pattern of fungiform papillae (score 5).

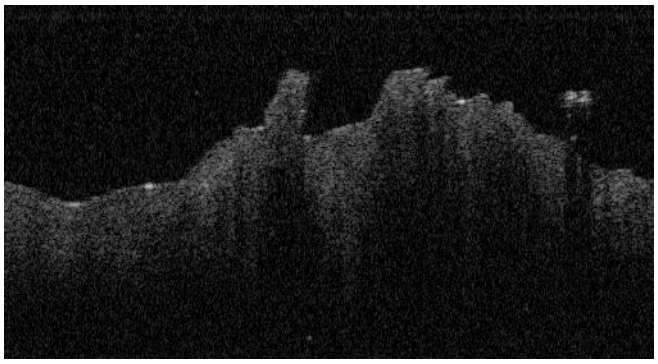

Figure 6.17: Filiform papilla (Score 2).

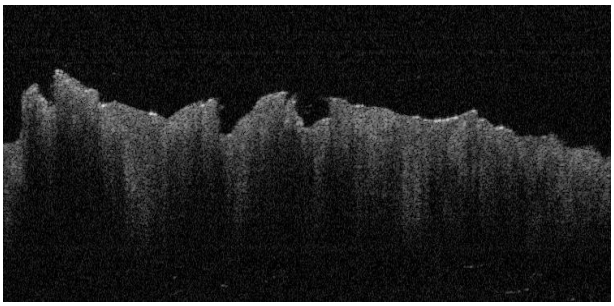

Figure 6.18: Filiform papilla (Score 3).

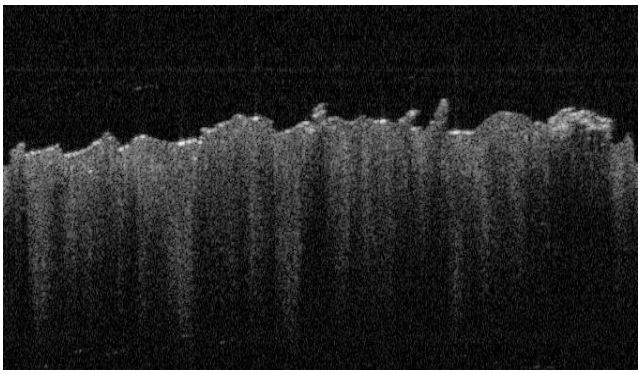

Figure 6.19: Filiform papilla (Score 4).

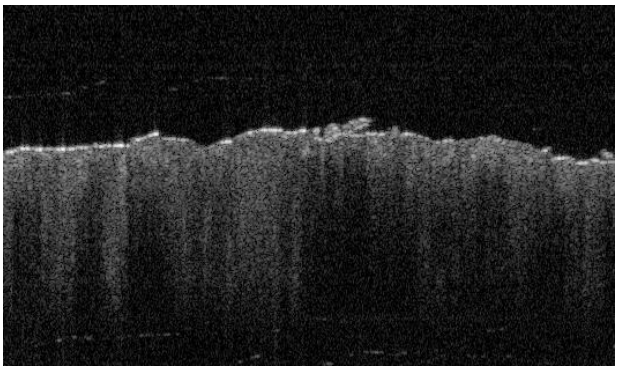

Figure 6.20: Filiform papilla (Score 5).

Table 6.2: Atrophic scores of tongue papillae

Fungiform papilla (I) Normal pattern with clear morphology; Papillae are clear in shape with heights between 400-750µm. (II) Slight decreases in the papillae height (300-400µm); the base of papillae at this stage range from 50-80µm. (III) Moderate decreases in height to between 100µm and 300µm. (IV) Severe decreases of height to between 10µm and 100µm. (V) Extreme, compıetely flattened patterns, with diminished papillae.
Filiform papilla (I) Papillae are pointed and normally keratinised (250-500µm). (II) Papillae are rounded and less keratinised (150-250µm). (III) Papillae are flattened and not keratinised (50-150µm). (IV) Stub of the papillae range from 10-50µm. (V) Papillae are diminished.

Section III: Risk assessment of oral epithelium thickness

Background

The normal epithelium and staged tongue papillae in previous sections were studied by instant *ex-vivo* scanning under the assumption that the identification of early structural changes in the oral mucosa can help in predicting premalignant and malignant changes.

Objectives

OCT was used for the evaluation of oral epithelial changes and thickness for high risk patients.

Subjects investigated

74 patients recruited into the study who had benign oral lesions needing excisional biopsy with normal margins were included. 17 of them were non-smokers who drank alcohol, 15 were smokers but non-alcoholic drinkers, 12 were smokers who drink alcohol, and 30 were non-smokers and non–drinkers. All subjects were aged between 30 and 60 years. A ‘‘drink’’ was defined for the study participants as a 12-ounce beer, a 4-ounce glass of wine, and a 1.5-ounce shot of hard liquor. Participants who reported drinking 3–6 drinks per week for 2 years were included in this study.

Non-drinkers were defined as patients who drank 'never or almost never’, ‘infrequent drinkers' (once a month or less), 'occasional' (one to three days a week).

The criteria for enrolment in the study with regards to smoking included subjects who smoked average numbers of 5-10 cigarettes per day for 2 years. Patients who had not smoked tobacco on a regular basis during their lifetime for 1 year or more were considered to be non-smokers. Former use was defined as not having used tobacco for at least 1 year prior to this interview.

47 subjects suffered from at least 1 pre-malignant disease PMD without having risk factors, with the exception of oral submucous fibrosis (OSF) with a history of betel nut chewing. These individuals attended the outpatient clinic of the Oral and

Maxillofacial Surgery clinic of the UCLH Medical Centre. Those groups are either histopathologically proved by biopsy or referred as patients with a high suspicion, all of which need excisional biopsies. Patients having PMD were interviewed face to face by well-trained research workers. Clinically, a distinction was made between a homogeneous and a non-homogeneous OL. Age, gender, location, size and clinical appearance of the lesions were recorded.

The lesions to be excluded were those belonging to other entities, such as lichen planus (acknowledging that some of them were included later in a separate group), lupus erythematosus, leukoedema and white sponge nevus, and lesions for which an aetiology can be established, such as frictional keratosis, cheek/lip/tongue biting, contact lesions and smoker's palate.

Subjects were also excluded if they had treatment with photosensitising or retinoid chemo preventative drugs within the previous 3 months, or treatment with ionising radiation or cytotoxic chemotherapy agents within the previous 6 months. Ethical clearance and informed consent from the participants were obtained in accordance with the Helsinki Declaration for Humane Research.

Clinical diagnosis of OSF was made when a patient showed the characteristic features of OSF in the clinics, including blanching and stiffness of the oral mucosa, fibrous bands in the buccal or labial mucosa, and difficulty in opening the mouth. All of the OSF lesion samples were diagnosed following biopsy.

Results

Suspicious lesions

Forty seven patients with clinically suspicious lesions were examined by OCT, 26 of them were proven to be dysplasia by biopsy, 10 patients were diagnosed with submucosa fibrosis and 5 with lichen planus. Six patients with a previous history of dysplasia and a high clinical suspicion underwent a biopsy that revealed SCC. For each patient diagnosed with OSF, pan oral biopsy was performed. Five areas of biopsies were included (lip, buccal mucosa, tongue and floor of mouth).

Morphometrical analysis

Risk group

No clear structural differences were observed between the smoking and non-smoking groups, and the same was observed for the drinking and non-drinking groups. In the smoking group, the Keratin cell layer showed a slight hyper-reflection in the majority of individuals, but had normal epithelium, basement membranes and lamina properia (Figure 6.21). This was similar for the drinking group, with the exception of the normal reflection of the keratin cell layer. Blood-supporting capillaries could be identified with clear visible capillary loops, without the contrast agent penetrating into the surrounding areas. In the smoking group, information regarding blood vessel status in the LP, either normal looking or hyperemic, shows what appear to be dilated vessels.

Lichen planus group

Mucosa appears to be normal from the OCT appearance, with an unclear wavy surface, in some areas of the epithelium. However, the junctions between EP and LP show smooth patterns with small cavity-like structures, which may represent liquifactive necrosis of the basal cell laser. Furthermore, a slight intensity of the LP signal was observed in some cases, which may reflect lymphocytic cell infiltration. Blood vessels appear similar in the normal mucosa (Figure 6.22), and the saw tooth appearance of the rete pegs was not seen in all of the cases.

Submucosal fibrosis

In the OSF mucosa, the EP layer is significantly thinner and the boundary between the EP and LP layers is smoother. The difference in contrast intensity between the EP and LP is also strong. Furthermore, the LP appears to be more signal reflective than normal, possibly due to the high percentage of collagen within the tissue structures with a lower blood supply (Figure 6.23). Salivary gland atrophy or absent glands have been seen in the majority of the cases, and blood vessels in the LP become reduced in number or absent.

Dysplasia

The results of this study show that when a lesion begins to evolve through the stages of epithelial dysplasia, from mild to moderate and then severe, the EP layer is thicker when the EP/LP boundary can still be identified. This increased thickness can be used as an effective diagnostic indicator for lesions. Large variations in EP thicknesses have been seen from stage to stage and from site to site, which may lead to difficulties in differentiating between different stages (Figures 6.24 and 6.25).

Cancer

In the early stage of oral cancer, the tumour cell starts developing in the EP layer and then migrates towards the LP. In the cancerous tissue, the boundary between the EP and LP layers disappeared with a stronger signal intensity in the LP representing the epithelial invasion. The epithelial cells aggregated into a cluster structure, which leads to non-homogenous distribution. However, in advanced cancerous mucosa, the tumour cells replaced epithelial cells and LP (Figure 6.26). In some benign oral lesions, false elevation of the epithelial layer may be confused with increases in the thickness (Figure 6.27)

Histometric analysis

By analyzing the thickness of the oral epithelium, smokers presented with significantly thicker epithelial tissue than the non-smoking patients. Women and men with a history of drinking showed no significant differences in the thickness measurements of the epithelium when compared to those who have never drunk. By grouping the risks according to smoking and alcohol drinking status, the oral epithelium was not significantly different in comparison to the non-smoking or drinking groups (Table 6.4).

Regarding the patients with lichen planus, there was no significant difference observed between this group and normal tissue (Table 6.5 and 6.6). Nevertheless, the epithelium thickness was significantly higher in patients with dysplasia compared with normal margins (Tables 6.7-6.10) and patients with SCC (Tables 6.11 and 6.12). Contrary to what has been previously thought, a decrease in mucosal thickness in the group with OSF was observed (Figure 6.28).

EP thickness values of the normal control samples are similar to those of the lichen planus group and are significantly smaller than those of the dysplasia group. The mean epithelial thickness of oral dysplasia is thicker in different anatomical sites.

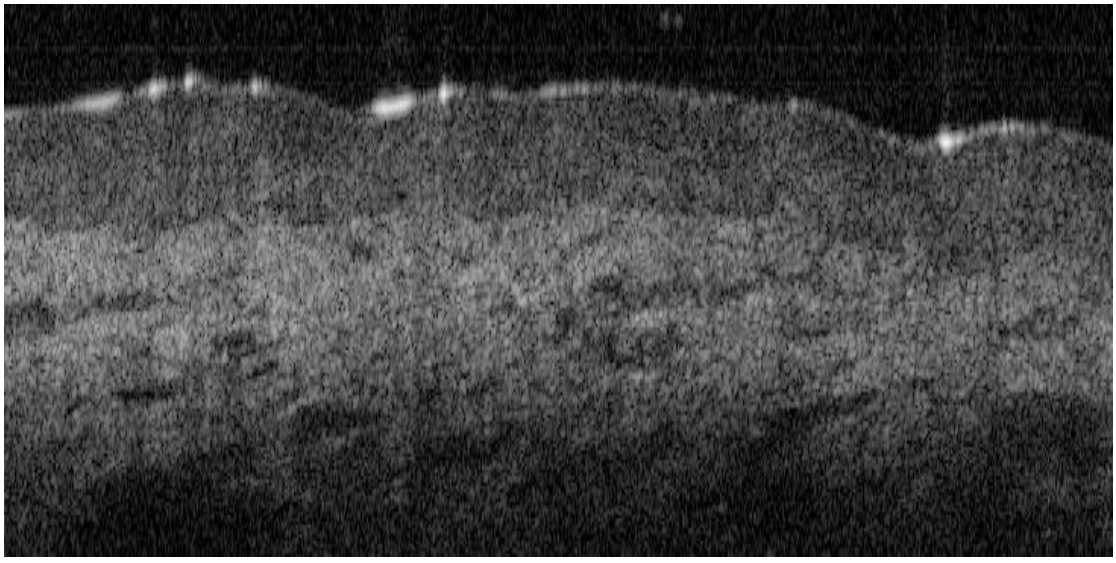

Figure 6.21: OCT scan for a biopsy from the floor of the mouth for a smoking patient, showing slight hyper-reflection in the top-most part of the epithelium (stratum corneum layer). Normal EP, basement membrane and LP with normal looking blood vessels.

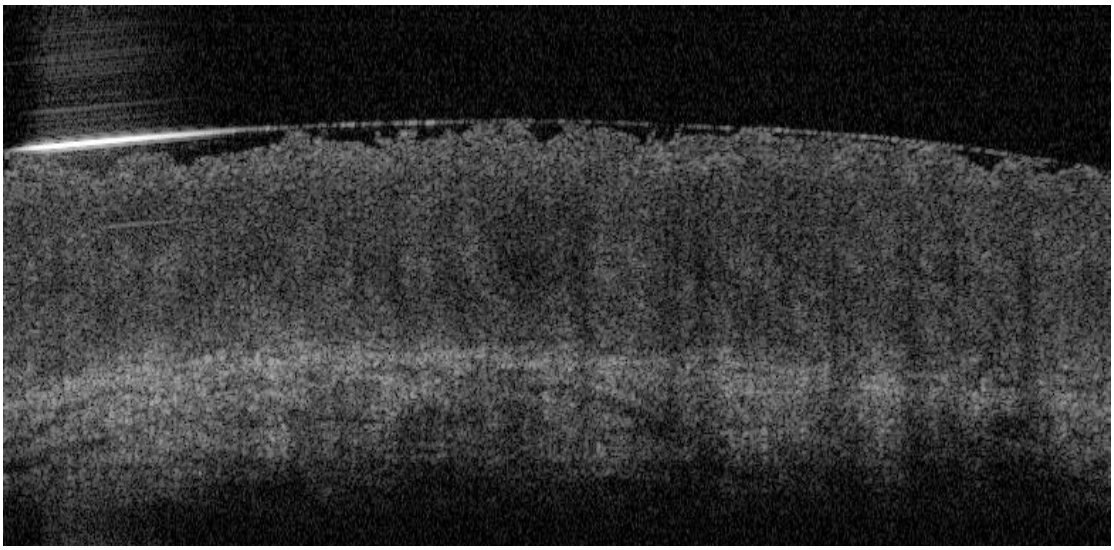

Figure 6.22: OCT scan for a biopsy for patient with lichen planus showing wavy structures in the epithelium. The basement membrane shows a smooth pattern with small cavity-like structures, which may represent liquifactive necrosis of the basal cell layer. Signal intense LP are also seen, which may reflect lymphocytic cell infiltration with less blood vessels.

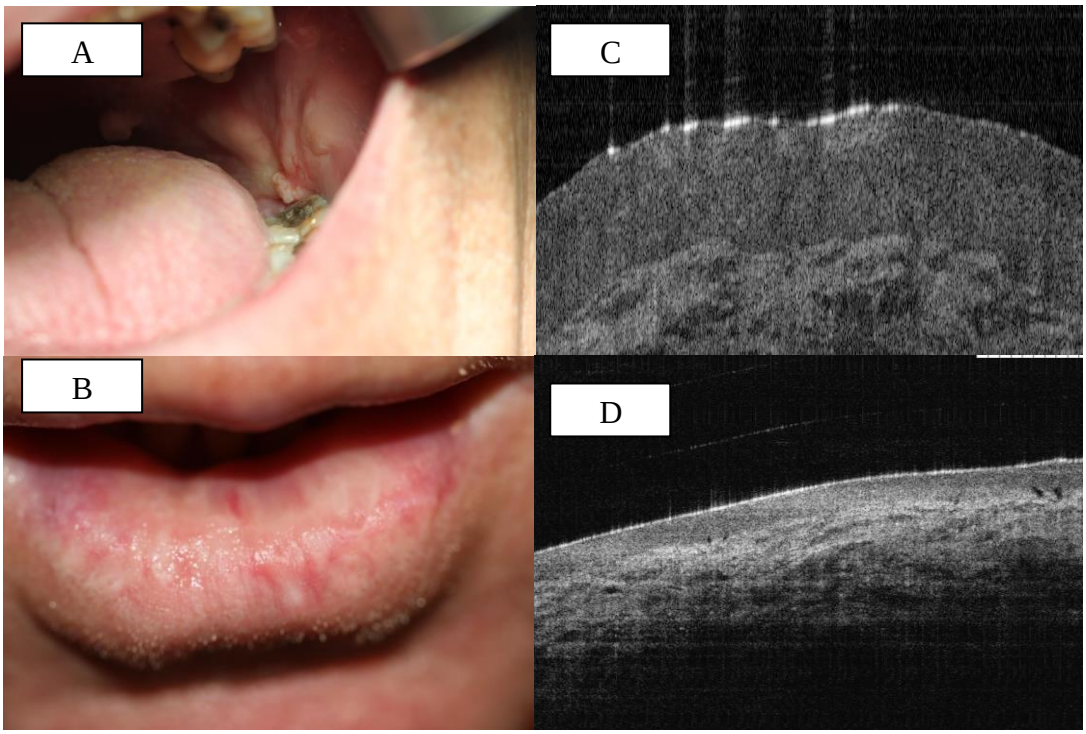

Figure 6.23: Submucosal fibrosis affecting the buccal mucosa and lip (A, B). Significant OCT measurements differences in epithelium thickness for the vermilion of the borders of the lower lip biopsy from a normal non OSF patient (C) and an epithelium for the biopsy from OSF paient(D). The EP layer in OSF patient becomes significantly thinner and the boundary between the EP and LP layers becomes smoother. The difference in contrast intensity between EP and LP is also strong.

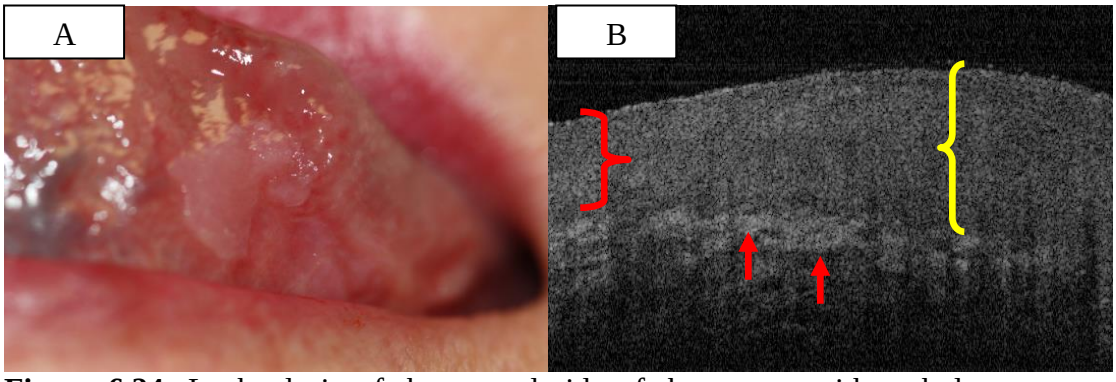

Figure 6.24: Leukoplasia of the ventral side of the tongue with pathology proven moderate dyplasia (A). Instant OCT scanning of the biopsy showing the transitional thickening of epithelium thickness from normal (red bracket 250μm) to the white area (yellow bracket 510), without breakdown of the basement membrane. The EP and LP layers can be clearly differentiated and two blood vessels (indicated by red arrows) can also be seen in the LP layer (B).

Figure 6.25: Sever dysplasia over the vermilion border of lower lip. Instant OCT scanning of the biopsy show that the EP layer is thickened (red bracket), dysplastic cells are found in the lower third of the EP, which creates a thicker epithelium, and a thick keratinised cell layer is found on the EP surface .

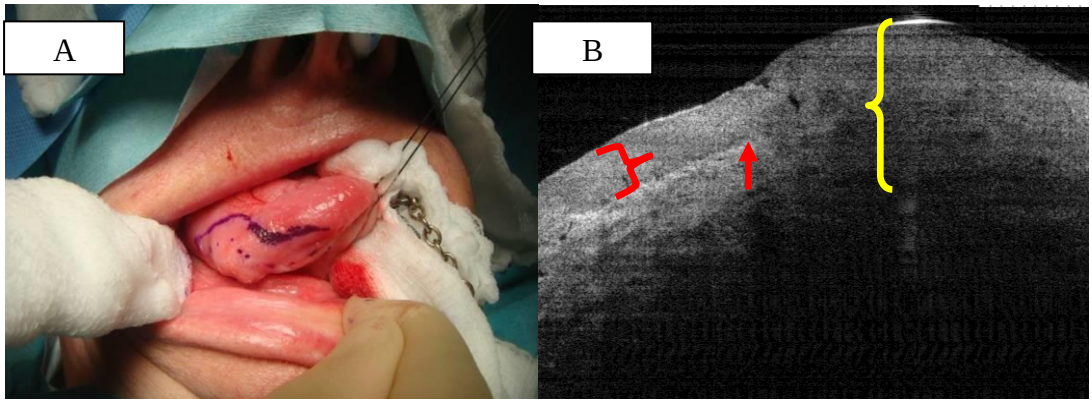

Figure 6.26: SCC ventral side of tongue (A). Instant OCT scanning of the excisional biopsy at the margin show that the epithelium thickness at the normal margins is 210µm (red bracket) while the central tumour zone is 730µm (yellow bracket) with a damaged basement membrane (red arrow) (B).

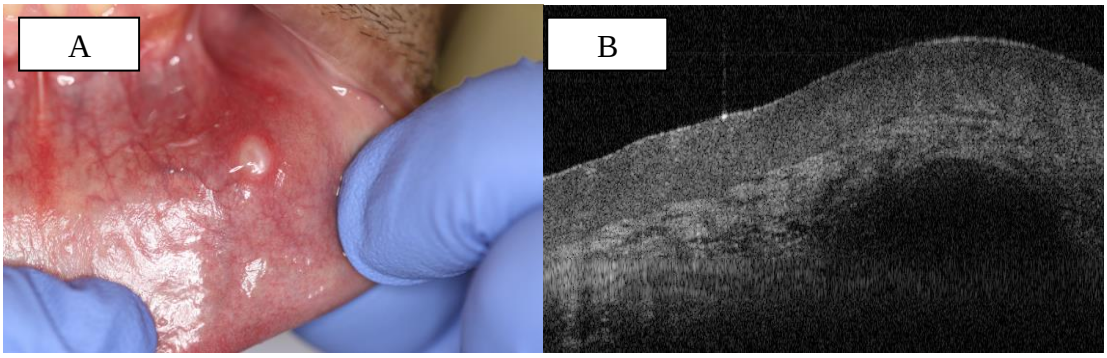

Figure 6.27: Mucoceel over the mucosal surface of lower lip (A). OCT image of he biopsy. The EP layer becomes elevated with no thickening or evidence of dysplastic cells found in the lower two-thirds of the EP in cases of cystic lesions. The basement membrane is intact with a well-circumscribed echogenic area (B).

Table 6.3: The Duncane test shows the difference between the control group and risk group for the mucosal surface of the buccal mucosa.

		Subset for alpha = 0.05		
CODE		1	2	3
5		302.0000		
1			362.3333	
3				481.7647
4				488.6667
2				500.8333
Sig.		1.000	1.000	.105

1: Normal control, 2: drinker& smoker, 3: Drinker,

4: Smoker, 5: Submocosal Fibrosis

Table 6.4: No significant difference was seen between the lichen planus of the lip with regards to the control margins, $P < 0.01$.

	CODE		Mean	Std. Deviation	Std. Error Mean
MUCOSA	1		372.5000	25.00000	12.50000
	2		415.0000	7.07107	5.00000

		t-test for Equality of Means				
		t	df	Sig. (2-tailed)	Mean Difference	Std. Error Difference
MUCOSA	Equal variances assumed	-2.237	4	.089	-42.5000	18.99836

Table 6.5: No significant difference was seen between the lichen planus of the buccal mucosa with regards to the control margins, P < 0.01.

	CODE		Mean	Std. Deviation	Std. Error Mean
BUCCAL	1		385.0000	28.80972	11.76152
	2		390.0000	10.00000	5.77350

		t-test for Equality of Means				
		t	df	Sig. (2-tailed)	Mean Difference	Std. Error Difference
BUCCAL	Equal variances assumed	-.284	7	.785	-5.0000	17.62709

Table 6.6: Significant differences in dysplasia of the lip with regards to the control margins, P < 0.01.

	CODE		Mean	Std. Deviation	Std. Error Mean
MUCOSA	1		372.5000	25.00000	12.50000
	2		593.3333	15.27525	8.81917

		t-test for Equality of Means				
		t	df	Sig. (2-tailed)	Mean Difference	Std. Error Difference
MUCOSA	Equal variances assumed	-13.361	5	.000	-220.8333	16.52859

Table 6.7: Significant differences in dysplasia of the ventral side of the tongue with regards to the control margins, P < 0.01.

	CODE		Mean	Std. Deviation	Std. Error Mean
floor	1		200.0000	16.51446	4.76731
	2		417.0000	43.21779	13.66667

		t-test for Equality of Means				
		t	df	Sig. (2-tailed)	Mean Difference	Std. Error Difference
floor	Equal variances assumed	-16.103	20	.000	-217.0000	13.47560

Table 6.8: Significant differences in the dysplasia of the buccal mucosa with regards to the normal margins, P < 0.01.

	CODE		Mean	Std. Deviation	Std. Error Mean
BUCCAL	1		385.0000	28.80972	11.76152
	2		590.0000	15.81139	7.07107

		t-test for Equality of Means				
		t	df	Sig. (2-tailed)	Mean Difference	Std. Error Difference
BUCCAL	Equal variances assumed	-14.153	9	.000	-205.0000	14.48499

Table 6.9: Significant differences in dysplasia of the floor of the mouth with regards to the normal margins, P < 0.01.

	CODE		Mean	Std. Deviation	Std. Error Mean
FLOOR	1		175.0000	17.79513	5.62731
	2		430.0000	37.79645	13.36306

		t-test for Equality of Means				
		t	df	Sig. (2-tailed)	Mean Difference	Std. Error Difference
FLOOR	Equal variances assumed	-18.970	16	.000	-255.0000	13.44259

Table 6.10: Significant differences between invasive carcinomas of the ventral side of the tongue with regards to the control margins, P < 0.01.

	CODE		Mean	Std. Deviation	Std. Error Mean
VENTAL	1		200.0000	16.51446	4.76731
	2		720.0000	14.14214	10.00000

		t-test for Equality of Means				
		t	df	Sig. (2-tailed)	Mean Difference	Std. Error Difference
VENTAL	Equal variances assumed	-41.693	12	.000	-520.0000	12.47219

Table 6.11: Significant differences between invasive carcinomas of the floor of the mouth with regards to the normal margins, P < 0.01.

	CODE		Mean	Std. Deviation	Std. Error Mean
FLOOR	1		175.0000	17.79513	5.62731
	2		635.0000	21.21320	15.00000

		t-test for Equality of Means				
		t	df	Sig. (2-tailed)	Mean Difference	Std. Error Difference
FLOOR	Equal variances assumed	-32.691	10	.000	-460.0000	14.07125

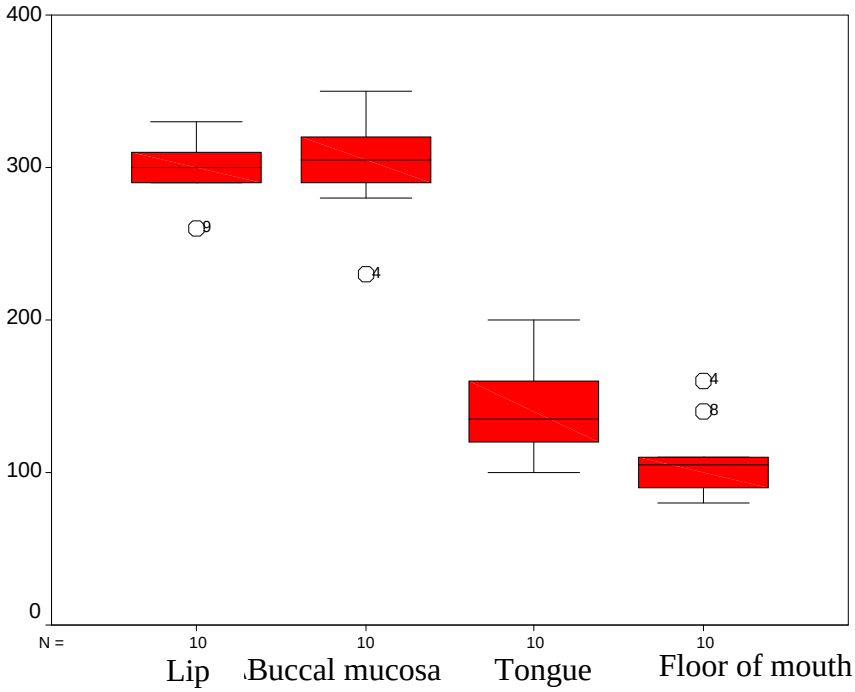

Figure 6.28: Thickness of the epithelium in patients with Submucosal fibrosis in µm scale.

Discussion

The knowledge of the oral epithelium thickness is of great significance in many areas of medical and biological research. For example, in chapter 4, results revealed that continuous epithelial thickening as a function of the grade of dysplasia occurs due to an altered nucleus–plasma-relation, an enlargement of nuclei and an increase of nucleus containing cells. This process begins in the basement layer and is confined to one or more epithelial layer until all three epithelial layers are affected by severe dysplasia or carcinoma in situ.

Arens *et al*. revealed a progressive thickening of the vocal epithelium from 147µm in normal tissue to 974µm in an early-stage invasive carcinoma. In such a manner, moderate dysplasia showed a double increase, carcinoma *in situ* showed a triple increase and early-stage invasive carcinoma showed up to a six-fold increase of the mean epithelial thickness compared to normal laryngeal mucosa (Arens *et al*., 2007).

In previous *ex-vivo* studies, mucosal appendages including gland ducts were identified by OCT. In addition, our pilot study on ET demonstrated a high correlation between OCT measurements and formalin-based histology with a satisfactory agreement between both methods. As a result, OCT can be considered a very useful tool for the study of ET *in-vivo*.

The determination of ET is strongly dependent on the definition of markers. For example, minimum ET is defined by the top of the uppermost papillae, and maximum ET by the valleys of the papillae. Our previous study showed that OCT resolution is not always able to detect fine rete pegs, resulting in the decision to assess the mean minimum ET. Generally speaking, this study found higher measurements compared with delayed *ex-vivo* studies. This may be explained as an action of the vertical collagen fibres.

It has to be stressed, however, that the entire range of ET values over all anatomic sites was smaller than the theoretical depth resolution (2mm) of the OCT scanner used in the current study. As a result, small differences in the ET may have been missed due to the limited resolution of the OCT device. However, using high-output

broadband light sources, such as a femtosecond Ti:sapphire laser, ultra-high OCT images can be generated, similar to those of conofocal microscopy (CM), which can be used to investigate tissues on a cellular level.

EP measurements do not significantly decrease in females, regardless of the anatomic sites assessed. Conversely, relatively uniform mean values for ET were observed throughout the oral sites investigated. The results presented here may serve as basic reference data for a variety of clinical and experimental matters.

Compared with Chapter 4 section II, mean epithelium thickness in instant *ex vivo* study show lower measurements except buccal mucosa. These significant differences confirm the theory of contraction which increases by the time after tissue excision and dehydration. Second important point which might contribute to this change is the higher resolution of the machine used in this study. Good resolution gives more details about the structure of epithelium especially near the basement membrane.

Auto-fluorescence and contact endoscopy allow for the study of certain parts of the normal oral mucosa (Chen *et al.,* 2005), while high-frequency ultrasound and optical coherence tomography determine the vertical assessment of the tissue. Through these studies, a certain prediction of malignancy or benignity of an oral lesion might be possible. Therefore, reliable values of epithelial thickness in early oral cancers and precursor lesions could be of great interest.

However, the fluorescent intensity of the epithelium using auto-fluorescence microscopy did not change perceptibly from mild dysplasia to early invasive carcinoma. As a result, it is thought that the epithelial thickening and not the tumour cells themselves are responsible for the endoscopically observed loss of auto-fluorescence in these lesions. In addition, enlarged nuclei with an altered nucleus–plasma-relationship and the altered metabolism of tumour cells with an increased amount of reduced flavins play only secondary roles (Fryen *et al*., 1997).

One of the major limitations of auto-fluorescence microscopy is that measurements of thicknesses greater than 300µm may result in the excitatory light used during endoscopic examination being prevented from reaching the sub-mucosal connective

tissue. In such a manner, less and lower energetic photons are emitted, which have longer wavelengths and, therefore, provide a reddish violet fluorescence. Hence, the change of colour in the emission spectrum reflects an energetic attenuation of detectable emitted photons.

Another clinical application of OCT is the evaluation of tongue papilla. Histologically, the different types of tongue papillae can be found on the dorsal surface, including fungiform, circumvallate, foliate and filiform papillae. These papillae are distributed in a specific pattern, with the fungiform, foliate and circumvallate papillae being known as the gustatory papillae, which contain taste buds and work as sensory organs.

The gustatory papillae are comprised of an epithelial covering over a broad core of connective tissue. Taste buds, which are discrete collections of approximately 40 to 60 cells within the papilla epithelium, are an oval sensory end organ that is involved in the perception of chemical stimuli and in taste transduction. The filiform papillae, which contain no taste buds, cover the entire anterior part of the dorsal surface of the tongue and consist of cone-shaped structures. Each of these structures has a core of connective tissue is covered by an epithelium expressing hair-related keratins.

This is the first study showing the feasibility of OCT for studying the normal morphology of papilla in the human tongue. The visualisation was most effective on the tip of the tongue (fungiform papilla) and the dorsum of tongue (filiform papilla).

One of the major strengths of this study is the comparison of the results of diseased groups with those of normal individuals. Most of the previous studies lacked a uniform measurement and a staging system for human papilla. Therefore, the data and determinations of staging systems presented here are difficult to compare with those of earlier studies, especially with regards to the conofocal data. Recently, Maeda 2006, reported dermoscopic patterns of the filiform papilla of the tongue. However, the criteria of atrophy of filiform papilla in that study were similar to those in the current study, although the changes seen in fungiform papilla were not evaluated.

A second strength of the current study was that the determination of the greatest length of papilla was feasible, due to the high resolution of the OCT with penetration depths of 2mm. As a consequence, in these cases it was estimated that the approximate normal height of fungiform papilla is between 400µm and 750µm. Normal heights of filiform papillae range between 250µm and 500µm. The display of normal structures without any contrast agent was also good in comparison with confocal microscopy, which is not meant to be used without the application of fluorescent contrast agents. Additionally, it was possible to differentiate between the different papillae of the tongue, in contrast with other methods.

The current study clearly demonstrated that the atrophic score of the tongue papillae was significantly higher in RT than in chemotherapy patients and healthy subjects. The initial atrophic change of filiform papillae appears to be decreased keratinisation and the rounding of the papillae. As atrophy progresses, it is speculated that the papillae lose their keratinisation and become flattened, and finally diminish completely, based on the findings of this study.

In parallel with the changes of filiform papilla, fungiform papilla also show characteristic changes. In RT patients, atrophy of tongue papillae correlated with decreased salivary secretion. An atrophic score equal to or greater than 2 was also well-correlated with the dose of RT. These correlations have not been reported previously. Fernando *et al*. 1995 found that taste loss was significantly associated with the proportion of the tongue contained within the radiation field. As a result, because the anterior two thirds of the tongue were not in the field of radiation in RCT patients, the damage to the mucosa seen in the present study may be best explained as a predominant indirect effect of the radiation.

Scattered radiation may indirectly damage oral epithelium and direct irradiation may impair salivary gland function. In such circumstances, various complications may develop as the result of severe dryness of the oral mucous membrane, which can therefore be a parameter for monitoring disease progress (Temmel *et al*., 2005). However, xerostomia was observed in patients who received radiotherapy during oral inspection in this study, and most of the patients complained of dry mouth.

Although histologic examination of tongue papillae was performed in the current study, the findings suggest that atrophic changes of the tongue papillae in chemotherapy patients may be partly related to the mucotoxic potential of both 5-FU and cisplatin (Kiewe *et al*., 2004). Direct damage of the mucosa occurs through the inhibition of DNA replication and mucosal cell proliferation, as these changes result in mucosal atrophy and ulceration. The mucotoxic changes of the epithelium usually start a few days after initiation of the therapy and exhibit their maximum at days 7 or 10 after the onset of the first treatment. While epithelial lesions typically heal within 5 weeks, taste disorders usually persist for a much longer period of time (Pico *et al.*, 1998; Guggenheimer *et al*., 1977).

The major advantages of OCT include the facts that no pressure is applied to the papilla, negligible thermal energy is transmitted to the biopsy, and papilla can be visualised reliably up to depths of 1.5mm. This could not be achieved with confocal microscopy (Just *et al*., 2005). However, the investigation of epithelia with its cellular and sub-cellular structures is not possible. The reason for this is the poor image resolution.

The final clinical application in oral cancer that was tested in this chapter was the used of OCT to predict the establishment of pre-malignant and malignant lesions, or their progression. It is believed that cigarette smoking and alcohol consumption are the major risk factors for cancers of the oral cavity, pharynx and larynx. However, it has been difficult to separate these factors since alcohol drinkers also tend to be smokers. Alcohol appears to act principally as a co-carcinogen, enhancing the effects of tobacco smoking.

Identification of high-risk populations is thought to be an effective way of controlling oral cancer. Knowledge of risk factors allows for the identification of populations which should undergo a screening test. Currently, the most common and recommended method for screening includes physical examination, vital staining with toluidine blue, and, if positive, incisional or excisional biopsy for definitive diagnosis in patients experiencing PMDs of the oral cavity.

Because early detection depends on the awareness and experience of the examiner, this may be a useful objective method, with low costs and high sensitivity, which can reduce uncertainty related to the operator and allows, wherever possible, for early degenerating epithelium to be highlighted with high accuracy.

Real-time information from high-risk group individuals or patients with early mucosal alterations could lead to an immediate definitive treatment and yield more information on the surrounding tissue. This is especially true for some patients who handle carcinogenic substances or already have pre-cancerous oral conditions. In the literature, there are no studies which have performed morphometric measurements of epithelial thickness in different lesions of the oral epithelium.

Continuous epithelial thickening as a function of the grade of dysplasia occurs due to an altered nucleus–plasma-relationship, an enlargement of nuclei and an increase of nucleus-containing cells. This process begins in the basement layer and is confined to one or more epithelial layers until it is completed for all three epithelial layers with severe dysplasia or carcinoma in situ.

In addition to a slight epithelial thickening in dysplasia, depending on the degree of severity, the mild to marked loss of stratification may be explained by the epithelial thickening causing absorption and the scattering of light. On the other hand, the hem molecules in dilated sub-epithelial vessels absorb the incidental light and contribute to a further loss of homogenicity.

Previous data, comparing *in-vitro* OCT imaging of the pathology of oral tissue with histology, established the foundation for *in vivo* OCT imaging for disease detection in oral mucosa. The OCT images correlated well with histology for dysplasia and cancer both qualitatively and quantitatively. The normal thickness of oral epithelium was then measured. In this study, the instant *ex-vivo* results show the same results with better quantitative information.

OCT was used *in vivo* to study oral dysplasia and malignancy in a hamster model using subjective criteria (Matheny *et al*., 2004; Wilder-Smith *et al*., 2004). Wilder-Smith *et al*. more recently extended this work to a human study involving 50 patients,

reporting differentiation of normal tissue, dysplastic tissue and squamous cell carcinoma of the oral mucosa. These studies identified the potential of OCT to provide early detection and regular monitoring of suspicious lesions in the oral cavity. However, the lack of sub-cellular detail in OCT and the dependence on subjective visual evaluation limits the absolute diagnostic efficacy (Wilder-Smith *et al*., 2009)

However, in this investigation, thickness measurements were used to completely assess epithelial alterations from a certain vertical thickness onwards. In the daily practice, an additional measurement of epithelial thickness might be performed for suspicious lesions in OCT by means of these two methods. In the early stages of oral cancer, the cells start accumulating in the EP layer, and in pre-cancerous lesions, the EP layer usually becomes thicker. The boundary between the EP and LP layers eventually disappears if the cancerous condition continues to evolve. Therefore, before the boundary disappears, the EP thickens.

In such a manner, values over 500μm are diagnosed as dysplastic lesions without breakdown of the basement membrane. Further prospective investigations in this direction are in preparation at this clinic, with the aim of gaining better pre-operative information about the character of oral lesions and to contribute to the early diagnosis of oral cancer. No difficulty has been observed in comparing the mean ET, in particular comparing the ET of dysplasia and non-dysplasia. However, difficulties have been found in some wide-spread cases due to the topographic location.

Histometric measurements have demonstrated that the thickness of epithelium for dysplasia in the ventral side of the tongue was 510μm. Furthermore, thicker epithelium has been noticed in SCC lesions from the same anatomic area for different patients, up to 730μm, and that SCC showed a triple increase in compression to normal epithelium (210μm). The EP thicknesses of healthy mucosa are always a minimum of 150μm smaller than those of dysplasia.

Increased epithelial thickness as a result of exposure to extrinsic risk factors, such as smoking or drinking, may result from epithelial hyperplasia as a precursor to cellular dysplasia. However, it is clear that most of the epithelial thicknesses range below 500μm regardless of the type of oral epithelium.

The OCT is capable of distinguishing between benign and malignant mucosal lesions. The results of the current study support the examiner in terms of considering increased epithelium thickness as an important sign of dysplasia in cases of clinically unsuspicious oral lesions. Still, signs of malignancy could be identified, primarily by disturbed tissue architecture and an increased density of blood vessels with irregular, elongated and enlarged appearances.

Because of the atraumatic, non-invasive approach of the OCT technique, measurements may be repeated immediately and averaged to minimise outliers. Examiners should be trained in this method to reduce reading errors, and repeated measures should be performed. From a practical point of view, manufacturers should aim for further reduce the size of the B mode transducers combined with an integrated stand-off in order to facilitate OCT diagnosis in the oral cavity.

Conclusion

It has been demonstrated unequivocally that instant *ex-vivo* OCT images distinguish the individual layers of the wall of the oral tissue with superior sharpness compared with delayed *ex-vivo*. Determination of epithelial thickness by OCT may allow conclusions on whether or not an oral lesion is malignant. No gender-related differences of EP were observed with respect to the other anatomic sites investigated. The influence of risk factors on the epithelium thickness is well established. Differences between different risk factors were insignificant in comparison to the counterpart group alone, but differences were significant when compared to normal. These encouraging data mandate prospective studies to determine whether the sensitivity and specificity of this technique can differentiate between carcinoma and abnormal mucosa that is either non-cancerous or pre-cancerous.

Also the results generated demonstrate that OCT is a feasible tool for the morphometric analysis of papilla. It showed that the atrophic changes of tongue papilla were significant in RT patients and were correlated with the characteristic features of the disease

Chapter 7
Instant *ex-vivo* for pathologic skin

Introduction

The thickness of the epidermis of healthy human skin varies depending on the localisation (Whitton and Everall, 1973; Sandby-Møller *et al*., 2003). An understanding of epidermal thickness at various facial sites allows for improved reconstructive outcomes when matching donor and recipient tissues. In particular, it provides consistent results while considering recipient site colour and contour, additionally, thickness is important in optimizing facial skin reconstruction. Normalisation of facial epidermal thickness is important in cosmetic science as well as in dermo oncology (thickness of actenic keratosis and basal cell carcinoma).

The appearance of confocal laser microscopy has allowed researchers for the first time to the ability perform morphometric measurements in vivo. However, the first report provided only limited data with limited penetration deph, although the precision of the thickness measures were remarkable (Branchet *et al.,* 1990).

Another work presented data from different localisations obtained from ten volunteers using the OCT (Welzel *et al.,* 2004). The thicknesses of the stratum corneum, stratum granulosum and the depths of the suprapapillary plate and the rete pegs were measured by reading of the penetration depth during visual inspection and topographic variations were observed. The main deficiency is that they used experimental laboratoy equipment constructed specifically for the purpose of research. Presently, no study has been performed using a commercially approved system.

In the current study we examine: (a) Differences between localisations in adults that have been observed by OCT for the purpose of calculating benchmark averages among normal facial skin samples. (b) The nature and extent of commonly encountered skin tumours using a commercially approved machine utilizing the instant *ex vivo* study design with 7.5 μm axial resolution.

Section I: Evaluation of epidermal layer thickness in facial skin

Background

Measurement of epidermal thickness in facial skin is variable for different parts of the anatomy. Although ultrasound and confocal laser microscopy are used with moderate success, this issue has not been addressed by OCT.

Objectives

In the present study, instant *ex-vivo* morphometric measurements of the epidermal layer of different facial anatomy is performed using a new OCT machine with higher axial resolution.

Subjects and sites investigated

In accordance with the Declarations of Helsinki and after approval by Moorfields & Whittington Local Research Ethics Committee, 50 patients with skin cancer requiring surgical excision were included in the study. The study group consisted of 31 men and 19 women of various skin phototypes (27 subjects of skin phototypes I–III and 23 of skin phototypes IV–VI). All the patients had indoor occupations. All of them gave written informed consent. The study population consisted of only one age group: middle-aged (35-45 years.). Lesions located within ten anatomic sites were included. These sites specifically were, the frontal skin, tip of nose, nasal dorsum, and lateral side of nose, lower eyelid, check, upper lip, lower lip, chin and malar eminence.

Results

Analysis of topographic variations - quantitative analysis (morphometric analysis)

The measurement of epidermal thickness by eye is less variable due to smooth layer borders, e.g. at the surface or the dermo-epidermal junction. In all imaged skin sites, the depths (in μm), of various viable epidermal layers were obtained by reading the calibrated depth micrometer. Descriptive features of stratum corneum in terms of brightness, presence of fissures or wrinkles, and hair shafts were not analysed. Qualitative analysis of the stratum corneum was not feasible due to the thin structure of this layer on all facial sites.

Quantitative measurement

Average thickness (cheek 160–180 µm, malar eminent 70 µm, lower eyelid 50 µm, lower lip 90 µm, upper lip 100 µm, chin 150 µm, tip of nose 120–130 µm, bridge of nose 130–140 µm, lateral side of nose 120 µm, forehead 130–140 µm.) Table 7.1 & Figure 7.1.

Analysis of topographic variations - qualitative analysis

The stratum corneum appears much brighter on sun-exposed sites. The stratum corneum was fissured and wrinkled on the cheek, upper lip and frontal skin when compared with the tip of the nose. Hair shafts were more frequently seen on cheek, nose, upper and lower eyelid and forehead than in any of the remaining sites.

Table 7.1: Minimum, maximum, range and mean value for the epidermal layer thickness among different facial anatomy.

Facial Site	Range	Minimum	Maximum	Mean
Frontal area				
Ep thickness	55µm	175µm	230µm	140µm
Tip of the nose				
Ep thickness	70µm	160µm	230µm	120µm
Dorsum of nose				
Ep thickness	110µm	140µm	250µm	130µm
Lateral side of nose				
Ep thickness	350µm	150µm	250µm	100µm
Lower eyelid				
Ep thickness	130µm	30µm	160µm	50µm
Cheek				
Ep thickness	200µm	100µm	300µm	170µm
Upper lip				
Ep thickness	150µm	50µm	200µm	100µm
Lower lip				
Ep thickness	130µm	70µm	200µm	90µm
Chin				
Ep thickness	160µm	90µm	350µm	150µm
Malar eminence				
Ep thickness	190µm	50µm	240µm	70µm

Figure 7.1: Box plot summary of epidermal layer thickness distribution for different facial anatomy.

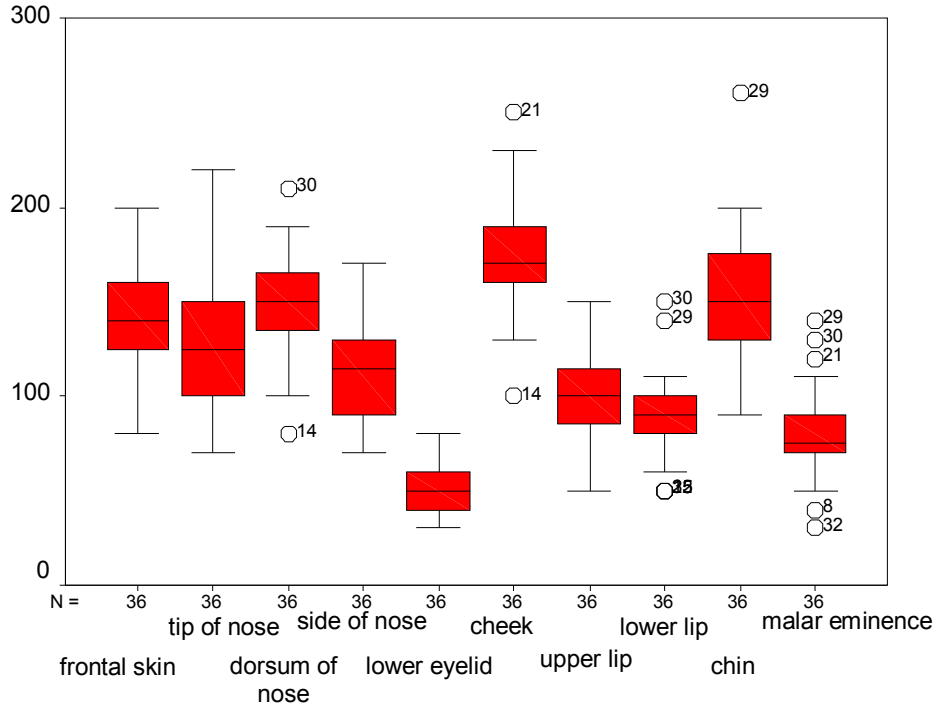

Section II: Qualitative instant *ex vivo* OCT for pathologic skin lesions

Background

The pre-clinical application of OCT on *ex vivo* skin lesions has validated this tool structurally and morphometrically. However, knowledge of instant *ex vivo* pathological skin architectural and morphological properties would be of significant interest to improve contrast.

Objectives

This study describes morphologic features of diverse skin lesions, and features of normal and pathologic skin, and assesses the diagnostic applicability of instant *ex vivo* OCT.

Patients

The study was performed on 60 patients (from 24 males, 36 females, age range: 35 - 70 years). The study was approved by an Ethics Committee from Moorfields & Whittington Local Research Ethics Committee. The patients were recruited in conformity with the Declaration of Helsinki and informed of the procedures and risks regarding the use of the OCT. They gave written informed consent. Pigmented skin lesions (e.g. melanocytic nevi, seborrheic keratosis, malignant melanoma), inflammatory skin disorders (e.g. atopic dermatitis, psoriasis), connective tissue diseases (e.g. systemic sclerosis), autoimmune bullous diseases (e.g. pemphigus vulgaris) and hemangioma were not included in this study due to small sample size.

Results

The 84 skin specimens, which were evaluated prospectively, comprised 45 BCCs, 22 AKs and 17 SCCs. Within the group of histologically verified BCCs, 20 were nodular, 11 were cystic, four were superficial spreading and 10 were mixed. Clinical presentation, anatomical distribution and clinical signs and symptoms of lesions were characterised in detail (Table 7.2).

Transitional zone between normal and abnormal skin

A change in image characteristics was seen in the transitional zone between normal and disease skin. The signal is generally attenuated more rapidly with increasing severity of the superficial damage, especially in case of hyperkeratosis, leading to decreased image penetration depth. This decrease could be as a result of an increase in skin pigmentation, which scatters light effectively due to its high index of refraction (Figure 7.2).

Acinic Keratosis (AK)

AK represents the early stages of cancer initiation. OCT of AK images show very heterogeneous layers, a strong entrance signal (hyper-reflection), composed of thick un-parallel scales, which may cause signal shadows due to total reflection of the light from the compacted keratin. These scales lead to a decrease of light scattering in the dermis. Acanthosis of the epidermis due to proliferation is identified in many cases (Figure 7.3).

The epidermis in AK images often exhibited slight to moderate light penetration due to flaking within the keratinized region. In cases where a thick keratinized layer was present, a distinct boundary was observed between the keratinized region and the underlying epidermis (Figure 7.4).

An increase in epidermal thickness, compared to non-diseased skin, was unusually observed in OCT images. Unlike non-diseased skin, the epidermis in AK images appeared relatively hyper-intense, possibly because of increased backscatter from the dysplastic cells or parakeratosis.

Squamous cell carcinoma (SCC) and SCC *in situ*

In SCCs, distinction between the EP and dermis is difficult with the whole epidermis being elevated in some occasions. The characteristic spike-like hyperkeratosisis visible in AK can be seen in SCC, as well as a significantly thickened epidermis. The stratum corneum is also thickened and shows stronger light scattering. All of these changes can be quantified by measurement of distances between the stratum-

epidermal junction and the dermal-epidermal junction of the adjacent normal skin (Figure 7.5).

Advanced SCC is characterised by hypoechoic signal free spaces within the dermis, and sometimes epidermis, due to tumour necrosis. In these tumours, demarcation between the epidermis and dermis may become difficult due to extensive damage to the dermal-epidermal junction, resulting in the squamous cell nest extending beyond the dermis-subcutis border, because subcutaneous fatty tissue is also hypoechoic (Figure 7.6).

At the early stage of tumour invasion, subtle damage to the dermal-epidermal junction may be hard to detect, however, a hyperechoic deposit can be seen below the junction which represents the dense cluster of tumour invasion, with little or no blood supply from the papillary dermis. Distinction between early SCC and SCC *in situ* depends upon the homogeneity of the dermis layer and a clear, smooth junction between the epidermis and dermis layer (Figure 7.7 & 7.8).

Basal cell carcinomas (BCC)

Basal cell carcinomas are usually are visualised as hypoechoic structures, but they can show a mixed echogenicity (Figure 7.9). The normal keratotic epidermis in basal cell carcinoma is unlike SCCs and AKs, giving negligible reflection of light, which means that measurement of tumour thickness is more achievable in these cases.

An axial resolution of 7.5 μm allowed detection of cell aggregates and layers in skin diseases and tumours. Tumour cell aggregates from the epidermis are visible. Solid nodular BCCs appear as oval or round, high signal, single or multiple areas, with no clear arrangement of surrounding low-reflectivity lobular structures (Figure 7.10 & 7.11). Cystic structures are identifiable by signal-free areas adjacent to healthy skin. The inner structure of a tumour (hypoechoic/hyperechoic, homogenous/inhomogenous, calcification foci and necrosis) depend upon the BCC subclass (Figure 7.12).

In many cases, a distinct boundary at a depth consistent with the epidermal-dermal junction was observed. Vertical shadowing from skin flakes was common. Attenuation in the dermis, however, was often weak, unlike severely sun damaged sites (AK or SCC). However, a great deal of variability existed from site to site and from in different pathological subtypes. In superficial spreading BCC, peripheral palisading in the papillary dermis, in continuity with the overlying epidermis, was observed. This palisading projected toward the papillary dermis (Figure 7.13).

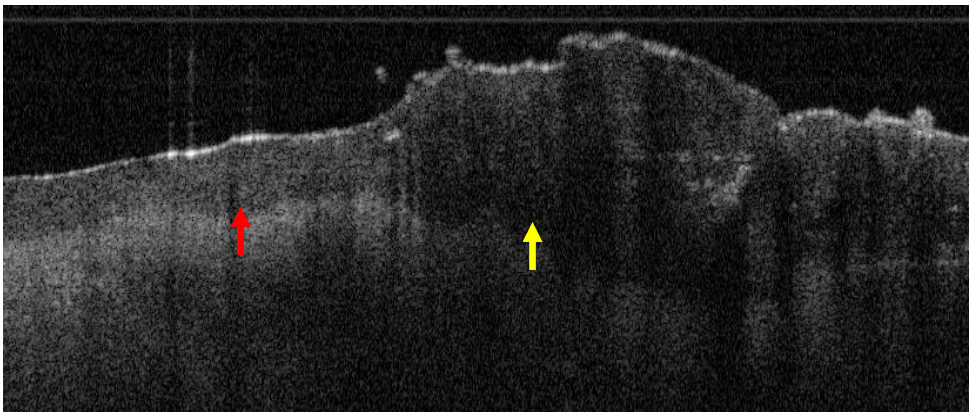

Figure 7.2: Transition from the normal area (red arrow) toward diseased area (yellow arrow)

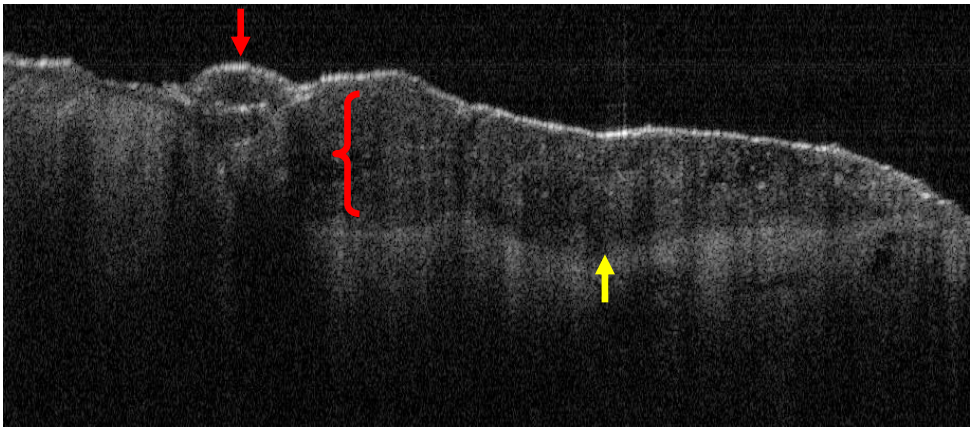

Figure 7.3: Actinic keratosis showing flaked hyperrflective stratum corneum layer (red arrow) with moderate thickening of epidermis layer (red bracket area represent acanthosis) and intact DEJ (yellow arrow)

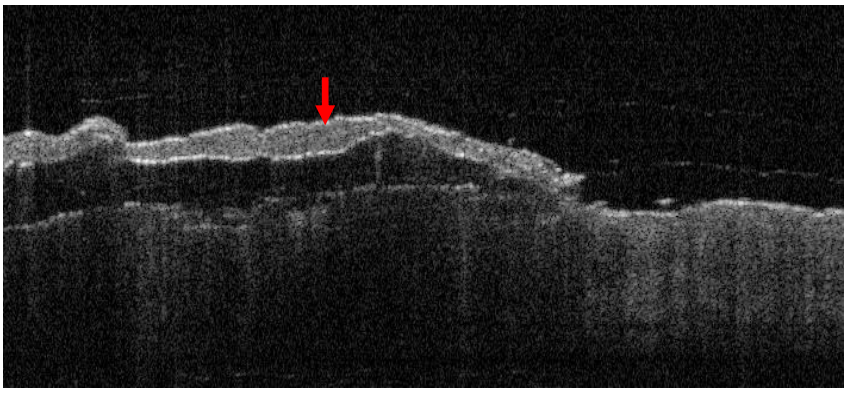

Figure 7.4: Early stage AK with strong signal reflection at the stratum corneum layer which is already separated from the epidermis (red arrows)

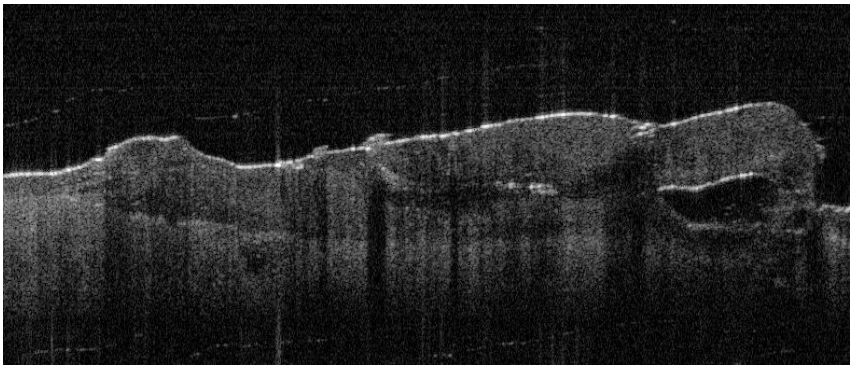

Figure 7.5: Squamous cell carcinoma with area of epidermal separation from the underlining dermis at the level of DEJ

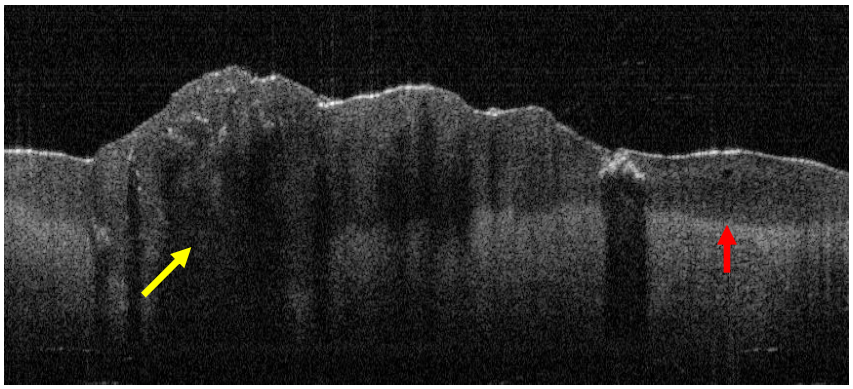

Figure 7.6: Advanced squamous cell carcinoma of check with area of transition from normal (red arrow) toward thickened epidermis with dermis invasive (yellow arrow) . The area of advance invasion show hypoechoic feature as a sign of tumor cells necrosis

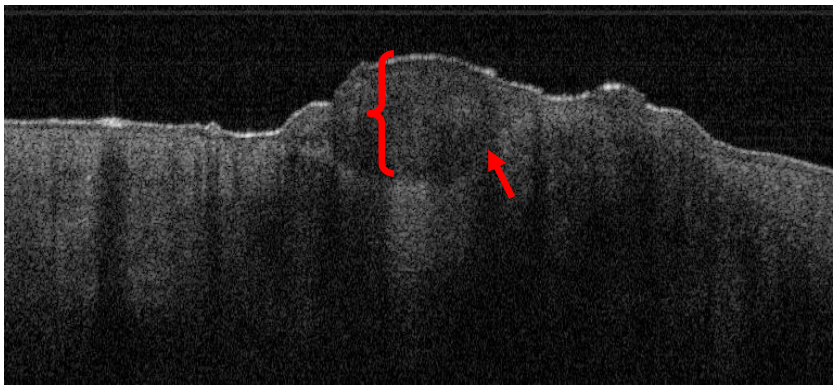

Figure 7.7: Focal squamous cell carcinoma with localized thickening of epidermis (red bracket) and damaged DEJ (red arrow). Localized hypoechoic area in the papillary dermis represent tumour invasion

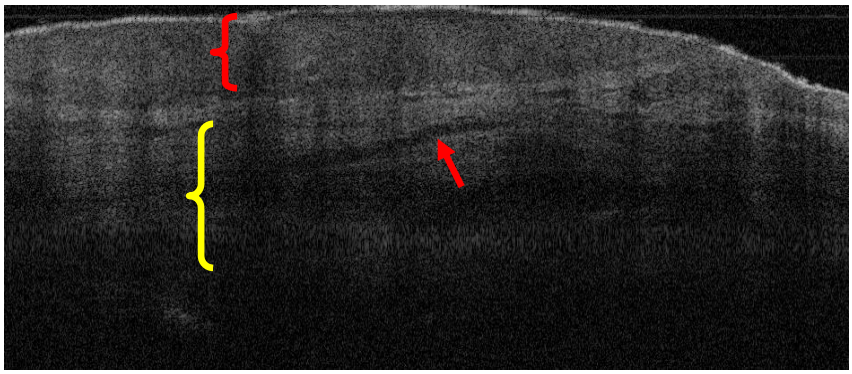

Figure 7.8: SCC in situ showing thickening of the epidermis without break down of DEJ (red bracket) with homogenous papillary dermal layer (yellow bracket) and clear blood vessels (arrow)

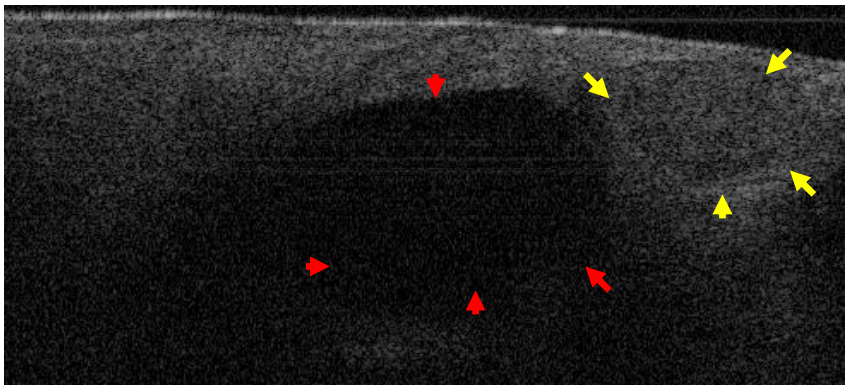

Figure 7.9: Mixed cystic and nodular basal cell carcinoma lesion showing two distinctive hyporeflective (red arrows) and hyperreflective (yellow arrows) areas

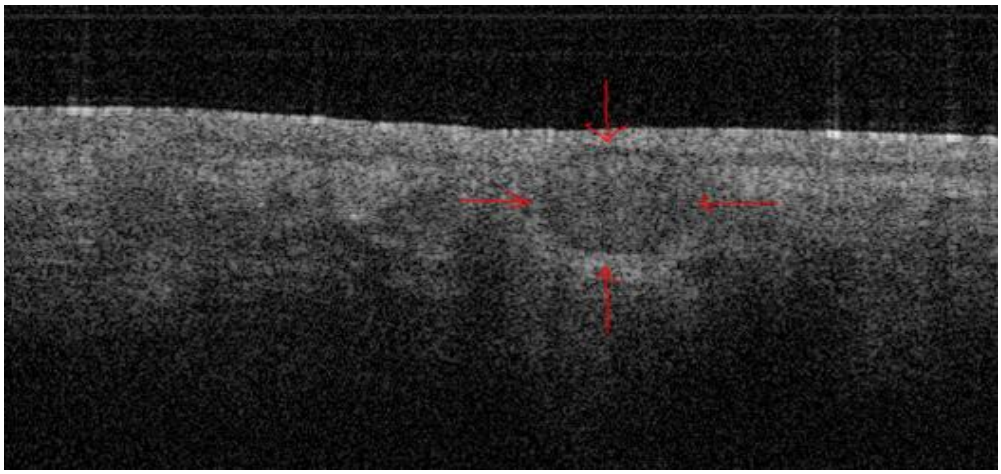

Figure 7.10: Single nodular basal cell carcinoma lesion showing a single moderately hyporeflective tumour nest surrounded by hyperreflective band (red arrows)

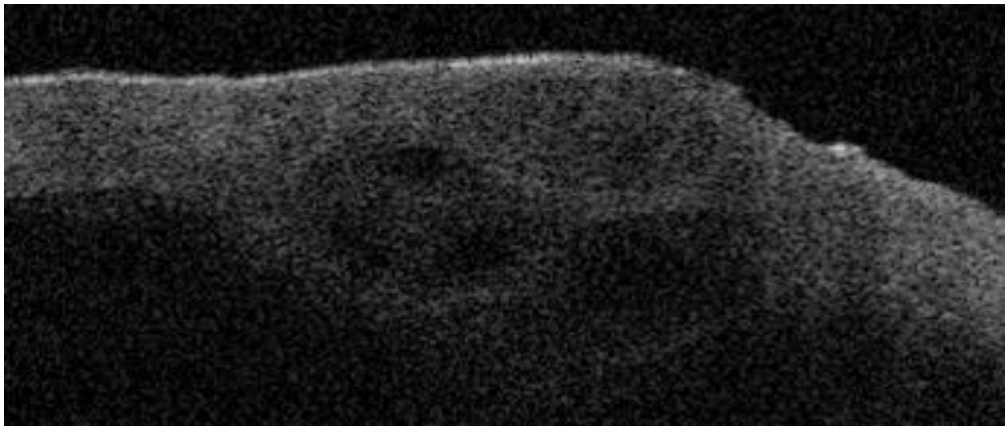

Figure 7.11: Multinodular basal cell carcinoma presenting as multiple, closely arranged, distinct cancer lobule. The cancer nests appear as hyporeflective circular regions compared to the surrounding skin layers

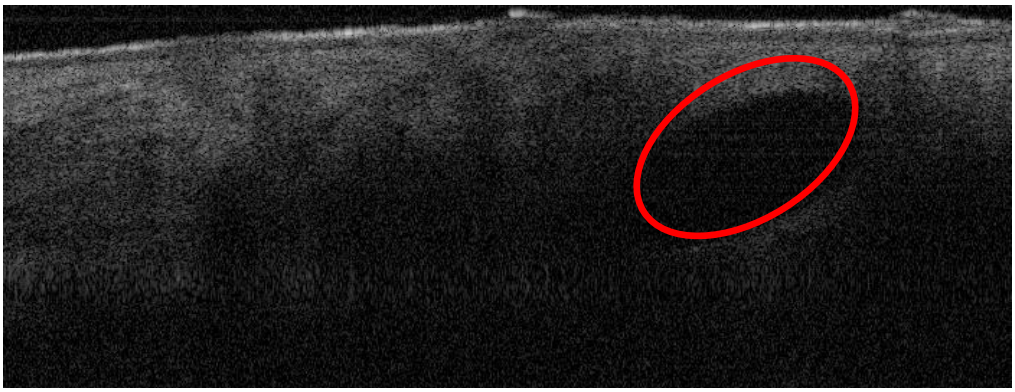

Figure 7.12: Cystic basal cell carcinoma lesion showing a single intensive hyporeflective empty tumour (red oval)

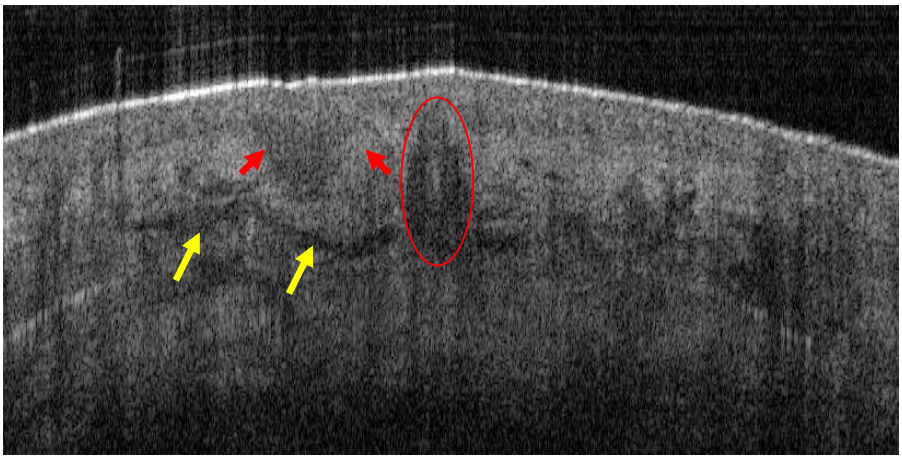

Figure 7.13: Superficial spreading basal cell carcinoma showing cellular nest protruding from epidermis toward the papillary dermal layer (red arrows). Papillary dermis show dilated blood vessels (yellow arrows) and hair follicle assembly (red oval)

Table 7.2: Characteristics of the demographic location of imaged lesions.

	No. (%)			No. (%)
Gender			**Skin type**	
Male	24 (40)		Type I	3(5)
Female	36 (60)		Type II	10(16.6)
			Type III	29(48.4)
Location			Type VI	18 (30)
Cheek	25 (29.7)			
Nose	23(27.3)		**Clinical features**	
Lip	17(20.2)		Erosion	12(14.2)
Forehead	11(13)		Ulcer	20(23.8)
Ear	8(9.5)		Nodule	22(26.1)
			Others	6(7.1)
Colour				
Mixed	30 (35.7)		**Histologic diagnosis**	
Red	20(23.8)		BCC	45 (53.5)
Brown	13 (15.4)		SCC	17 (20.2)
Black	3 (3.5)		AK	22 (26)
White	7 (8.3)			
Non-specific	11 (13)			

Discussion

Absolute values of epidermal thickness have demonstrated variability among the different modalities, leaving questions regarding the ability to standardize or compare results of different studies. Differences in epidermal layer measurement also depend on the tool used. The result obtained from measuring epithelium thickness using instant *ex vivo* measurement hold fantastic future applications.

The epidermal layer constitutes a varying proportion of thickness at any given anatomical site. For example, in the upper eyelid there is very little rete pegs, and in the frontal region there is a greater amount of subcutaneous fat and fibrous tissue. Upper eyelid skin is the thinnest of all the sites reviewed in this study. Skin at all other sites (malar eminence, lower lip) is at least twice as thick as the upper eyelid. This research design was not chosen to facilitate tissue biopsy sites within subjects as this would not be feasible in a clinical study.

For the facial skin study, our samples were obtained from an age group between 35–45 years. Further investigation with a larger and more representative group regarding age and sex may add more useful information for clinical purposes. Using the upper eyelid average skin thickness, the nasal tip skin thickness was only 20 μm thicker and the forehead was 40 μm thicker. The skin over the cheek is 70 μm thicker than the upper eyelid.

In the last section of this chapter, OCT have shown that there are qualitative differences in OCT image features of skin with varying degrees of pathology, and between diseased and undiseased skin. The ultimate goal, however, is to use OCT in instant *ex vivo* using an upgraded machine (7.5 μm).

This clinical study of OCT in dermatology revealed that the method is of value for diagnosis of skin cancer, for example, between different type of basal cell carcinoma (solid or cystic). Compared to confocal scanning laser microscopy (Corcuff *et al*., 1999; Veiro and Cummings 1994), which provides a higher resolution, the detection depth and the image size of OCT is much greater. Furthermore, the technique is much simpler than magnetic resonance imaging of the skin (El Gammal *et al*., 1996; Song

et al., 1997). Information about the size and the thickness of a cutaneous tumour is feasible in this study. The measurement has no side effects and can be performed nearly in real time. However, measuring tumour thickness is out of the scope of our feasibility study.

Bechara *et al*. 2004 reported similar morphologic structures and formations both in histologic examination and OCT in their series of six patients with BCC and naevi. In their study, the OCT images were taken in vivo before lesion excision. While Strasswimmer *et al*. 2004 devised a pilot study using polarisation-sensitive OCT to identify features of (BCC). Before surgical excision, they scanned different portions of the tumour. A loss of birefringence was noted in the tumour itself, which was more marked in the infiltrative type of BCC.

The quality of image and depth of penetration obtained from this study is far superior to our previous in vitro experiment. It is recognised that water content and temperature of the body tissue can affect image quality (Troy and Thennadil, 2001). Normal skin temperature is approximately 37 °C, and it contains 60% to 70% water. These constants are affected in excised tissue and can modify the optical properties of the skin.

Schmitt *et al*. 1990 have shown that differences exist in the optical properties when measurements are taken at different temperatures. In addition, Bonner *et al*. 1987 reported that the absorption spectrum of water in the near-infrared region depends on temperature. Differences may also exist due to local conditioning of the skin by the application of an ointment or glycerol to reduce reflection of the skin surface by making the skin more transparent. However, we found no clinical benefit from using any resolution enhancing cream. Vargas *et al*. investigated the influence of glycerol on the light scattering properties of skin. They found a reduction in the lack of layers and structures can be distinguished in the OCT image (Vargas *et al*., 1999).

The OCT measurement is inconspicuous and safe. It is not noticeable by the subject and has no side effects. Because of the fast scanning mode and the low output power of the light source (in a range of a few milliwatts), the technique meets the safety standards for irradiation of tissue. Furthermore, our OCT studies were approved by

the local ethics committee. For the special demands of practical dermatological operation, an OCT system with a flexible cord was constructed at the by Michelson diagnostic, UK; the system is commercially available.

Generally in the OCT images, the papillary ridges were clearly defined. This effect may be heightened in this study because of the powerful resolution. However, compression should always be avoided as this may result in false thinning and flattening of the epidermis or superficial tissue distortion which is necessary for the diagnosis.

Conclusion

We observed relatively uniform mean values for ET throughout the facial sites investigated. Furthermore, the upgraded OCT machine turns out to be sensitive in identifying differences in human skin properties between the two groups studied.

Optical coherence tomography has been identified as a successful tool in distinguishing normal from abnormal skin, as well as accurately identifying different skin pathologies. A further *in vivo* study to evaluate the sensitivity, specificity and accuracy of this technology is important.

Chapter 8

Summery & Suggestions

Summary

1-Correlation between OCT and gold standard pathology is not easily achieved. Further technical advances will be needed before it can match conventional histopathology.

2-*Ex-vivo* tissues lack a blood supply which affects negatively image resolution and contrast.

3- Measurements made with the *ex-vivo* OCT were reproducible with underestimation comparing with histology due to tissue shrinkage as excision.

4- OCT demonstrates mild to moderate ability to discriminate cancerous oral lesions which is attributed to poor light penetration.

5- Epithelial thickness and the status of the basement membrane play key roles in OCT image interpretation in oral dysplasia.

6- OCT interrogation of the margins of oral cancer specimens is potentially applicable only for thin tumors and a high percentage of false negative results occurred due to technical limitations in the machine used.

7- Instant *ex-vivo* OCT images using an upgraded machines distinguishes the individual layers of the wall of the oral tissue with good resolution compared with delayed *ex-vivo*.

8- OCT is a feasible tool for the morphometric analysis of papilla, however, this needs to be proven *in-vivo*.

9- OCT may not only be able to discriminate between various skin pathologies specially the melanoma group.

10- Considerable challenges exist in distinguishing different histological layers using the Niris OCT system.

Suggested further studies

1-*In vivo* OCT for assessment of suspicious oral lesions with phase 1 clinical trial.

1-Phase 2 trials are expanded to a larger group of patients.

2-*In vivo* OCT for assessment of oral cancer resection margins.

3-Comparing OCT with MOHES surgery in skin cancer.

4-Phase 3 trials are traditionally multicenter studies and are carried out to confirm the effectiveness of the new technology, compare it to other commonly used diagnostic methods, and collect any information on anomalies or adverse effects that may occur as side effects.

5-Phase 4 trials to be carried out by the private sector in an effort to determine the risks, benefits, and optimal uses of the technology.

References

References

Alfano RR, Pradhan A, Tang GC. Optical spectroscopic diagnosis of cancer and normal breast tissues. J Opt Soc Am A. 1989;6:1015-1023.

Al-Rawi NH, Talabani NG. Squamous cell carcinoma of the oral cavity: a case series analysis of clinical presentation and histological grading of 1,425 cases from Iraq. Clin Oral Investig 2008;12(1):15–8.

Andrea M, Dias O, Macor C, Santos A. Contact endoscopy of the nasal mucosa. Acta Otolaryngol (Stockh) 1997;117:307-11.

Andrea M, Dias O, Santos A. Contact endoscopy during microlaryngeal surgery. A new technique for endoscopic examination of the larynx. Ann Otol Rhinol Laryngol 1995;104:333-9.

Andrea M, Dias O, Santos A. Contact endoscopy of the vocal cord. Normal and pathological patterns. Acta Otolaryngol (Stockh) 1991;15:3145-6.

Andreasen JO. Oral lichen planus: a clinical evaluation of 115 cases. Oral Surg Oral Med Oral Pathol. 1968;25:31-41.

Archard JA, Carlson KP, Stanley HR. Leukoedema of the human oral mucosa. Oral Surg Oral Med Oral Pathol. 1968;25:71 7-728.

Arens C, Glanz H, Wönckhaus J, Hersemeyer K, Kraft M. Histologic assessment of epithelial thickness in early laryngeal cancer or precursor lesions and its impact on endoscopic imaging. Eur Arch Otorhinolaryngol. 2007 Jun;264(6):645-9.

Armstrong WB, Ridgway JM, Vokes DE, Guo S, Perez J, Jackson RP, Gu M, Su J, Crumley RL, Shibuya TY, Mahmood U, Chen Z, Wong BJ. Optical coherence tomography of laryngeal cancer. Laryngoscope. 2006 Jul;116(7):1107-13.

Balch CM, Buzaid AC, Soong SJ, Atkins MB, Cascinelli N, Coit DG, Fleming ID, Gershenwald JE, Houghton A Jr, Kirkwood JM, McMasters KM, Mihm MF, Morton DL, Reintgen DS, Ross MI, Sober A, Thompson JA, Thompson JF. Final version of the American joint committee on cancer stage system for cutaneous melanoma. J Clin Oncol 2001; 19: 3635– 4648.

Barton JK, Gossage KW, Xu W, Ranger-Moore JR, Saboda K, Brooks CA, Duckett LD, Salasche SJ, Warneke JA, Alberts DS. Investigating sun-damaged skin and actinic keratosis with optical coherence tomography: a pilot study. Technol Cancer Res Treat. 2003 Dec;2(6):525-35.

Bechara FG, Gambichler T, 5Stücker M, Orlikov A, Rotterdam S, Altmeyer P, Hoffmann K. Histomorphologic correlation with routine histology and optical coherence tomography. Skin Res Technol. 2004 Aug;10(3):169-73.

Bell RB, Kademani D, Homer L, Dierks EJ, Potter BE. Tongue cancer: is there a difference in survival compared with other subsites in the oral cavity? J Oral Maxillofac Surg 2007;65(2):229–36.

Berg AO, Atkins D. US Preventive Services Task Force: Recommendations and rationale. Screening for skin cancer: Am Fam Phys 2002; 65:925.

Bettendorf O, Piffkò J, Bànkfalvi A. Prognostic and predictive factors in oral squamous cell cancer: important tools for planning individual therapy? Oral Oncol 2004 Feb;40(2):110-9.

Betz CS, Stepp H, Janda P, Arbogast S, Grevers G, Baumgartner R, Leunig A. A comparative study of normal inspection, autofluorescence and 5-ALA-induced PPIX fluorescence for oral cancer diagnosis. Int J Cancer. 2002 Jan 10;97(2):245-52.

Bibas AG, Podoleanu AG, Cucu RG, Bonmarin M, Dobre GM, Ward VM, Odell E, Boxer A, Gleeson MJ, Jackson DA. 3-D optical coherence tomography of the laryngeal mucosa. Clin Otolaryngol Allied Sci. 2004 Dec;29(6):713-20.

Bonner RF, Nossal R, Havlin S, Weiss GH. Model for photon migration in turbid biological media. J Opt Soc Am A. 1987 Mar;4(3):423-32.

Bornstein MM, Kalas L, Lemp S. Oral lichen planus and malignant transformation : a retrospective follow up study of clinical and histopathologic data. Quintessence Int. 2006;37:261-71.

Branchet MC, Boisnic S, Frances C, Robert AM. Skin thickness changes in normal aging skin. Gerontology. 1990;36(1):28-35.

Brand S, Poneros JM, Bouma BE, Tearney GJ, Compton CC, Nishioka NS. Optical coherence tomography in the gastrointestinal tract. Endoscopy. 2000 Oct;32(10):796-803.

Brandizzi D, Gandolfo M, Velazco ML, Cabrini RL, Lanfranchi HE. Clinical features and evolution of oral cancer: a study of 274 cases in Buenos Aires, Argentina. Med Oral Patol Oral Cir Bucal 2008;13:E544–8.

Brantsch KD, Meisner C, Schönfisch B, Trilling B, Wehner-Caroli J, Röcken M, Breuninger H. Analysis of risk factors determining prognosis of cutaneous squamous-cell carcinoma: a prospective study. Lancet Oncol 2008; 9: 713–20.

Brennan M, Migliorati CA, Lockhart PB, Wray D, Al-Hashimi I, Axéll T, Bruce AJ, Carpenter W, Eisenberg E, Epstein JB, Holmstrup P, Jontell M, Nair R, Sasser H, Schifter M, Silverman B, Thongprasom K, Thornhill M, Warnakulasuriya S, van der Waal I. Management of oral epithelial dysplasia: a review. Oral Surg Oral Med Oral Pathol Oral Radiol Endod. 2007 Mar;103 Suppl:S19.e1-12.

Breslow A. Thickness, cross-sectional areas and depth of invasion in the prognosis of cutaneous melanoma. Ann Surg 1970; 172: 902–908.

Bricker SL. Oral lichen planus: a review. Semin Dermatol. 1994;13: 87-90.

Buchwald HJ, Müller A, Kampmeier J, Lang GK. Optical coherence tomography versus ultrasound biomicroscopy of conjunctival and eyelid lesions. Klin Monbl Augenheilkd. 2003 Dec;220(12):822-9.

Chak A, Wallace MB, Poneros JM. Optical coherence tomography of Barrett's esophagus. Endoscopy. 2005 Jun;37(6):587-90.

Chauhan DS, Marshall J. The interpretation of optical coherence tomography images of the retina. invest Ophthalmol Vis Sci. 1999 Sep;40(10):2332-42.

Chen HM, Chiang CP, You C, Hsiao TC, Wang CY. Time-resolved autofluorescence spectroscopy for classifying normal and premalignant oral tissues. Lasers Surg Med. 2005 Jul;37(1):37-45.

Cherpelis BS, Marcusen C, Lang PG. Prognostic factors for metastasis in squamous cell carcinoma of the skin. Dermatol Surg 2002; 28: 268–73.

Cör A, Gale N, Kambic V. Quantitative pathology of laryngeal epithelial hyperplastic lesions. Acta Otolaryngol Suppl. 1997;527:57-61.

Corcuff P, Hadjur C, Chaussepied C, Toledo-Crow R. Confocal laser microscopy of the in vivo human skin revisited. In: Proceedings of three-dimensional and multidimensionalmicroscopy: image acquisition and processing VI. SocPhoto-Opt InstrEng 1999: 3605: 73–81.

Cox NH, Eedy DJ, Morton CA, Therapy Guidelines and Audit Subcommittee, British Association of Dermatologists. Guidelines for management of Bowen's disease: 2006 update. Br J Dermatol 2007; 156: 11–21.

Crawford J, "Optics and the pathology gold standard," in Optical Imaging 2006: Fifth Inter-Institute Workshop on Optical Diagnostic Imaging from Bench to Bedside at the National Institutes of Health, Bethesda, MD (2006).

Crawley EP, Kerr DA. Lichen planus. Oral Surg Oral Med Oral Pathol. 1952;5:1069-1076.

Dachi SF: Experimental production of carcinoma of the hamster tongue. Dent Res 1967 Nov-Dec;46(6):1480.

de Araújo Jr RF, Barboza CA, Clebis NK, de Moura SA, Lopes Costa Ade L. Prognostic significance of the anatomical location and TNM clinical classification in oral squamous cell carcinoma. Med Oral Patol Oral Cir Bucal. 2008 Jun 1;13(6):E344-7.

de Boer JF, Milner TE. Review of polarization sensitive optical coherence tomography and Stokes vector determination. J Biomed Opt. 2002 Jul;7(3):359-71.

de Giorgi V, Stante M, Massi D, Mavilia L, Cappugi P, Carli P. Possible histopathologic correlates of dermoscopic features in pigmented melanocytic lesions identified by means of optical coherence tomography. Exp Dermatol. 2005 Jan;14(1):56-9.

De Veld DC, Witjes MJ, Sterenborg HJ, Roodenburg JL. The status of in vivo autofluorescence spectroscopy and imaging for oral oncology, Oral Oncol. 2005. 41(2), 117– 131.

Diepgen TL, Mahler V. The epidemiology of skin cancer. Br J Dermatol 2002; 146 (Suppl. 61): 1–6.

Diffey BL, Langtry JA. Skin cancer incidence and the ageing population. Br J Dermatol 2005; 153:679–80.

Dormand EL, Ridha H, Vesely MJ Long-term outcome of Squamous Cell Carcinoma of the upper and lower limbs. J Plast Reconstr Aesthet Surg. 2010 Oct;63(10):1705-11.

Durocher RT, Thalman R, Ginseppe F. Leukoedema of the oral mucosa. J Am Dent Assoc. 1972;85:1 105-1109.

Egger K, Werner M, Meining A, Ott R, Allescher HD, Hofler H, Classen M, Rosch T. Biopsy surveillance is still necessary in patients with Barrett's oesophagus despite new endoscopic imaging techniques. Gut 2003;52:18–23.

Eichelberg C, Erbersdobler A, Haese A, Schlomm T, Chun FK, Currlin E, Walz J, Steuber T, Graefen M, Huland H. Frozen section for the management of intraoperatively detected palpable tumor lesions during nerve-sparing scheduled radical prostatectomy. Eur Urol. 2006 Jun;49(6):1011-6.

Eisen D. The oral mucosal punch biopsy. Report of 140 cases. Arch Dermatol 1992; 128: 815-817.

El Gammal S, Hartwig R, Aygen S, Bauermann T, el GammalC, Altmeyer P. Improved resolution of magnetic resonancemicroscopy in examination of skin tumors. J Invest Dermatol 1996: 106: 1287–1292.

Elizabeth M. Kanter, Shovan Majumder, Elizabeth Vargis, Amy Robichaux-Viehoever, Gary J. Kanter, Heidi Shappell, Howard W. Jones III, Anita Mahadevan-Jansen. 2009. Multiclass discrimination of cervical precancers using Raman spectroscopy. Journal of Raman Spectroscopy 40:2, 205-211. 3.

Epstein JB, Gorsky M, Lonky S, Silverman S Jr, Epstein JD, Bride M. The efficacy of oral lumenoscopy (ViziLite) in visualizing oral mucosal lesions. Spec Care Dentist. 2006 Jul-Aug;26(4):171-4.

Epstein JB, Güneri P. The adjunctive role of toluidine blue in detection of oral premalignant and malignant lesions Curr Opin Otolaryngol Head Neck Surg.2009 Apr;17(2):79-87.

Epstein JB, Silverman S Jr, Epstein JD, Lonky SA, Bride MA. Analysis of oral lesion biopsies identified and evaluated by visual examination, chemiluminescence and toluidine blue. Oral Oncol. 2008 Jun;44(6):538-44.

Farahati B, Stachs O, Prall J, Guthoff R, O, Paul HW, Just T. Rigid conofocal endoscopy for in vivo imaging of experimental oral squamous intra-epithelial lesions. J Oral Pathol Med. 2010 Apr;39(4):318-27.

Faruqi SA, Arantes V, Bhutani MS. Barrett's esophagus: current and future role of endosonography and optical coherence tomography. Dis Esophagus. 2004;17(2):118-23.

Fernando IN, Patel T, Billingham L, Hammond C, Hallmark S, Glaholm J, Henk JM. The effect of head and neck irradiation on taste dysfunction: a prospective study. Clin Oncol (R Coll Radiol) 1995;7:173–178.

Flaitz CM: Oral frictional hyperkeratosis. E-Medicine from WebMD. Available at: http://www.emedicine.com/DERM/ topic643.htm. Accessed October 5, 2006.

Florence Draux, Pierre Jeannesson, Abdelilah Beljebbar, Ali Tfayli, Nicolas Fourre, Michel Manfait, Josep Sulé-Suso, Ganesh D. Sockalingum. 2009. Raman spectral imaging of single living cancer cells: a preliminary study. The Analyst 134:3, 542.

Fomina IuV, Gladkova ND, Leont'ev VK, Urutina MN, Gazhva SI, Snopova LB, Gelikonov VM, 2Kamenskiĭ VA. Optical coherence tomography in the evaluation of the oral cavity mucosa. Part II. Benign and malignant diseases. Stomatologiia (Mosk). 2004;83(4):25-32.

Freeman RG, Cockerell EG, Armstrong J, Knox JM. Sunlight as a factor influencing the thickness of epidermis. J Invest Dermatol 1962; 39: 295 – 298.

Fryen A, Glanz H, Lohmann W, Dreyer T, Bohle RM. Significance of autofluorescence for the optical demarcation of field cancerisation in the upper aerodigestive tract. Acta Otolaryngol. 1997 Mar;117(2):316-9.

Fujino H, Chino T, Imai T. Experimental production of labial and lingual carcinoma by local application of 4-nitroquinoline N-oxide. 223J Natl Cancer Inst. 1965 Dec;35(6):907-18.

Gambichler T, Boms S, Stu¨ cker M. Epidermal thickness assessed by optical coherence tomography and routine histology: preliminary results of method comparison. J Eur Acad Dermatol Venereol 2006; 20: 791–795.

Gambichler T, Matip R, Moussa G, Altmeyer P, Hoffmann K. In vivo data of epidermal thickness evaluated by optical coherence tomography: effects of age, gender, skin type, and anatomic site. J Dermatol Sci. 2006 Dec;44(3):145-52.

Gambichler T, Orlikov A, Vasa R, Moussa G, Hoffmann K, Stücker M, Altmeyer P, Bechara FG. In vivo optical coherence tomography of basal cell carcinoma. J Dermatol Sci 2007;45:167-73.

Gambichler T, Regeniter P, Bechara FG, Orlikov A, Vasa R, Moussa G, Stücker M, Altmeyer P, Hoffmann K. Characterization of benign and malignant melanocytic skin lesions using optical coherence tomography in vivo. J Am Acad Dermatol. 2007 Oct;57(4):629-37.

Garbe C, McLeod GR, Buettner PG. Time trends of cutaneous melanoma in Queensland, Australia and Central Europe. Cancer 2000; 89: 1269–78.

Gardner LC, Smith SJ, Cox TM. Biosynthesis of delta-aminolevulinic acid and the regulation of heme formation by immature erythroid cells in man. J Biol Chem. 1991 Nov 15;266(32):22010-8.

Gimenez-Conti IB, Slaga TJ. The hamster cheek pouch model of carcinogenesis and chemoprevention. Adv Exp Med Biol. 1992; 320:63-7.

Gladkova ND, Petrova GA, Nikulin NK, Radenska-Lopovok SG, Snopova LB, Chumakov YP, Nasonova VA, Gelikonov VM, Gelikonov GV, Kuranov RV, Sergeev AM, Feldchtein FI. In vivo optical coherence tomography imaging of human skin: norm and pathology. Skin Res Technol. 2000 Feb;6(1):6-16.

Glogau RG. The risk of progression to invasive disease. J Am Acad Dermatol 2000; 42 (1 Pt 2): 23–24.

Golden D P, Hooley J R. Oral mucosal biopsy procedures. Excisional and incisional. Dent Clin North Am 1994; 38: 279-300.

Gossage KW, Tkaczyk TS, Rodriguez JJ, Barton JK. Texture analysis of optical coherence tomography images: feasibility for tissue classification. J Biomed Opt 2003;8:570-5.

Guggenheimer J, Verbin RS, Appel BN, Schmutz J. Clinicopathologic effects of cancer chemotherapeutic agents on human buccal mucosa. Oral Surg Oral Med Oral Pathol 1977;44:58–63.

Hammer JE, Mekta FS, Pindborg JJ, Daftary DK. An epidemiologic and histopathologic study of leukoedema among 50915 rural Indian villagers. Oral Surgery. 1971 ;32:58-63.

Hanlon EB, Manoharan R, Koo TW, Shafer KE, Motz JT, Fitzmaurice M, Kramer JR, Itzkan I, Dasari RR, Feld MS. Prospects for in vivo Raman spectroscopy. Phys Med Biol. 2000 Feb;45(2):R1-59.

Hayes RC, Leonfellner S, Pilgrim W, Liu J, Keeling DN. Incidence of nonmelanoma skin cancer in New Brunswick, Canada, 1992 to 2001. J Cutan Med Surg 2007; 11: 45–52.

Heaphy MR Jr, Ackerman AB: The nature of actinic keratosis: a critical review in a historical perspective. J Am Acad Dermatol 2000; 43: 138–150.

Heissler E, Steinkamp HJ, Heim T, Zwicker C, Felix R, Bier J. Value of magnetic resonance imaging in staging carcinomas of the oral cavity and oropharynx. Int J Oral Maxillofac Surg 1994: 23: 22–27.

Holme SA, Malinovszky K, Roberts DL. Changing trends in nonmelanoma skin cancer in South Wales 1988–98. Br J Dermatol 2000; 143:1224–9.

Howie NM, Trigkas TK, Cruchley AT, Wertz PW, Squier CA, Williams DM. Short-term exposure to alcohol increases the permeability of human oral mucosa. Oral Dis. 2001 Nov;7(6):349-54.

Huber MA, Bsoul SA, Terezhalmy GT. Acetic acid wash and chemiluminescent illumination as an adjunct to conventional oral soft tissue examination for the detection of dysplasia: a pilot study. Quintessence Int. 2004 May;35(5):378-84.

Hung J, Lam S, LeRiche JC, Palcic B. Autofluorescence of normal and malignant bronchial tissue. Lasers Surg Med. 1991;11:99-105.

Huang D, Swanson EA, Lin CP, Schuman JS, Stinson WG, Chang W, Hee MR, Flotte T, Gregory K, Puliafito CA, et al. Optical coherence tomography. Science. 1991 Nov 22;254(5035):1178-81.

Hutcheson AC, Fisher AH, Lang Jr PG. Basal cell carcinomas with unusual histological patterns. J Am Acad Dermatol 2005;53(5): 833-7.

Ingafou M, Leao JC, Porter SR. Oral Lichen Planus: a retrospective study of 690 british patients. Oral Dis. 2006;12:463-8.

Ingrams DR, Dhingra JK, Roy K, Perrault DF Jr, Bottrill ID, Kabani S, Rebeiz EE, Pankratov MM, Shapshay SM, Manoharan R, Itzkan I, Feld MS. Autofluorescence characteristics of oral mucosa. Head Neck 1997;19(1):27–32.

Isenberg G, Sivak MV Jr, Chak A, Wong RC, Willis JE, Wolf B, Rowland DY, Das A, Rollins A. Accuracy of endoscopic optical coherence tomography in the detection of dysplasia in Barrett's esophagus: a prospective, double-blinded study. Gastrointest Endosc 2005 Dec;62(6):825-31.

Ismail SB, Kumar SK, Zain RB. lichenoid reactions: etiopathogenesis, diagnosis, management and malignant transformation. J Oral Sci. 2007;49:89-106.

Jaber MA, Porter SR, Scully C, Gilthorpe MS, Bedi R. The role of alcohol in non-smokers and tobacco in non-drinkers in the aetiology of oral epithelial dysplasia. Int J Cancer 1998;77:333–6.

Jäckle S, Gladkova N, Feldchtein F, Terentieva A, Brand B, Gelikonov G, Gelikonov V, Sergeev A, Fritscher-Ravens A, Freund J, Seitz U, Soehendra S, Schrödern N. In vivo endoscopic optical coherence tomography of the human gastrointestinal tract--toward optical biopsy. Endoscopy. 2000 Oct;32(10):743-9.

Jakobsson A, Nilsson GE..Prediction of sampling depth and photon path length in laser Doppler flowmetry. Med Biol Eng Comput. 1993 May;31(3):301-7.

Jay F. Piccirillo, Irene Costas, and Marsha E. Reichman Cancers of the Head and Neck Chapter 2 National Cancer Institute 2008.

Jeon MY, Zhang J, Wang Q, Chen Z. High-speed and wide bandwidth Fourier domain mode-locked wavelength swept laser with multiple SOAs. Opt Express 2008;16:2547–2554.

Jerjes W, Swinson B, Johnson KS, Thomas GJ, Hopper C. Assessment of bony resection margins in oral cancer using elastic scattering spectroscopy: a study on archival material Arch Oral Biol. 2005 Mar;50(3):361-6.

Jerjes W, Swinson B, Pickard D, Thomas GJ, Hopper C. Detection of cervical intranodal metastasis in oral cancer using elastic scattering spectroscopy Oral Oncol. 2004 Aug;40(7):673-8.

Jerjes W, Upile T, Hamdoon Z, Nhembe F, Bhandari R, Mackay S, Shah P, Mosse CA, Brookes JA, Morley S, Hopper C. Ultrasound-guided photodynamic therapy for deep seated pathologies: prospective study. Lasers Surg Med. 2009 Nov;41(9):612-21.

Johnson MD, Schilz J, Djordjevic MV, Rice JR, Shields PG Evaluation of In vitro Assays for Assessing the Toxicity of Cigarette Smoke and Smokeless Tobacco Cancer Epidemiol Biomarkers Prev. 2009 Dec;18(12):3263-304.

Johnson RE, Sigman JD, Funk GF, Robinson RA, Hoffman HT. Quantification of surgical margin shrinkage in the oral cavity. Head Neck 1997 Jul;19(4):281-6.

Jørgensen TM, Tycho A, Mogensen M, Bjerring P, Jemec GB. Machine-learning classification of non-melanoma skin cancers from image features obtained by optical coherence tomography. Skin Res Technol. 2008 Aug;14(3):364-9.

Jovanovic A, Schulten EA, Kostense PJ, Snow GB, van der Waal I. Tobacco and alcohol related to the anatomical site of oral squamous cell carcinoma. J Oral Pathol Med 1993;22(10):459–62.

Just T, Stave J, Boltze C, Wree A, Kramp B, Guthoff RF, Pau HW. Laser scanning microscopy of the human larynx mucosa: a preliminary, ex vivo study. Laryngoscope. 2006 Jul;116(7):1136-41.

Just T, Stave J, Kreutzer HJ, Guthoff R, Pau HW. Confocal microscopic evaluation of epithelia of the larynx. Laryngorhinootologie 2007; 86: 644–8. (in German).

Just T, Stave J, Pau HW, Guthoff R. In-vivo observation on papillae of the human tongue using confocal laser scanning microscopy. ORL J Otorhinolaryngol Relat Spec 2005;67: 207–212.

Jüttner FM, Fellbaum C, Popper H, Arian K, Pinter H, Friehs G. 2%Pitfalls in intraoperative frozen section histology of mediastinal neoplasms. Eur J Cardiothorac Surg. 1990;4(11):584-6.

Kaiser ML, Rubinstein M, Vokes DE, Ridgway JM, Guo S, Gu M, Crumley RL, Armstrong WB, Chen Z, Wong BJ. Laryngeal epithelial thickness: a comparison between optical coherence tomography and histology. Clin Otolaryngol. 2009 Oct;34(5):460-6.

Kameyama T: Experimental production of lingual carcinoma by local application of 4-nitroquinoline l-oxide. J Jpn Stomatol Sot 1969 18: 609-624.

Kerr AR, Sirois DA, Epstein JB. Clinical evaluation of chemiluminescent lighting: an adjunct for oral mucosal examinations. J Clin Dent. 2006;17(3):59-63.

Kiewe P, Jovanovic S, Thiel E, Korfel A. Reversible ageusia after chemotherapy with pegylated liposomal doxorubicin. Ann Pharmacother 2004;38:1212–1214.

Kimura M, Tayama N, Chan RW. Geometrical deformation of vocal fold tissues induced by formalin fixation. Laryngoscope. 2003 Apr;113(4):607-13.

King R, Page RN, Googe PB, Mihm MC Jr. Lentiginous melanoma: a histologic pattern of melanoma to be distinguished from lentiginous nevus. Mod Pathol. 2005;18(10):1397–1401.

Klein-Szanto AJ, Schroeder HE. Architecture and density of the connective tissue papillae of the human oral mucosa. J Anat. 1977;123:93-109.

Korde VR, Bonnema GT, Xu W, Krishnamurthy C, Ranger-Moore J,Saboda K, Slayton LD, Salasche SJ, Warneke JA, Alberts DS, Barton JK. Using optical coherence tomography to evaluate skin sun damage and precancer. Lasers Surg Med. 2007 Oct;39(9):687-95.

Kossard S, Commens C, Symons M, Doyle J. Lentinginous dysplastic naevi in the elderly: a potential precursor for malignant melanoma. Australas J Dermatol. 1991;32(1):27–37.

Kossard S. Atypical lentiginous junctional naevi of the elderly and melanoma. Australas J Dermatol. 2002;43(2):93–101.

Kraft M, 5Lüerssen K, Lubatschowski H, Woenckhaus J, Schöberlein S, Glanz H, Arens C. Mucosal lesions in the larynx: predictive value of new imaging modalities for a histological diagnosis HNO. 2008 Jun;56(6):609-13.

Kume T, Akasaka T, Kawamoto T, Ogasawara Y, Watanabe N, Toyota E, Neishi Y, Sukmawan R, Sadahira Y, Yoshida K. Assessment of coronary arterial thrombus by optical coherence tomography. Am J Cardiol 2006;97:1713–1717.

Kyrgidis A, Vahtsevanos K, Tzellos TG, Xirou P, Kitikidou K, Antoniades K, Zouboulis CC, Triaridis S. Clinical, histological and demographic predictors for recurrence and second primary tumours of head and neck basal cell carcinoma. A 1062 patient-cohort study from a tertiary cancer referral hospital. Eur J Dermatol. 2010 May-Jun;20(3):276-82.

L'Estrange P, Bevenius J, Williams L. Intraoral application of microcolpohysteroscopy. A new technique for clinical examination of oral tissues at high magnification. Oral Surg Oral Med Oral Pathol 1989;67:282-5.

Lee CK, Tsai MT, Lee HC, Chen HM, Chiang CP, Wang YM, Yang CC. Differentiating oral lesions in different carcinogenesis stages with optical coherence tomography. J Biomed Opt. 2009 14: 044028.

Leiter U, Garbe C Epidemiology of melanoma and nonmelanoma skin cancer--the role of sunlight. Adv Exp Med Biol. 2008;624:89-103.

Levi F, La Vecchia C, Te VC, Mezzanotte G. Descriptive epidemiology of skin cancer in the Swiss Canton of Vaud. Int J Cancer. 1988 Dec 15;42(6):811-6.

Levy BM: The experimental production of carcinoma of the tongue in mice. J Dent Res 1958 Sep-Oct;37(5):950.

Lingen MW, Kalmar JR, Karrison T, Speight PM. Critical evaluation of diagnostic aids for the detection of oral cancer. Oral Oncol. 2008 Jan;44(1):10-22.

Llewellyn CD, Johnson NW, Warnakulasuriya S. Factors associated with delay in presentation among younger patients with oral cancer. Oral Surg Oral Med Oral Pathol Oral Radiol Endod 2004;97:707–13.

Lo Muzio L, Mignona MD, Favia G. The possible association between oral lichen planus and oral squamous cell carcinoma : a clinical evaluation of 14 cases and a review of literature. Oral Oncol 1998;34:239-46.

Looser KG, Shah JP, Strong EW. The significance of 'positive' margins in surgically resected epidermoid carcinomas. Head Neck Surg 1978; 1:107–11.

Macdonald DG, Rennie JS. Oral epithelial atypia in denture induced hyperplasia, lichen planus and squamous cell papilloma. Int J Oral Surg. 1975 Jan;4(1):40-45.

MacDonald DG. Comparison of epithelial dysplasia in hamster cheek pouch carcinogenesis and human oral mucosa. J Oral Pathol 1981;10:186–191.

Maeda K, Suzuki T, Ooyama Y, Nakakuki K, Yamashiro M, Okada N, Amagasa T. Colorimetric analysis of unstained lesions surrounding oral squamous cell carcinomas and oral potentially malignant disorders using iodine. Int J Oral Maxillofac Surg. 2010 May;39(5):486-92.

Maeda M. Dermoscopic pattern of the filiform papillae of the tongue in patients with Sjögren's syndrome. J Dermatol 2006; 33:96-102.

Mahmood U, Weissleder R. Near-infrared optical imaging of proteases in cancer. Mol Cancer Ther 2003 May;2(5):489-96.

Margarone JE, Natiella JR, Vaughan CD. Artifacts in oral biopsy specimens. J Oral Maxillofac Surg. 1985 Mar;43(3):163-72.

Marks R, Rennie G, Selwood TS. Malignant transformation of solar keratosis to squamous cell carcinoma. Lancet 1998; 331: 795–97.

Martin JL, Buenahora AM, Bolden TE. Leukoedema of the buccal mucosa. The Meharri-Dent. 1970;29:7-9.

Martin JL, Crump EP. Leukoedema of the buccal mucosa in Negro children and youth. Oral Surg Oral Med Oral Pathol. 1972;34:49-59.

Mashberg A, Merletti F, Boffetta P, Gandolfo S, Ozzello F, Fracchia F, Terracini B. Appearance, site of occurrence, and physical and clinical characteristics of oral carcinoma in Torino, Italy. Cancer 1989;63(12):2522–7.

Massoud TF, Gambhir SS. Molecular imaging in living subjects: seeing fundamental biological processes in a new light. Genes Dev 2003 Mar 1;17(5):545-80.

Matheny ES, Hanna NM, Jung WG, Chen Z,Wilder-Smith P, Mina-Araghi R, Brenner M. Optical coherence tomography of malignancy in hamster cheek pouches. J Biomed Opt. 2004 Sep-Oct;9(5):978-81.

MCarrozzo M. Oral mucosal disease: Lichen planus. Br J Oral Maxillofac Surg. 2008 Jan;46(1):15-21.

McCormack CJ, Kelly JW, Dorevitch AP. Differences in age and body site distribution of the histological subtypes of basal cell carcinoma: a possible indicator of differing causes. Arch Dermatol 1997; 133: 593–96.

McGurk M, Chan C, Jones J, O'Reagan EO, Sherriff M. Delay in diagnosis and its effect on outcome in head and neck cancer. Br J Oral Maxillofac Surg 2005;43:281–4.

McMahon J, O'Brien CJ, Pathak I, Hamill R, McNeil E, Hammersley N, Gardiner S, Junor E. Influence of condition of surgical margins on local recurrence and disease-specific survival in oral and oropharyngeal cancer. Br J Oral Maxillofac Surg. 2003 Aug;41(4):224-31.

Mehrotra R, Gupta A, Singh M, Ibrahim R. Application of cytology and molecular biology in diagnosing premalignant or malignant oral lesions. Mol Cancer. 2006 Mar 23;5:11.

Mehrotra R, Hullmann M, Smeets R, Reichert TE, Driemel O. Oral cytology revisited. J Oral Pathol Med. 2009 Feb;38(2):161-6.

Miller DL, Weinstock MA. Nonmelanoma skin cancer in the United States: incidence. J Am Acad Dermatol 1994;30(5 Pt 1):774-8.

Mogensen M, Joergensen TM, Nürnberg BM, Morsy HA, Thomsen JB, Thrane L, Jemec GB. Assessment of optical coherence tomography imaging in the diagnosis of non-melanoma skin cancer and benign lesions versus normal skin: observer-blinded evaluation by dermatologists and pathologists. Dermatol Surg. 2009a Jun;35(6) : 965-72.

Mogensen M, Nürnberg BM, Forman JL, Thomsen JB, Thrane L, Jemec GB. In vivo thickness measurement of basal cell carcinoma and actinic keratosis with optical coherence tomography and 20-MHz ultrasound. Br J Dermatol. 2009b May;160(5):1026-33.

Mogensen M, Thrane L, Jørgensen TM, Andersen PE, Jemec GB. OCT imaging of skin cancer and other dermatological diseases. J Biophotonics. 2009c Jul;2(6-7):442-51.

Mogensen M, Morsy HA, Thrane L, Jemec GB. Morphology and epidermal thickness of normal skin imaged by optical coherence tomography. Dermatology. 2008;217(1):14-20.

Molckovsky A, Song LM, Shim MG, Marcon NE, Wilson BC. Diagnostic potential of near-infrared Raman spectroscopy in the colon: differentiating adenomatous from hyperplastic polyps. Gastrointest Endosc 2003 Mar;57(3):396-402.

Moule I, Parsons P A, Irvine G H. Avoiding artefacts in oral biopsies: the punch biopsy versus the incisional biopsy. Br J Oral Maxillofac Surg 1995; 33: 244-247.

Nair DR, Pruthy R, Pawar U, Chaturvedi P. Oral cancer: Premalignant conditions and screening - an update. J Cancer Res Ther. 2012 Jan;8 Suppl:S57-66.

Natarajan E, Woo SB: Benign alveolar ridge keratosis (oral lichen simplex chronicus): A distinct clinicopathologic entity. J Am Acad Dermatol 2008 Jan;58(1):151-7.

Negoro A, Umemoto M, Fukazawa K, Terada T, Sakagami M. Observation of tongue papillae by video microscopy and contact endoscopy to investigate their correlation with taste function. Auris Nasus Larynx 2004;31:255-9.

Nelson DB, Block KP, Bosco JJ, et al. Technology status evaluation report: highresolution and high-magnification endoscopy. Gastrointest Endosc. 2000;52: 864-866.

Nemet AY, Deckel Y, Martin PA, Kourt G, Chilov M, Sharma V, Benger R. Management of periocular basal and squamous cell carcinoma: a series of 485 cases. Am J Ophthalmol. 2006 Aug;142(2):293-7.

Newbold PC Pre-cancer and the skin. Br J Dermatol. 1972 Apr;86(4):417-34.

Niepsuj K, Niepsuj G, Cebula W, Zieleznik W, Adamek M, Sielanczyk A, Adamczyk J, Kurek J, Sieron A. Autofluorescence endoscopy for detection of high-grade dysplasia in short-segment Barrett's esophagus. Gastrointest Endosc 2003;58:715–719.

Oliver AJ, Helfrick JF, Gard D. Primary oral squamous cell carcinoma: a review of 92 cases. J Oral Maxillofac Surg 1996;54(8):949–54. Discussion 955.

Oliver RJ, Sloan P, Pemberton MN Oral biopsies: methods and applications. Br Dent J. 2004 Mar 27;196(6):329-33.

Olmedo JM, Warschaw KE, Schmitt JM, Swanson DL. Correlation of thickness of basal cell carcinoma by optical coherence tomography in vivo and routine histologic findings: a pilot study. Dermatol Surg. 2007 Apr;33(4):421-5; discussion 425-6.

Olmedo JM, Warschaw KE, Schmitt JM, Swanson DL. Optical coherence tomography for the characterization of basal cell carcinoma in vivo: a pilot study. J Am Acad Dermatol. 2006 Sep;55(3):408-12.

Onizawa K, Saginoya H, Furuya Y, Yoshida H, Fukuda H. Usefulness of fluorescence photography for diagnosis of oral cancer. Int J Oral Maxillofac Surg 1999;28(3):206–10.

Onizawa K, Saginoya H, Furuya Y, Yoshida H. Fluorescence photography as a diagnostic method for oral cancer. Cancer Lett 1996;108(1):61–6.

Parkin DM, Bray F, Ferlay J, Pisani P. Global cancer statistics, CA Cancer J Clin. 2005 Mar-Apr;55(2):74-108.

Patton LL, Epstein JB, Kerr AR. Adjunctive techniques for oral cancer examination and lesion diagnosis: a systematic review of the literature J Am Dent Assoc. 2008 Jul;139(7):896-905.

Paulsen F, Thale A. Epithelial-connective tissue boundary in the oral part of the human soft palate. J Anat. 1998;193:457-467.

Pearson J. "Informatics platforms to support collaboration and drive standardization," in Optical Imaging 2006: Fifth Inter- Institute Workshop on Optical Diagnostic Imaging from Bench to Bedside at the National Institutes of Health, Bethesda, MD (2006).

Perelman LT, Backman V, Wallace M, Zonios G, Manoharan R, Nusrat A, Shields S, Seiler M, Lima C, Hamano T, Itzkan I, Van Dam J, Crawford JM, Feld MS. Observation of periodic fine structure in reflectance from biological tissue: a new technique for measuring nuclear size distribution. Phys Rev Lett 1998;80: 627–630.

Pervaiz S, Olivo M. Art and science of photodynamic therapy. Clin Exp Pharmacol Physiol 2006;33:551–556.

Pico JL, Avila-Garavito A, Naccache P. Mucositis: its occurrence, consequences, and treatment in the oncology setting. Oncologist 1998;3:446–451.

Pierce MC, Strasswimmer J, Park BH, Cense B, de Boer JF. Advances in optical coherence tomography imaging for dermatology. J Invest Dermatol. 2004 Sep;123(3):458-63.

Pindborg JJ, Reichart P, Smith CJ, van der Waal I. World Health Organization. Histological typing of cancer and precancer of the oral mucosa. Berlin: Springer-Verlag; 1997.

Pinholt EM, Rindum J, Pindborg JJ. Oral cancer: a retrospective study of 100 Danish cases. Br J Oral Maxillofac Surg. 1997 Apr;35(2):77-80.

Pitris C, Jesser C, Boppart SA, Stamper D, Brezinski ME, Fujimoto JG. Feasibility of optical coherence tomography for high-resolution imaging of human gastrointestinal tract malignancies. J Gastroenterol. 2000;35(2):87-92.

Porter SR, Fedele S, Habbab KM. Taste dysfunction in head and neck malignancy. Oral Oncol. 2010 Jun;46(6):457-9.

Potsaid B, Gorczynska I, Srinivasan VJ, Chen Y, Jiang J, Cable A, Fujimoto JG. Ultrahigh speed spectral/Fourier domain OCT ophthalmic imaging at 70,000 to 312,500 axial scans per second. Opt Express. 2008 Sep 15;16(19):15149-69.

Prakash G, Agarwal A, Jacob S, Kumar DA, Agarwal A, Banerjee R. Comparison of fourier-domain and time-domain optical coherence tomography for assessment of corneal thickness and intersession repeatability Am J Ophthalmol. 2009 Aug;148(2):282-290.

Ramanujam N, Mitchell MF, Mahadevan A, Thomsen S, Malpica A, Wright T, Atkinson N, Richards-Kortum R. Development of a multivariate statistical algorithm to analyze human cervical tissue fluorescence spectra acquired in vivo. Lasers Surg Med. 1996;19:46-62.

Reibel J. Prognosis of oral pre-malignant lesions: significance of clinical, histopathological, and molecular biological characteristics Crit Rev Oral Crit Rev Oral Biol Med. 2003;14(1):47-62.

Reintgen C, Shivers S, Reintgen M, Giuliano R, Reintgen D. The changing face of malignant melanoma. J Surg Oncol. 2010 May 1;101(6):443-6.

Riedl O, Fitzal F, Mader N, Dubsky P, Rudas M, Mittlboeck M, Gnant M, Jakesz R. Intraoperative frozen section analysis for breast-conserving therapy in 1016 patients with breast cancer. Eur J Surg Oncol. 2009 Mar;35(3):264-70.

Rippey JJ. Why classify basal cell carcinomas? Histopathology 1998 May;32(5):393-8.

Römer TJ, Fitzmaurice M, Cothren RM, Richards-Kortum R, Petras R, Sivak MV Jr, Kramer JR Jr. Laser-induced fluorescence microscopy of normal colon and dysplasia in colonic adenomas: implications for spectroscopic diagnosis. Am J Gastroenterol. 1995;90:81-87.

Röwert-Huber J, Patel MJ, Forschner T, Ulrich C, Eberle J, Kerl H, Sterry W, Stockfleth E. Actinic keratosis is an early in situ squamous cell carcinoma: a proposal for reclassification. Br J Dermatol 2007; 156: 8–12.

Roy HK, Liu Y, Wali RK, Kim YL, Kromine AK, Goldberg MJ, Backman V. Four-dimensional elastic light-scattering fingerprints as preneoplastic markers in the rat model of colon carcinogenesis. Gastroenterology 2004;126:1071–1081.

Rubinstein M, Fine EL, Sepehr A, Armstrong WB, Crumley RL, Kim JH, Chen Z, Wong BJ. Optical coherence tomography of the larynx using the Niris system. J Otolaryngol Head Neck Surg. 2010 Apr;39(2):150-6.

Russ HC. Oral leukoplakia: a review of the literature. Journal of Oral Surgery. 1957 Jan;15(1):40-9.

Sackett DLHR, Guyatt GH, Tugwell P. Clinical epidemiology: a basic science for clinical medicine. 2nd ed. Boston: Little Brown; 1991, p. 53–7.

Sandstead HR, Lowe JW. Leukoedema and keratosis in relation to leukoplakia of the buccal mucosa in man. J Nat Cancer Inst. 1953 Oct;14(2):423-37.

Sandby-Møller J, Poulsen T, Wulf HC. 11 . Epidermal thickness at different body sites: relationship to age, gender, pigmentation, blood content, skin type and smoking habits. Acta Derm Venereol. 2003;83(6):410-3.

Savini G, Zanini M, Barboni P. Influence of pupil size and cataract on retinal nerve fiber layer thickness measurements by stratus OCT. J Glaucoma 2006 Aug;15(4):336-40.

Schaffer AB, Sachs SW. Observations on the fluorescent tongue pattern and its relation to the deficiency state. Oral Surg Oral Med Oral Pathol 1953 Dec;6(12):1425-34.

Scheer M, Neugebauer J, Derman A, Fuss J, Drebber U, Zoeller JE Autofluorescence imaging of potentially malignant mucosa lesions. Oral Surg Oral Med Oral Pathol Oral Radiol Endod. 2011 May;111(5):568-77.

Schmitt JM, Zhou GX, Walker EC, Wall RT. Multilayer model of photon diffusion in skin. J Opt Soc Am A. 1990 Nov;7(11):2141-53.

Scott J, Valentine JA, St Hill CA, West CR: Morphometric analysis of atrophic changes in human lingual epithelium in iron deficiency anemia. 1985 Sep;38(9):1025-9.

Scully C, Beyli M, Ferreiro MC, Ficarra G, Gill Y, Griffiths M, Holmstrup P, Mutlu S, Porter S, Wray D. . Update on oral lichen planus: etiopathogenesis and management. Crit Rev Oral Biol Med. 1998;9(1):86-122.

Scully C, Carrozzo M. Oral mucosal disease: lichen planus. Br J Oral Maxillofac Surg. 2008;46:15-21.

Sepehr A, Armstrong WB, Guo S, Su J, Perez J, Chen Z, Wong BJ. Optical coherence tomography of the larynx in the awake patient. Otolaryngol Head Neck Surg 2008 Apr;138(4):425-9.

Sexton M, Jones DB, Maloney ME. Histologic pattern analysis of basal cell carcinoma. Study of a series of 1039 consecutive neoplasms. J Am Acad Dermatol 1990 Dec;23(6 Pt 1):1118-26.

Shafer WG, Waldron CA. Erythroplakia of the oral cavity. Cancer. 1975 Sep;36(3):1021-8.

Shafir R, Hiss J, Tsur H, Bubis JJ. Pitfalls in frozen section diagnosis of malignant melanoma. Cancer. 1983 Mar 15;51(6):1168-70.

Sharwani A, Jerjes W, Salih V, Swinson B, Bigio IJ, El-Maaytah M, Hopper C Assessment of oral premalignancy using elastic scattering spectroscopy. Oral Oncol. 2006 Apr;42(4):343-9.

Shim MG, Song LM, Marcon NE, Wilson BC. In vivo near-infrared Raman spectroscopy: demonstration of feasibility during clinical gastrointestinal endoscopy. Photochem Photobiol 2000;72:146–150.

Shintani S, Nakayama B, Matsuura H, Hasegawa Y. Intraoral ultrasonography is useful to evaluate tumor thickness in tongue carcinoma. Am J Surg 1997 Apr;173(4):345-7.

Silverman S Jr, Gorsky M, Lozada-Nur F. A prospective follow-up study of 570 patients with oral lichen planus: persistence, remission and malignant association. Oral Surg Oral Med Oral Pathol. 1985 Jul;60(1):30-4.

Simić D, Prohić A, Situm M, Zeljko Penavić J. Risk factors associated with the occurrence of basal cell carcinoma. Coll Antropol. 2010 Mar;34 Suppl 1:147-50.

Slaughter DP, Southwick HW, Smejkal W. Field cancerization in oral stratified squamous epithelium; clinical implications of multicentric origin, Cancer. 1953 Sep;6(5):963-8.

Song HK, Wehrli FW, Ma J. In vivo MR microscopy of human skin. MagnReson Med 1997 Feb;37(2):185-91.

Songra AK, Ng SY, Farthing P, Hutchison IL, Bradley PF. Observation of tumour thickness and resection margin at surgical excision of primary oral squamous cell carcinoma—assessment by ultrasound. Int. J. Oral Maxillofac. Surg. 2006 Apr;35(4):324-31.

Southwood WF. The thickness of the skin. Plast Reconstr Surgery 1955 May;15(5):423-9.

Steffen C, Dupree M. Louis-Frederic Wickham and the Wickham's Striae of Lichen Planus. Le Jacq Communications Inc; 2004. p. 287-9.

Strasswimmer J, Pierce MC, Park BH, Neel V, de Boer JF. Polarization-sensitive optical coherence tomography of invasive basal cell carcinoma. J Biomed Opt. 2004 Mar-Apr;9(2):292-8.

Talbot S, Hitchcock B. Incomplete primary excision of cutaneous basal and squamous cell carcinomas in the Bay of Plenty. 2004 Apr 23;117(1192):U848.

Tanaka T, Kojima T, Okumura A, Yoshimi N, Mori H. Alterations of the nucleolar organizer regions during 4-nitroquinoline 1-oxide-induced tongue carcinogenesis in rats. Carcinogenesis. 1991 Feb;12(2):329-33.

Tang XH, Knudsen B, Bemis D, Tickoo S, Gudas LJ. Oral cavity and esophageal carcinogenesis modeled in carcinogen-treated mice. Clin Cancer Res. 2004 Jan 1;10(1 Pt 1):301-13.

Tearney GJ, Brezinski ME, Southern JF, Bouma BE, Boppart SA, Fujimoto JG. Optical biopsy in human gastrointestinal tissue using optical coherence tomography. Am J Gastroenterol. 1997 Oct;92(10):1800-4.

Temmel AFP, Quint C, Schickinger-Fischer B, Hummel T. Taste function in xerostomia before and after treatment with salvia substitute containing carboxy methyl cellulose. J Otolaryngol 2005 Apr;34(2):116-20.

Testoni PA, Mariani A, Mangiavillano B, Arcidiacono PG, Di Pietro S, Masci E. Intraductal optical coherence tomography for investigating main pancreatic duct strictures. Am J Gastroenterol 2007 Feb;102(2):269-74.

Therkildsen P, Hædersdal M, Lock-Andersen J, de Fine Olivarius F, Poulsen T, Wulf HC. Epidermal thickness measured by light microscopy: a methodological study. Skin Res Technol 1998; 4: 174 – 179.

Thomson PJ. Field change and oral cancer: new evidence for widespread carcinogenesis? Int J Oral Maxillofac Surg. 2002 Jun;31(3):262-6.

Tran PH, Mukai DS, Brenner M, Chen Z. In vivo endoscopic optical coherence tomography by use of a rotational microelectromechanical system probe. Opt Lett. 2004 Jun 1;29(11):1236-8.

Troy TL, Thennadil SN. Optical properties of human skin in the NIR wavelength range of 1000 to 2200 nm. J Biomed Opt 2001 Apr;6(2):167-76.

Tsai MT, Lee HC, Lee CK, Yu CH, Chen HM, Chiang CP, Chang CC, Wang YM, Yang CC. Effective indicators for diagnosis of oral cancer using optical coherence tomography. Opt Express. 2008(a) Sep 29;16(20):15847-62.

Tsai MT, Lee HC, Lu CW, Wang YM, Lee CK, Yang CC, Chiang CP. Delineation of an oral cancer lesion with swept-source optical coherence tomography. J Biomed Opt. 2008(b) Jul-Aug;13(4):044012.

Ulrich M, Stockfl eth E, Roewert-Huber J, Astner S. Noninvasive diagnostic tools for nonmelanoma skin cancer. Br J Dermatol 2007 Dec;157 Suppl 2:56-8.

Upil T, Fisher C, Jerjes W, Elmaayta M, Singh S, Sudhoff H. Recent technical developments: in situ histopathological interrogation of surgical tissues and resection margins. Head Face Med 2007(a) Mar 1,3:13.

Upile T, Jerjes W, Sterenborg HJ, El-Naggar AK, Sandison A, Witjes MJ, Biel MA, Bigio I, Wong BJ, Gillenwater A, MacRobert AJ, Robinson DJ, Betz CS, Stepp H, Bolotine L, McKenzie G, Mosse CA, Barr H, Chen Z, Berg K, D'Cruz AK, Stone N, Kendall C, Fisher S, Leunig A, Olivo M, Richards-Kortum R, Soo KC, Bagnato V, Choo-Smith LP, Svanberg K, Tan IB, Wilson BC, Wolfsen H, Yodh AG, Hopper C. Head & neck optical diagnostics: vision of the future of surgery. Head Neck Oncol. 2009 Jul 13;1:25.

Upile T, JerjesW, Betz CS, El Maaytah M, Wright A, Hopper C. Optical diagnostic techniques in the head and neck. Dent Update 2007(b); Sep;34(7):410-2.

Valentine JA, Scott J,West CR, St Hill CA. A histological analysis of the early effects of alcohol and tobacco usage on human lingual epithelium. J Oral Pathol 1985 Sep;14(8):654-65.

Van Tuyll van Serooskerken AM, van Marion AM, de Zwart-Storm E, Frank J, Poblete-Gutiérrez P. Lichen planus with bullous manifestation on the lip. Int J Dermatol. 2007 Nov;46 Suppl 3:25-6.

Vargas G, Chan EK, Barton JK, Rylander HG, Welch AJ. Use of an agent to reduce scattering in skin. Lasers Surg Med 1999;24(2):133-41.

Veiro JA, Cummings PG. Imaging of skin epidermis fromvarious origins using confocal laser scanning microscopy.Dermatology 1994: 189: 16–22.

Velich N, Vaszilkó M, Németh Z, Szigeti K, Bogdán S, Barabás J, Szabó G. Overall survival of oropharyngeal cancer patients treated with different treatment modalities J Craniofac Surg. 2007 Jan;18(1):133-6.

Veness MJ. Defining patients with high-risk cutaneous squamous cell carcinoma. Australas J Dermatol 2006 Feb;47(1):28-33.

Wagnières GA, Star WM, Wilson BC. In vivo fluorescence spectroscopy and imaging for oncological applications. Photochem Photobiol. 1998 Nov;68(5):603-32.

Wallace MB, Perelman LT, Backman V, Crawford JM, Fitzmaurice M, Seiler M, Badizadegan K, Shields SJ, Itzkan I, Dasari RR, Van Dam J, Feld MS. Endoscopic detection of dysplasia in patients with Barrett's esophagus using light-scattering spectroscopy. Gastroenterology 2000 Sep;119(3):677-82.

Wardrop PJ, Sim S, McLaren K. Contact endoscopy of the larynx:a quantitative study. J Laryngol Otol 2000 Jun;114(6):437-40.

Warnakulasuriya S, Johnson NW, Van Der Waal I. Nomenclature and classification of potentially malignant disorders of the oral mucosa. Journal of Oral Pathology & Medicine. 2007(a) Nov;36 (10):575–80.

Warnakulasuriya S, Mak V, Möller H. Oral cancer survival in young people in South East England. Oral Oncol. 2007(b) Nov;43(10):982-6.

Warnakulasuriya S. Causes of oral cancer—an appraisal of controversies. Br Dent J. 2009(a) Nov 28;207(10):471-5.

Warnakulasuriya S. Global epidemiology of oral and oropharyngeal cancer Oral Oncol. 2009(b) Apr-May;45(4-5):309-16.

Welzel J, Lankenau E, Birngruber R, Engelhardt R. Optical coherence tomography of the skin. Curr Probl Dermatol. 1998;26:27-37.

Welzel J, Lankenau E, Birngruber R, Engelhardt R. Optical coherence tomography of the human skin. J Am Acad Dermatol. 1997 Dec;37(6):958-63.

Welzel J, Reinhardt C, Lankenau E, Winter C, Wolff HH. "Changes in function and morphology of normal human skin: evaluation using optical coherence tomography Br J Dermatol. 2004 Feb;150(2):220-5.

Welzel J. Optical coherence tomography in dermatology: a review. Skin Res Technol. 2001 Feb;7(1):1-9.

White WM, Rajadhyaksha M, Gonzalez S, Fabian RL, Anderson RR. Noninvasive imaging of human oral mucosa in vivo by confocal reflectance microscopy. Laryngoscope 1999 Oct;109(10):1709-17.

Wilder-Smith P, Jung WG, Brenner M, Osann K, Beydoun H, Messadi D, Chen Z. In vivo optical coherence tomography for the diagnosis of oral malignancy. Lasers Surg Med. 2004;35(4):269-75.

Wilder-Smith P, Lee K, Guo S, Zhang J, Osann K, Chen Z, Messadi D. In vivo diagnosis of oral dysplasia and malignancy using optical coherence tomography: preliminary studies in 50 patients. Lasers Surg Med. (2009) Jul;41(5):353-7.

Wilder-Smith P, Holtzman J, Epstein J, Le A. Optical diagnostics in the oral cavity: an overview. Oral Dis. 2010 Nov;16(8):717-28.

Wildt J, Bundgaard T, Bentzen SM. Delay in the diagnosis of oral squamous cell carcinoma. Clin Otolaryngol Allied Sci. 1995 Feb;20(1):21-5.

Wirbelauer C, Winkler J, Bastian GO, Häberle H, Pham DT. Histopathological correlation of corneal diseases with optical coherence tomography. Graefes Arch Clin Exp Ophthalmol. 2002 Sep;240(9):727-34.

Wong BJ, Jackson RP, Guo S, Ridgway JM, Mahmood U, Su J, Shibuya TY, Crumley RL, Gu M, Armstrong WB, Chen Z. In vivo optical coherence tomography of the human larynx: normative and benign pathology in 82 patients. Laryngoscope 2005;115:1904–1911.

Woo SB, Lin D: Morsicatio mucosae oris—A chronic oral frictional keratosis, not a leukoplakia. J Oral Maxillofac Surg 2009 Jan;67(1):140-6.

Woolgar JA, Triantafyllou A. A histopathological appraisal of surgical margins in oral and oropharyngeal cancer resection specimens. Oral Oncol. 2005 Nov;41(10):1034-43.

Xie T, Xie H, Fedder GK, Pan Y. Endoscopic optical coherence tomography with a modified microelectromechanical systems mirror for detection of bladder cancers. Appl Opt. 2003 Nov 1;42(31):6422-6.

Yazdanfar S, Kulkarni M, Izatt J. High resolution imaging of in vivo cardiac dynamics using color Doppler optical coherence tomography. Opt Express. 1997 Dec 22;1(13):424-31.

Yen AM, Chen SC, Chang SH, Chen TH. The effect of betel quid and cigarette on multistate progression of oral pre-malignancy J Oral Pathol Med. 2008 Aug;37(7):417-22.

Yuen AP, Lam KY, Wei WI, Lam KY, Ho CM, Chow TL, Yuen WF. A comparison of the prognostic significance of tumor diameter, length, width, thickness, area, volume and clinicopathological features of oral tongue carcinoma. Am J Surg 2000 Aug;180(2):139-43.

Yuen PW, Lam KY, Chan AC, Wei WI, Lam LK. Clinicopathological analysis of local spread of carcinoma of the tongue. Am J Surg 1998 Mar;175(3):242-4.

Zegarelli DJ. The treatment of oral lichen planus. Ann Dent. 1993 Winter;52(2):3-8.

Prize and grant

HEAD AND NECK OPTICAL DIAGNOSTICS SOCIETY

The International Society of Minimally Invasive Diagnostics

Best Oral Communication Prize
Junior Trainee
2009

Awarded jointly to:

Muriel Abbaci and Zaid Hamdoon

For best oral communication presented at the Scientific Meeting.

Title of the Muriel Abbaci's paper **"Characterization of laryngeal carcinoma by confocal endomicroscopy"**.

Title of the Zaid Hamdoon's paper **"Immediate ex-vivo optical coherence tomography of suspicious oral lesions"**.

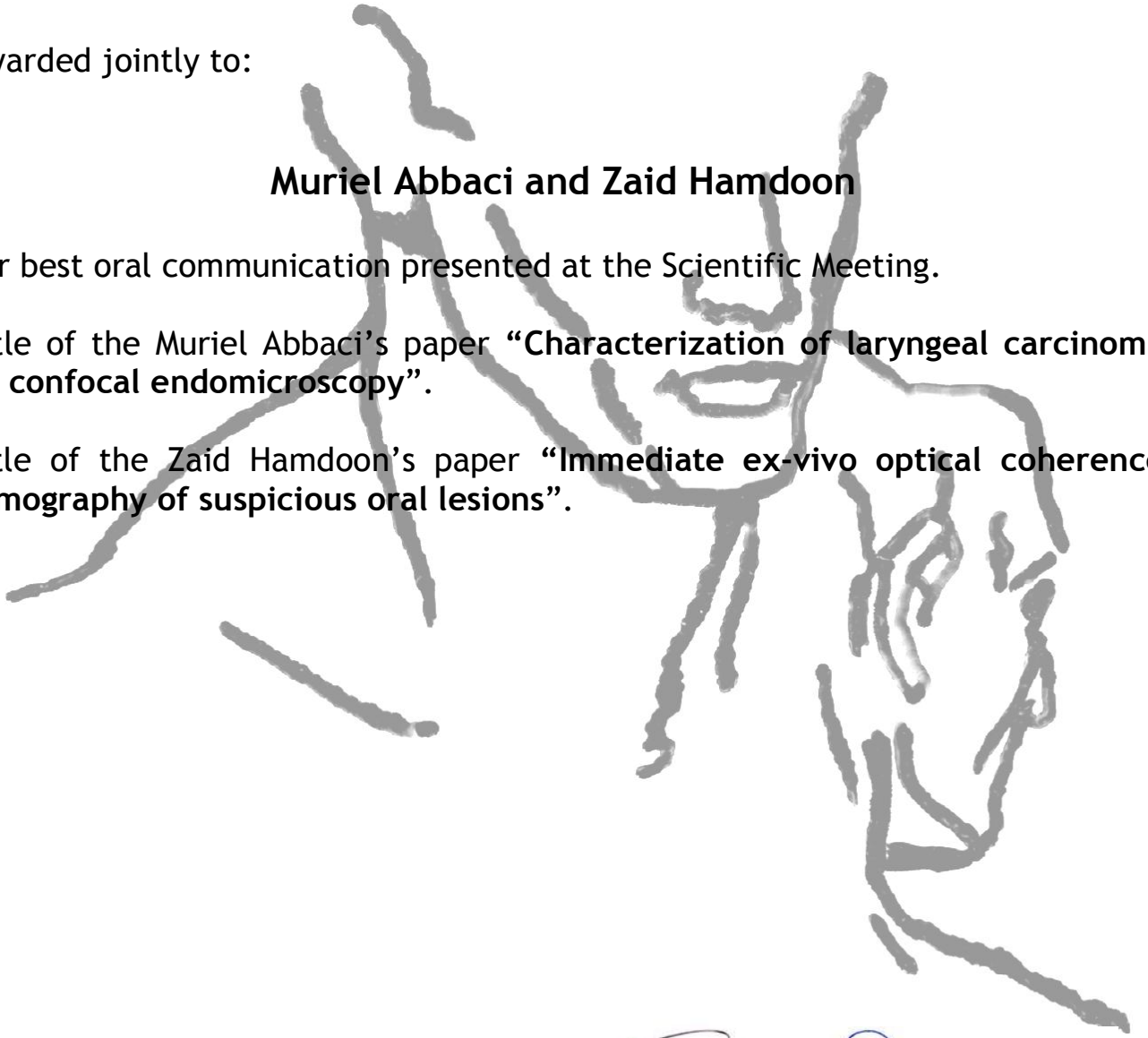

Colin Hopper
Chairman

HJCM Sterenborg
Secretary

HEAD AND NECK OPTICAL DIAGNOSTICS SOCIETY

The International Society of Minimally Invasive Diagnostics

HNODS/SPIE Young Researcher Bursary 2009

Awarded to:

Zaid Hamdoon

The grant is for the sum of $500.00 towards the expenses of attending and presenting at the 2nd Scientific Meeting of the HNODS in conjunction with SPIE Photonics West/Otolaryngology and Head and Neck Section, Jan, 2010 in San Francisco. The funding of this bursary is supported by SPIE.

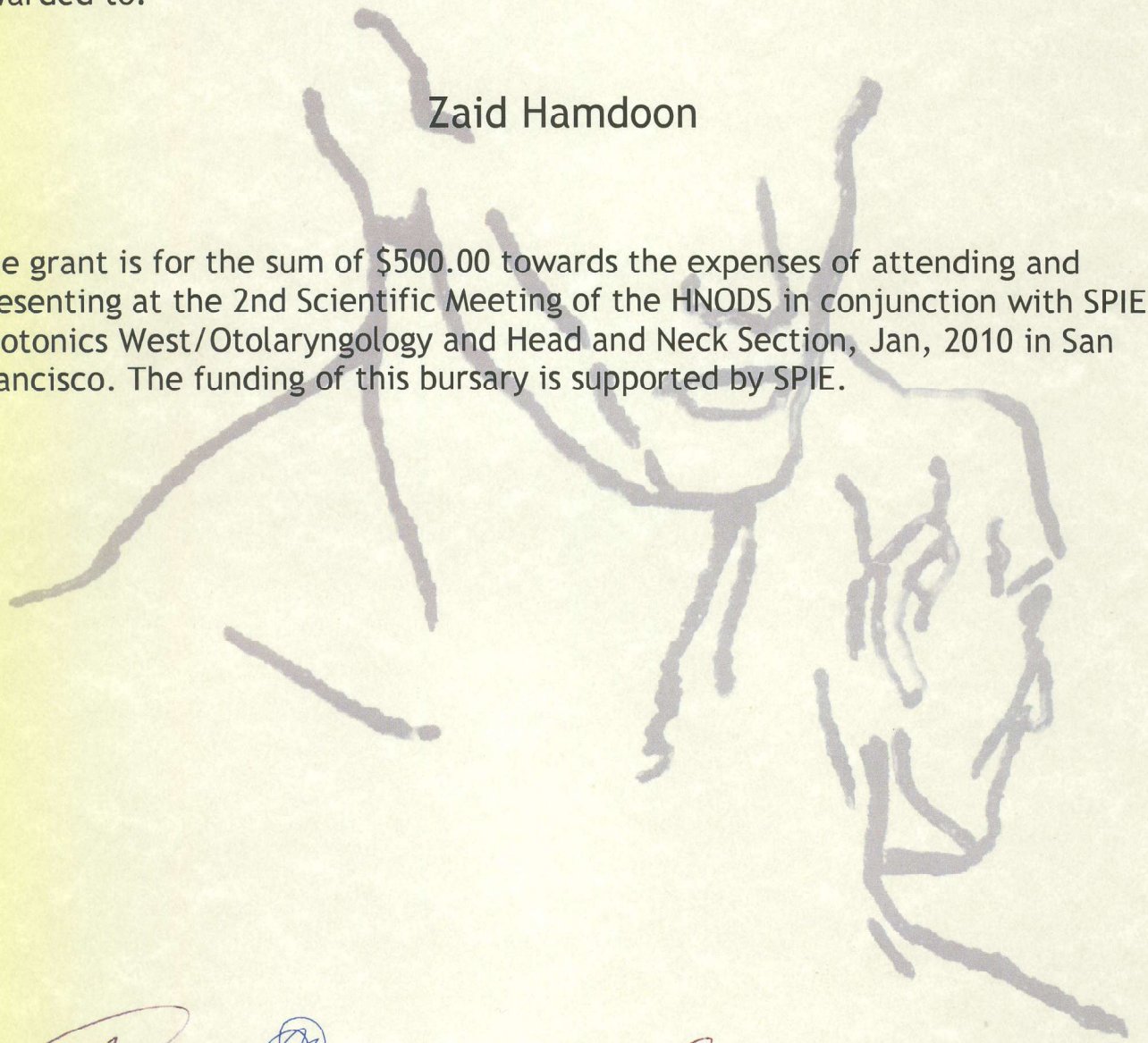

Colin Hopper	HJCM Sterenborg	Waseem Jerjes	Brian Jet-Fei Wong
Chairman	Secretary	Vice Chairman	Conference Chair

Publications and conferences

Hamdoon et al. Head & Neck Oncology 2012, 4:29
http://www.headandneckoncology.org/content/4/1/29

Head & Neck Oncology

RESEARCH Open Access

Structural validation of oral mucosal tissue using optical coherence tomography

Zaid Hamdoon[1,2,3,4*], Waseem Jerjes[3,5,6], Raed Al-Delayme[3], Gordon McKenzie[4,6], Amrita Jay[4] and Colin Hopper[2,4,5]

Abstract

Background: Optical coherence tomography (OCT) is a non-invasive optical technology using near-infrared light to produce cross-sectional tissue images with lateral resolution.

Objectives: The overall aims of this study was to generate a bank of normative and pathological OCT data of the oral tissues to allow identification of cellular structures of normal and pathological processes with the aim to create a diagnostic algorithm which can be used in the early detection of oral disorders.

Material and methods: Seventy-three patients with 78 suspicious oral lesions were referred for further management to the UCLH Head and Neck Centre, London. The entire cohort had their lesions surgically biopsied (incisional or excisional). The immediate *ex vivo* phase involved scanning the specimens using optical coherence tomography. The specimens were then processed by a histopathologist.
Five tissue structures were evaluated as part of this study, including: keratin cell layer, epithelial layer, basement membrane, lamina propria and other microanatomical structures. Two independent assessors (clinician and pathologist trained to use OCT) assessed the OCT images and were asked to comment on the cellular structures and changes involving the five tissue structures in non-blind fashion.

Results: Correct identification of the keratin cell layer and its structural changes was achieved in 87% of the cohort; for the epithelial layer it reached 93.5%, and 94% for the basement membrane. Microanatomical structures identification was 64% for blood vessels, 58% for salivary gland ducts and 89% for rete pegs. The agreement was "good" between the clinician and the pathologist.
OCT was able to differential normal from pathological tissue and pathological tissue of different entities in this immediate *ex vivo* study. Unfortunately, OCT provided inadequate cellular and subcellular information to enable the grading of oral premalignant disorders.

Conclusion: This study enabled the creation of OCT bank of normal and pathological oral tissues. The pathological changes identified using OCT enabled differentiation between normal and pathological tissues, and identification of different tissue pathologies.
Further studies are required to assess the accuracy of OCT in identification of various pathological processes involving the oral tissues.

Introduction

Over the past few years, there have been very successful attempts in the diagnosis of oral tissue pathologies using optical biopsy or optical diagnostics. In theory, a beam of light fired into tissue should provide an optical signature of that tissue highlighting the abnormal characteristics on cellular and subcellular levels. The mechanism of the optical diagnostics technologies varies but they are all non-invasive with the aim to provide *in vivo*, real time and cost effective diagnosis. The successful application of this technology would reduce the workload on pathology units and reduce the time the anxious patient has to wait for a diagnosis [1,2].

When it comes to oral tissues, the aim of these technologies is to identify premalignant disorders and early cancer. Oral cancer is the sixth most common cancer worldwide. It represents about 2% of the cancers in the

* Correspondence: zaid19772000@yahoo.com
[1]Department of Oral & Maxillofacial Surgery, Dental School, Mosul, Iraq
[2]Unit of Oral & Maxillofacial Surgery, UCL Eastman Dental Institute, London, United Kingdom
Full list of author information is available at the end of the article

BioMed Central

© 2012 Hamdoon et al.; licensee BioMed Central Ltd. This is an Open Access article distributed under the terms of the Creative Commons Attribution License (http://creativecommons.org/licenses/by/2.0), which permits unrestricted use, distribution, and reproduction in any medium, provided the original work is properly cited.

UK with incidence of 5.9/100.000 and prevalence of 1 in 1000. Unfortunately, with all advances in surgery, medical and radiation oncology, the 5-year survival continues to be slightly above 50%. The single greatest determinant of long-term patient survival remains early detection and intervention [1,2].

The most commonly used optical diagnostic technologies include elastic scattering spectroscopy (identification of cellular and subcellular changes), Raman spectroscopy (identification of molecular vibration), microendoscopy (identification of surface morphology changes) and fluorescence spectroscopy (identification of biochemical changes in tissue). The results from the immediate *ex vivo* and the *in vivo* studies, where applicable, were very promising [2].

Optical coherence tomography (OCT), another technology which was first applied in 1991 by Huang et al., is a non-invasive interferometric (superimposing or interfering waves) tomographic imaging modality which allows millimeter penetration with micrometer-scale axial and lateral resolution and provides morphological information similar to pathology [3].

For OCT to become clinically interpretable and relevant, the structures visualized must be correlated with the corresponding tissue microstructures. To date, the interpretation of OCT images has been largely intuitive and empiric.

We aimed in this immediate *ex vivo* study to generate a bank of normative and pathological OCT data of the oral tissues to allow identification of cellular structures of normal and pathological processes and compare it to "gold standard" histopathology with the aim to create a diagnostic algorithm which can be used in the early detection of oral disorders.

Material and methods

This immediate *ex vivo* study involved 73 patients (29 males and 44 females), with 78 suspicious oral lesions. The mean age was 50 years (range 32–68 years). The patients were referred to the UCLH Head & Neck Centre, London, for further management of their oral lesions.

The study protocol was approved by the Moorfields and Whittington Local Research Ethics Committee. The protocol was devised in cooperation with the Departments of Pathology at University College London and Imperial College.

Informed consent was obtained from each patient explaining the nature of the study. Exclusion criteria involved patients under 18 years of age and those with previous history of cancer of the oral cavity and the oropharyngeal/laryngeal regions.

In this study, we used swept-source frequency-domain optical coherence tomography microscope (Michelson Diagnostics EX1301 OCT Microscope V1.0); the components of which were discussed in a previous study [1-3]. The light source used is a Santec HSL-2000, with an imaging wavelength of 1310 nm, axial optical resolution of <10 μm, and lateral optical resolution of <10 μm. The system provides an image resolution of 5.3μmpixel with a maximum image width of 6 mm, a sub-surface imaging depth of 1.5 mm, and a focal depth of 1 mm. Samples can be manipulated to see the full quality results on the screen instantly, with an image capture time of <100 ms and refresh rate of >1 Hz.

The multi-beam swept source OCT EX1301 (Michelson Diagnostics Ltd., Orpington, UK) utilizes a novel optical set-up involving multiple optical channels which does not suffer from loss of sensitivity or other serious drawbacks. The idea is to partition the depth of field into sub-fields and to provide a separately focused beam for each sub-field.

The laser beam in the SS-OCT EX1301 is split into 5 'beam-lets' using an etalon-type 'rattle plate' prior to the interferometer beam splitter. Four of these beams are used to scan the specimens and are relayed back to an array of photodiodes where they interfere with four reference beams in the conventional manner. The fifth beam is imaged onto a 5^{th} photodiode to generate a balance signal.

The entire cohort has had their lesions surgically biopsied (incisional or excisional). The specimens were kept in normal saline before being transferred to be scanned. The OCT instrument captured b-mode scans of the tissue. The specimens were then processed by a histopathologist.

Prior to this, digital pictures and diagrams were produced to ensure that the histopathologist would be able to identify the scanned planes accurately and provide an exact histopathological image. Our co-registration method was enhanced by using dyes and sutures for better orientation.

A histopathological diagnosis was then achieved after several steps including tissue sample embedding in paraffin wax, staining with haematoxylin and eosin (H&E), and examination by light microscopy. Close attention was paid to tissue shrinkage in formalin when comparing microanatomical structures of immediate *ex vivo* OCT images and paraffin wax slides.

Five tissue structures were evaluated as part of this study, including: keratin cell layer, epithelial layer, basement membrane, lamina propria and other microanatomical structures. Two independent assessors (clinician and pathologist trained to use OCT) assessed the OCT images and were asked to comment on cellular structures and changes involving the five tissue structures in non-blind fashion.

Seven variables were studied on the OCT images to identify normal oral mucosa microanatomical structures

Table 1 Characteristics of imaged lesions demographic location

	No. (%)		No. (%)
Gender		**Clinical features**	
Male	44 (60.2)	Papule	26 (33.3%)
Female	29 (39.8)	Plague	22 (28.2)
		Ulcer	18 (23%)
Location		Others	12 (15.3)
Tongue	30 (38.4)		
Buccal mucosa	21 (26.9)	**Symptoms**	
Floor of mouth	13 (16.6)	Oral discomfort	29 (39.7)
Hard palate	8 (10.2)	Symptomless	20 (27.3)
Soft palate	6 (7.6)	Pain	13 (17.8)
		Bleeding	11 (15)
Colour			
Leukoplakia	26 (33.3)	**Histologic diagnosis**	
Speckled leukoplakia	24 (30)	Dysplasia	30 (38.4)
Erythroplakia	10 (12.8)	Carcinoma in situ	4 (5.1)
Bluish	10 (12.8)	Invasive carcinoma	25 (32)
Normal	8 (10.2)	Frictional keratosis	5 (6.5)
		Other Benign lesion	14 (18)

and architectural changes in these areas caused by the pathological processes. This included visibility of keratin layer, epithelial layer and lamina propria, identification of the basement membrane and identification of blood vessels, minor salivary gland ducts, rete pegs and taste bud papilla (where applicable). Structural changes of keratin layer, epithelial layer and lamina propria were also examined and highlighted.

OCT measurements were taken from the edges of the macroscopically normal oral mucosa of the surgical biopsy (assumed to be normative data); while pathological data were acquired from the centre of the lesion.

Statistical analysis

All data were entered and stored in a computerized database (Microsoft Excel 2010). The statistical analysis was performed by using the statistical software package SPSS 13.0 (SPSS, Chicago, Ill).

Results

Clinical examination of the suspicious oral lesions was reported and is highlighted in Table 1. The lesions were mainly identified in the tongue, buccal mucosa and floor of mouth. Histopathological diagnosis revealed that dysplasia (oral potentially malignant disorder) was identified in 30 patients, carcinoma *in situ* in 4 patients and squamous cell carcinoma (SCC) in 25 patients (Table 1).

OCT and histopathology correlation

OCT imaging showed distinct zones of normal and altered architectural changes. Basic histological layers (keratin cell layer, epithelium, lamina propria) and microanatomical structures (i.e. blood vessels, tongue papillae, and glandular ducts) were identified in most of the images (Figures 1, 2, 3, 4, 5). The basement membrane was clearly identified in many specimens.

Structural identification and validation with histopathology was variable. This was achieved in 97% when assessing the basement membrane, 93.5% in identifying epithelial layer and its changes and 94% in assessing keratin cell layer and its changes. Correlation was less achievable when it comes to blood vessels (77%) and salivary gland ducts (60%). Rete ridges were correlated in 89% of the OCT specimens and validated histopathologically

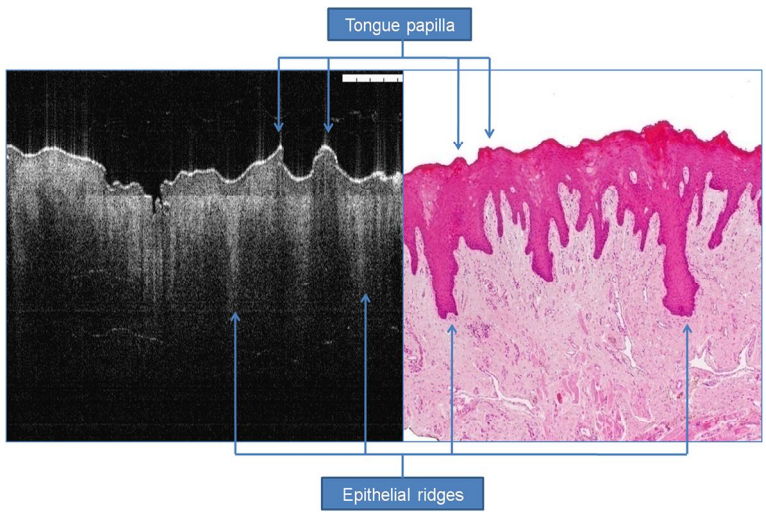

Figure 1 H&E and OCT corresponding images of tongue biopsy showing prominent epithelium ridges and tongue papilla.

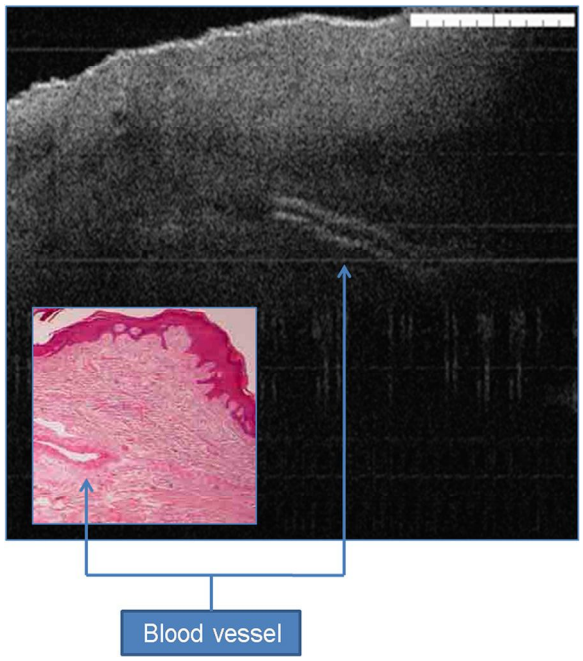

Figure 2 Prominent blood vessel appears as two lines with hyper-ecoic signal and central hypo-ecoic shadow.

(Table 2). For normal resection margins, OCT and histology images were compared and high correlation was achieved (Table 3).

Description of keratin layer

In normal keratinised mucosa, the keratin layer appears as thin bright line on the most upper part of epithelium. This layer is absent in non-keratinised epithelium. In frictional keratosis, this layer shows hyper-reflection features with moderate thickening. Similarly, other benign oral conditions show high backscattering signals similar to reactive keratosis (Figure 4).

Dysplasia cases (mild, moderate) mainly demonstrate hyper-signal, however, severe dysplasia and carcinoma *in situ* have hypo-reflective keratin layer due to the disorganised tissue differentiation. Invasive carcinoma can either have hypo-reflective keratin layer or no layer due to structural damage from ulceration.

Description of epithelial layer

Epithelial layer in normal mucosa has relatively lower signal intensity than keratin cell layer and lamina propria. This layer has homogenous structure with hard distinction between spinous and granular cell layers (Figure 5). In benign lesions this layer may show slight increase in the thickness mainly when the lesion show tissue hyperplasia.

In dysplastic cases, slight to moderate increase in this layer thickness and is usually associated with architectural changes in severe dysplasia and carcinoma *in situ*. In cases of invasive carcinoma, epithelial layer shows significant increase in the thickness in the areas of focal invasion.

Description of lamina propria layer

In normal tissue, this layer show noticeable demarcation from the upper epithelium with high signal. Small blood vessels may be seen as poor signal surrounded by two high signal lines (Figure 2).

Description of basement membrane

The demarcation between two different signal intensity of epithelium and lamina propria represents the basement membrane. This junction may appear as linear of undulated structure due to tissue formalin shrinkage effect. Small projections towards the lamina propria may be seen which represent ret pegs. Intact basement membrane is seen in benign and dysplastic cases, while complete or partial loss (breach) of the basement membrane is usually evident in cases of invasive carcinoma (Figure 3).

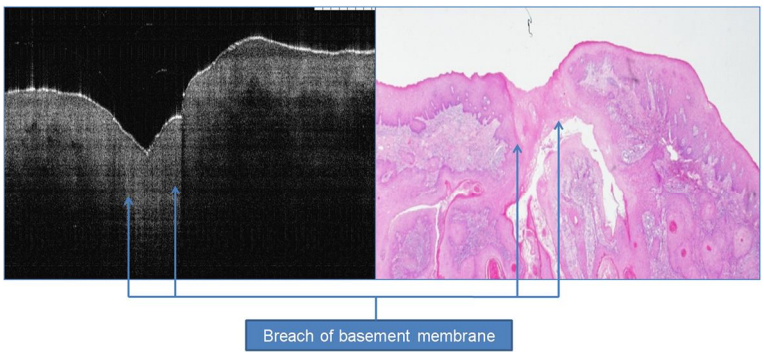

Figure 3 Focal invasive carcinoma of buccal mucosa with localized breach of basement membrane and thin or no keratin cell layer.

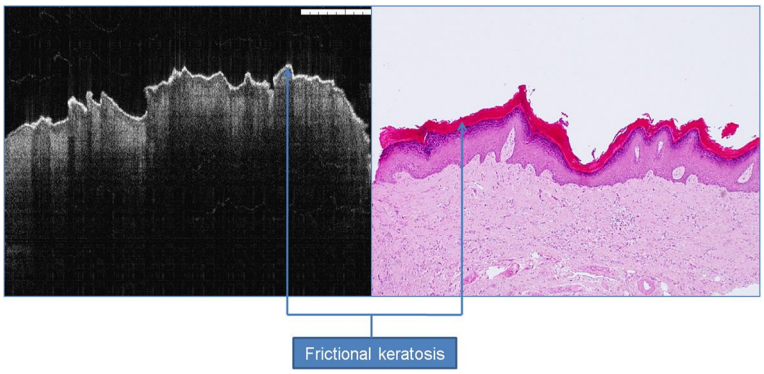

Figure 4 Frictional keratosis showing hyper-reflective OCT signal.

Description of other microanatomical structures

In the normal part of dorsum of tongue biopsy, mushroom or feather-like humps can be identified and represent the fungi-form and filli-form papilla (Figure 1). Minor salivary gland ducts may be seen in some biopsies as tiny tortuous signal free cavities which can be difficult to differentiate from blood vessels. Rete pegs appear as shadow extension from the epithelium holding the same signal intensity.

Agreement between the clinician and the histopathologist

With regards to hyperkeratosis, agreement was achieved in 100% of the specimens in identifying the basement membrane and epithelial layer and its changes. 100% of the keratin cell layer demonstrated hyper-reflective features. With regards to other benign oral lesions, agreement was achieved in 78% of the specimens in identifying the basement membrane as demarcated structure, 78% in identifying epithelial layer as normal thickness and 92% in keratin cell layer described as normal reflective.

In the oral dysplasia group, agreement was achieved in 90% of the specimens in identifying the basement membrane, 83% in identifying epithelial layer as increased, and 13% in identifying hypo-reflective keratin cell layer. For oral cancer, agreement was achieved in 100% of the specimens in identifying the status of the basement membrane and 100% in identifying thickened epithelial layer (Table 4).

Diagnostic criteria

By analysing an OCT image, the normal oral mucosa exhibited three layers. The upper portion of the mucosa (keratin cell layer) appeared distinct and more reflective than the rest of the epithelium. Basement membrane appeared as change of contrast between the hyper-reflective epithelium and hypo-reflective lamina propria. Some epithelium characterized by prominent ret peg ridges which clearly demarcate the intact basement membrane. Microanatomical structures including blood vessels, salivary gland ducts were seen in the third layer, which was the lamina propria.

In the examination of an invasive carcinoma, OCT images showed break down of the basement membrane which correlated well with the histological findings of the same specimen. Cancerous lesions also showed

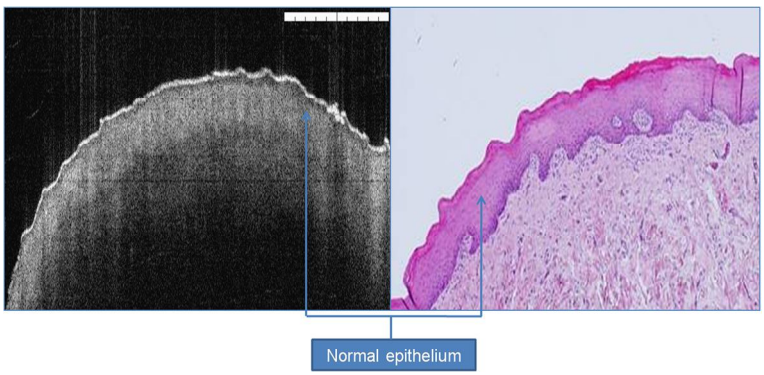

Figure 5 Normal epithelium showing normal reflective keratin cell layer, basement membrane and homogenous lamina propria. The area between the basement membrane and upper most layers represent oral epithelium.

Table 2 Common descriptive features between OCT and pathology from oral tissue agreed by two observers

	No.	No.	No.
Keratin cell layer	**OCT**	**Pathology**	**Total**
Clearly seen	62	66	128
Not seen	16	12	28
Total	78	78	156
Basement membrane	**OCT**	**Pathology**	**Total**
Clearly identified	70	68	138
Not identified	8	10	18
Total	78	78	156
Blood vessel in the lamina propria	**OCT**	**Pathology**	**Total**
Clearly seen	17	22	39
Not seen	61	56	117
Total	78	78	156
Tongue papilla	**OCT**	**Pathology**	**Total**
Clearly seen	14	16	30
Not seen	16	14	30
Total	30	30	60
Epithelium boundary	**OCT**	**Pathology**	**Total**
Clearly seen	69	70	139
Not seen	9	8	17
Total	78	78	156
Salivary gland duct	**OCT**	**Pathology**	**Total**
Clearly seen	6	10	16
Not seen	72	68	140
Total	78	78	156
Rete ridges	**OCT**	**Pathology**	**Total**
Clearly seen	55	62	117
Not seen	23	16	39
Total	78	78	156

irregular and unclear architecture in the lower lamina propria as non-homogenous structure. The majority of the invasive lesions had hypo-reflective signals for the keratin cell layer, while epithelium thickness increased in all OCT images scanned. Advanced malignant lesions extended in deeper tissue layers were beyond the scope of this technology as OCT cannot penetrate deeper than 2 mm in tissue.

OCT was able to differentiate normal from pathological tissue and pathological tissue of different entities. OCT failed to provide enough cellular and subcellular information for staging of oral premalignant disorders (potentially malignant). Differentiation between normal and pathological tissue was mainly based on the identification of thickened oral epithelium and disorganized keratin layer and subepithelial structures.

Differentiation between invasive carcinoma and other benign entities was accurate based on basement membrane status (intact or breached). The epithelium in the early invasive carcinoma is highly variable in thickness, with areas of invasion into the subepithelial layers with invisible basement membrane. However, the OCT image of a dysplastic lesion showed epithelial thickening without frank breach of the basement membrane; this was sometimes difficult to be differentiated from some benign lesions. Thickness of the epithelium for two lesions with carcinoma *in situ* has higher value for benign lesions removed from the same anatomic area.

Discussion

The term "optical biopsy" refers to the method that uses the properties of light to enable the operator to make a "real time" diagnosis. However, the term optical biopsy is misnomer as biopsy mean surgical tissue removal.

Table 3 Common descriptive features between OCT and histology from normal resection oral tissue agreed by two observers.

	No.	No.	No.
Keratin cell layer	**OCT**	**Histology**	**Total**
Clearly seen	30	30	60
Not seen	0	0	0
Total	30	30	60
Basement membrane	**OCT**	**Histology**	**Total**
Clearly identified	30	30	60
Not identified	0	0	0
Total	30	30	60
Blood vessel in the lamina properia	**OCT**	**Histology**	**Total**
Clearly seen	12	15	27
Not seen	18	15	33
Total	30	30	60
Tongue papilla	**OCT**	**Histology**	**Total**
Clearly seen	10	10	20
Not seen	20	20	40
Total	30	30	60
Epithelium boundary	**OCT**	**Histology**	**Total**
Clearly seen	30	30	60
Not seen	0	0	0
Total	30	30	60
Salivary gland duct	**OCT**	**Histology**	**Total**
Clearly seen	6	7	13
Not seen	24	23	47
Total	30	30	60
Rete ridges	**OCT**	**Histology**	**Total**
Clearly seen	22	25	47
Not seen	8	5	13
Total	30	30	60

Table 4 Descriptive interpretation of OCT image changes. KL: keratin cell layer, EP: epithelium, BM: basement membrane, LP: lamina propria. Increase: ↑, decrease: ↓, no change: ↔

Pathology entity	KL hyper-reflective	KL hypo-reflective	KL normo-reflective	Not applicable	EP ↑	EP ↓	EP ↔	EP not identified	BM demarcated	BM non-demarcated	Not applicable	LP homogenous	LP non-homogenous
Keratosis (n = 5)	5	0	0	0	1	0	4	0	5	0	0	5	0
Benign oral lesions (n = 14)	2	0	9	3	1	1	11	1	11	2	1	12	2
Oral dysplasia (n = 30)	13	4	10	3	25	0	3	2	27	1	2	26	4
Carcinoma in situ (n = 4)	1	1	2	0	4	0	0	0	4	0	0	4	0
Invasive carcinoma (n = 25)	10	10	5	0	25	0	0	0	1	24	0	0	25
Normal margin (n = 30)	0	0	30	0	0	0	30	0	30	0	0	30	0

Optical diagnostics seems a correct terminology for these techniques [1-3].

Although OCT can accurately evaluate frank cancer, oral premalignant disorders can be difficult to stage. Dysplasia is identified by cytological and architectural changes. The former including nuclear size and shape, nuclear/cytoplasmic ratio and nuclear stratification, are beyond the resolution of OCT. Visualization of subcellular features, such as nuclei (size, number, and chromatin content) and organelles was impossible in the current premises.

Several studies have sought to investigate the diagnostic utility of OCT to detect and diagnose oral and oropharyngeal/laryngeal pre-malignancy and malignancy [4-6]. No study adhered to solid diagnostic criteria to reach the diagnosis mainly for oral premalignant disorders.

In one study, involving 50 patients with suspicious lesions including oral leukoplakia or erythroplakia, the effectiveness of OCT was evaluated for detecting oral premalignant disorders and malignancy [7]. OCT images of the dysplastic lesions revealed visible epithelial thickening, loss of epithelial stratification and epithelial down growth. This criterion is not adamant enough to draw firm conclusion and to grade oral premalignant disorders.

Criteria for oral cancer diagnosis was established using OCT images by the absence or disruption of the basement membrane and the epithelial layer that was highly variable in thickness, with areas of erosion and extensive epithelial down growth and invasion into the subepithelial layers.

In another study [8], 97 patients were subjected to OCT imaging to detect neoplasia in the oral cavity. The results revealed that the main diagnostic criterion for high-grade dysplasia and carcinoma *in situ* was the lack of a layered structural pattern. Diagnosis based on this criterion for dysplastic/malignant vs. benign / reactive conditions was achieved. In a similar study conducted by our group, OCT images of suspicious oral lesions obtained in *ex vivo* form. It was found that OCT was able to distinguish various layers of oral mucosa. In addition segregating benign from malignant lesion was easily feasible [9].

One limitation of the current study is the co-registration of images with histopathology. The method used in this study provides an accurate registration of OCT and pathology. However, the exact control of the histopathological plane may be difficult due to the formalin shrinkage effect and the processing artifacts in histology.

A second limitation is the relatively small sample size which prevents us from determining the sensitivity and specificity as well as the accuracy for assessment of oral diseases. This study has been sufficient to suggest possible applications of this technique in the oral cavity. Also, further advances and modification of OCT probe technology will be needed to make OCT suitable for routine *in vivo* clinical use.

A third limitation is that the image quality was affected due to lack of tissue perfusion (*ex vivo* nature of the study). The use of high resolution *in vivo* optical imaging may offer a clinically useful adjunct to standard histopathological techniques.

Ridgway et al. examined the mucosa of the oral cavity and the oropharynx using OCT in 41 patients during operative endoscopy [10]. OCT imaging was combined with endoscopic photography for correlation of gross and histological images. They concluded that OCT images of the oral cavity and oropharynx provided microanatomical information about the epithelium, basement membrane, and supporting lamina propria of the mucosa, and showed distinct zones of normal, altered, and ablated tissue microstructures for each pathological process studied.

Building on the results from this study, the diagnostic criteria should be applied through a blind study to judge robustly the sensitivity and accuracy for diagnosis of oral lesions before considering these criteria as gold standard for future work.

Conclusion

This study validates the use of OCT in identifying structural changes in healthy and pathological oral mucosa. Further studies to prove its *in vivo* usefulness are required.

Competing interests

Mr Colin Hopper is an Advisory Board Member at Michelson Diagnostics, Kent, UK. Dr Gordon McKenzie is a Medical Applications Director at Michelson Diagnostics, Kent, UK.

Acknowledgement

We would like to acknowledge Tahwinder Upile for his support at the initial writing up of this manuscript.

Author details

[1]Department of Oral & Maxillofacial Surgery, Dental School, Mosul, Iraq. [2]Unit of Oral & Maxillofacial Surgery, UCL Eastman Dental Institute, London, United Kingdom. [3]Department of Surgery, Al-Yarmouk University College, Baghdad, Iraq. [4]UCLH Head and Neck Unit, London, United Kingdom. [5]UCL Department of Surgery, University College London Medical School, London, United Kingdom. [6]Leeds Institute of Molecular Medicine, University of Leeds, Leeds, UK.

Authors' contribution

ZH, WJ, AJ, CH designed and performed the study, carried out the literature research and manuscript preparation. **ZH, WJ, RA, GM, AJ, CH** were responsible for critical revision of scientific content and manuscript review. All authors approved the final version of the manuscript.

Received: 16 March 2012 Accepted: 6 June 2012
Published: 6 June 2012

References

1. Upile T, Jerjes W, Sterenborg HJ, El-Naggar AK, Sandison A, Witjes MJ, Biel MA, Bigio I, Wong BJ, Gillenwater A, MacRobert AJ, Robinson DJ, Betz CS, Stepp H, Bolotine L, McKenzie G, Mosse CA, Barr H, Chen Z, Berg K,

D'Cruz AK, Stone N, Kendall C, Fisher S, Leunig A, Olivo M, Richards-Kortum R, Soo KC, Bagnato V, Choo-Smith LP, Svanberg K, Tan IB, Wilson BC, Wolfsen H, Yodh AG, Hopper C: **Head & neck optical diagnostics: vision of the future of surgery.** *Head Neck Oncol.* 2009 Jul 13, **1**:25.

2. Upile T, Jerjes WK, Sterenborg HJ, Wong BJ, El-Naggar AK, Ilgner JF, Sandison A, Witjes MJ, Biel MA, van Veen R, Hamdoon Z, Gillenwater A, Mosse CA, Robinson DJ, Betz CS, Stepp H, Bolotine L, McKenzie G, Barr H, Chen Z, Berg K, D'Cruz AK, Sudhoff H, Stone N, Kendall C, Fisher S, MacRobert AJ, Leunig A, Olivo M, Richards-Kortum R, Soo KC, Bagnato V, Choo-Smith LP, Svanberg K, Tan IB, Wilson BC, Wolfsen H, Bigio I, Yodh AG, Hopper C: **At the frontiers of surgery: review.** *Head Neck Oncol.* 2011 Feb 9, **3**(1):7.
3. Jerjes WK, Upile T, Wong BJ, Betz CS, Sterenborg HJ, Witjes MJ, Berg K, van Veen R, Biel MA, El-Naggar AK, Mosse CA, Olivo M, Richards-Kortum R, Robinson DJ, Rosen J, Yodh AG, Kendall C, Ilgner JF, Amelink A, Bagnato V, Barr H, Bolotine L, Bigio I, Chen Z, Choo-Smith LP, D'Cruz AK, Gillenwater A, Leunig A, MacRobert AJ, McKenzie G, Sandison A, Soo KC, Stepp H, Stone N, Svanberg K, Tan IB, Wilson BC, Wolfsen H, Hopper C: **The future of medical diagnostics: review paper.** *Head Neck Oncol.* 2011 Aug 23, **3**:38.
4. Wong BJ, Jackson RP, Guo S, Ridgway JM, Mahmood U, Su J, Shibuya TY, Crumley RL, Gu M, Armstrong WB, Chen Z: **In vivo optical coherence tomography of the human larynx: normative and benign pathology in 82 patients.** *Laryngoscope* 2005 Nov, **115**(11):1904–1911.
5. Tsai MT, Lee HC, Lee CK, *et al*: **Effective indicators for diagnosis of oral cancer using optical coherence tomography.** *Opt Express* 2008, **16:**15847–15862.
6. Tsai MT, Lee HC, Lu CW, *et al*: **Delineation of an oral cancer lesion with swept-source optical coherence tomography.** *J Biomed Opt* 2008, **13:**044012.
7. Wilder-Smith P, Lee K, Guo S, Zhang J, Osann K: **In vivo diagnosis of oral dysplasia and malignancy using optical coherence tomography: preliminary studies in 50 patients.** *Lasers Surg Med* 2009b, **41:**353–357.
8. Tsai MT, Lee CK, Lee HC, Chen HM, Chiang CP, Wang YM, Yang CC: **Differentiating oral lesions in different carcinogenesis stages with optical coherence tomography.** *J Biomed Opt* 2009, **14:**044028.
9. Jerjes W, Upile T, Conn B, Hamdoon Z, Betz CS, McKenzie G, Radhi H, Vourvachis M, El Maaytah M, Sandison A, Jay A, Hopper C: **In vitro examination of suspicious oral lesions using optical coherence tomography.** *Br J Oral Maxillofac Surg* 2010 Jan, **48**(1):18–25.
10. Ridgway JM, Armstrong WB, Guo S, Mahmood U, Su J, Jackson RP, Shibuya T, Crumley RL, Gu M, Chen Z, Wong BJ: **In vivo optical coherence tomography of the human oral cavity and oropharynx.** *Arch Otolaryngol Head Neck Surg* 2006, **132:**1074–1081.

doi:10.1186/1758-3284-4-29
Cite this article as: Hamdoon *et al.*: Structural validation of oral mucosal tissue using optical coherence tomography. *Head & Neck Oncology* 2012 **4**:29.

Submit your next manuscript to BioMed Central and take full advantage of:

- **Convenient online submission**
- **Thorough peer review**
- **No space constraints or color figure charges**
- **Immediate publication on acceptance**
- **Inclusion in PubMed, CAS, Scopus and Google Scholar**
- **Research which is freely available for redistribution**

Submit your manuscript at
www.biomedcentral.com/submit

BioMed Central

Upile et al. Head & Neck Oncology 2011, 3:7
http://www.headandneckoncology.org/content/3/1/7

Head & Neck Oncology

MEETING REPORT Open Access

At the frontiers of surgery: review

Tahwinder Upile[1,2,3], Waseem K Jerjes[1,2,3,4], Henricus J Sterenborg[1,5], Brian J Wong[1,6], Adel K El-Naggar[1,7], Justus F Ilgner[8], Ann Sandison[1,9], Max J Witjes[1,10], Merrill A Biel[1,11], Robert van Veen[5], Zaid Hamdoon[2,3,4], Ann Gillenwater[1,12], Charles A Mosse[1,13], Dominic J Robinson[1,14], Christian S Betz[1,15], Herbert Stepp[1,16], Lina Bolotine[1,17], Gordon McKenzie[1,2,18], Hugh Barr[1,19], Zhongping Chen[1,20], Kristian Berg[1,21], Anil K D'Cruz[1,22], Holger Sudhoff[23], Nicholas Stone[1,19], Catherine Kendall[1,19], Sheila Fisher[1,24], Alexander J MacRobert[1,13], Andreas Leunig[1,15], Malini Olivo[1,25], Rebecca Richards-Kortum[1,26], Khee C Soo[1,27], Vanderlei Bagnato[1,28], Lin-Ping Choo-Smith[1,29], Katarina Svanberg[1,30], I Bing Tan[1,31], Brian C Wilson[1,32,33], Herbert Wolfsen[1,33,34], Irving Bigio[1,35], Arjun G Yodh[1,36], Colin Hopper[1,2,4*]

Abstract

The complete surgical removal of disease is a desirable outcome particularly in oncology. Unfortunately much disease is microscopic and difficult to detect causing a liability to recurrence and worsened overall prognosis with attendant costs in terms of morbidity and mortality. It is hoped that by advances in optical diagnostic technology we could better define our surgical margin and so increase the rate of truly negative margins on the one hand and on the other hand to take out only the necessary amount of tissue and leave more unaffected non-diseased areas so preserving function of vital structures. The task has not been easy but progress is being made as exemplified by the presentations at the 2nd Scientific Meeting of the Head and Neck Optical Diagnostics Society (HNODS) in San Francisco in January 2010. We review the salient advances in the field and propose further directions of investigation.

Introduction

Optical technologies are being used not only to detect disease but also direct treatment (laser) and activate photodynamic therapy as well as in cases aid in the activation of nano-devices to deliver a therapeutic effect. We briefly outline some of the excellent evidence presented in the 2nd Scientific Meeting of the Head and Neck Optical Diagnostics Society (HNODS), (Figure 1) in San Francisco in January 2010.

I. Diagnostic

Disease detection

Optical diagnostics have proved to be a reliable resource that can be used to provide an instant diagnosis of soft and, more recently, hard tissue diseases. In the field of head and neck malignancy, most of the experimental spectroscopy work has been performed using fluorescence spectroscopy, Raman spectroscopy, elastic scattering spectroscopy, micro-endoscopy and optical coherence tomography. These have all shown a marked increase in the sensitivity and specificity when compared to both clinical examination and frozen section analysis [1].

Optical biopsies can be acquired through different modalities; each has it own mechanism of action and requires different modes of data analysis. However, they share the ability of being able to provide a real time, non-invasive and *in situ* optical signature. Most of these techniques have been applied only in clinical trials and are yet to be employed in clinical practice, with the exception of fluorescence spectroscopy. Results from these trials are very promising and current results indicate the possibility of these techniques being applied in clinical practice in the next few years. This could have a great impact on diagnostics, by reducing the histopathology workload, reducing patient's anxiety, and allowing rapid surgical or adjuvant intervention [1]. Further miniaturization has reduced the size of micro-endoscopic multi-photon imaging devices allowing further clinical applications to be developed [2].

* Correspondence: c.hopper@ucl.ac.uk
[1]The "Head and Neck Optical Diagnostics Society" Council, Head & Neck Centre, University College Hospital, 250 Euston Road, London, NW1 2PG, UK
Full list of author information is available at the end of the article

BioMed Central

© 2011 Upile et al; licensee BioMed Central Ltd. This is an Open Access article distributed under the terms of the Creative Commons Attribution License (http://creativecommons.org/licenses/by/2.0), which permits unrestricted use, distribution, and reproduction in any medium, provided the original work is properly cited.

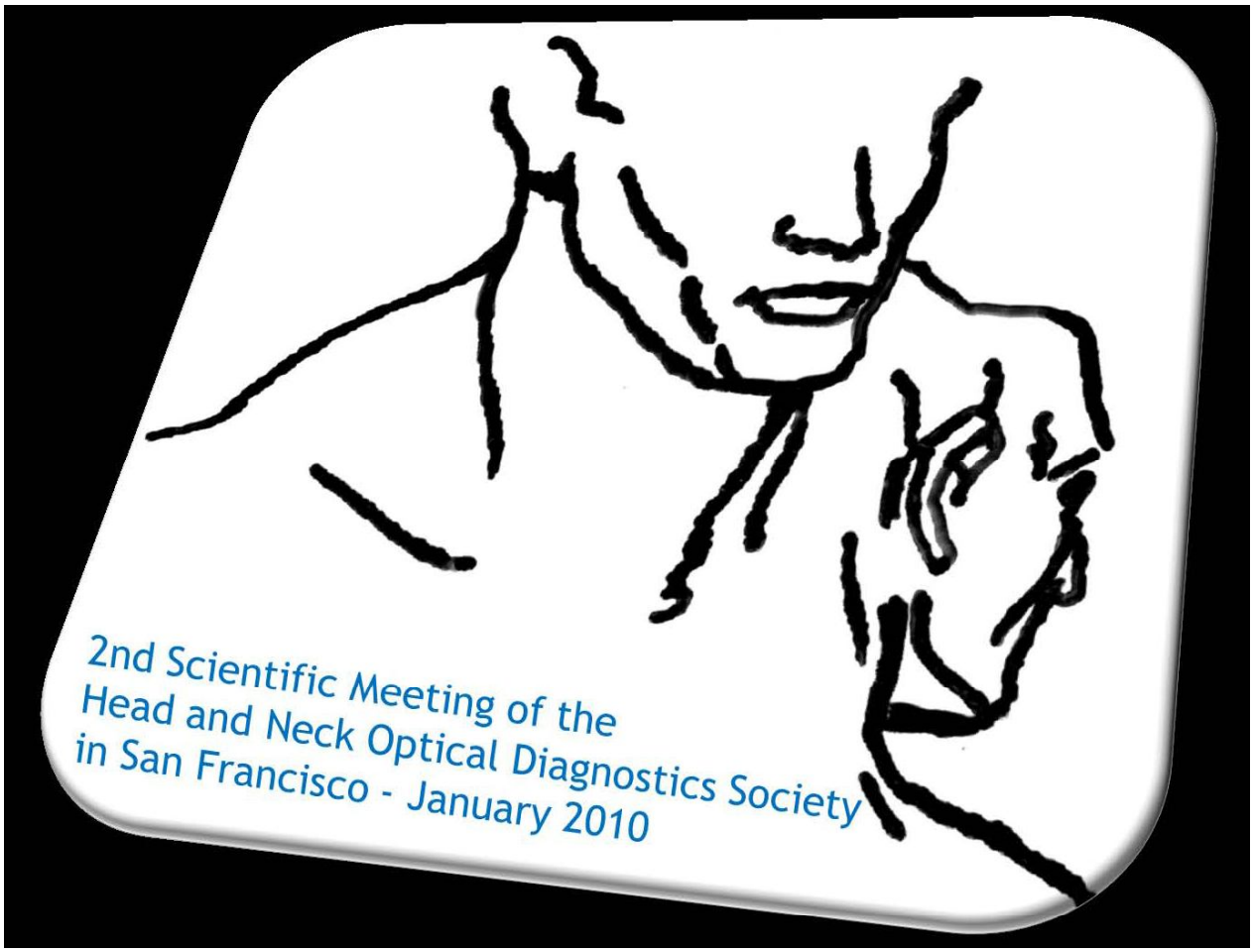

Figure 1 The Head and Neck Optical Diagnostics Society (HNODS) logo.

Applications of optical technologies for diagnosis of lung pathology

Visualizing the respiratory mucosa in pulmonary airways at the sub-cellular level could yield new insights into pathogenesis of many important diseases. However, current imaging modalities to study the respiratory mucosa lack the required resolution to visualize critical sub-cellular detail such as nuclei and respiratory epithelial cilia [3].

Full-field optical coherence microscopy (FFOCM) is an emerging technique capable of providing reflectance images *in situ* with high spatial resolution in all three dimensions. Liu et al. have developed a FFOCM with an axial sectioning thickness of 1 μm and a high transverse resolution of 0.6 μm. Individual epithelial cells and goblet cells, including their sub-cellular morphologies, were seen. Their results demonstrated the potential of FFOCM to provide detailed micro-structural imaging of pulmonary airways without administration of a contrast medium [3].

Investigating the structure and function of pulmonary alveoli *in vivo* is crucial for understanding the normal and diseased lung. In particular, understanding the three-dimensional geometry and relationship of the terminal alveoli to their neighboring alveoli, alveolar ducts and acini during respiration would be a major advance. However, the lung is an inherently difficult organ to image *in vivo* and the peripheral lung has many compounding challenges not limited to its highly scattering micro architecture, large motion artifacts and difficult access through the bronchial tree. Namati et al. used a high-speed high-resolution optical frequency domain imaging (OFDI) system that is endoscopically compatible for future *in vivo* imaging of human alveoli. They showed that OFDI images reveal clear delineation of alveolar septal walls, demonstrating that high-speed three-dimensional visualization of air filled alveoli is feasible [4].

Lung disease involving the alveoli and distal bronchioles are poorly understood and most commonly studied indirectly via lung function tests. Unglert et al. showed that alveolar microstructure could be resolved in three

dimensions in images obtained by intra-vital fluorescence microscopy and optical coherence tomography [5].

Furthermore, lung cancer is the leading cause of cancer-related death, and despite recent efforts to reduce the mortality associated with the disease, patient prognosis remains poor with the current 5-year survival rate under 15%. Detection and diagnosis of lesions arising in the bronchial mucosa remains problematic and as a result they are typically well advanced upon discovery.

Suter et al. described their experience in using optical frequency domain imaging (OFDI) to interrogate the bronchial mucosa of patients with the suspicion of lung cancer. During bronchoscopic evaluation, regions of interest suspicious of cancer or precursor lesions were identified and imaged, in addition to regions of normal appearing mucosa. OFDI imaging of the pulmonary airways may enable the early detection of airway features associated with the development of cancer. When used as a screening tool in high-risk patients, it is hoped that early detection of airway-associated cancer with OFDI will result in a decrease in patients' mortality [6].

Applications of optical technologies for diagnosis of oral and head and neck pathology

Non-invasive differentiation of pre- and early malignant mucosal changes may be helpful to reduce the morbidity and shorten the time to diagnosis for the patients concerned. Optical Coherence Tomography (OCT) seems to be well suited to reach this goal. Volgger et al. reviewed 82 primary leukoplakic or erythroplakic mucosal lesions of the upper aero-digestive tract (UADT) prospectively using an *in vivo*, time-domain OCT. They found that down to a depth of 1.5 mm, micro-anatomical structures were clearly identifiable on the OCT images. OCT reached a sensitivity of 100% and a specificity of 92% or 75% (investigator unblinded or blinded to visual inspection), respectively. This method seems highly promising for early, non-invasive tumour diagnosis in the UADT [7].

Optical biopsy systems have been investigated for various clinical applications; however the main interest remains in the diagnosis and monitoring of premalignant and malignant conditions. Hamdoon et al. acquired suspicious oral lesions from 120 patients which were then subjected to immediate *ex vivo* Swept-Source Frequency-Domain OCT. They suggested that the use of OCT in clinical examination and monitoring can be invaluable tool for inexperienced clinicians [8]. Optical coherence tomography (OCT) is a promising method in the early diagnosis of oral cavity cancer. Prestin et al. showed that depending on the location within the oral cavity, the epithelium demonstrated a varying thickness. The highest values were found in the region of the tongue and the cheek, whereas the floor of the mouth showed the thinnest epithelium [9].

Rubinstein et al. found that the OCT system is non-invasive and easy to incorporate into the operating room as well as to the outpatient clinic. It requires minimal set-up and requires only one person to operate the system. OCT has the distinctive capability to obtain high-resolution images, where the microanatomy of different sites can be observed. OCT technology has the potential to offer a quick, efficient and reliable imaging method to help the surgeon not only in the operating room but also in the clinical setting to guide surgical biopsies and aid in the decision making of different head and neck pathologies [10].

For oral cancer, biopsy has a low specificity because of a thick keratin layer that often covers potential malignancies. Sterenborg et al. investigated the possibility to distinguishing potentially malignant visible lesions from benign ones using differential pathlength spectroscopy (DPS) to reduce the number of unnecessary biopsies in 75 suspicious lesions and 35 clinically normal locations that were not biopsied. They showed that the area under the ROC curve was 0.951 [11]. Pierce et al. developed a portable system to enable high-resolution evaluation of cellular features within the oral mucosa *in situ*. This system is essentially a wide-field epi-fluorescence microscope coupled to a 1 mm in diameter flexible fiber-optic imaging bundle capable of imaging nuclear size and nuclear-to-cytoplasmic ratio following topical application of a fluorescent labeling solution [12].

The development of lymphadenopathy in the neck has many causes, in children it is often found in relation to infection and in a small but significant number it is the first presentation of lymphoma. In adults neoplastic causes predominate for example, lymphoma, squamous cell carcinoma and adenocarcinoma. The treatment modalities and prognosis for these conditions varies enormously and in the case of squamous cell carcinoma, an excision biopsy can lead to significant morbidity. Orr et al. investigated the ability of Raman spectroscopy to differentiate between the major neoplastic diseases of lymph nodes presenting within the neck. Pre-treatment accurate diagnosis is imperative and is a compelling argument for investment in the development of accurate, sensitive and minimally invasive diagnostic techniques, such as Raman spectroscopy [13].

Thyroid cancer is the most common endocrine malignancy. The standard of care in the management of a patient with a thyroid nodule is fine-needle aspiration (FNA) biopsy with cytological evaluation. While 5-10% of nodules are malignant, 10-25% of FNAs' are indeterminate. Consequently, about twice as many patients undergo surgery for a suspicious lesion that turns out to be benign to patients undergo surgery for a known malignant lesion. A more accurate molecular and ultrastructural based algorithm would be useful to improve

diagnostic accuracy. Non-invasive optical tissue diagnosis mediated by fiber-optic probes can be used to perform non-invasive, or minimally-invasive, real-time assessment of tissue pathology *in situ*. Elastic light-scattering spectroscopy (ESS) is a point spectroscopic measurement technique, which is sensitive to cellular and sub-cellular morphological features. Normal and abnormal tissues can generate different spectral signatures as a result of changes in nuclear size, density, and other sub-cellular features, the optical-spectroscopy equivalent of histopathological readings. ESS is optimal for use in the small-volume area as found in thyroid FNA. An important advantage of ESS is that it provides an objective and quantitative assessment of tissue pathology that may not require on-site special expertise and subjective image interpretation as in conventional histopathology. Rosen et al. described their experience in the clinical application of elastic scattering spectroscopy in the thyroid [14].

Within the discipline of Otology, Just et al. used OCT images and 3D reconstructions demonstrate the usefulness of OCT to measure the drilling cavity, to visualize the inner ear structures, and to obtain micro-anatomical information about the round and oval window niche. They suggested that OCT-guided drilling allows identification of the intact inner ear more precisely [15]. Optical coherence tomography is a unique technique to visualize subsurface tissue structures with a resolution below 10 μm during microsurgery without tissue contact. A non-contact volumetric imaging with less than 15 μm resolution can guide microsurgery in Otolaryngology (i.e. middle ear or tumor surgery of the vocal fold) and in other medical disciplines [16].

Visible light is a source of energy known to activate the visual system through absorption by photoreceptors in the eye. When the "stress-confinement" condition is fulfilled, laser light can induce an acoustic signal through an opto-acoustic effect. Wenzel et al. sought to assess if visible light with parameters that induce an optoacoustic effect (i.e., 532 nm, 10 ns pulses) could be used to stimulate the peripheral hearing organ at ear drum and middle ear level. The group demonstrated that visible light can be used to activate the peripheral hearing organ when applied at the ear drum level or on bony structures within the middle ear that can transmit vibrations to the cochlea or inner ear. They suggested that the technique could be used to improve implantable and non-implantable hearing [17].

Wisweh et al. showed that automated classification of laryngeal lesions using optical coherence tomography data can be helpful in making a faster and safer diagnosis. A change in the epithelial layer thickness seems to be an effective indicator for laryngeal cancer and its precursors [18].

Within the discipline of dentistry, Choo-Smith et al. are developing a combined optical coherence tomography (OCT) and polarized Raman spectroscopy (PRS) system for the detection of early non-cavitated dental caries. OCT provides high resolution morphological depth imaging of incipient caries. In combination, OCT and PRS have potential for detecting and monitoring early lesions with high sensitivity and high specificity [19].

Guidance of therapies

Optical technologies improve a clinician's ability to discriminate between normal and diseased tissue. This has obvious advantages including automation, objectivity and reproducibility to give consistent results with defined accuracies.

In the treatment of cancer, the fundamental surgical goal is to remove all local malignant disease and leave no residual malignant cells. Studies have demonstrated the benefit of achieving negative resection margins in terms of disease free local recurrence and overall survival. The surgical margins for head & neck cancer may vary widely depending on the site of disease. Assessment of tumour resection margins using optical coherence tomography was performed by Hamdoon et al. in 25 patients with early stage oral squamous cell carcinoma (OSCC) who underwent local resection. The group found that the junctional epithelium (between positive and negative margins) can be identified by gradual change in epithelial thickness and basement membrane organisation (integrity) from the normal to pathological. They also identified changes in tumour positive margins including hyper-keratinisation, breach of the basement membrane and dis-organised epithelial structure. Moreover, the tumour spread pattern could be identified on the majority of the interrogated tissue [20].

Tissue remodeling

The use of optical technologies to reshape tissue structures is important in reconstructive and cosmetic surgery. Electromechanical reshaping (EMR) of cartilage is a promising non-invasive technique with potential for broad application in reconstructive surgery. EMR involves applying direct current electrical fields to localized stress regions and then initiating a series of oxidation-reduction reactions, thus effecting a shape change. Previous EMR studies have focused on macroscopic structural measurements of the shape change effect or monitoring of electrical current flow. OCT provides a means to gauge structural changes in the tissue matrix during EMR. Chen et al. described the application of OCT to image the EMR process to improve our understanding of the mechanisms of action involved and potentially facilitate optimization of this process [21].

Furthermore, in 1992, laser-induced stress relaxation in cartilage was identified. This led to the development

of non-ablative laser reshaping of cartilage. Laser septochondral correction is non-invasive, bloodless, painless procedure which takes only 10 minutes to complete and can be performed in outpatient settings. The efficacy and safety of this technology can be improved with the feed back control system measuring temperature and stress distribution in the course of laser treatment. Sobol et al. presented recent results of the research and clinical applications of the technology and equipment for laser reshaping of cartilage in the ENT in 120 patients. The positive results were obtained for 95 percent of the patients in two years follow-up [22].

Grafts obtained from peripheral regions of costal cartilage have an inherent tendency to warp over time. Laser irradiation provides a potential method to control the warping process, thus yielding stable grafts for facial reconstructive surgery. Foulad et al. proposed a model for assessing the effect of laser irradiation on the warping process of costal cartilage using optical technology [23].

II. Therapeutic

The therapeutic use of optical techniques ranges from the direct use of optical wavelengths for delivering treatment to the use of light to specifically activate photochemicals to affect tumour lysis with minimal bystander tissue effects. Since many of these technologies are surgically or microscopically directed, the accuracy and resolution of the treatment volume far exceeds that obtained by radiotherapy.

Stepp & Betz showed the feasibility of semi-quantitative endoscopic guided perfusion measurements using ICG-angiographies in 25 patients with free-tissue transfer to the upper aero-digestive tract. The method was shown to be easy to perform with no adverse events. A method for simultaneous ICG-fluorescence and white light imaging was presented. The team suggested that the methodology was suited to situations with questionable flap vasculature Doppler signals, or when flaps are otherwise difficult to monitor [24,25].

Direct use of optical technology

Lasers have been used by a number of researchers to close wounds in controlled laboratory tests over the last 15 years. Larson et al. presented their experience using a device to fuse tissue membranes as an alternative to sutures or staples for the coaptation of mucoperichondrial membranes. Coaptation is accomplished through the controlled application of laser heating to induce protein denaturation and subsequent renaturation across the interface. They identified the important parameters involved in fusing biological tissues using radiation from laser sources following computational modeling of the fusion process based on engineering first-principles from heat transfer, fluid dynamics and optics, and from experimental results on a particular tissue system [26].

An interesting application was presented by Fishman et al. Advancements in implantable auditory prostheses now demand preservation of residual auditory function following the surgery. Atraumatic cochleostomy formation is essential to this goal. Clinically reported hearing outcomes in human implantation are still quite variable in this regard. It was suggested that CO_2 laser operated with a handheld hollow waveguide can consistently produce cochleostomies without damaging the residual auditory function. Fishman et al. demonstrated that for a careful selection of the laser's power, the safety range for the laser is superior to the safety range of drilling. Particularly important is the finding that multiple laser pulses through the same cochleostomy do not further increase the initial compound action potential (CAP) threshold elevation. Moreover, multiple laser pulses at different locations of the cochlea do not further increase the initial CAP threshold elevation observed after the first laser pulse [27].

Eustachian tube dysfunction is very common and is the predominant cause of otitis media with effusion. Negative middle ear pressure generated by Eustachian tube dysfunction can cause deformation of the collagen layer in the ear drum. Kaylie and Miller presented their findings after laser myringoplasty using the Omniguide hand-held flexible fiber CO_2 laser in 22 patients which showed immediate hearing improvement and eardrum contraction [28].

CO_2 trans-oral laser microsurgery (TLM) is an emerging technique for the management of laryngeal cancer and other head and neck malignancies. This technique has become more widely used by head and neck surgeons progressively replacing traditional open surgical procedures because it is better at preserving organ function with lower overall morbidity. The CO_2 laser is coupled to a micromanipulator and microscope, which provides enhanced tumor visualization and the ability to perform precise tissue cuts, obtain excellent haemostasis, and avoid damaging the surrounding tissues and structures that are transected during open surgical procedures. Armstrong et al. reflected upon their decade of experience in TLM, they felt that the improved instrumentation, demonstration of oncologic effectiveness, clinical experience using TLM and decreased morbidity has led to an increased utilization of TLM by head and neck surgeons. Successful surgery requires adequate visualization, precise cutting, controlled depth of tissue penetration, and ability to obtain tissue haemostasis. The full spectrum of laser power settings, spot sizes and energy pulse delivery modes is utilized to resect mucosa, fat, muscle, connective tissue and cartilage while avoiding inadvertent damage to nerves and large vessels, and obtaining adequate haemostasis [29].

The use of CO_2 laser in the management of oral dysplastic lesions has been put into practice for more than

a few years now. The main advantage is the decrease in local tissue morbidity. Very few studies have evaluated recurrence, malignant transformation and overall outcome in patients undergoing such procedure. Jerjes et al. applied CO_2 laser in a prospective study of 123 oral dysplastic lesions followed-up for 6.4 years. Recurrence and/or malignant transformation of oral dysplasia were observed following laser surgery. They recommended laser resection/ablation for oral dysplasia to prevent not only recurrence and malignant transformation, but also postoperative oral dysfunction encountered by other conventional modalities. The use of trans-oral robotic flexible CO_2 laser with fluorescence and narrow band imaging control was commended [30].

The incidence of oral squamous cell carcinoma (OSCC) remains high. Oral carcinomas are the sixth most common cancer in the world. Squamous cell carcinoma of the oral cavity has a poor overall prognosis with a high tendency to recur at the primary site and extend to involve the cervical lymph nodes. Jerjes et al. followed-up 73 patients for 3 years in prospective study to evaluate the oncological outcomes following trans-oral CO_2 laser resection of T_1/T_2 N_0 OSCC. Tumour clearance was primarily achieved in 73 patients. Follow-up resulted in a 3-year survival of 87.8%. Recurrence was identified in 12% of the patients. The mean age of 1^{st} diagnosis of the recurrence group was 76.4 years. Most common oral sites included the lateral border of tongue and floor of mouth. Recurrence was associated with clinical N-stage disease. The surgical margins in this group were also evaluated [31].

Vocal fold scarring can arise from disease or post-surgical wound healing and is one of the predominant causes of voice disorders. Focused ultrafast laser pulses have been demonstrated to create tightly confined sub-surface ablation in a variety of tissue, including vocal folds. Ben-Yakar et al. demonstrated how the unique ability of ultrafast laser ablation to create sub-surface vocal fold microsurgeries could be used for eventually creating a plane in tough sub-epithelial scar tissue into which biomaterials can be injected. They found that the use of relatively high repetition rates, with a small number of overlapping pulses, is critical to achieving ablation in reasonable amounts of time while still avoiding significant heat deposition. Additionally, they used multi-photon fluorescence of the ablation region and SHG imaging of collagen fibers to obtain visual feedback of tissue structure and confirm successful ablation [32].

Photodynamic therapy

Analogous to 3D dosimetry planning for radiotherapy attempts are being made to plan interstitial photodynamic therapy (iPDT), using multiple linear light sources positioned within the tumour. In an on-going feasibility study in the Netherlands, 16 patients with incurable SCC at the base tongue have been treated with iPDT as a last treatment option. Preliminary results are encouraging with a long-term complete response in 8 out of 16 patients who have failed standard treatment. There is strong evidence that the partial responders are a direct result of inadequate light delivery [33].

Accurate light dosimetry has not yet been performed during iPDT in the head and neck. van Veen et al. proposed the development of dedicated iPDT verification and planning technology to improve the clinical response and reduce the occurrence of side effects. Their results so far indicate good conservation of functions i.e. swallowing, and excellent local control of the tumour. Interstitial PDT may offer an excellent alternative or adjuvant for conventional treatment modalities [33].

Photodynamic therapy with m-THPC is an established treatment for superficial squamous cell carcinoma and is also being considered for treatment of larger head and neck tumors. Recently, clinical implementation of m-THPC-mediated PDT in the head and neck has not been optimal; a subset of patients has experienced incomplete response. It is well-understood that sufficient quantities of light, drug and oxygen must be present in the targeted tissue in order to deliver sufficient damage. This requirement is complicated by variations in the tissue optical properties and in the photo-sensitizer uptake rates; however, most clinical protocols do not measure the effect of these factors on the PDT dose delivered to individual patients [34,35].

Kanick and de Visscher et al. described the use of optical techniques developed to monitor PDT treatments in pre-clinical models into the clinical treatment of head and neck cancer. Their techniques incorporated reflectance and fluorescence spectroscopic measurements into the PDT-treatment protocol. They found that spectral analysis allowed the extraction of m-THPC concentrations and the quantitative determination of tissue physiological parameters that are important to the PDT-delivered dose (i.e. blood volume and hemoglobin saturation). They described the practical and technical challenges of translating these techniques into the clinical setting [34,35].

Photodynamic therapy, the fourth oncological interventional modality has proved its successfulness in the management of variety of pathologies involving the human body. University College London (UCL) researchers evaluated the outcome following ultrasound-guided iPDT of pathologies involving the head and neck region as well as the upper and lower limbs in 110 patients. Clinical assessment showed that more than half of the patients had "good response" to the treatment and a third reported "moderate response". Radiological assessment comparing imaging 6-week post-PDT to the

baseline showed moderate response in half of the patients and significant response in 20% of patients [36].

Optical technologies can be used to activate therapy in a particular location directed by imaging modalities to improve co-location of therapy to disease states. Photodynamic therapy (PDT) is a minimally invasive surgical intervention used in the management of tissue disorders. It can be applied before, or after, any of the conventional modalities, without compromising these treatments or being compromised itself. PDT is valuable for potentially malignant disorders. Hopper et al. on a study of 147 patients showed that 5-ALA-PDT and/or mTHPC-PDT offer an effective alternative treatment for potentially malignant oral disorders. It is associated with excellent functional and cosmetic results and can be used in conjunction with other standard therapies [37].

Shafirstein et al. further showed the safety and efficacy of photodynamic therapy (PDT) in the treatment of oral leukoplakia with 5-aminolevulinic acid (5-ALA) and pulsed dye laser (PDL) confirmed with fluorescence diagnosis system. They determined that high power laser activation allowed completing the laser therapy within 1-3 minutes with a significant response in up to 46% [38].

Professor Biel presented an excellent account of the clinical application of photodynamic therapy for ENT cancers. Carcinoma of the larynx accounts for 25-30% of all carcinomas of the head and neck. Early carcinomas of the larynx (Tis or T1) and severe dysplasia are presently treated with either radiation therapy or surgery alone. Photodynamic therapy has been demonstrated to be effective in the treatment of early carcinomas of the larynx, T_{is} and T_1, with cure rates of 90% with follow-up to 236 months. The advantage of PDT for early carcinomas of the larynx is the ability to preserve normal endo-laryngeal tissue while effectively treating the carcinomas. This results in improved laryngeal function and voice quality. Furthermore, PDT requires a short duration of therapy as compared to radiation therapy. PDT is repeatable and carries less risk than surgical therapy and is performed as an outpatient non-invasive treatment. Importantly, the use of PDT does not preclude the use of radiotherapy or surgery in the future for new primary or recurrent disease [39].

Within oro-pharyngeal oncology the management of base of tongue carcinoma continues to be a major challenge in head and neck oncology especially after chemo-radiation failure and the poor reconstructive prospects of total glossectomy with laryngectomy as the remaining salvage option. Without advances in pathological confirmation of previously irradiated fibrotic tongue base tissue the efficacy of robotic trans-oral laser resection is still unproven but very promising. Jerjes et al. evaluated the outcome following ultrasound-guided interstitial photodynamic therapy (US-iPDT) of stage IV tongue base carcinoma in 33 patients followed-up for 18 months. Their clinical assessment showed that two-thirds of the patients had "good response" to the treatment and a third reported "moderate response" [40].

Advances in diagnosis and therapy

Jerjes et al. also described their experiences with a phase I dose escalating study of photochemical internalization (PCI), which is a novel technology that facilitates the delivery of oncotoxic macromolecules into cytoplasm. The initial mechanism and practical application was described by Berg et al. in 1999. The group evaluated the safety and tolerance of the photo-sensitizer (amphinex) that is used to initiate the photochemical internalization process with bleomycin as the chemotherapeutic agent. The most striking finding was the dramatic tumour responses. The starting dose of Amphinex for the study was set at a level not expected to trigger a PCI response, however there appeared to be a localized synergistic effect with photo-activation [41].

It is now known that the presence of biofilms in the upper aero-digestive tract prevents the adequate treatment of infections because the infecting agents remain sequestered in an environment away from circulating or topical agents such as antibiotics. The treatment of these recidivist infections is difficult although the use of selected detergents has shown promise. An alternative treatment option is the use of PDT which was shown to be effective *in vivo* by Rhee et al. using *H. Influenza* biofilms with over 66% resolution of otitis media, one of the most common childhood diseases [42].

Naturally the next step in the utilization of optical technologies is in the shaping and control of nano devices. An innovative use of optical technology in the activation of nano-devices to promote chondrocyte growth across Ti:Sapphire Femto second laser microstructured titanium prosthesis coated with bioactive proteins was shown by Ilgner et al. to improve biointegration and sound transmission [43].

In summary, we briefly outlined some of the excellent evidence presented in the 2nd Scientific Meeting of the Head and Neck Optical Diagnostics Society (HNODS) in San Francisco initially relating to disease diagnostics, including detection and guidance for biopsies and treatment and then focusing upon the therapeutic use of optical technologies either directly or by activating treatments.

Author details

[1]The "Head and Neck Optical Diagnostics Society" Council, Head & Neck Centre, University College Hospital, 250 Euston Road, London, NW1 2PG, UK. [2]Department of Surgery, University College London Medical School, London, UK. [3]Department of Otolaryngology/Head and Neck Surgery, Barnet and Chase Farm Hospitals NHS Trust, London, UK. [4]Unit of Oral & Maxillofacial Surgery, Division of Maxillofacial, Diagnostic, Medical and Surgical Sciences,

UCL Eastman Dental Institute, London, UK. [5]Center for Optical Diagnostics and Therapy, Erasmus University Medical Center, Rotterdam, the Netherlands. [6]The Beckman Laser Institute and Medical Clinic, The University of California Irvine, Irvine, CA, USA. [7]Department of Pathology, The University of Texas M. D. Anderson Cancer Center, Houston, Texas, USA. [8]Department of Otorhinolaryngology, Plastic Head and Neck Surgery, Aachen University Hospital, RWTH Aachen, Germany. [9]Department of Histopathology, Imperial College and The Hammersmith Hospitals, London, UK. [10]Department of Oral & Maxilofacial Surgery, University Medical Center Groningen, the Netherlands. [11]Virginia Piper Cancer Institute-Abbott Northwestern Hospital, Minnesota, USA. [12]Department of Head and Neck Surgery, Division of Surgery, The University of Texas M. D. Anderson Cancer Center, Houston, TX, USA. [13]National Medical Laser Centre, University College London, London, UK. [14]Center for Optical Diagnostics and Therapy, Department of Radiation Oncology, Erasmus University Medical Center, Rotterdam, the Netherlands. [15]Department of Otorhinolaryngology, Head & Neck Surgery, Ludwig Maximilian University, Munich, Germany. [16]LIFE Center, University Clinic Munich, Munich, Germany. [17]Research Centre for Automatic Control (CRAN), Nancy-University, UMR CNRS, France. [18]Michelson Diagnostics, 11A Grays Farm Production Village, Grays Farm Road, Orpington, Kent, BR5 3BD, UK. [19]Gloucestershire Hospitals NHS Foundation Trust, Gloucester, UK. [20]Department of Biomedical Engineering, Beckman Laser Institute, University of California, Irvine, USA. [21]Dept. of Radiation Biology, The Norwegian Radium Hospital, Montebello, Norway. [22]Department of Oral & Maxillofacial Surgery, Tata Memorial Hospital, Mumbai, India. [23]Department of Otorhinolaryngology, Head and Neck Surgery, Klinikum Bielefeld, Bielefeld, Germany. [24]Department of Oral & Maxillofacial Surgery, Leeds Dental Institute, Leeds, UK. [25]National University of Ireland, Galway, Ireland. [26]Department of Bioengineering, Rice University, Houston, USA. [27]National Cancer Centre, Singapore 169610, Singapore. [28]University of Sao Paulo, Sao Carlos, SP, Brazil. [29]National Research Council Canada-Institute for Biodiagnostics, Winnipeg, Manitoba, Canada. [30]Division of Oncology, Lund University Hospital, Lund, Sweden. [31]Department of Head & Neck Oncology & Surgery, The Netherlands Cancer Institute - Antoni van Leeuwenhoek Hospital, Amsterdam, the Netherlands. [32]Division of BioPhysics and BioImaging, Ontario Cancer Institute, Ontario, Canada. [33]Department of Medical Biophysics, Faculty of Medicine, University of Toronto, Toronto, Canada. [34]Division of Gastroenterology and Hepatology, Mayo Clinic, Florida, USA. [35]Department of Biomedical Engineering, Electrical & Computer Engineering, Physics, Boston University, Boston, USA. [36]Physics and Astronomy, University of Pennsylvania, Philadelphia, USA.

Authors' contributions

All authors have contributed to conception and design, drafting the article or revising it critically for important intellectual content and final approval of the version to be published.

Competing interests

The authors declare that they have no competing interests.

Received: 7 February 2011 Accepted: 9 February 2011
Published: 9 February 2011

References

1. Hopper C, Jerjes W, Upile T: **Our experience with optical diagnostics of the head and neck.** *Head & Neck Oncology* 2010, **2(Suppl 1)**:O1.
2. Liu G, Kieu K, Wise FW, Wong B, Chen Z: **Fiber-based microendoscopic multiphoton imaging.** *Head & Neck Oncology* 2010, **2(Suppl 1)**:O35.
3. Liu L, Oh W, Bouma B, Rowe S, Tearney G: **Ultrahigh-resolution 3D full-field optical coherence micropscopy of the pulmonary airways ex vivo.** *Head & Neck Oncology* 2010, **2(Suppl 1)**:O10.
4. Namati E, Unglert C, Bouma B, Tearney G: **High-speed three-dimensional imaging of the pulmonary alveoli.** *Head & Neck Oncology* 2010, **2(Suppl 1)**:O11.
5. Unglert C, Namati E, Liu L, Yoo H, Kang D, Bouma B, Tearney G: **Reflectance microscopy techniques for 3D imaging of the alveolar structure.** *Head & Neck Oncology* 2010, **2(Suppl 1)**:O12.
6. Suter Melissa, Riker David, Bouma Brett, Beamis John, Guillermo Tearney: **Three-dimensional microscopy of the human bronchial mucosa.** *Head & Neck Oncology* 2010, **2(Suppl 1)**:O13.
7. Volgger V, Stepp H, Jerjes W, Upile T, Leunig A, Hopper C, Betz C: **Current Munich status concerning in-vivo optical coherence tomography for differentiating lesions of the upper aerodigestive tract.** *Head & Neck Oncology* 2010, **2(Suppl 1)**:O39.
8. Hamdoon Z, Jerjes W, McKenzie G, Jay A, Hopper C: **Assessment of suspicious oral lesions using optical coherence tomography.** *Head & Neck Oncology* 2010, **2(Suppl 1)**:O6.
9. Prestin S, Betz C, Kraft M: **Measurement of epithelial thickness within the oral cavity using optical coherence tomography (OCT).** *Head & Neck Oncology* 2010, **2(Suppl 1)**:O42.
10. Rubinstein M, Kim J, Armstrong W, Djalilian H, Chen Z, Wong B: **Emerging applications for OCT in the head and neck.** *Head & Neck Oncology* 2010, **2(Suppl 1)**:O41.
11. Sterenborg HJCM, Witjes M, Visscher S, Amelink A: **Differential Pathlength Spectroscopy for diagnosis of head and neck cancer.** *Head & Neck Oncology* 2010, **2(Suppl 1)**:O3.
12. Pierce M, Rosbach K, Roblyer D, Muldoon T, Williams M, El-Naggar A, Gillenwater A, Richards-Kortum R: **Wide-field and high-resolution optical imaging for early detection of oral neoplasia.** *Head & Neck Oncology* 2010, **2(Suppl 1)**:O2.
13. Orr L, Kendall C, Hutchings J, Isabelle M, Horsnell J, Stone N: **Raman spectroscopy as a tool for the identification and differentiation of neoplasias contained within lymph nodes of the head and neck.** *Head & Neck Oncology* 2010, **2(Suppl 1)**:O4.
14. Rosen J, Suh H, Lee S, Aamar O, Bigio I: **Design, conduct and challenges of a clinical trial utilizing elastic light scattering spectroscopy in the thyroid.** *Head & Neck Oncology* 2010, **2(Suppl 1)**:O36.
15. Just T, Lankenau E, Hüttmann G, Pau H: **An optical coherence tomography study for imaging the round window niche and the promontorium tympani.** *Head & Neck Oncology* 2010, **2(Suppl 1)**:O5.
16. Hüttmann G, Probst J, Just T, Pau H, Oelckers S, Hillmann D, Koch P, Lankenau E: **Real-time volumetric optical coherence tomography OCT imaging with a surgical microscope.** *Head & Neck Oncology* 2010, **2(Suppl 1)**:O8.
17. Wenzel G, Lim H, Zhang K, Balster S, Massow O, Lubatschowski H, Reuter G, Lenarz T: **Laser hearing aids.** *Head & Neck Oncology* 2010, **2(Suppl 1)**:O31.
18. Wisweh H, Mateu LM, Kraft M, Krüger A, Lubatschowski H: **Automatic segmentation of clinical OCT images for the determination of epithelial thickness changes in laryngeal lesions.** *Head & Neck Oncology* 2010, **2(Suppl 1)**:O9.
19. Choo-Smith L, Hewko M, Sowa M: **Towards early dental caries detection with OCT and polarized Raman spectroscopy.** *Head & Neck Oncology* 2010, **2(Suppl 1)**:O43.
20. Hamdoon Z, Jerjes W, McKenzie G, Jay A, Hopper C: **Assessment of tumour resection margins using optical coherence tomography.** *Head & Neck Oncology* 2010, **2(Suppl 1)**:O7.
21. Chen H, Yu L, Manuel C, Wong BJ: **Using optical coherence tomography to monitor effects of electromechanical reshaping in septal cartilage.** *Head & Neck Oncology* 2010, **2(Suppl 1)**:O19.
22. Sobol E, Sviridov A, Vorobieva N, Svistushkin V: **Feedback controlled laser system for safe and efficient reshaping of nasal cartilage.** *Head & Neck Oncology* 2010, **2(Suppl 1)**:O17.
23. Foulad A, Manuel C, Kim J, Wong BJF: **Numerical analysis of costal cartilage warping after laser modification.** *Head & Neck Oncology* 2010, **2(Suppl 1)**:O22.
24. Stepp H: **Endoscopic ICG perfusion imaging for flap transplants: technical development.** *Head & Neck Oncology* 2010, **2(Suppl 1)**:O14.
25. Betz C: **Endoscopic ICG perfusion imaging for flap transplants: clinical results.** *Head & Neck Oncology* 2010, **2(Suppl 1)**:O15.
26. Larson M, Sooklal V, McClure J, Hooper L, Sieber J: **A laser device for fusion of nasal mucosa.** *Head & Neck Oncology* 2010, **2(Suppl 1)**:O23.
27. Fishman A, Moreno L, Rivera A, Richter C: **Lasers, a tool for soft cochleostomies.** *Head & Neck Oncology* 2010, **2(Suppl 1)**:O38.
28. Kaylie D, Miller J: **CO_2 laser myringoplasty using handheld waveguide.** *Head & Neck Oncology* 2010, **2(Suppl 1)**:O32.
29. Armstrong WB, Rubinstein M: **CO_2 Laser Transoral Laser Microsurgery of Head and Neck Cancer: Lessons Learned over Ten Years.** *Head & Neck Oncology* 2010, **2(Suppl 1)**:O37.
30. Jerjes W, Upile T, Hamdoon Z, Hopper C: **CO_2 laser ablation of oropharyngeal dysplasia.** *Head & Neck Oncology* 2010, **2(Suppl 1)**:O34.

31. Jerjes W, Upile T, Hamdoon Z, Hopper C: **The use of CO2 laser in tumour resection of the oropharyngeal region.** *Head & Neck Oncology* 2010, **2(Suppl 1)**:O33.
32. Ben-Yakar A, Hoy C, Everett WN, Kobler J: **Toward endoscopic ultrafast laser microsurgery of vocal folds.** *Head & Neck Oncology* 2010, **2(Suppl 1)**: O29.
33. van Veen RLP, Robinson DJ, Sterenborg HJCM, Aans JB, Tan IB, Hamming Vrieze O, Hoebers F, Witjes MJH, Levendag PC: **Treatment planning for Interstitial Photodynamic Therapy for head and neck cancer.** *Head & Neck Oncology* 2010, **2(Suppl 1)**:O45.
34. Kanick S, Karakullukcu B, van Veen R, Sterenborg H, Tan IB, Witjes M, Amelink A, Robinson D: **In vivo monitoring of Foscan-mediated photodynamic therapy in clinical head and neck procedures using optical spectroscopy.** *Head & Neck Oncology* 2010, **2(Suppl 1)**:O16.
35. de Visscher S, Witjes M, Kascáková S, Robinson D, Sterenborg H, Roodenburg J, Amelink A: **Non-invasive measurement of photosensitiser concentration using fluorescence differential path-length spectroscopy: validation for different liposomal formulations of m-THPC: Foscan, Foslip and Fospeg.** *Head & Neck Oncology* 2010, **2(Suppl 1)**:O46.
36. Osher J, Jerjes W, Upile T, Hamdoon Z, Nhembe F, Bhandari R, Mackay S, Shah P, Mosse CA, Morley S, Hopper C: **Ultrasound-guided interstitial photodynamic therapy for deeply seated pathologies: assessment of outcome.** *Head & Neck Oncology* 2010, **2(Suppl 1)**:O26.
37. Hopper C, Jerjes W, Hamdoon Z, Upile T: **The role of photodynamic therapy in the management of oral dysplasia.** *Head & Neck Oncology* 2010, **2(Suppl 1)**:O24.
38. Shafirstein G, Bäumler W, Sigel E, Fan C, Berry K, Vural E, Stack BC, Suen JY: **Utilizing 5-Aminolevulinic Acid and Pulsed Dye Laser for Photodynamic Therapy of Oral Leukoplakia - Pilot study.** *Head & Neck Oncology* 2010, **2(Suppl 1)**:O40.
39. Biel M: **Photodynamic therapy of laryngeal cancers.** *Head & Neck Oncology* 2010, **2(Suppl 1)**:O25.
40. Jerjes W, Upile T, Hamdoon Z, Nhembe F, Bhandari R, Mackay S, Mosse CA, Morley S, Hopper C: **Photodynamic therapy as the "last hope" for tongue-based carcinoma.** *Head & Neck Oncology* 2010, **2(Suppl 1)**:O27.
41. Jerjes W, Mosse C, Hamdoon Z, Carnell D, Berg K, Høgset A, Hopper C: **Photochemical internalization.** *Head & Neck Oncology* 2010, **2(Suppl 1)**: O44.
42. Rhee C, Chang S, Chung P, Jung J, Ahn J, Suh M: **The effect of PDT on H. influenzae biofilm in vivo.** *Head & Neck Oncology* 2010, **2(Suppl 1)**:O28.
43. Ilgner JF, Biedron S, Fadeeva E, Cichkov B, Klee D, Loos A, Sowa-Soehle E, Westhofen M: **Femtosecond laser microstructuring and bioactive nanocoating of titanium surfaces in relation to chondrocyte growth.** *Head & Neck Oncology* 2010, **2(Suppl 1)**:O30.

doi:10.1186/1758-3284-3-7
Cite this article as: Upile *et al.*: At the frontiers of surgery: review. *Head & Neck Oncology* 2011 **3**:7.

Submit your next manuscript to BioMed Central and take full advantage of:

- **Convenient online submission**
- **Thorough peer review**
- **No space constraints or color figure charges**
- **Immediate publication on acceptance**
- **Inclusion in PubMed, CAS, Scopus and Google Scholar**
- **Research which is freely available for redistribution**

Submit your manuscript at
www.biomedcentral.com/submit

BioMed Central

Hamdoon et al. Head & Neck Oncology 2010, 2(Suppl 1):O7
http://www.headandneckoncology.org/content/2/S1/O7

Head & Neck Oncology

ORAL PRESENTATION Open Access

Assessment of tumour resection margins using optical coherence tomography

Zaid Hamdoon*, Waseem Jerjes, Gordon McKenzie, Amrita Jay, Colin Hopper

From 2nd Scientific Meeting of the Head and Neck Optical Diagnostics Society
San Francisco, CA, USA. 23-24 January 2010

Introduction/aims

In the treatment of cancer, the fundamental surgical goal is to remove all local malignant disease and leave no residual malignant cells. Studies have demonstrated the benefit of achieving negative resection margins in terms of disease free local recurrence and overall survival. The surgical margins for head & neck cancer may vary widely depending on the site of disease.

Optical coherence tomography (OCT) is an imaging modality that uses light to determine cross-sectional anatomy in turbid media such as living tissues.

In this study, we used this technology to evaluate resection margins acquired from patients with oral squamous cell cancer (OSCC).

Material/methods

Twenty-five patients with newly diagnosed T1-T2 OSCC underwent local resection. In the immediate ex-vivo phase, OCT was used to interrogate the surgical margins of these specimens and the results were, then, compared to histopathology. Inter, Intra-observer differences, sensitivity and specificity was calculated.

Results

The junctional epithelium (between positive and negative margins) can be identified by gradual change in epithelial thickness and basement membrane organisation (integrity) from the normal to pathological. Identified changes in tumour positive margins include hyperkeratinisation, breach of the basement membrane and disorganised epithelial structure. Tumour spread pattern could be identified on the majority of the interrogated tissue. Sensitivity and specificity were calculated and proved to be encouraging.

Conclusions

The results from this study are encouraging and suggest the feasibility of using OCT in differentiating between positive and negative surgical margins.

Acknowledgment
We would like to thank the BAOMS for supporting this research project.

Published: 29 October 2010

doi:10.1186/1758-3284-2-S1-O7
Cite this article as: Hamdoon *et al.*: Assessment of tumour resection margins using optical coherence tomography. *Head & Neck Oncology* 2010 **2**(Suppl 1):O7.

UCL Department of Surgery, University College London Medical School, London, UK

Submit your next manuscript to BioMed Central and take full advantage of:

- Convenient online submission
- Thorough peer review
- No space constraints or color figure charges
- Immediate publication on acceptance
- Inclusion in PubMed, CAS, Scopus and Google Scholar
- Research which is freely available for redistribution

Submit your manuscript at
www.biomedcentral.com/submit

BioMed Central

BioMed Central © 2010 Hamdoon et al; licensee BioMed Central Ltd.

BioOptics WORLD | Advances in lasers, optics, and imaging for the life sciences

Multiple beams boost resolution of OCT

Social Media Tools

11/01/2008

The freqency-domain approach broke the first significant barrier to optical coherence tomography's potential. Now a multibeam approach promises similar improvement, as an oral-cancer study demonstrates.

By Gordon McKenzie, Waseem Jerjes, Zaid Hamdoon, and Colin Hopper

Optical coherence tomography (OCT), a powerful cross-sectional modality allowing noninvasive imaging of samples in real time and at high resolution, has become the new gold standard in ophthalmic care. But while it is extremely promising for other clinical applications, its use in those areas is not widespread. That is due at least in part to technical constraints, which equipment makers are addressing. One approach, multibeam OCT, promises to advance the use of OCT in cancer detection.

OCT was conceived independently by Tanno and Chiba of Yamagata University in 1990, and by Huang and Fujimoto at MIT in 1991.[1, 2] It is normally based around a Michelson interferometer, an invention dating back to 1887.[3] The technology uses a coherence gate to spatially locate a reflected signal from within a sample. An optical focus provides lateral resolution, and beam-scanning enables 2-D and 3-D scans.

Early OCT systems operated in the time domain. Improvements such as broad-band light sources and dynamic focusing supported its development, but first-generation OCT had a significant limitation: speed. The scanning mechanism's mechanical limitations meant image capture would take multiple seconds–too slow for use in vivo. Fercher's group overcame that bottleneck in the mid 1990s by collecting the interferogram in the frequency domain (FD-OCT), which gave a signal-to-noise

advantage of about three orders of magnitude.[4, 5] Advances in light sources and detectors since then have enabled very rapid image capture.

But even FD-OCT has a significant disadvantage: it is not possible to achieve high lateral resolutions by dynamic focusing because the method involves collection of light from all depths simultaneously (followed by a Fourier transform to recover the depth data). While axial resolution is determined by light source properties, the lateral resolution is a function of the numerical aperture (N.A.), which is a function of the desired depth of focus.

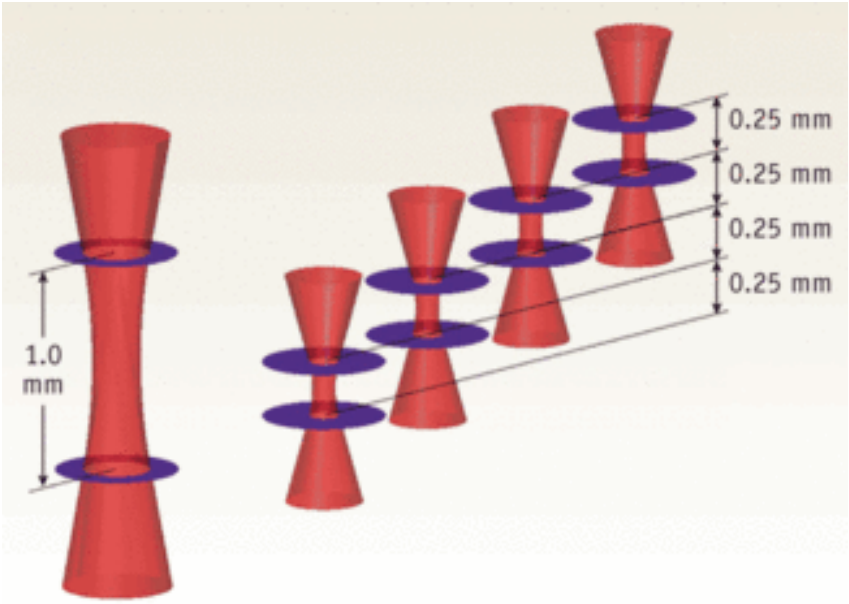

Figure 1. The four-beam configuration of the mulitbeam OCT microscope is focused over 1 mm with each sub-beam focused over 0.25 mm, producing double the resolution possible from a single beam. Each sub-beam has a theoretical FWHM diameter of just 10.3 µm.

The Gaussian beam waist radius w_0 is related to the depth of focus Z_R (using the well-known Rayleigh criteria) by the following formula:

$$w_0 = \sqrt{\frac{\lambda z_R}{n\pi}}$$

At the usual wavelength of 1300 nm used for imaging tissue ($n \approx 1.35$), a 1 mm depth of focus implies a minimum Gaussian beam radius of 17.5 µm (equivalent to 20.6 µm FWHM). This is often too large for useful clinical images.

Multibeam OCT

To overcome this fundamental limitation of traditional, single-beam FD-OCT systems, Michelson Diagnostics has developed a solution to simultaneously scan multiple beams, focused at slightly different depths, and compile an image mosaic from the resulting multiple FD-OCT interferograms. Using a multichannel interferometer, the beams are sufficiently close together to be effectively simultaneous, so motion artifacts are not a problem. For example, a four-beam system focused over 1.0 mm, with each sub-beam focused over 0.25 mm, produces double the resolution possible from a single beam (see Fig. 1). Each sub-beam has a theoretical FWHM diameter of just 10.3 µm.

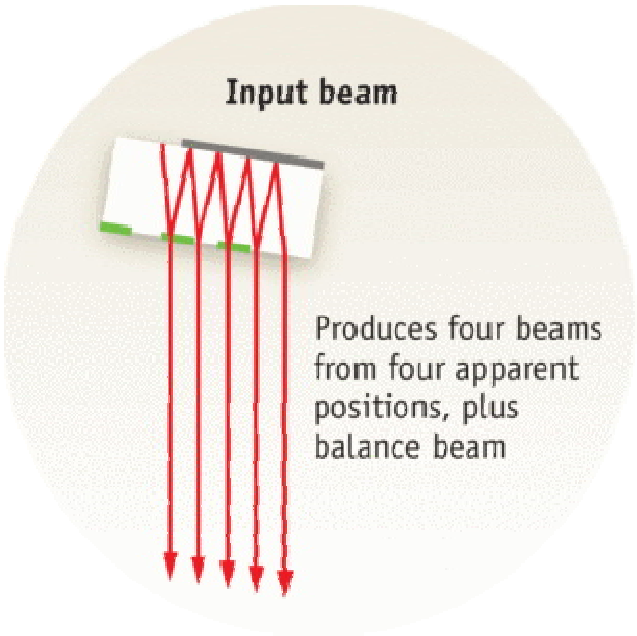

Michelson Diagnostics first implemented the multibeam OCT approach in its EX1301 OCT Microscope (see Fig. 2). This microscope is based on a free-space Michelson interferometer, using a “rattle plate” to generate a series of virtual sources at the input to the interferometer. The instrument achieves the required lateral resolution of less than 10 µm (see Fig. 3); blending algorithms eliminates minor mismatch of intensity across the mosaic-tile boundaries.

Figure 2. The housing (eft) and interior (right) of Michelson Diagnostics' first multibeam OCT microscope, the EX1301. The design is based on a free-space Michelson interferometer, using a "rattle plate" to generate a series of virtual sources at the input to the interferometer (inset).

Another way of generating multibeam OCT is to use a probe with multiple fibers. This approach was pioneered by Victor Yang et al. at Ontario Cancer Institute, Princess Margaret Hospital, University Health Network (Toronto, Canada). A collaboration between Michelson Diagnostics and UHN Toronto has demonstrated successful in vivo imaging of a lapine colon with a prototype four-beam fiber-optic probe (see Fig. 4).

Oral cancer: the case for OCT

OCT has the potential to greatly improve the effectiveness of detection and management of oral cancer, the 11th most common cancer worldwide. World Health Organization figures show 405,000 new cases annually, with an upward trend. The five-year survival rate, approximately 50%, has not changed significantly in 30 years despite the fact that cancers detected early are much more survivable. The usual treatment is surgical removal of the tumor; early detection enables less invasive surgery with greatly reduced effects on appearance as well as on eating and speaking functions. Late detection requires more expensive, invasive and disfiguring surgery, and requires costly aftercare.

After a patient with oral cancer is treated, continuous monitoring is necessary to ensure recurrence is picked up and treated at an early stage. A delay in diagnosis can lead to the spread of new disease, increasing morbidity and mortality. The current state of the art for monitoring lesions is very far from ideal: it requires a combination of objective (clinical examination, including visual inspection) and subjective (surgical biopsy and histopathology processing) techniques.

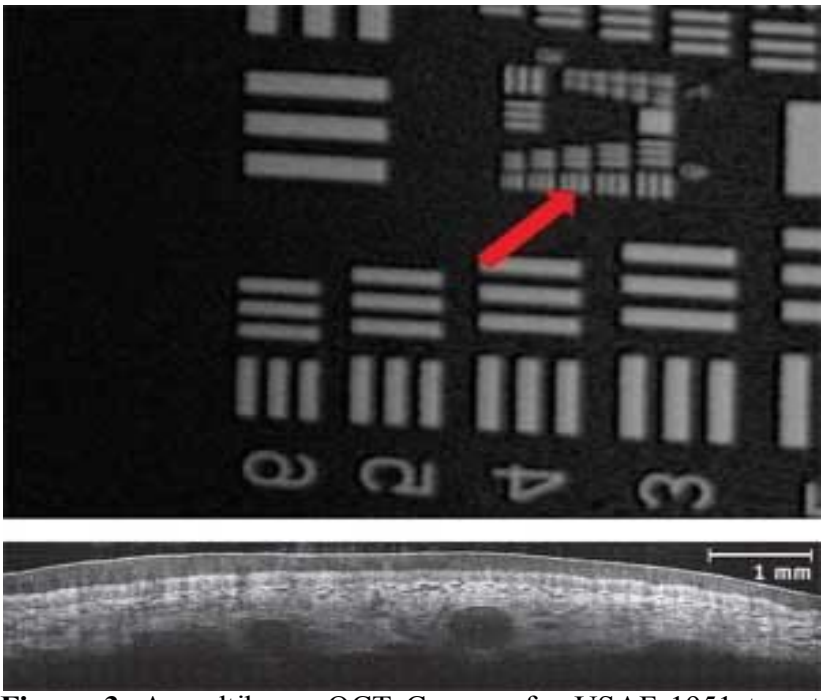

Figure 3. A multibeam OCT C-scan of a USAF 1951 target (top) shows the 90.5-line-pairs-per-mm element resolved clearly (each bar is 5.5 μm wide). In vivo multibeam OCT image of skin (bottom), clearly shows the keratinized layer, epidermis, dermis, capillary networks, and the top of large blood vessels.

A thorough surveillance program would be unacceptably painful, stressful, and damaging to the patient's oral tissues, with biopsies impacting both aesthetic and functional structures (multiple biopsies can cause fibrosis). OCT, with its ability to precisely monitor changes in tissue architecture, could regularly and noninvasively alert the clinical team to any changes needing further attention (for example, a more senior opinion or a surgical biopsy).

Standard diagnosis and treatment

A patient suspected of oral cancer today is typically referred to a specialist clinic by a doctor or dentist who notices initial symptoms such as nonhealing red (erythroplakia), white (leukoplakia) or mixed (speckled erythroplakia) lesions. The first job of the clinical specialist is to try to eliminate the worried well patients from those who are of clinical concern.

A patient judged to be of clinical concern must undergo surgical biopsy, and will have to return to the clinic one to two weeks later to receive the results. If the diagnosis shows oral dysplasia/cancer, further treatment and/or follow-up will be advised. The patient will typically fall into one of three groups.

Figure 4. This prototype four-beam fiber-optic probe with 10 µm lateral resolution is the result of a partnership between Michelson Diagnostics and UHN Toronto.

If the patient's pathology is benign or mildly dysplastic, he/she will not be treated, but will be recalled to the clinic for monitoring every few months. This process will last for years and can involve further painful and destructive biopsies.

If the patient has a moderate or severe dysplasia or a combination (for example, mild to moderate, moderate to severe), he/she will require immediate treatment. The lesion will be treated using a variety of methods, which may include surgical excision, CO_2 laser excision, ablation, or photodynamic therapy (PDT). Once the treatment has been completed, these patients will also be put into a monitoring cycle, attending the clinic every month initially, then every three to six months. The clinical specialist will give advice on risk factors and self-examination. Most of the patients in this group end up being reviewed annually for life; surgical biopsy may be acquired many times.

A final group will be found to have invasive cancer and require a more complex treatment process, which is, frankly, beyond the scope of this article.

Where OCT adds most value

Histopathology is severely lacking in its ability to predict or observe progression, and it provides only a snapshot of a part of the lesion, destroying the tissue and the pathology in the process. Clearly, there is a pressing need for a tool that allows accurate monitoring of oral tissue lesions for the first two groups of patients. OCT is noninvasive, nondestructive, can be used to systematically scan the whole lesion, and is able to quantify tissue architecture in terms of depth and size. It is ideal for monitoring change in patients in the first two groups. Even for patients in the third group, OCT can be of major benefit.

A recent study carried out at the National Medical Laser Centre, University College London and the Head and Neck Unit, University College Hospital (England), compared the potential of the multibeam Michelson Diagnostics EX1301 OCT microscope with histopathology.5 The comparison involved 24 suspicious oral lesions

(from 19 patients) that were excised and scanned. The study's key conclusions were that OCT can serve effectively as an adjunct to clinical examination. The OCT scanner can be used by the examining clinical specialist to assess the need for surgical biopsy, in vivo and in real time. The clinical specialist can examine the OCT image for worrying signs including thinning and thickening of the keratin layer, thinning (atrophy) and thickening (acanthosis) of the epithelial layer, thickening (breach) of the basement membrane, and thickening (corium) of the submucosal layers, plus tumor cell aggregation (crowding) and pattern of invasion.

The study provides the basis for recognizing four major initial opportunities for multibeam OCT to assist in the clinical pathway.

During the initial clinical (visual) exam, multibeam OCT can be used to help exclude the worried well from the clinical process as quickly and safely as possible, by providing more information than is currently available to the clinician from visual examination.

During follow-ups, multibeam OCT can enable quantitative analysis of disease progression. The ability of OCT to record the thickness, architectural changes of specific tissue layers, and breach of the basement membrane is the key to allowing accurate measurement of progression.

Multibeam OCT can provide out-patient assessment of precancerous (dysplastic) oral lesions. Initially this is likely to be for localizing and guiding biopsy sites for nonhomogenous large lesions. This capability has the dual benefit of reducing the flow of healthy tissue into the histopathology process, and ensuring that the most relevant samples are taken quickly and analyzed quickly.

During treatment, to image tissue structure changes due to cancer, to enable detection of early-stage cancers, avoiding major ablative surgery and chemoradiation. It is possible that OCT could reduce oral cancer deaths.

A powerful and flexible imaging tool, multibeam OCT overcomes resolution limitations of FD-OCT. with the ability to provide more detailed imaging of tissue architecture and pathologies and better contrast, it has significant near-term potential to address such pressing clinical needs as early detection of oral cancer.

References

1. N. Tanno, T. Ichikawa & A. Saeki (1990). "Lightwave Reflection Measurement," Patent JP2010042
2. D. Huang et al., (1991) *Science 254*(5035), 1178 (1991).
3. http://en.wikipedia.org/wiki/michelson_interferometer
4. A.F. Fercher, C.K. Hitzenberger, G. Kamp and S.Y. El-Zaiat *Optics Communications* 117(1) 43 (1995).
5. A.F. Fercher, W. Drexler, C.K. Hitzenberger & G. Kamp (1994) "Measurement of optical distances by optical spectrum modulation" Ed. A.F. Fercher et al. Vol. 2083, 263. Presented at Microscopy, Holography, and Interferometry in Biomedicine, SPIE, Budapest, Hungary (1994).
6. W. Jerjes et al., *British J. of Oral & Maxillofacial Surgery,* In Press.

to the Department of Oral and Maxillofacial Surgery, University College London Hospitals. Management included conservative, intermaxillary fixation and open reduction and internal fixation. In all, 50 males and 18 females (age range 16–54 years) evaluated in this study: 33 had unilateral condylar fractures, while the remainder also had another mandibular fracture. Fourty-five of the patients had allegedly been assaulted. Open reduction and internal fixation of the mandibular condyle seems to carry low morbidity and may be of considerable functional benefit to the patient.

doi:10.1016/j.bjoms.2011.03.127

P120

Septic thrombosis of the cavernous sinus: systematic review

W. Jerjes, Z. Hamdoon*, S. Abbas, Z. Algamal

UCL Department of Surgery, University College London Medical School, London, UK

Background: Septic thrombosis of the cavernous sinus is a rare condition that may lead to significant morbidity and mortality if not diagnosed and treated urgently. Numerous risk factors have been reported but the evidence and strength of association is variable. We aimed to identify those risk factors with strong levels of evidence.

Methods: A systematic review identified 18 reports of cases of septic thrombosis of the cavernous sinus. Fixed-effects meta-analyses were conducted for each factor to combine odds ratio (OR) and/or relative risk (RR) outcomes across studies by study design. Overall raw point estimates of each risk factor and associated 95% confidence intervals (CI) were calculated.

Results: Poor dental hygiene and sphenoid sinusitis showed strong and consistent associations with this pathology. Also, the infection may spread from facial regions via the facial venous plexus. The primary source of sepsis may be a distant focus with septicemia preceding thrombosis.

Conclusion: Early recognition and management with broad spectrum intravenous antibiotics is essential for full recovery.

doi:10.1016/j.bjoms.2011.03.128

P121

Percutaneous dilational tracheostomy and open surgical tracheostomy: systematic review

W. Jerjes*, Z. Hamdoon, S. Abbas, Z. Algamal

UCL Department of Surgery, University College London Medical School, London, UK

Background: Tracheostomy is a common surgical procedure, and is increasingly performed in the intensive care units as well as operating rooms. Tracheostomy tubes are placed for a variety of reasons, including upper-airway obstruction, failure to wean from mechanical ventilation, inability to protect the airway due to impaired mental status and inability to manage excessive secretions.

Methods: The authors conducted a systematic review and meta-analysis of studies comparing percutaneous dilational tracheostomy and open surgical tracheostomy. We outlined the potential acute and chronic complications of tracheostomy and their management, and we reviewed the different tracheostomy tubes, their indications and when to remove them.

Results and conclusion: The percutaneous method has a comparable, safety profile and lower cost compared with the open surgical approach. The surgical tracheostomy approach is preferred in oral and maxillofacial and ENT procedures. Studies comparing early versus late tracheostomy suggest morbidity benefits that include less nosocomial pneumonia, shorter mechanical ventilation and shorter hospital stay.

Complications include tracheal stenosis, bleeding, infection, aspiration pneumonia, and fistula formation (to either the esophagus or the innominate artery). Final removal of the tracheostomy tube is an important step in the recovery from chronic critical illness and can usually be done once the indication for the tube placement has resolved. There is currently no higher evidence-based study to recommend MDTs being involved in tacheostomy care.

doi:10.1016/j.bjoms.2011.03.129

P122

Optical diagnostics: an update on the most commonly applied techniques in the head and neck

W. Jerjes*, Z. Hamdoon

UCL Department of Surgery, University College London Medical School, London, UK

Introduction: While histopathology remains the gold standard for tissue diagnosis, several new diagnostic techniques are being developed that rely on physical and biochemical changes that precede and mirror malignant change within tissue. The technique involves the use of novel optical techniques which have an advantage of being simple non-invasive methods of tissue interrogation.

Optical diagnostics "biopsy" involves the use of light, of varying wavelength, to examine suspect tissue. Optical biopsy aims to investigate areas of pathology including: hyperkeratosis, inflammation, dysplasia, carcinoma in situ and neoplasia.

Most commonly used in vitro/immediate ex vivo modalities, include elastic scattering spectroscopy, deferential path-length spectroscopy, near infrared spectroscopy, Raman spectroscopy, confocal spectroscopy, fluorescence imaging, microendoscopy, and optical coherence tomography.

Method: The clinical application of these modalities in the head and neck, the pro and contra of optical diagnos-

tics and future combinations of optical modalities are being discussed.

Conclusion: Optical diagnosis of the head and neck is a rapidly developing area of clinical research that can be readily translated to inform patient treatment and overall quality of life. Much still needs to be achieved and granting organisations are directed to pay attention to this area where relatively small investments may lead to enormous dividends in terms of improvements in treatments throughout the fields of medicine and surgery.

doi:10.1016/j.bjoms.2011.03.130

P123

Endoscopic repair of orbital floor fractures: systematic review

W. Jerjes*, Z. Hamdoon, S. Abbas, Z. Algamal

UCL Department of Surgery, University College London Medical School, London, UK

Background: Recent studies have suggested that no high quality evidence is available in relation to endoscopic repair of orbital floor fractures and no conclusions could be reached about its effectiveness. The purpose of this systematic review was to evaluate the successes and challenges of endoscopic orbital floor fracture repairs.

Methods: The PubMed and EMBASE databases were used to perform a systematic review of the English literature. Our inclusion criteria were fractures due to trauma, patients greater than 18 years of age, more than 15 patients in the study or subgroup of interest, at least 18 months follow-up, at least one relevant functional outcome score, and quality outcome score of at least 5/10. Studies that did not meet these criteria were excluded.

Results and conclusion: Repairs of smaller injuries confined entirely to the medial floor were readily accomplished. Endoscopic repair became very difficult and often not possible when a large amount of soft tissue was herniated through the floor defect. Duration of follow-up was short for most studies, but no adverse trends in outcomes were identified. The technical challenge of working from below with an endoscope tends to increase the difficulty of many repairs without improving results.

doi:10.1016/j.bjoms.2011.03.131

P124

Temporomandibular joint dysfunction in orthognathic surgery: systematic review

W. Jerjes*, Z. Hamdoon, S. Abbas, Z. Algamal

UCL Department of Surgery, University College London Medical School, London, UK

Purpose: There are various opinions concerning TMJ dysfunction in orthognathic surgery. The aim of the present study was to conduct a systematic review of the published data on this controversial area. Orthognathic surgical interventions included mandibular ramus osteotomy and bilateral saggital split osteotomy. We have evaluated TMJ disorders changes before and after orthognathic surgery, and assessed the risk of developing new symptoms in asymptomatic patients.

Materials and methods: Selected reports from the PubMed and Embase databases for studies conducted from 1980 to 2008 were evaluated. Of the 88 reports examined and evaluated, 11 were included in the critical analysis conducted as a part of the present systematic review.

Results and conclusion: TMJ symptoms were significantly reduced after treatment for patients with pre-operative symptoms. Pain levels can be reduced by orthognathic treatment; a percentage of dysgnathic patients who were pre-operatively asymptomatic can develop TMJ disorders after surgery but this risk is low.

doi:10.1016/j.bjoms.2011.03.132

P125

The management of periorbital skin tumours using surface illumination photodynamic therapy: case series

W. Jerjes*, Z. Hamdoon, C. Hopper

UCL Department of Surgery, University College London Medical School, London, UK

Objective: The purpose of this prospective case series was to assess the outcome following photodynamic therapy (PDT) in patients with basal cell carcinomas (BCCs) and squamous cell carcinomas (SCCs) involving the periorbital skin.

Materials and methods: Twenty-two patients were referred to the UCLH Head and Neck Centre for treatment of SCCs and BCCs of the periorbital skin. After multidisciplinary discussion, all patients underwent surface illumination photodynamic therapy under local anaesthesia, using 0.05 mg/kg mTHPC as the photosensitising agent. Following treatment, patients were followed-up for a mean of 12 months.

Results: Clinical assessment showed that 20 patients had "excellent response" to the treatment (no residual disease, no recurrence and good cosmetic outcome). The other two patients were classified as having "good response" to the treatment (no residual disease, no recurrence and hypopigmentation of the treated area).

Head & Neck Oncology

BioMed Central

Poster presentation

Open Access

Optical coherence tomography in the diagnosis of oral dysplasia

Syeda Amna Azim, Tina Kumar, Tahwinder Upile, Zaid Hamdoon and Colin Hopper*

Address: UCLH Head and Neck Centre, London, UK
* Corresponding author

from 1st Scientific Meeting of the Head and Neck Optical Diagnostics Society
London, UK. 14 March 2009

Published: 28 July 2009

Head & Neck Oncology 2009, **1**(Suppl 1):P2 doi:10.1186/1758-3284-1-S1-P2

This abstract is available from: http://www.headandneckoncology.org/content/1/S1/P2

© 2009 Azim et al; licensee BioMed Central Ltd.

To date histopathological examination has been considered the gold standard for diagnosing early dysplastic to late cancerous lesions. The prime concern for early detection of the cancer and its precursors in patients is to ensure the appropriate treatment in response to disease progression and also to improve the survival and prognosis. The time taken for conventional invasive histopathological analysis is about 1–2 weeks, whereas the spread of the disease may require diagnosis in real time. Recently new optical non invasive methods has had been introduced to acquire biopsies through different modalities through which diseased tissues can be distinguished from healthy tissues in real time. Optical diagnosis techniques have proved to be a reliable method that can be used to obtain instant diagnosis of soft and recently hard tissue pathologies. During the past few decades most of the experimental spectroscopy work has been performed in head and neck malignancy using Fluorescence spectroscopy, Raman spectroscopy, Elastic scattering spectroscopy, Micro-endoscopy and Optical coherence tomography. All these modalities have shown a marked increase in the sensitivity and specificity when compared to both clinical and histopathological analysis with promising results. Optical coherence tomography is a non invasive, interferometric, topographic imaging modality which allows the millimetre penetration with millimetre-scale axial and lateral resolution. Optical coherence tomography findings when compared with the histopathological results of suspected oral lesions confirm the feasibility of optical coherence tomography to detect the architectural changes in pathological tissues.

46

Deaths following chemotherapy—lessons to be learnt

Ian C. Martin*, Neil Smith, Heather Cooper

National Confidential Enquiry into Patient Outcome and Death (NCEPOD), United Kingdom

This study examines the process of care for 1044 patients who died within 30 days of receiving chemotherapy. The majority of patients received chemotherapy for palliation of disease, but there was a high level of toxicity, and in many cases, decisions were not being taken within the MDT, and information and consent were inadequate. Less than 50% of cases were judged by specialist advisors to have received good care. Seven patients received chemotherapy for head and neck cancers, and none of these were judged to have received good care. Recommendations for improving the quality of care will be presented.

doi:10.1016/j.bjoms.2009.06.073

47

Incidence of wound dehiscence and lower lid ectropion after infraorbital access incision closure with Indermil following naso-orbital and orbito-malar trauma. Prospective study of 30 consecutive patients

Gillian Greenhill*, Barry O'Regan, S. Bhopal

Maxillo-Facial Unit, Queen Margaret Hospital, Dunfermline, Fife, Scotland

Introduction: Standard wound closure using conventional suture techniques is the established method for access skin incision closure following skeletal orbital trauma. The completion of a prospective study using the technique for elective parotid surgery encouraged us to expand the application of this method to post-traumatic orbital surgery access incision closure.[1] Some concern exists in the literature regarding a possible higher rate of wound dehiscence associated with the use of tissue adhesives. We set up this study to explore this association further.

Aim: To study the incidence of post-operative wound dehiscence and lower lid ectropion following Indermil use in infra-orbital/blepharoplasty access incision wound closure.

Method: A prospective study of 30 consecutive patients was undertaken over 2 years. Cutaneous closure of each infra-orbital incision was achieved using Indermil. A data collection form was completed for each patient. The collected data included details of injury, fracture type, treatment and routine complications. Patient satisfaction with postoperative cosmesis was included. All patients were followed up at 1 week, 1 month and 3 months.

Results: M/F ratio was 10/1 with an age range of 19–58 years. The range of surgical procedures included isolated orbital floor, naso-orbital and orbito-malar fractures. No patient developed a wound dehiscence or lower lid ectropion.

Conclusion: The technique has not been associated with any wound dehiscence or lower lid ectropion. Indermil can be used safely and effectively to close post-traumatic infra-orbital access incisions. The technique and its advantages over conventional suture closure methods are described.

Reference

1. Greenhill GA, O'Regan B. Incidence of hypertrophic and keloid scars after N-butyl 2-cyanoacrylate tissue adhesive had been used to close parotidectomy wounds: a prospective study of 100 consecutive patients. *BJOMS* 2009;**47**:290–3.

doi:10.1016/j.bjoms.2009.06.074

48

Immediate ex vivo optical coherence tomography of suspicious oral lesions

Zaid Hamdoon, Waseem Jerjes, Tahwinder Upile, Gordon McKenzie, Christian S. Betz, Ann Sandison, Amrita Jay, Colin Hopper

UCLH Head & Neck Centre, London, United Kingdom

Introduction: Optical biopsy systems have been investigated for various clinical applications; however, the main interest remains in the diagnosis and monitoring of premalignant and malignant conditions. In this study, we compared findings of optical coherence tomography (OCT) with histopathology results of suspicious oral lesions to assess the feasibility of OCT in identifying pathological tissue.

Materials and methods: Suspicious oral lesions from 70 patients were subjected to immediate ex vivo OCT. Five OCT parameters were assessed (keratin, epithelial, sub-epithelial layers changes, basement membrane and micro-anatomical structures). Two clinicians and two pathologists, who were blind to clinical and histopathological diagnosis, examined the OCT images autonomously, provided deferential diagnosis, the most probable diagnosis and provided judgment on the need for surgical biopsy. Inter-, intra-observer differences, sensitivity and specificity were calculated.

Results: Basic histological tissue structures were identified on the mainstream of the OCT images. Recognition of the basement membrane was achieved in the majority of the lesions. Identification of changes in the parameters ruled areas of architectural changes. There was a high inter- and intra-observer agreement among the two clinicians and two pathologists, who recommended a surgical biopsy when examined all the histologically proven dysplasia and cancer OCT images. Sensitivity and specificity were calculated and proved to be encouraging.

Conclusion: At this phase, OCT can definitely aide clinical examination and monitoring and can be invaluable tool for inexperienced clinicians.

The in vivo, real time tissue perfusion, system images are expected to provide better demarcation between tissue layers and better description of pathological lesions.

doi:10.1016/j.bjoms.2009.06.075

49

The management of the penetrating ocular injury

Simon Holmes*, Andrew Coombes, Vicky Cohen, Chris Bridle, Sonia Alam

Barts and The London NHS Trust, United Kingdom

We present our experience of 25 traumatically injured globes over a period of four years.

The mechanism of injury was bomb blast (3 cases), gunshot (2 cases), glass (15 cases), knife (2), dog assault (1 case), military RPG (1 case) and firework injury (1 case).

Management was dependent upon type of globe injury, severity of other injuries, and degree of orbital injury.

All wounds were managed operatively, and affected eyes were primarily closed (15 cases), eviscerated (7 cases) or enucleated (3 cases).

Indications for enucleation included complex lacerations or large ocular tissue loss both making closure impossible.

Evisceration or enucleation was performed when closure was judged inadequate, or loss of contents was severe. Removal of all of the retina was mandatory to avoid loss of immunological privilege. Insertion of an implant was deferred to a secondary stage. Insertion of a conformer was performed wherever possible to maintain lid shape.

Repair of orbital wall defects was carried out within 18 days post injury in the acute phase or after 6 months in the secondary phase.

Secondary reconstructions involved orbital wall reconstruction, insertion of implants (medpore), and ocular prosthesis, together with optimisation of orbital soft tissues. There were no cases of sympathetic ophthalmitis

Conclusion: Recovery of normal visual acquity was low at 3 cases. Aesthetic results were generally good. Retention of the globe remnant allowed limited ocular movement allowing for improved cosmesis.

doi:10.1016/j.bjoms.2009.06.076

50

Randomised controlled trial of Lugol's iodine in head and neck cancer surgery (LIHNCS trial)

James Anthony McCaul*, D.N. Sutton, J.C. Devine, D. Gouldesbrough, G. Bryson, D. McLelland, J.D. McMahon

Bradford Teaching Hospitals NHS Foundation Trust, United Kingdom

Introduction: Dysplasia at surgical margins is a predictor of local recurrence in surgical treatment of oral and oropharyngeal cancer. Normal cells store increasing glycogen from basal layer to surface. Dysplastic cells do not and this metabolic difference can be exploited to identify epithelial dysplasia by staining with Lugol's iodine. We have previously shown that Lugol's Iodine reduced margins positive for dysplasia, carcinoma-in situ, and invasive carcinoma in patients undergoing primary SCCHN surgery (32% [control] to 4% [intervention]). We report interim data from a multicentre randomised controlled trial evaluating this technique.

Methods: Patients are randomised to control or Lugol's iodine staining using a web based method stratified by centre and surgeon. Controls undergo removal of mucosal SCC with a 1 cm margin and adjacent leukoplakia. Intervention subjects have the same surgery with Lugol's iodine used to identify dyplasia at margins and remove this where feasible. The RCPath minimum dataset is analysed for the presence of dysplasia, Ca-in situ, or invasive SCC at mucosal margins. After resection and before formalin fixation specimens have carbocisteine and Lugol's iodine applied to ensure histopathologist blinding. Subjects are followed up for five years.

Results: We present interim data from our trial. Recruitment is on target to achieve 164 patients in multiple centres within the study period. At time of writing 33 patients have been recruited. In the control group 16.7% had margin dysplasia. Intervention group 0% dysplasia.

Discussion: Lugols iodine may be an effective method for reducing margin dysplasia at resection of SCCHN. This may reduce locoregional recurrence in SCCHN.

doi:10.1016/j.bjoms.2009.06.077

51

Ballistic injuries of the head and neck—managing unconventional injuries

Colin MacIver*, Andrew Monaghan

West of Scotland Regional Maxillofacial Unit, United Kingdom

Background: The conflict in Afghanistan has given Military Maxillofacial surgeons a unique challenge in dealing with ballistic injuries. UK maxillofacial surgeons based at the Role 3 Multinational Medical Unit (MMU) at Kandahar have faced a high intensity of challenging cases providing both resuscitative care and definitive surgery. The recent emergence of global terrorism has meant that these kind of injuries are no longer confined to the battlefield. The principles of dealing with their consequences should be a part of every maxillofacial surgeons armamentarium.

Aim: To highlight how ballistic injuries differ from conventional injuries and the reconstructive problems that they cause.

Methods: A number of index cases will show how patients that have sustained ballistic injuries present with unique challenges in resuscitation, stabilization and reconstruction.

Reference(s)

Berg K, Selbo PK, Prasmickaite L, Tjelle TE, Sandvig K, Moan J, Gaudernack G, Fodstad O, Kjølsrud S, Anholt H, Rodal GH, Rodal SK, Høgset A. Photochemical internalization: a novel technology for delivery of macromolecules into cytosol. Cancer Res 1999 Mar 15; 59(6): 1180–3.

P21

Early outcomes after transoral CO_2 laser resection of oral squamous cell carcinoma: prospective evaluation of outcome

J. Osher, W. Jerjes, T. Upile, Z. Hamdoon, P. Hoonjan, S. Akram, C. Hopper. *UCLH Head and Neck Centre, UK*

Introduction and Aims: The incidence of oral squamous cell carcinoma (OSCC) remains high. Oral carcinomas are the sixth most common cancer in the world. This prospective study evaluated the oncological outcomes following transoral CO_2 laser resection of T1/T2 N0 OSCC. Patients' three-year disease-specific survival and disease-free survival were evaluated, including postoperative complications.

Material and Methods: The patients' data included a range of clinical, operative and histopathological variables related to the status of the surgical margins. Data collection also included recurrence, cause of death, date of death and last clinic review.

Ninety patients participated in this study. Their mean age at the 1st diagnosis of OSCC was 63.5 years. Two-thirds of the patients were Caucasians. Primary sites were mainly identified in the tongue, floor of mouth and buccal mucosa. Pathological analysis revealed that half of the patients had moderately differentiated OSCC.

Results: Tumour clearance was primarily achieved in 73 patients. Follow-up resulted in a 3-year survival of 87.8%. Recurrence was identified in 12% of the patients. The mean age of 1st diagnosis of the recurrence group was 76.4 years. Most common oral sites included the lateral border of tongue and floor of mouth. Recurrence was associated with clinical N-stage disease. The surgical margins in this group were also evaluated.

Conclusions: Squamous cell carcinoma of the oral cavity has a poor overall prognosis with a high tendency to recur at the primary site and extend to involve the cervical lymph nodes. The overall results of this study were comparable with those of other, larger studies.

P22

Photodynamic therapy as the "last hope" palliative modality for patients with tongue base carcinoma

J. Osher, W. Jerjes, T. Upile, Z. Hamdoon, R. Bhandari, P. Hoonjan, S. Akram, C.A. Mosse, S. Morley, C. Hopper. *UCLH Head and Neck Centre, UK*

Introduction: The management of base of tongue carcinoma continues to be a major challenge in head and neck oncology.

Our aim in this prospective study was to evaluate the outcome following ultrasound-guided interstitial photodynamic therapy (US-iPDT) of stage IV tongue base carcinoma. Patients' reports on quality of life with clinical and radiological evaluation were the main end point parameters used to assess the outcome.

Material and Methods: Thirty-three consecutive patients were referred to the UCLH Head and Neck Centre for treatment of advanced tongue base cancer. Two-thirds of the patients had not been offered further treatment. It was decided that the only available option is to offer US-iPDT under general anaesthesia, using mTHPC as the photosensitising agent. Following treatment, patients were followed-up for a mean of 18 months (Min 8, Max 44).

Results: 11/14 patients who presented with breathing problems reported improvement after treatment. Also, 28/33 reported improvement of swallowing. Improvement of speaking was reported by 15/18 patients.

Clinical assessment showed that two-thirds of the patients had "good response" to the treatment and a third reported "moderate response". Radiological assessment comparing imaging 6-week post-PDT to the baseline showed stable pathology with no change in size in 6 patients, minimal response in 7 patients, moderate response in 12 patients and significant response in 5 patients.

Eleven patients died, seven of whom due to locoregional metastasis. Kaplan–Meier survival curve was generated from the survival and follow-up data.

Conclusions: Photodynamic therapy is a successful palliative modality in the treatment of advanced tongue base carcinoma.

P23

Assessment of premalignant/malignant oral lesions using optical coherence tomography

Z. Hamdoon, W. Jerjes, T. Upile, G. McKenzie, A. Jay, C. Hopper. *UCLH Head and Neck Centre, UK*

Introduction and Aims: Optical biopsy systems have been investigated for various clinical applications; however the main interest remains in the diagnosis and monitoring of premalignant and malignant conditions. In this study, we compared findings of optical coherence tomography (OCT) with histopathology results of suspicious oral lesions to assess the feasibility of OCT in identifying pathological tissue.

Material and Methods: Suspicious oral lesions acquired from 120 patients were subjected to immediate ex-vivo Swept-Source Frequency-Domain OCT. Five OCT parameters were assessed (keratin, epithelial, sub-epithelial layers changes, basement membrane and microanatomical structures). Two clinicians and two pathologists, who were blind to clinical and histopathological diagnosis, examined the OCT images autonomously, provided deferential diagnosis, the most probable diagnosis and provided judgment on the need for surgical biopsy. Inter, Intra-observer differences, sensitivity and specificity was calculated.

Results and Statistics: Basic microanatomical tissue structures were identified on the mainstream of the OCT images. Recognition of the basement membrane was achieved in the majority of the lesions. Identification of changes in the parameters ruled areas of architectural changes. There was a high inter and intra-observer agreement among the two clinicians and two pathologists, who recommended a surgical biopsy when examined all the histologically proven dysplasia and cancer OCT images. Sensitivity and specificity were calculated and proved to be encouraging.

Conclusions and Clinical relevance: At this phase, OCT can definitely aide clinical examination and monitoring and can be invaluable tool for inexperienced clinicians.

Acknowledgment: We would like to thank the BAOMS for supporting this research project.

P24

Tumour resection margins subjected to optical coherence tomography

Z. Hamdoon, W. Jerjes, T. Upile, G. McKenzie, A. Jay, C. Hopper. *UCLH Head and Neck Centre, UK*

Introduction and Aims: In the treatment of cancer, the fundamental surgical goal is to remove all local malignant disease and leave no residual malignant cells. Studies have demonstrated the benefit

of achieving negative resection margins in terms of disease free local recurrence and overall survival. The surgical margins for head & neck cancer may vary widely depending on the site of disease.
Optical coherence tomography (OCT) is an imaging modality that uses light to determine cross-sectional anatomy in turbid media such as living tissues. In this study, we used this technology to evaluate resection margins acquired from patients with oral squamous cell cancer (OSCC).
Material and Methods: Twenty-five patients with newly diagnosed T1-T2 OSCC underwent local resection. In the immediate ex-vivo phase, OCT was used to interrogate the surgical margins of these specimens and the results were, then, compared to histopathology. Inter, Intra-observer differences, sensitivity and specificity was calculated.
Results: The junctional epithelium (between positive and negative margins) can be identified by gradual change in epithelial thickness and basement membrane organisation (integrity) from the normal to pathological. Identified changes in tumour positive margins include hyperkeratinisation, breach of the basement membrane and disorganised epithelial structure. Tumour spread pattern could be identified on the majority of the interrogated tissue. Sensitivity and specificity were calculated and proved to be encouraging.
Conclusions: The results from this study are encouraging and suggest the feasibility of using OCT in differentiating between positive and negative surgical margins.
Acknowledgment: We would like to thank the BAOMS for supporting this research project.

P25

CO_2 laser of oral dysplasia: clinicopathological features of recurrence and malignant transformation

W. Jerjes, T. Upile, Z. Hamdoon, C. Hopper. *UCLH Head and Neck Centre, UK*

Introduction and Aims: Recurrence and/or malignant transformation of oral dysplasia have infrequently been observed following laser surgery. It is reported that the rate of recurrence was 7.7–38.1%, while malignant transformation was 2.6–9% following CO_2 laser ablation.
Material and Methods: In this prospective study, a total of 123 oral dysplastic lesions from 77 patients were treated with CO_2 laser. Comparisons with the rate of recurrence, malignant transformation and clinical features, epithelial dysplasia, anatomical location, and treatment procedure were made.
Results and Statistics: The results were cross tabulated and the Chi-squared statistic was used to test for differences in the case-mix. The rate of recurrence had no association with the location or the severity of epithelial dysplasia. The rate of recurrence in laser surgery was approximately 8.1%. Malignant transformation was observed in 8 lesions. They were observed in tongue and floor of mouth.
Conclusions and Clinical relevance: Laser ablation is recommended for oral dysplasia. Management of oral dysplasia prevents not only recurrence and malignant transformation, but also postoperative dysfunction.

P26

Survey of the handling of primary oral and oropharyngeal malignant tumours during their surgical resection – UK OMFS Units

J. Rao, E. Bailey, K. Grimes, M. Patel. *University Hospital of South Manchester, UK*

Introduction and Aim: Reports of intra-operative tumour seeding in the head and neck have been documented. Factors believed to influence this range from, the microscopic cell biology of the tumour, to the macroscopic shedding of tumour to distant sites. Though very small the risk is present and methods to reduce the risk have been adopted. These include the use of irrigants acting against tumour cells, draping of open wounds and the tumour, the change of gloves and instruments.
The aim of the survey was to establish current practice and beliefs amongst UK Consultant OMF Surgeons, regarding the seeding of oral and oropharyngeal tumours.
Materials and Methods: A postal questionnaire was sent to 357 UK Consultant OMF Surgeons to establish current practice in relation to, the order of surgical tracheostomy, use of irrigants, wound and tumour draping, glove and instrument changes and opinion on tumour seeding.
Results: The response rate was 148 (41%), of which 83 (56%) were practicing oncology surgery. A tracheostomy was inserted as a first stage by 69 (83%), with 10 (12%) as a last stage. Irrigants were used by 49 (59%), 62 (75%) draped non-primary wounds; 22 (27%) draping the tumour. A change of gloves was performed by 73 (88%) and instruments by 50 (60%). 55 (66%) of surgeons believed tumour seeding to other sites was feasible.
Conclusion: Although the risk of tumour seeding in the head and neck is small, there appears to be a significant belief it can occur. Precautions to prevent this are being taken mainly in the form of change of gloves and draping wounds.

P27

Complications of percutaneous endoscopic gastrostomy (PEG) and radiological inserted gastrostomy (RIG) in patients with head and neck cancer

P. McAllister, C. MacIver, J. Devine, J. McMahon, C. Wales. *Regional Maxillofacial Unit, Southern General Hospital, Glasgow, UK*

Introduction: Patients with treatment for Head and Neck (H&N) cancer typically require implementation of nutritional support prior to treatment. Traditionally, percutaneous endoscopic gastrostomy (PEG) or radiologically inserted gastrostomy (RIG) have been used to prevent aspiration and supplement nutrition in patients following treatment for head and neck cancer. The aim of this study was to identify complications arising from PEG or RIG insertion in patients with H&N Cancer over a five-year period of 2005–2009 inclusive.
Materials and Methods: This study is a retrospective analysis of PEG/RIG data from the time of gastrostomy insertion until removal due to either adequate oral intake or patient death. Data forms were completed by the nutritional support nurse to whom the referral was made to. Any complications throughout the duration of gastrostomy placement were documented on individual patient audit forms.
Results: In one of the years reviewed (2006), 35 primary feeding tubes (20 PEGs, 15 RIGs) were placed in patients with head and neck cancer. In this study, 6 (17%) experienced "major" complications as classified by Shapiro and Edmundowicz [2] compared with 2.8% for previous studies [1]. In a comparable study [3] on complications of PEG placement in head and neck cancer patients, a similarly high number of patients (22.5%) suffered major complications of gastrostomy insertion.
Conclusion: Insertions of gastrostomy feeding tubes (PEG/RIG) are essential in providing nutritional support for patients with impaired swallowing following treatment of H&N Cancer. There is considerable morbidity and mortality associated PEG/RIG placement and this must be considered to ensure patient selection is always appropriate.

Head & Neck Oncology

BioMed Central

Poster presentation

Open Access

Optical diagnostic techniques in the head and neck

Waseem Jerjes*[1], Tahwinder Upile[1], Zaid Hamdoon[1], Christian S Betz[2] and Colin Hopper[1]

Address: [1]UCLH Head and Neck Centre, London, UK and [2]Department of Otorhinolaryngology, Head & Neck Surgery, Ludwig Maximilian University Munich, Marchioninistr, Munich, Germany

* Corresponding author

from 1st Scientific Meeting of the Head and Neck Optical Diagnostics Society
London, UK. 14 March 2009

Published: 28 July 2009

Head & Neck Oncology 2009, **1**(Suppl 1):P1 doi:10.1186/1758-3284-1-S1-P1

This abstract is available from: http://www.headandneckoncology.org/content/1/S1/P1

© 2009 Jerjes et al; licensee BioMed Central Ltd.

Optical biopsies can be acquired through different modalities; each has it own mechanism of action and requires different modes of data analysis. However, they share the ability of being able to provide a real time, non-invasive and *in situ* optical signature. Most of these techniques have been applied only in clinical trials and are yet to be employed in clinical practice, with the exception of fluorescence spectroscopy. Results from these trials are very promising, and current results indicate the possibility of these techniques being applied in clinical practice in the next few years. This could have a great impact on diagnostics, by reducing the histopathology workload, reducing patient's anxiety, and allowing rapid surgical or adjuvant intervention.

Elastic scattering spectroscopy (ESS) has proved to be a promising method for detecting premalignant and malignant changes in oral tissues, with high sensitivity and specificity. Several head and neck tissues, including lymph nodes and bones, have been interrogated using ESS, which detects changes at the cellular and subcellular level, with very promising results. Fluorescence spectroscopy, unlike ESS, can identify changes through the fluorophores detected in the tissue, and has been found to be very accurate in detecting oral dysplasia. Raman spectroscopy can detect biochemical changes in tissue, but it has limited clinical applications due to its weak signal. The first application of Microendoscopy in the head and neck was described by Upile et al. at University College Hospital, London; resected tumour margins were examined and the results were impressive; however, a fundamental understanding of histopathology is essential for achieving a high sensitivity and specificity.

46

Deaths following chemotherapy—lessons to be learnt

Ian C. Martin*, Neil Smith, Heather Cooper

National Confidential Enquiry into Patient Outcome and Death (NCEPOD), United Kingdom

This study examines the process of care for 1044 patients who died within 30 days of receiving chemotherapy. The majority of patients received chemotherapy for palliation of disease, but there was a high level of toxicity, and in many cases, decisions were not being taken within the MDT, and information and consent were inadequate. Less than 50% of cases were judged by specialist advisors to have received good care. Seven patients received chemotherapy for head and neck cancers, and none of these were judged to have received good care. Recommendations for improving the quality of care will be presented.

doi:10.1016/j.bjoms.2009.06.073

47

Incidence of wound dehiscence and lower lid ectropion after infraorbital access incision closure with Indermil following naso-orbital and orbito-malar trauma. Prospective study of 30 consecutive patients

Gillian Greenhill*, Barry O'Regan, S. Bhopal

Maxillo-Facial Unit, Queen Margaret Hospital, Dunfermline, Fife, Scotland

Introduction: Standard wound closure using conventional suture techniques is the established method for access skin incision closure following skeletal orbital trauma. The completion of a prospective study using the technique for elective parotid surgery encouraged us to expand the application of this method to post-traumatic orbital surgery access incision closure.[1] Some concern exists in the literature regarding a possible higher rate of wound dehiscence associated with the use of tissue adhesives. We set up this study to explore this association further.

Aim: To study the incidence of post-operative wound dehiscence and lower lid ectropion following Indermil use in infra-orbital/blepharoplasty access incision wound closure.

Method: A prospective study of 30 consecutive patients was undertaken over 2 years. Cutaneous closure of each infra-orbital incision was achieved using Indermil. A data collection form was completed for each patient. The collected data included details of injury, fracture type, treatment and routine complications. Patient satisfaction with postoperative cosmesis was included. All patients were followed up at 1 week, 1 month and 3 months.

Results: M/F ratio was 10/1 with an age range of 19–58 years. The range of surgical procedures included isolated orbital floor, naso-orbital and orbito-malar fractures. No patient developed a wound dehiscence or lower lid ectropion.

Conclusion: The technique has not been associated with any wound dehiscence or lower lid ectropion. Indermil can be used safely and effectively to close post-traumatic infra-orbital access incisions. The technique and its advantages over conventional suture closure methods are described.

Reference

1. Greenhill GA, O'Regan B. Incidence of hypertrophic and keloid scars after N-butyl 2-cyanoacrylate tissue adhesive had been used to close parotidectomy wounds: a prospective study of 100 consecutive patients. *BJOMS* 2009;**47**:290–3.

doi:10.1016/j.bjoms.2009.06.074

48

Immediate ex vivo optical coherence tomography of suspicious oral lesions

Zaid Hamdoon, Waseem Jerjes, Tahwinder Upile, Gordon McKenzie, Christian S. Betz, Ann Sandison, Amrita Jay, Colin Hopper

UCLH Head & Neck Centre, London, United Kingdom

Introduction: Optical biopsy systems have been investigated for various clinical applications; however, the main interest remains in the diagnosis and monitoring of premalignant and malignant conditions. In this study, we compared findings of optical coherence tomography (OCT) with histopathology results of suspicious oral lesions to assess the feasibility of OCT in identifying pathological tissue.

Materials and methods: Suspicious oral lesions from 70 patients were subjected to immediate ex vivo OCT. Five OCT parameters were assessed (keratin, epithelial, sub-epithelial layers changes, basement membrane and micro-anatomical structures). Two clinicians and two pathologists, who were blind to clinical and histopathological diagnosis, examined the OCT images autonomously, provided deferential diagnosis, the most probable diagnosis and provided judgment on the need for surgical biopsy. Inter-, intra-observer differences, sensitivity and specificity were calculated.

Results: Basic histological tissue structures were identified on the mainstream of the OCT images. Recognition of the basement membrane was achieved in the majority of the lesions. Identification of changes in the parameters ruled areas of architectural changes. There was a high inter- and intra-observer agreement among the two clinicians and two pathologists, who recommended a surgical biopsy when examined all the histologically proven dysplasia and cancer OCT images. Sensitivity and specificity were calculated and proved to be encouraging.

Conclusion: At this phase, OCT can definitely aide clinical examination and monitoring and can be invaluable tool for inexperienced clinicians.

The in vivo, real time tissue perfusion, system images are expected to provide better demarcation between tissue layers and better description of pathological lesions.

doi:10.1016/j.bjoms.2009.06.075

49

The management of the penetrating ocular injury

Simon Holmes*, Andrew Coombes, Vicky Cohen, Chris Bridle, Sonia Alam

Barts and The London NHS Trust, United Kingdom

We present our experience of 25 traumatically injured globes over a period of four years.

The mechanism of injury was bomb blast (3 cases), gunshot (2 cases), glass (15 cases), knife (2), dog assault (1 case), military RPG (1 case) and firework injury (1 case).

Management was dependent upon type of globe injury, severity of other injuries, and degree of orbital injury.

All wounds were managed operatively, and affected eyes were primarily closed (15 cases), eviscerated (7 cases) or enucleated (3 cases).

Indications for enucleation included complex lacerations or large ocular tissue loss both making closure impossible.

Evisceration or enucleation was performed when closure was judged inadequate, or loss of contents was severe. Removal of all of the retina was mandatory to avoid loss of immunological privilege. Insertion of an implant was deferred to a secondary stage. Insertion of a conformer was performed wherever possible to maintain lid shape.

Repair of orbital wall defects was carried out within 18 days post injury in the acute phase or after 6 months in the secondary phase.

Secondary reconstructions involved orbital wall reconstruction, insertion of implants (medpore), and ocular prosthesis, together with optimisation of orbital soft tissues. There were no cases of sympathetic ophthalmitis

Conclusion: Recovery of normal visual acquity was low at 3 cases. Aesthetic results were generally good. Retention of the globe remnant allowed limited ocular movement allowing for improved cosmesis.

doi:10.1016/j.bjoms.2009.06.076

50

Randomised controlled trial of Lugol's iodine in head and neck cancer surgery (LIHNCS trial)

James Anthony McCaul*, D.N. Sutton, J.C. Devine, D. Gouldesbrough, G. Bryson, D. McLelland, J.D. McMahon

Bradford Teaching Hospitals NHS Foundation Trust, United Kingdom

Introduction: Dysplasia at surgical margins is a predictor of local recurrence in surgical treatment of oral and oropharyngeal cancer. Normal cells store increasing glycogen from basal layer to surface. Dysplastic cells do not and this metabolic difference can be exploited to identify epithelial dysplasia by staining with Lugol's iodine. We have previously shown that Lugol's Iodine reduced margins positive for dysplasia, carcinoma-in situ, and invasive carcinoma in patients undergoing primary SCCHN surgery (32% [control] to 4% [intervention]). We report interim data from a multicentre randomised controlled trial evaluating this technique.

Methods: Patients are randomised to control or Lugol's iodine staining using a web based method stratified by centre and surgeon. Controls undergo removal of mucosal SCC with a 1 cm margin and adjacent leukoplakia. Intervention subjects have the same surgery with Lugol's iodine used to identify dyplasia at margins and remove this where feasible. The RCPath minimum dataset is analysed for the presence of dysplasia, Ca-in situ, or invasive SCC at mucosal margins. After resection and before formalin fixation specimens have carbocisteine and Lugol's iodine applied to ensure histopathologist blinding. Subjects are followed up for five years.

Results: We present interim data from our trial. Recruitment is on target to achieve 164 patients in multiple centres within the study period. At time of writing 33 patients have been recruited. In the control group 16.7% had margin dysplasia. Intervention group 0% dysplasia.

Discussion: Lugols iodine may be an effective method for reducing margin dysplasia at resection of SCCHN. This may reduce locoregional recurrence in SCCHN.

doi:10.1016/j.bjoms.2009.06.077

51

Ballistic injuries of the head and neck—managing unconventional injuries

Colin MacIver*, Andrew Monaghan

West of Scotland Regional Maxillofacial Unit, United Kingdom

Background: The conflict in Afghanistan has given Military Maxillofacial surgeons a unique challenge in dealing with ballistic injuries. UK maxillofacial surgeons based at the Role 3 Multinational Medical Unit (MMU) at Kandahar have faced a high intensity of challenging cases providing both resuscitative care and definitive surgery. The recent emergence of global terrorism has meant that these kind of injuries are no longer confined to the battlefield. The principles of dealing with their consequences should be a part of every maxillofacial surgeons armamentarium.

Aim: To highlight how ballistic injuries differ from conventional injuries and the reconstructive problems that they cause.

Methods: A number of index cases will show how patients that have sustained ballistic injuries present with unique challenges in resuscitation, stabilization and reconstruction.

Head & Neck Oncology

Oral presentation

Open Access

Immediate ex-vivo optical coherence tomography of suspicious oral lesions

Zaid Hamdoon, Waseem Jerjes, Tahwinder Upile, Gordon McKenzie, Christian S Betz, Ann Sandison, Amrita Jay and Colin Hopper*

Address: UCLH Head & Neck Unit, London, UK
* Corresponding author

from 1st Scientific Meeting of the Head and Neck Optical Diagnostics Society
London, UK. 14 March 2009

Published: 28 July 2009

Head & Neck Oncology 2009, **1**(Suppl 1):O16 doi:10.1186/1758-3284-1-S1-O16

This abstract is available from: http://www.headandneckoncology.org/content/1/S1/O16

© 2009 Hamdoon et al; licensee BioMed Central Ltd.

Background

Optical biopsy systems have been investigated for various clinical applications; however the main interest is in the diagnosis of premalignant lesions.

The aim of this study was to compare findings of optical coherence tomography (OCT) with histopathology of various oral lesions to see if this technique could be used as an adjunct or alternative to histopathology in assessing oral dysplasia. The technique is a non-invasive interferometric tomographic imaging modality which allows millimetre penetration with micrometer-scale axial and lateral resolution.

Materials and methods

Suspicious oral lesions, from 87 patients, were excised and subjected to Swept-Source Fourier-Domain OCT. The acquired OCT images were then compared with histopathology images.

Results

Epithelium, basement membrane, lamina properia, microanatomical histological structures and pathological processes were clearly identified. Normal microanatomical structures identified in these tissues included an overlying keratin layer, papillae, ducts, glands, and blood vessels. Regions of pathologic features studied included leukoplakias, and erythroplakias. Areas of architectural changes were clearly visible and correlated well with the histopathological slides to a depth of approximately 1.5 mm.

Conclusion

This study confirms the feasibility of using OCT to identify various histological structures as well as changes that occurs in these tissues. These preliminary results suggest that OCT may be able to identify dysplasia in oral tissues.

Appendices

Moorfields & Whittington Local Research Ethics Committee
South House, Block A
Royal Free Hospital
Pond Street
London
NW3 2QG

Telephone: 020 7794 0552
Facsimile: 020 7794 0714

Mr. Colin Hopper
Senior Lecturer Hon Consultant Maxillofacial Surgeon
University College London
Department of Oral & Maxillofacial Surgery
Mortimer Market
London
WC1E 8AU

21 February 2007

Dear Mr. Hopper

Full title of study: **Prospective, diagnostic study using Fourier-Domain Optical Coherence Tomography for the assessment of pre- and early malignant lesions of the facial skin and the oral cavity as compared to histopathological results**

REC reference number: **07/Q0504/4**

Thank you for your letter of 13 February 2007, responding to the Committee's request for further information on the above research and submitting revised documentation.

The further information was considered at the meeting of the Sub-Committee of the REC held on 20 February 2007. A list of the members who were present at the meeting is attached.

Confirmation of ethical opinion

On behalf of the Committee, I am pleased to confirm a favourable ethical opinion for the above research on the basis described in the application form, protocol and supporting documentation as revised.

However, the Committee would like to comment that under the Risk Section, the word 'neglectable' should be replaced by 'negligible' and in the 'What will happen' section '...a digital photo will be taken *of* the site.'

Ethical review of research sites

The Committee has not yet been notified of the outcome of any site-specific assessment (SSA) for the research site(s) taking part in this study. The favourable opinion does not therefore apply to any site at present. I will write to you again as soon as one Local Research Ethics Committee has notified the outcome of a SSA. In the meantime no study procedures should be initiated at sites requiring SSA.

Conditions of approval

The favourable opinion is given provided that you comply with the conditions set out in the attached document. You are advised to study the conditions carefully.

Approved documents

The final list of documents reviewed and approved by the Committee is as follows:

Document	*Version*	*Date*
Application		03 January 2007
Investigator CV		
Protocol	1	02 January 2007
Covering Letter		
GP/Consultant Information Sheets	2	
Participant Information Sheet	2	09 February 2007
Participant Consent Form	2	
Response to Request for Further Information		13 February 2007

Research governance approval

The study should not commence at any NHS site until the local Principal Investigator has obtained final research governance approval from the R&D Department for the relevant NHS care organisation.

Statement of compliance

The Committee is constituted in accordance with the Governance Arrangements for Research Ethics Committees (July 2001) and complies fully with the Standard Operating Procedures for Research Ethics Committees in the UK.

07/Q0504/4 **Please quote this number on all correspondence**

With the Committee's best wishes for the success of this project

Yours sincerely

Chair

Email: katherine.clark@royalfree.nhs.uk

Enclosures: *List of names and professions of members who were present at the meeting and those who submitted written comments*
Standard approval conditions
Site approval form

Copy to: UCLH NHS Trust - Research and Development Directorate
1st Floor, Maple House
149 Tottenham Court Road
London
W1P 9LL

Rijksuniversiteit Groningen Dierexperimentencommissie

Secretariaat:
A. Deusinglaan 50
9713 AZ Groningen
Tel. (050) 363 2999

Voor informatie:
Dr. J. Prop
Tel. (050) 361 4494

Dhr. S.A.H.J. de Visscher
Mondziekten, Kaakchirurgie & Bijzondere Tandheelkunde
Hanzeplein 1
9713 GZ GRONINGEN

23 mei 2007.

Betreft Dierexperiment: Pilot studie naar de inductie van Plaveiselcel carcinoom (PCC) op de tong van de Wistar rat met 4NQO in drinkwater.
DECnr.: 4767A

Geachte collega,

De Dierexperimentencommissie RuG heeft uw bovengenoemde aanvraag besproken in overleg met de proefdierdeskundige, daarbij is rekening gehouden met uw antwoord op vragen.

Het oordeel van de DEC-RuG is **positief** met inachtneming van de onderstaande **voorwaarde.**

- Bij dit onderzoek moet het welzijn van de ratten goed in de gaten worden gehouden en de humane eindpunten consequent worden gehanteerd. Daarbij komt de maximale grootte van de tumor van 10% van het lichaamsgewicht wel overeen met de *Code of practice*, maar dat lijkt bij locatie op de tong te extreem: met een tumor van meer dan 25 gram kan het dier niet leven. U zult de proefdierdeskundige geregeld op de hoogte moeten houden van het beloop van de experimenten.

Uw DEC-nummer is:	**4767A**
Toegewezen diersoort en aantal:	**Rat niet transgeen 12**
De toewijzing geldt tot:	**01-07-2008**
Doel van de proef:	**Wetenschappelijke vraag m.b.t.: kanker bij mensen #30** (voor toelichting zie hieronder)

Wij vragen uw aandacht voor de volgende punten:

- Deze goedkeuring is gebaseerd op de door u verstrekte informatie bij de aanvraag.
- Indien het onderzoek wijzigingen in protocol of proefopzet nodig maakt, dient u hiervoor toestemming van de DEC aan te vragen.

Wij wensen u succes met uw onderzoek.

Met vriendelijke groet,

Dr. Jochum Prop
secretaris DEC-RuG

Institute of Biology

Incorporated by Royal Charter

This is to certify that

Zaid Ghanem Hamdoon

has been assessed as having satisfactorily completed accredited training for personnel working under the Animals (Scientific Procedures) Act 1986

Modules: 1,2,3 & 4 (General Principles) ***

Species: rat, mouse, rabbit, guinea-pig, hamster ***

Training organised by: Biological Services, University College London

Certificate Number: UCL/08/142

Date: 08-10 July 2008

Course Organiser

For the Institute of Biology

This is <u>not</u> a licence to perform procedures under the Animals (Scientific Procedures) Act 1986

University College London Hospitals NHS
NHS Foundation Trust

Appendix A: Patient consent form

Centre Number:
Patient Identification Number for this study:

UCLH Project ID number:
Form version: 2

RESEARCH PARTICIPANT CONSENT FORM

Title of project: OCT for early tumour diagnosis in the head & neck region

Name of Principal investigator: Mr. Colin Hopper (Consultant Maxillofacial Surgeon)

Please initial box

1. I confirm that I have read and understood the Research Participant Information Sheet dated 09/02/2007 (Version 2) for the above study. I have had the opportunity to consider the information, ask questions and have had these answered satisfactorily. ☐

2. I understand that my participation is voluntary and that I am free to withdraw at any time without giving any reason, without my medical care or legal rights being affected. ☐

3. I understand that relevant sections of my medical notes and data collected during the study may be looked at by individuals from Michelson Diagnostics Limited, from regulatory authorities or from the NHS Trust, where it is relevant to my taking part in this research. I give permission for these individuals to have access to my records. ☐

4. I agree to my GP being informed of my participation in the study. ☐

5. I agree to take part in the above study. ☐

Continued on next page/
1 form for Patient;
1 to be kept as part of the study documentation,

1 to be kept with hospital notes

Centre Number:
Patient Identification Number for this study:

UCLH Project ID number:
Form version: 2

RESEARCH PARTICIPANT CONSENT FORM

Title of project: OCT for early tumour diagnosis in the head & neck region

Name of Principal investigator: Colin Hopper (Consultant Maxillofacial Surgeon)

Name of patient	Date	Signature
Name of Person taking consent (if different from researcher)	Date	Signature
Researcher (to be contacted if there are any problems)	Date	Signature

Comments or concerns during the study

If you have any comments or concerns you may discuss these with the investigator. If you wish to go further and complain about any aspect of the way you have been approached or treated during the course of the study, you should write or get in touch with the Complaints Manager, UCL hospitals. Please quote the UCLH project number at the top this consent form.

1 form for Patient;
1 to be kept as part of the study documentation,
1 to be kept with hospital notes

UCL HOSPITALS

UCL Hospitals is an NHS Trust incorporating the Eastman Dental Hospital, Elizabeth Garrett Anderson & Obstetric Hospital, The Heart Hospital, Hospital for Tropical Diseases, The Middlesex Hospital, National Hospital for Neurology & Neurosurgery, The Royal London Homoeopathic Hospital and University College Hospital.

University College London Hospitals NHS
NHS Foundation Trust

Appendix C: letter to GP

Maxillofacial Unit
Mortimer Market
London
WCIE 6AU

Telephone: 020 7380 9862/59
Fax: 020 7380 9855
Appointments: 020 7380 9856/57
E-mail: mb.maxfax@uclh.org

Name of GP

Address 1
Address 2
Address 3

Date

Dear Mr / Mrs.

Name of Patient, Date of Birth
Address of Patient

OCT FOR EARLY TUMOUR DIAGNOSIS IN THE HEAD & NECK REGION

We would hereby like to inform you that the above patient will, in addition to the routine diagnostic workup for the suspicious lesion of her / his face or oral cavity, take part in a diagnostic study to assess the feasibility of Optical Coherence Tomography (OCT) for non-invasively determining the histopathological features of precancerous or early malignant epithelial lesions.

There is solid evidence that an early detection and treatment of head and neck cancer will dramatically increase the survival of the patients and reduce the socio-economical damage this disease inflicts on society. At present, screening for this kind of cancer is done by visual inspection followed by tissue biopsy, whereas common imaging techniques (ultrasound, CT, MRI) are not sensitive enough for detecting these early changes. This is an expensive, time- and labour-intensive procedure. At the same time, single biopsies do not always result in the correct diagnosis.

The present project aims to investigate the potential of OCT for differentiating between pre- and early malignant lesions of the head and neck region and for determining the three-dimensional extents (3D-mapping) of early malignant head and neck cancers. OCT has recently advanced to become a prominent biomedical tissue imaging technique and is particularly suited for tissue imaging requiring micrometer resolution and millimetre penetration depth.

In this *ex vivo* diagnostic study on initially 50 patients, routinely taken tissue biopsies from clinically diagnosed precancerous head and neck lesions will be scanned using OCT before being sent off for regular histopathological diagnosis. The acquired images will then be assessed concerning important histopathological features and subsequently compared to the results from regular H&E stained sections. No measurements will be performed on the patients themselves. Please also be assured that no additional tissue biopsies will be taken within the course of this study.

Yours sincerely,

Mr Colin Hopper FRCS (Ed), FDSRCS, MBBS (Lond), BDS (Lond), LRCP, MRCS
Senior Lecturer/Consultant Maxillofacial Surgeon, UCLH
Head of Academic Surgery Unit at Eastman Dental Institute for Oral Health Care Sciences
Senior Research Fellow at the National Medical Laser Centre, UCLH

UCL HOSPITALS

UCL Hospitals is an NHS Trust incorporating the Eastman Dental Hospital, Elizabeth Garrett Anderson & Obstetric Hospital, The Heart Hospital, Hospital for Tropical Diseases, The Middlesex Hospital, National Hospital for Neurology & Neurosurgery, The Royal London Homoeopathic Hospital and University College Hospital.

Appendix D: PATIENT INFORMATION SHEET

Version: 2
Date: 09/02/2007
Project ID:

PATIENT INFORMATION SHEET

OCT FOR EARLY TUMOUR DIAGNOSIS IN THE HEAD & NECK REGION

We would like to invite you to take part in a research study. Before you decide you need to understand why the research is being done and what it would involve for you. Please take time to read the following information carefully. Talk to others about the study if you wish.
The Patient Information Sheet consists of two parts. **Part 1** tells you the purpose of this study and what will happen to you if you take part. **Part 2** gives you more detailed information about the conduct of the study.
Ask us if there is anything that is not clear or if you would like more information. Take time to decide whether or not you wish to take part.

Part 1 of the Patient Information Sheet

What is the purpose of the study?
In the present study, we are trying to evaluate a new imaging method called "Optical Coherence Tomography" to establish a tissue diagnosis by optically scanning tissue biopsies. If successful, the equipment might later be used routinely for examining skin lesions in a completely "bloodless manner", i.e. without the need to take actual tissue biopsies.

Why have I been invited?
We would like to include you into this study as you have been diagnosed with a skin condition in the head and neck field that requires a tissue biopsy to be taken in order to establish a final diagnosis. Scanning biopsies with the Optical Coherence Tomography equipment (before sending them off for routine pathological diagnosing) is the first stage of evaluating this method for routine clinical use.

Do I have to take part?
It is up to you to decide. We will describe the study and go through this information sheet, which we will then give to you. We will then ask you to sign a consent form to show you have agreed to take part. You are free to withdraw at any time, without giving a reason. This would not affect the standard of care you receive.

What will happen to me if I take part?

Participation in the study would be restricted to the same visit that your routine tissue biopsy is taken and would involve the following:
1) Before the tissue biopsy is taken, a digital photo will be taken of the site of the lesion.
2) Once the tissue biopsy is taken, the tissue sample will be scanned by Optical Coherence Tomography before being sent off to the Pathology Laboratory for regular processing and diagnosing. The regular diagnostic process will not be hindered by this and no additional biopsies than those required for routine diagnosis will be taken.
Please be assured that if you take part in the study, no normal diagnostic or therapeutic procedures will be withheld from you.

Expenses and payments
For this study, we can unfortunately not offer any expenses to the participants.

What will I have to do?
Apart from an approximately additional 5 minutes for your visit (for taking the picture of the lesion), there is no active involvement of the patient in the study.

What is the imaging technique that is being tested?
Optical Coherence Tomography is an optical method for the imaging of tissue. The term "optical" refers to the fact that the system works with low intensity light only (not ultrasound, ionising radiation,…). The most important difference to other imaging methods such as Ultrasound, Magnetic Resonance Imaging or Computed Tomography is that Optical Coherence Tomography works with very small tissue volumes, but at a very high resolution.

What are the alternatives for diagnosis or treatment?
In this study, you will get the normal, state-of-the-art diagnostic workup for the condition you have been diagnosed with. The optical scanning is simply performed "in addition" to this.

What are the possible disadvantages and risks of taking part?
As you won't be withheld any procedures considered normal standard of care, taking part in the study should in no way be disadvantageous for you. The scanning is performed on tissue samples; therefore, the risk of taking part in the study should be negligible.

What are the possible benefits of taking part?
Even though this study was not designed to benefit you directly, your participation will hopefully be helpful for future patients with similar conditions. We will, however, inform you about your individual results of the examinations if you wish so.

What if there is a problem?
Any complaint about the way you have been dealt with during the study or any possible harm you might suffer will be addressed. The detailed information on this is given in Part 2.

Will my taking part in the study be kept confidential?
Yes. We will follow ethical and legal practice and all information about you will be handled in confidence. The details are included in Part 2.

Part 2 of the Patient Information Sheet

What if relevant new information becomes available?
As your active participation in this study is restricted to one visit only, the results from this study or other new information on the imaging technique investigated will not affect your individual further diagnostic workup or treatment.

What will happen if I don't want to carry on with the study?
If you decide to take part you are still free to withdraw at any time and without giving a reason. A decision to withdraw will not affect the standard of care you receive. If you withdraw from the study, we will only use the data collected up to your withdrawal.

What if there is a problem?
If you have a concern about any aspect of this study, you should ask to speak to the researchers (Dr. Zaid Hamdoon, Mr. Colin Hopper) who will do their best to answer your questions. If you remain unhappy and wish to complain formally, you can do this through the NHS Complaints Procedure. Details can be obtained from the hospital.
In the unlikely event that something does go wrong and you are harmed during the research and this is due to someone's negligence then you may have grounds for a legal action for compensation against the UCLH NHS Trust but you may have to pay your legal costs. Please note that there are no compensatory mechanisms in place for "non-negligent harm" (i.e. the harm is not due to somebody's fault). In this case, the normal National Health Service complaints mechanisms will still be available to you (if appropriate).

Will my taking part in this study be kept confidential?
All information which is collected about you during the course of the research will be kept strictly confidential, and any information about you which leaves the hospital will have your name and address removed so that you cannot be recognised.
The scanning images as well as identifiable information will be kept on one single, password-protected computer with access only by the researchers themselves. Following anonymisation, these images will be compared to the actual tissue sections that are prepared at the Pathology Laboratory and the results of this comparison will be statistically evaluated. The Chief Investigator will be personally responsible for safety and security of the data, and only the chief and the other investigators have access to the data.

Involvement of the General Practitioner/Family doctor (GP)
If you wish so (see Patient Consent Form) we will inform your GP about your participation in the study.

What will happen to any samples I give?
In this study, we will not take more samples (i.e. tissue biopsies) than necessary for your normal standard of care. All samples will be passed on to the Pathology Laboratory for routine processing and diagnosing after the optical scanning is performed. No samples will be kept with the researchers.

Will any genetic tests be done?
We will not perform any genetic tests on the tissue biopsies.

What will happen to the results of the research study?
Even though the outcome of the study won't have an influence on your personal diagnostic and therapeutic treatment plan, we will inform you about your individual results of the optical scanning if you so wish.
Once the study is finished, we plan to publish its results in the scientific and clinical press. Please be assured that you will not be identified in any report or publication.

Who is organising and funding the research?
This study has no financial support outside of UCLH. There will be no payment other than that to cover necessary expenses, i.e. the investigators will not be paid for including you into the study.

Who has reviewed the study?
All research in the NHS is looked at by independent group of people, called a Research Ethics Committee to protect your safety, rights, wellbeing and dignity. This study has been reviewed and given favourable opinion by Moorfields and the Whittington Research Ethics Committee.

Further information and contact details
If you have any further questions, please don't hesitate to ask me or one of the sub-investigators.

Thank you very much for your cooperation.

Mr Colin Hopper FRCS (Ed), FDSRCS, MBBS (Lond), BDS (Lond), LRCP, MRCS
Senior Lecturer/Consultant Maxillofacial Surgeon, UCLH
Head of Academic Surgery Unit at Eastman Dental Institute for Oral Health Care Sciences
Senior Research Fellow at the National Medical Laser Centre, UCLH